The Expeditions ANTARKTIS-XXII/1 and XXII/2 of the Research Vessel „Polarstern“ in 2004/2005

Edited by
Saad El Naggar, Gerhard Dieckmann, Christian Haas, Michael Schröder and Michael Spindler
with contributions of the participants

Ber. Polarforsch. Meeresforsch. 551 (2007)
ISSN 1618 - 3193

CONTENTS

ANT-XXII/1

12 October - 4 November 2004

Bremerhaven - Cape Town

Fahrtleiter / Chief Scientist:
Dr. S. El-Naggar

Koordinator / Coordinator:
Prof. Dr. P. Lemke

CONTENTS

1. ZUSAMMENFASSUNG UND FAHRTVERLAUF

Saad El Naggar
Alfred Wegener Institute, Bremerhaven

Nach einem kurzen Hafenaufenthalt in Bremerhaven (03.10.04 -12.10.04) hat FS *Polarstern* seine 22. Antarktisreise am 12.10.04 angetreten. Der erste Fahrtabschnitt (ANT-XXII/1) wurde zur Erprobung von wissenschaftlichen Geräten und zur Durchführung von atmosphärischen Messungen genutzt. Die Reise hat am 12.10.2004 um 13:00 h in Bremerhaven begonnen und endete am 04.11.2004 10:00 h in Kapstadt. Das FS *Polarstern* fuhr auf kürzestem Wege nach Kapstadt (siehe Fahrtroute) und die Reisedauer betrug 22 Tage inklusive einem Tag für Stationsbetrieb.

Die wissenschaftlichen, atmosphärischen, meereschemischen und luftchemischen Messungen wurden bei voller Fahrt des Schiffes durchgeführt. Ein Besatzungsmitglied und 8 Personen aus der Testmannschaft (AWI, Fielax, Atlas Hydrographic) wurden am 19.10.2004 in Gran Canaria (Las Palmas) ausgeschifft, eine Person wurde eingeschifft.

Auf dem ersten Teilabschnitt (Bremerhaven - Las Palmas) wurden folgende technische Erprobungen und Tests durchgeführt:

- Das Fächersonar HYDROSWEEP von ATLAS Hydrographic, Bremen, wurde mit neuer Rechnerhardware ausgestattet. Das System wurde auf Integrität und Funktionalität geprüft. Eine neue Kalibrierung bezüglich der Navigationsplattform (MINS) wurde am 17.10.04 zwischen den Wegpunkten (35°53'N 13°15'W) und (35°28'N 13°17'W) vollzogen. Diese Maßnahme war nach dem Austausch einer defekten Navigationsplattform MINS erforderlich geworden.

- Das Tiefsee-Sedimentecholot PARASOUND DS II von ATLAS Hydrographic, Bremen, wurde im Juni 2004 modernisiert. Die Software hierfür wurde im Oktober 2004 modifiziert. Das System konnte bis Las Palmas nicht vollständig getestet werden, da erneut Hardware- und Softwareprobleme auftraten. Ein Ingenieur von ATLAS Hydrographic setzte deshalb seine Reise bis Kapstadt fort und konnte in Zusammenarbeit mit der Firma an Land alle Fehler beseitigen. Das System wurde als betriebsbereit abgenommen.

- Ein neues EDV-Massenspeichersystem, SUN-Systems, wurde im Oktober installiert. Es wurde durch die Mitarbeiter der Firma Fielax und des AWI-Rechenzentrums an Bord in Betrieb genommen und während der Fahrt im realen Betrieb getestet. Das System hat damit zur Zeit eine Kapazität von ca. 3 Terra Byte und arbeitet an Bord reibungslos. Nutzerdaten können ab sofort direkt abgespeichert werden.

- Die vorkommenden Beschleunigungen (Verzögerungen) in verschiedenen Orten an Bord der FS *Polarstern* wurden mit Hilfe eines dreiachsigen Beschleunigungsloggers gemessen und analysiert. Die damit gemessene Beschleunigung lag maximal bei ca. 2.2 g.

Der Pinger wurde am 01.11.04 bei ca. 23°12'S; 8°20'E und bei einer Wassertiefe von ca. 1100 m erfolgreich getestet.

Darüber hinaus wurden folgende wissenschaftliche Programme durchgeführt:

- Die UV-B-Gruppe des AWI hat während der Reise eine UV-B-Messkampagne durchgeführt, die die spektrale UV-Verteilungen (UV-B&UV-A) in Abhängigkeit vom Breitengrad ermitteln soll. Hierfür wurden kontinuierliche Spektralmessungen mit dem AWI-Spektrometer durchgeführt. Gleichzeitig fanden Dosismessungen mit dem UV-Biometer „Solar Light" statt. Begleitend zu den UV-B-Messungen wurden 19 Radiosonden zur Sondierung der Atmosphäre gestartet.

- Die IfM-GEOMAR-Gruppe hat kontinuierlich Proben aus dem Oberflächenwasser entnommen (ca. 60 Proben). Diese sollen Auskunft über die Langzeittrends und die saisonale Variabilität der 13C-Isotopie des gelösten anorganischen Kohlenstoffs (DIC) im Oberflächenwasser des Nordatlantiks geben.

- Die Gruppe aus Heidelberg (IUP) hat die Absorptionsspektren der atmosphärischen Spurengase mit Hilfe des DOAS (Differential Optical Absorption Spectroscopy) entlang der Fahrtroute gemessen. Die gesammelten Daten werden an Land ausgewertet, mit dem Ziel die Konzentrationen der Spurengase in der Atmosphäre zu bestimmen.

- Die Arbeitsgruppe der Universität Hamburg, Institut für Geochemie, hat an drei Stationen Tiefenwasserproben mit einem großen Wasserschöpfer (400 l) gesammelt. Diese Wasserproben sollen Informationen über die gelösten organischen Substanzen im Tiefenwasser des Atlantiks (DOM) liefern. Die Wasserproben wurden an Bord filtriert und für den Transport nach Hamburg vorbereitet.

ITINERARY AND SUMMARY

After a short harbour stop in Bremerhaven (03.10.04 - 12.10.04) RV *Polarstern* started its 22th cruise to Antarctica.The first leg of this cruise (ANT-XXII/1) started in Bremerhaven on 12 October 2004, 13:00 h and was completed in Cape Town on 4 November 2004, 10:00 h. During that cruise different scientific instrumentation were tested and a scientific atmospheric marine programme was carried out. The ship sailed to Cape Town on the shortest way (see route plan). The transfer time was about 22 days including one day for station works and sea trials of instrumentation. A part of the testing crew (AWI, Fielax, Atlas Hydrographic) disembarked on 19 October 2004 in Grand Canaria (Las Palmas).

The following sea trials and instrumentation tests were carried out between Bremerhaven and Las Palmas:

- The Multi-Beam Echo Sounder (HYDROSWEEP DS II, Atlas Hydrographic) was equipped with a new hardware. The complete system was tested under real conditions at sea and a sea trial was performed. In addition, a calibration of the system in connection to the replaced navigation platform (MINS) was carried out on 17 October 2004 at 35°53'N 13°15'W and 35°28'N 13°17'W. The stability, reliability and the functionality of the system were tested during the complete cruise. Modifications on the software were also done by Atlas Hydrographic.

- The Deep Sea Sediment Echo Sounder (PARASOUND DS II, Atlas Hydrographic) was upgraded in June 2004 to DS II. An upgrade of the software was performed in October 2004 in Bremerhaven. A sea trial and a final tuning of the complete system was carried out. New software and hardware problems occurred during the first test between Bremerhaven and Las Palmas. An engineer from Atlas Hydrographic continued the work on board during the complete cruise with the help of his company's software. The system is now complete and operational.

- The new Data Mass Storage Unit was installed on board of RV *Polarstern* during maintenance at the shipyard in Bremerhaven. The installations were completed during that cruise and a sea trial and an acceptance test had been carried out on real conditions during that time period. The Mass Storage has now a capacity of 3 Terra Byte and user data can now be stored online on the system.

- The accelerations had been measured at different locations on board of RV *Polarstern* by using a special mobile acceleration data logger. The data collected herewith will be used to specify sensitive equipment, which will have to be installed and used on board in future. The maximum acceleration measured on board at moderate weather conditions was about 2.2 g.

- The Pinger was successfully tested on 1 November 2004 at 23°12'S 8°20'E. The water depth was about 1100 m.

- In addition, the following scientific programmes were performed during the complete cruise:

- The UV-B-group of AWI measured the UV-B-distributions (spectral and doses measurements) as a function of latitude. The AWI-spectrometer (UV-B & UV-A) and a UV-Biometer “Solar Light” were used. Calibration of UV-dosimeter was also performed. In addition, sounding of the atmosphere by using the VAISALA radio sonde was carried out. In total 19 ascents were released.

- The IfM-GEOMAR group is studying the long-term trends and the seasonal variability of the 13C signature of dissolved inorganic carbon (DIC) in surface waters of the Atlantic Ocean. 60 water samples of surface water were collected and will be analysed in Kiel and USA.

- The institute of environmental Physics of the University of Heidelberg (IUP) carried out Differential Optical Absorption Spectroscopy (DOAS) measurements during the cruise to determine the distributions of different chemical tracers in the atmosphere. The collected data will be processed later.

- In a long-term programme the group of University of Hamburg will study the Dissolved Organic Matter (DOM) in the Atlantic deep water. Three stations with a giant water sampler (400 l) were performed in the Atlantic deep water (Angola Basin). The collected water samples were ultra-filtrated on board and prepared for further processing in the laboratory in Hamburg.

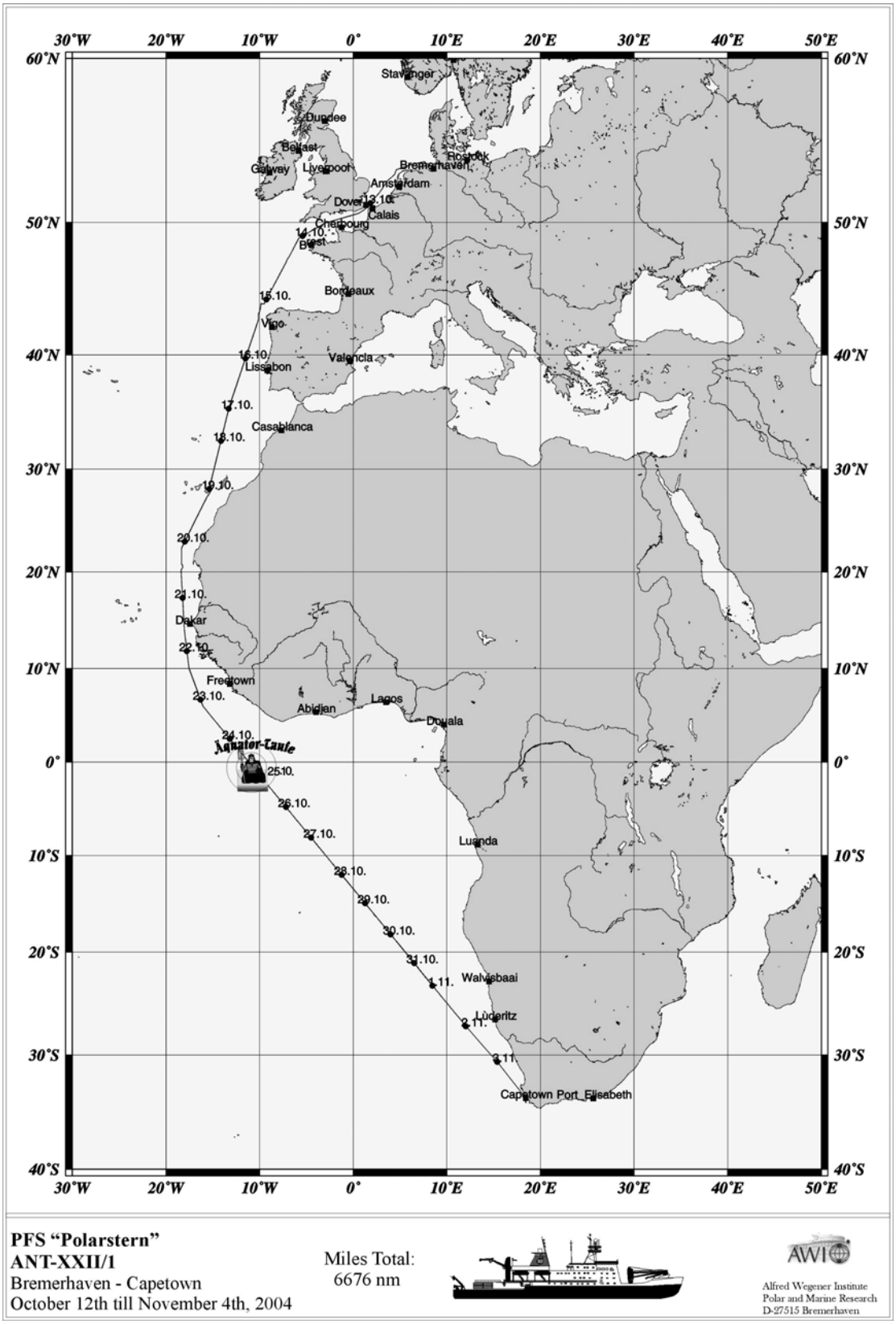

Abb. 1: Die Route auf ANT-XXII/1 FS Polarstern
Fig. 1: The Route of ANT-XXII/1 RV Polarstern

2. SEA TRIAL AND CALIBRATION OF THE HYDROSWEEP MULTIBEAM SYSTEM AND CONTINUOUSLY PERFORMED SURVEY OF THE SEAFLOOR

Fred Niederjasper[1)], Jörn Ewert[2)]

[1)] Alfred Wegener Institute, Bremerhaven
[2)] Atlas Hydrographic, Bremen

Objectives
The main goal of the cruise was the sea trial of the Hydrosweep system after a major update of its soft- and hardware components and the preparation for operation during leg 2-4 of ANT-XXII. In addition, data outside Exclusive Economic Zones (EEZ) were continuously recorded for further use.

Work at sea
The directions of the sound signals transmitted and received by the Hydrosweep system have to be corrected by use of roll and pitch angles, supplied by two laser gyro systems (MINS). Because of a small tilt angle of the transducer array and the laser gyro system against the horizontal, correction values have to be estimated (calibration). Both gyros failed at the beginning of the 2004 Arctic expedition. MINS 1 was replaced by a substitutional part and sent for repair. The substitutional part was used for Hydrosweep measurement during legs ARK-XX/2 and 3. During the last port call MINS 2 was replaced by the repaired MINS 1. Therefore MINS 1 has to be used for Hydrosweep during all subsequent ANT-XXII legs. For this reason both gyros had to be calibrated.

The estimation of the roll and pitch correction values was done by a repeated survey of a straight track line over approx. 7.5 nm in an area with a smoothly shaped seafloor near 35°35'N 13°15'W. The calibration work was finished after approx. 8 hours with good results. The differences between the correction values of the actual and the previously performed calibration of MINS 1 clearly pointed out, that after a replacement the gyro has to be calibrated.

Sea Trial
In autumn 2003 the Hydrosweep system was updated with the "High Definition Beam Estimation (HDBE)". HDBE increases the number of 59 hard beams to 240 soft beams. This results in a better resolution of the seafloor topography. During the last port time the computer hardware of the Hydrosweep control- and visualization software "Hydromap Online" was changed. The approx. seven years old HP UX workstations were replaced by PCs with the operating system SuSE Linux 9.0 installed. The new version of Hydromap Online includes two new features. An improved algorithm for calculating the mean sound velocity (C_{mean}) was added. The "HDBE" mode now comes with a variable receiver coverage, which can be changed in steps of 10°, depending of the reliability and quality of the outer beams.

In addition to the harbour acceptance test, these modifications had to be checked during a sea trial. We already started with Hydrosweep in the North Sea. The detection, analysis and correction of some major problems took some days. Since Las Palmas an extensive test programme had been performed. The track to Cape Town was planned parallel to the track of leg ANT-XIX/1, with an overlap of the old and new Hydrosweep measurements of about 50%. This enables a comparison between the new Hydrosweep data with the data derived during ANT-XIX/1. First results from the Hydromap online display demonstrate that HDBE makes it possible to use a transmit coverage of 120° also in deep waters with good results. In this mode the receiver coverage has to be set to 110° or 100°. For more precise results the Hydrosweep data must be post processed and analysed in Bremerhaven.

Bathymetry
The Hydrosweep system was operated during the whole leg. Outside the Exclusive Economic Zones (EEZ) the data was stored for further use. The validation and editing of the navigation and depth data will have to be done later because of lack of time. After the post processing, the data will be used for improvement of international bathymetric charts, like GEBCO. The high resolution data will be stored in a database and will be available for planning and detailed investigations.

3. SEA TRIAL AND SYSTEM TESTS OF ATLAS PARASOUND-DS2

Frank Niessen[1)], Gerd Kuhn[1)], Saad El Naggar[1)], Jörn Ewert[2)], Peter Gerchow[3)], Werner Dimmler[3)]

[1)] Alfred Wegener Institute, Bremerhaven
[2)] Atlas Hydrographic, Bremen
[3)]FIELAX, Gesellschaft für wissenschaftliche Datenverarbeitung mbH, Bremerhaven

Objectives
The hull-mounted PARASOUND sediment echo sounder belongs to the geological survey equipment on board RV *Polarstern*. On scientific expeditions it is in 24-hour operation along all cruise tracks. In June 2004, the RV *Polarstern* parasound system DS1 received a major upgrade by installation of ATLAS PARASOUND-DS2. The DS2 equipment consists of the transmitter/receiver electronics and its control/data acquisition system. The former remained mostly unchanged as compared to the previous DS1 version, whereas the latter was completely replaced by an operator personal computer (PC) working as control, processing, display and recording unit. The purpose of system testing during ANT-XXII/1 was to check the functions of the latest software versions of ATLAS PARASOUND-DS2. The aim was to provide a fully functioning system for the forthcoming expeditions ANT-XXII/2 and ANT-XXII/4, where PARASOUND is going to be used for intensive scientific data acquisition.

Bottom and sub-bottom reflection patterns obtained by PARASOUND characterize the uppermost sediments in terms of their acoustic behaviour. This can be used to interpret the sedimentary environments and their changes in space and time and to select coring locations for gravity and box cores. The PARASOUND system (ATLAS Hydrographic, GmbH, Bremen, Germany) generates two primary frequencies

between 18 and 23.5 kHz transmitting in a narrow beam of 4° at high power (70 kW electrical power per pulse). As a result of the interaction of the primary frequencies within the water column, a secondary frequency is created based on the parametric effect. The parametric frequency is the difference frequency of the two primary waves transmitted. As a result of the longer wavelength, the parametric frequency allows sub-bottom penetration up to 150 m (depending on sediment composition) with a vertical resolution of ca. 20 cm. The use and basic principles of the system are described in Spiess (1992). The specifications and different components of the new PARASOUND-DS2 are described and illustrated in Stein (2005).

Work at sea

During ANT-XXII/1 the parametric frequency was set to 4 kHz and the pulse length to 2 parametric periods. Since the water depths were 20 to 50 m in the North Sea and English Channel and up to 5200 m along the voyage across the Gulf of Biscay to the Canary Islands, the Parasound operation modes were switched between PAR (shallow and deep water), NBS-PAR or PAR-pilot.

ATLAS PARASOUND-DS2 is controlled by means of the ATLAS HYDROMAP CONTROL software via Operator PC. ATLAS PARASTORE-3 provides a user-friendly graphical interface and has been designed to acquire, visualize, process, store, convert, quality control, replay and print data from ATLAS PARASOUND-DS2 profiles via Operator PC. This includes not only the sub-bottom parametric data but also the primary narrow single-beam signal (NBS, 18 kHz). The recorded data of both parametric and NBS signals are stored in a hybrid raw data format (ASDF format) in either a ring buffer or into user selected folders on hard disc. The new Control Unit GE 6030 (CU) provides the link between the Operator PC, the largely unchanged Transceiver Cabinets GE 6019 A 003/004 and external interfaces. The latter are essential to provide importation of navigation (GPS-position, speed heading etc.) and ship-motion data (heave, roll, pitch) as well as water depth and sound velocity form the MINS interface (Werum, Germany) and ATLAS Hydrosweep (ATLAS Hydrographic, Germany), respectively. The former control and printing unit of DS1 ATLAS Deso-25 remained in the new DS2-system as black and white chart recorder operating as slave only.

The function of the new system was first checked during the Sea Acceptance Test (SAT) carried out during ARK-XX/1 in June 2004. The results are published in Budéus (2004). The system was successfully used and further tested during the expedition ARK-XX/3 in September 2004 (Stein, 2005). However, during ARK-XX/3 a total of 25 hardware and software errors were detected in the PARASOUND-DS2 system and mailed to ATLAS Hydrographic GmbH in Bremen. Based on the error descriptions, improved versions of both ATLAS HYDROMAP CONTROL and ATLAS PARASTORE-3 software were installed on board *Polarstern* prior to ANT-XXII/1. These versions were subjected to intensive testing during the voyage from Bremerhaven to Las Palmas (Grand Canaria) with particular emphasis on deep water operation (> 3000 m water depth) in rough seas because previous operations were restricted to relatively shallow water (mostly < 3000 m) and calm seas with lack of significant ship motion.

During the first part of the journey from Bremerhaven to the Gulf of Biscay, the system was tested in shallow water. Almost all of the previously detected software and hardware problems turned out to be solved. Two new printers (HP-Deskjet 5652) for online-profile and auxiliary-data printing respectively, were installed and functioned without problems. Acoustic artefacts in the recorded seismograms derived from the blanking-out signals of the TVG mode (Time Variable Gain) could be eliminated prior to the arrival in Las Palmas.

During the journey from the Gulf of Biscay to Las Palmas the system was tested in deep water (4000 to 5200 m). Due to bad weather conditions and relatively high waves (up to 6 m) the deep-water mode "PAR-Pilot" of PARASOUND-DS2 could be checked for functioning of ship-motion correction based on data imported from the MINS interface (heave, roll and pitch). It turned out that motion correction was insufficient in two ways: (1) For a large number of pulses (or pulse trains in PAR-Pilot mode) no motion data was received and traces were blanked out in the echogram window PAR accordingly. (2) Heave compensation was insufficient so that vertical displacements of several meters from pulse-train to pulse-train were observed in the in the echogram window PAR (Fig. 3.1).

Problem (1) was identified as caused by the MINS interface data protocol where heave data having question marks were blanked out. A new version of MINS software, which ignored the question marks, was transmitted to the vessel by the Werum company and solved this problem. Apparently, question marks appeared in the heave sensor data at high seas, but turned out to reflect correct measurements.

Problem (2) was analysed in more detail along the Hydrosweep test profiles between 35°35'N 13°14.95'W and 35°27.73'N 13°17.10'W, where the ship repeated data acquisition along one 7.5 nm long line nine times in total. Sub-bottom structures and water depth of almost 5000 m remained more or less constant, but the ship motion changed due to variable heading and alteration of sea conditions. In different time intervals, the PARASOUND-2 system was changed between PAR-Pilot, PAR-NBS and PAR modes. As illustrated in figure 3.1, heave compensation was insufficient in the PAR-Pilot mode, but appeared to be correct in modes PAR and PAR-NBS. This observation can only be explained by a software error in the Control Unit GE 6030 and/or ATLAS PARASTORE-3. This conclusion is consistent with simultaneous echogram recording in PAR-Pilot mode by DESO-25 not being affected by insufficient heave compensation, because DESO-25 is using direct analogue depth-motion data via CU. Therefore DESO-25 heave-compensation is decoupled from CU software and/or PARASTORE-3 software and thus not subjected to such errors. A report was sent to ATLAS Hydrographic in Bremen with the aim of receiving a correct software version prior to arrival of the vessel in Cape Town at the end of ARK-XXII/1. It cannot be excluded that the system is affected by further minor problems of insufficient motion-data corrections. These may be originated in ship-motion data acquisition and/or correction within PARASOUND-2. We were not able to analyse this in further detail during the cruise.

The slave chart recorder DESO-25 was properly installed for PAR-Pilot mode operation of PARASOUND-2 by removing a pre-trigger signal causing artefacts in the record. In addition, a list describing nine new problems of PARASOUND-2 hard and

software was compiled and send to ATLAS Hydrographic in Bremen. The problems include:

- insufficient depth detection in the PAR-pilot mode below 4000 m water depth,
- blanking out of train pulses in NBS echograms in PAR-Pilot mode, if a depth range of 10,000 m is used for pulse train transmission,
- inconsistency in HYDROMAP CONTROL software with respect of function and meaning of depth range and pulse train length,
- a few more minor problems causing inconveniences by using PARASTORE-3 and HYDROMAP-CONTROL software.

Mr. J. Ewert (Atlas Hydrographic) stayed on board until arrival in Cape Town on 4 November 2004, while the sea trial team of AWI had left the vessel in Las Palmas on 19 October 2004.

In co-operation with Atlas Hydrographic in Bremen Mr. Ewert was able to repair all the claims mentioned above during the time period 19 October to 4 November 2004. The ATLAS PARASOUND-DS2 was accepted as fully operational according to the Sea Acceptance protocol signed on Board at the end of the cruise.

References

Budéus, G. (2004) The *Polarstern* Expedition ARK-XX/1. Reports of Polar Research (in press)

Spiess, V. (1992): Digitale Sedimentechographie - Neue Wege zu einer hochauflösenden Akustostratigraphie.- Berichte aus dem Fachbereich Geowissenschaften der Universität Bremen, Nr.35, 199pp.

Stein, R. (2005), The *Polarstern* Expedition ARK-XX/3, Reports of Polar Research No. 517.

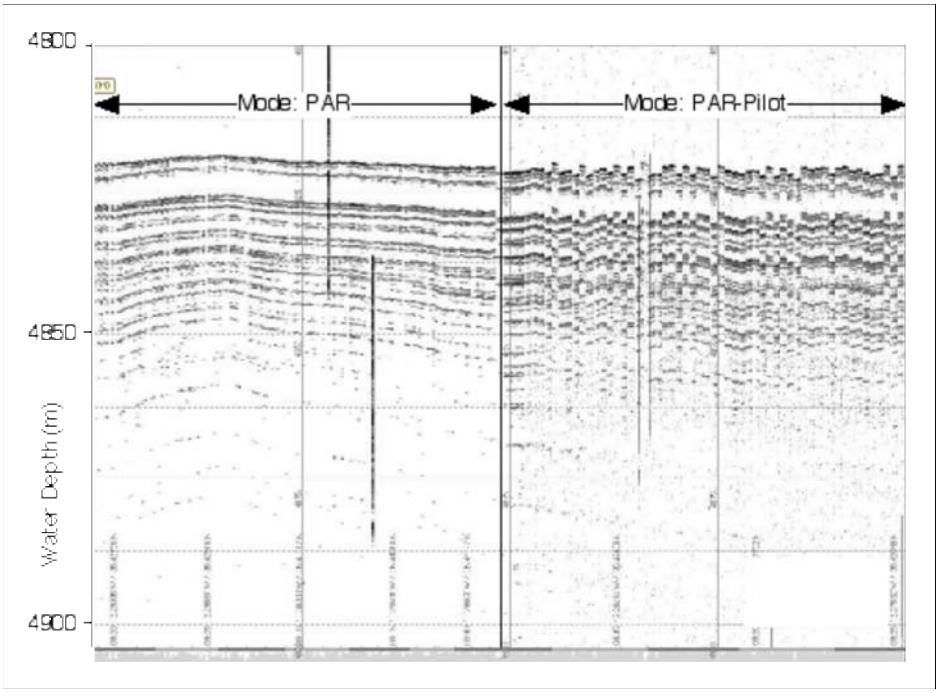

Fig. 3.1: Example of a Parasound profile recorded in both PAR and PAR-Pilot modes. Left-end and right-end positions are 35°26.4N 13°17.53W and 35°29.51N 13°16.556W, respectively. The distance bar (black or white) at the bottom of the figure corresponds to 1 km.

4. SEA TRIAL AND ACCEPTANCE TESTS OF THE DATA MASS STORAGE UNITS

Hans Pfeiffenberger[1)], Saad El Naggar[1)], Peter Gerchow[2)]

[1)] Alfred Wegener Institute, Bremerhaven
[2)]FIELAX, Gesellschaft für wissenschaftliche Datenverarbeitung mbH, Bremerhaven

Objectives
A Data Mass Storage Unit was installed on board of RV *Polarstern* during maintenance at the shipyard in Bremerhaven (3 October to 12 October 2004).

Due to the restricted time at the shipyard and since the systems on board were not completely running during that period, the installation of the system could not be accomplished in Bremerhaven. Consequently, the installation of hard and software had to be completed during the cruise ANT-XXII/1 between Bremerhaven and Las Palmas. A sea trial and acceptance test was carried out under real conditions during this time period.

Work at sea
The mass storage unit including all Sun-Servers, hard disks and buck-up tapes machine had been integrated into the computer systems and the network on board. A complete configuration and tuning were carried out to optimise this system.

This new system is able to store more than 3 terabytes of data and it is compatible with the main storage system at AWI.

The Data Storage Unit consists of 2 X Sun-Servers (VT 240), 2 X External RAID-Disk-Storage System and a Back-Up Library (96 Tapes of LTO2-System including 2 X LTO2-Tape Drives) with a Roboter System for tape positioning and transports.

This system will offer an efficient data transfer between RV *Polarstern* and AWI and will realise a high integrity of the data on board.

The following programme was carried out:

- Completion of the hard and software installation of the mass storage unit
- Configuration and tuning of the system
- Carrying out the sea trial and the acceptance tests

The system was successfully installed and tested during ANT-XXII/1. The system was accepted and has been operational since 19 October 2004.

5. MEASUREMENTS OF THE REAL ACCELERATION ON BOARD OF POLARSTERN

Saad El Naggar
Alfred Wegener Institute, Bremerhaven

Objectives and work at sea
The accelerations have been measured at different locations on board of RV *Polarstern* by using a special mobile acceleration data logger. The data collected herewith will be used to specify sensitive equipment, which will have to be installed and used on board in future. The maximum acceleration measured on board at moderate weather conditions was about 2.2 g.

6. SEA TRIAL OF THE 12 KHZ PINGER

Saad El Naggar[1)], Thomas Kahrs[2)]

[1)] Alfred Wegener Institute, Bremerhaven
[2)]FIELAX, Gesellschaft für wissenschaftliche Datenverarbeitung mbH, Bremerhaven

Objectives and work at sea
The board Pinger was successfully tested on 1 November 2004 at 23°12'S 8°20'E at a water depth of 1,100 m.

The main goals of this test were to find an optimal operation mode to use the existing Pinger system of 12 kHz with the SIMRAD Deep Water Sounder (DWS 500). External triggering was established by using a high precision function generator and an operation procedure was found.

The system can be now used as a pinger according to the mentioned procedure. The synchronisation between SIMRAD and the pinger usually takes about 30 minutes. The distance resolution between pinger and seafloor is about 5 meters.

7. MAX-DOAS MEASUREMENTS

Roman Sinreich
University of Heidelberg

Objectives
The University of Heidelberg (Institute of Environmental Physics) had installed a Multi-Axis Differential Optical Absorption Spectroscopy (MAX-DOAS) device on RV *Polarstern*. The DOAS method allows to obtain the identity and the amount of atmospheric trace gases due to their characteristic absorption of light passing through the atmosphere. By looking into different elevation angles (Multi-Axis) it is additionally possible to estimate height profiles of these trace gases. Lower elevation angles lead to measurements with more horizontal scattered light. Thus in the longer light path mainly absorptions of tropospheric gases take place. Against, measurements in direction of the zenith show mainly absorptions of stratospheric gases. These ship borne measurements allow a validation of DOAS measurements of the satellite instrument SCIAMACHY onboard ENVISAT.

Through this cruise we used a spectrograph with a wavelength range from about 290 to 430 nm. A telescope that collects the scattered solar light and leads it via a quartz fibre bundle to the spectrograph points to the direction of 3, 6, 10, 18 and 90 degrees of the horizon one after another. Each direction is measured about 3 minutes and thus every 15 minutes continuously. To reduce the effect of the ship's movements the telescope is mounted on a cardanic suspension. Since the instrument was installed through the ship maintenance in the shipyard of Bremerhaven the measurements could start from the beginning of the cruise and were continued with only several very short interruptions.

The DOAS analysis is focused on the trace gases NO_2, O_3, BrO and HCHO. As expected, first results show higher values of NO_2 through the English Channel. This is based on the air emissions of the adjacent countries.

The MAX-DOAS measurements were performed during the whole cruise ANT-XXII.

8. LARGE VOLUME WATER SAMPLING FOR DOM FRACTIONATION AND ANALYSIS

Alejandro Spitzy and Hayo Köhler
Institute of Biogeochemistry and Marine Chemistry, University of Hamburg

Objectives

DOM in the ocean represents a carbon pool comparable in size to atmospheric CO_2. Its cycling is only partially understood and less than 30 % of marine DOM have been characterized chemically so far. It is a heterogenous mix of molecules covering a wide range of sizes/molecular weights, whereby the “truly dissolved” fraction (<1000 Da) exceeds the colloidal fraction (>1000 Da). Radiocarbon dating of different size classes of DOM revealed increasing age with decreasing size (Loh et al. 2004). In previous work on the terrestrial source of marine DOM we studied molecular size, humic content and carbon isotopes of DOM in Siberian estuaries and the Kara Sea (Spitzy et al. 2002), which is characterized by high terrigenous inputs. For comparative investigations on pure marine DOM we sampled deep sea water of old age from the Angola Basin during this cruise and size-fractionated it by ultrafiltration on bord for further chemical and isotopic analysis in our home laboratories.

Work at sea

Stations

Along the prescribed cruise track of RV *Polarstern* we performed 3 deep water sampling stations in the Angola Basin. Detailed station data are given in table 8.1. All stations are within a regional box constrained by the hydrographic and geochemical WOCE profiles A14 and A13 in longitude and by profiles A7 and A9 in latitude (Schlitzer, 2000; eWOCE Gallery). The first station is located near the intersect of A14 and A7, the third station near the intersect of A13 and A9. For all stations the WOCE data, which were generated in the nineties, indicate no freons at depths below 1000 m. Their further downward penetration since would not have reached the depths we sampled (2000 m; 4000 m).

Tab. 8.1: Sampling stations during ANT-XX II/1

No.	date	Latitude	Longitude	sampling depth	water depth	Sampled volume
PS 67 001	26/10/04	5°00 S	7° 03 W	2000 m	4420 m	800 L
PS 67 002	29/10/04	14°59 S	01° 17 E	4000 m	5550 m	800 L
PS 67 003	30/10/04	18°13 S	04°01 E	4000 m	5430 m	800 L

Equipment
Samples were taken with a 400 liter stainless steel large volume sampler of Hydrobios, Kiel. At each station the sampler was lowered twice providing a total sample of 800 liters per station.

Sample treatment
Samples were permanently (except during ultra filtration) stored at 4°C in acid pre-rinsed PE carboys of 30 l volume. Ultra filtration followed sampling immediately. It was done on unfiltered samples in a serial 2-step fractionation starting with 10 kDa followed by 1 kDa. We used a ROCHEM disc tube module system operating at 2.5 bar and 10 bar for the 10 kDa and the 1 kDa module respectively. For station 1 we only retained the retentate fractions > 10 kDa and >1 kDa<10kDa, containing the colloidal DOM, and discarded the <1 kDa permeate, which contains the truly dissolved DOM. For stations 2 and 3 we additionally saved the < 1kDa permeate for further fractionation in our land based laboratory, to which all samples are transported in an uninterrupted cooling chain at 2-4°C.

Follow up land based work
Permeates will be further fractionated at 0.3 kDa and at 0.1 kDa (Reverse Osmosis) cutoffs. All fractions finally obtained will be anlysed for their humic and isotopic composition and further characteristic physical and chemical parameters.

References
Loh, A.N., J.E.Bauer & E.M. Druffel (2004) Variable aeging and storage of dissolved organic components in the open ocean. Nature, 430: 887-881.

Spitzy, A., S.Ertl & H.Köhler (2002), Dissolved humic matter in Arctic estuaries. EOS Trans. AGU, 83(47).

Schlitzer, R. (2000) Electronic Atlas of WOCE Hydrographic and Trader data now available. EOC Trans. AGU, 81 (5), 45.

Acknowledgements:
We thank captain Pahl and his crew for their continuous support during all phases of our sampling programme. Chief scientist Dr. Saad El Naggar ensured the possibility of several station sampling. Prof.Dr.Detlef Schulz-Bull (IOW) kindly provided the large volume sampler. This project is partially funded by a grant of Ancora AG (Hamburg) to A.S. Shipping of samples in a cooling container from Cape Town to Hamburg will be kindly provided courtesy DAL-Rantzau group (Hamburg).

9. LONG-TERM TRENDS AND SEASONAL VARIABILITY OF THE ^{13}C SIGNATURE OF DISSOLVED INORGANIC CARBON (DIC) IN SURFACE WATERS OF THE ATLANTIC OCEAN

Arne Kötzinger, Björn Fiedler,
Leibniz-Institut für Meereswissenschaften IFM-GEOMAR

Objectives
The primary goal of the ^{13}C sampling programme is to study the interannual variability and long term trends in the air-sea $\delta^{13}C$-DIC disequilibrium of surface waters in the Atlantic Ocean. The project is meant to be a long-term study which involves sampling during all RV *Polarstern* transits to/from the Southern Ocean. It is a joint project of Prof. Dr. Paul Quay of the School of Oceanography, University of Washington, Seattle/WA, U.S.A. and Prof. Dr. Arne Körtzinger of the Leibniz-Institut für Meereswissenschaften, Kiel.

Work at sea
During the cruise ANT-XXII/1 of RV *Polarstern* from Bremerhaven to Cape Town (12 October to 4 November 2004), surface seawater samples for $\delta^{13}C$-DIC measurements were taken in an 8 hour interval along the entire cruise track to get equidistant sampling points (overall 60 samples). These samples will be measured at Paul Quay's Stable Isotope Laboratory.

In order to enhance interpretation of the ^{13}C data, parallel sampling for dissolved inorganic carbon (DIC) and total alkalinity (A_T) was carried out with a similar number of samples. Measurements of DIC and A_T will be carried out in Kiel.

All these samples were taken from the clean seawater pump system, which is based on a stain less steel (V4A) centrifugal pump and Teflon tubing. The required environmental data set were collected by using the on board data system PODAS.

The sampling has already occurred in leg 1 and 5 of the RV *Polarstern* cruise ANT-XXI, now in leg 1 of the RV *Polarstern* cruise ANT-XXII and will be continued in ANT-XXII leg 5.

Tab.9.1: Summary of collected data of the ^{13}C samples during ANT-XXII/1

Date	Time (UTC)	Sample No.	Position lat.	Position lon.
14.10.2004	14:07:00	UW 1	48° 45.24 N	5° 55.12 W
14.10.2004	21:59:00	UW 2	47° 9.0015 N	7° 11.4048 W
15.10.2004	06:12:00	UW 3	45° 28.8399 N	8° 27.8291 W
15.10.2004	14:12:00	UW 4	44° 3.5682 N	9° 40.8482 W

Date	Time (UTC)	Sample No.	Position lat.	Position lon.
15.10.2004	22:32:00	UW 5	42° 23.2716 N	10° 19.1403 W
16.10.2004	06:34:00	UW 6	40° 34.0110 N	11° 7.8845 W
16.10.2004	14:24:00	UW 7	39° 9.5884 N	11° 44.6686 W
16.10.2004	22:40:00	UW 8	37° 18.2328 N	12° 32.0455 W
17.10.2004	06:39:00	UW 9	35° 56.7886 N	13° 5.9655 W
17.10.2004	18:50:00	UW (10-200)	35° 27.1195 N	13° 17.0108 W
17.10.2004	18:50:00	UW 11	35° 27.1195 N	13° 17.0108 W
18.10.2004	06:33:00	UW 12	33° 37.5066 N	13° 49.6310 W
18.10.2004	14:30:00	UW 13a	32° 2.5390 N	14° 17.0967 W
18.10.2004	14:30:00	UW 13b	32° 2.5390 N	14° 17.0967 W
18.10.2004	22:29:00	UW 14	30° 29.8001 N	14° 43.4760 W
19.10.2004	06:58:00	UW 15	29° 1.1809 N	15° 8.2811 W
19.10.2004	16:30:00	UW 16	27° 14.0249 N	15° 41.1838 W
19.10.2004	22:30:00	UW 17	25° 57.3168 N	16° 24.0547 W
20.10.2004	06:39:00	UW 18	24° 11.3593 N	17° 21.9929 W
20.10.2004	14:26:00	UW 19	22° 28.2043 N	18° 16.9994 W
20.10.2004	22:28:00	UW 20	20° 31.8972 N	18° 12.5516 W
21.10.2004	07:32:00	UW 21	18° 23.3981 N	18° 17.2887 W
21.10.2004	15:26:00	UW 22	16° 30.8103 N	18° 10.7139 W
21.10.2004	23:38:00	UW 23	14° 36.0452 N	18° 4.0696 W
22.10.2004	07:38:00	UW 24	12° 46.3989 N	17° 52.9275 W
22.10.2004	15:33:00	UW 25	10° 59,5521 N	17° 39,8261 W
22.10.2004	23:30:00	UW 26	9° 15,7534 N	17° 16,0340 W
23.10.2004	07:37:00	UW 27	7° 33,5427 N	16° 37,7044 W
23.10.2004	15:24:00	UW 28a	5° 55,7504 N	15° 59,8211 W
23.10.2004	15:24:00	UW 28b	5° 55,7504 N	15° 59,8211 W
23.10.2004	23:29:00	UW 29	4° 31,0320 N	14° 50,2923 W
24.10.2004	07:40:00	UW 30	3° 7,6332 N	13° 41,9719 W
24.10.2004	15:23:00	UW 31	1° 57,5519 N	12° 44,6272 W
24.10.2004	23:13:00	UW 32	0° 49,6907 N	11° 49,1552 W
25.10.2004	07:32:00	UW 33	0°28,1492 S	10° 45,5394 W
25.10.2004	16:45:00	UW 34	1° 40,0026 S	9 °46,7351 W
26.10.2004	00:04:00	UW 35	2° 52,2428 S	8° 47,6451 W
26.10.2004	08:32:00	UW 36	4°16,4323 S	7° 38,6802 W
26.10.2004	21:29:00	UW 37	5° 39,0100 S	6° 30,8826 W
27.10.2004	07:38:00	UW 38	7° 23,2632 S	5° 4,9752 W
27.10.2004	15:24:00	UW 39	8° 42,7113 S	3° 59,4630 W
27.10.2004	23:21:00	UW 40	10° 1,2396 S	2° 54,3688 W
28.10.2004	07:42:00	UW 41	11° 22,8524 S	1° 46,4351 W
28.10.2004	16:09:00	UW 42	12° 42,0035 S	0° 40,2491 W
28.10.2004	23:49:00	UW 43	13° 52,7575 S	0° 19,2082 E
29.10.2004	07:44:00	UW 44	14° 58,7035 S	1° 14,9057 E
29.10.2004	22:17:00	UW 441	16° 14,1169 S	2° 15,9909 E
30.10.2004	06:45:00	UW 45	17° 27,8113 S	3° 21,7874 E

Date	Time (UTC)	Sample No.	Position lat.	Position lon.
30.10.2004	20:58:00	UW 46	18° 57,0829 S	4° 38,5619 E
31.10.2004	06:49:00	UW 47	20° 21,5601 S	5° 51,8605 E
31.10.2004	14:23:00	UW 48	21° 29,2970 S	6° 51,0921 E
31.10.2004	22:20:00	UW 49	22° 26,5581 S	7° 39,5421 E
01.11.2004	13:12:00	UW 50	23° 33,5454 S	8° 38,8776 E
01.11.2004	21:34:00	UW 51	24° 57,8473 S	9° 54,7614 E
02.11.2004	05:45:00	UW 52	26° 18,6735 S	11° 8,3288 E
02.11.2004	13:23:00	UW 53	27° 31,9295 S	12° 15,7488 E
02.11.2004	21:27:00	UW 54	28° 50,3930 S	13° 28,7987 E
03.11.2004	06:51:00	UW 55	30° 19,5558 S	14° 53,2074 E
03.11.2004	14:07:00	UW 56a	31° 30,4409 S	16° 0,7347 E
03.11.2004	14:07:00	UW 56b	31° 30,4409 S	16° 0,7347 E

10. UV-B- IRRADIANCE AND DOSIMETRY DISTRIBUTIONS

Saad El Naggar, Otto Schrems
Alfred Wegener Institute, Bremerhaven

Objectives
Due to the ozone depletion in Antarctica during the last 21 years, increased UV-B-solar radiation was there observed. Since 1994 a personal dosimetry programme has been started at *Neumayer*-Station to quantify the impacts of the UV-B-radiation on human beings in Antarctica. This programme includes the use of different personal dosimeter and UV- spectrometer. An electronic dosimeter (ELUV-14) was especially developed at AWI.To support this programme, UV-measurements were carried out during the cruise ANT-XXII/1 of RV *Polarstern* between Bremerhaven and Cape Town.

The objectives of the work at sea are:

- to determine the global UV-B doses as a function of latitude, sun elevation and ozone column,
- to find out the maximal daily doses reaching the earth surface at sea level,
- to measure the spectral UV-B distributions during the cruises using the AWI-Spectrometer.

Work at sea
To achieve the above objectives, the following work was done:

- daily UV-measurements using the AWI-spectrometer, ELUV-14,
- dosimeter and the biometer measurements,
- data collection and validation.

Used Instruments

- AWI-UV-Spectrometer (32 Multi Channel Plade), full spectrum every 10 seconds, UV-B and UV-A. Data are stored in daily files at 5 minutes records.
- Personal UV-B-Dosimeter ELUV-14, Erythem similar action spectra. Data are stored in daily files at 1 minutes records.
- Biometer, Solar Light 501, erythemally weighted UV-B irradiances an doses. Data are stored in daily files at 5 minutes records.
- Ozone data of TOMS were used here to complete the data set, while no ozone sounding was carried out during this cruise.

Preliminary Results

UV-B and UV-A spectral measurements

Solar UV irradiance were measured during this cruise with a spectral radiometer unit mounted in a white box on the port side of the upper deck. The same instrument was used during ANT-XX/3 from Cape Town to Bremerhaven, except the colour of the housing box. The colour of the box was changed from dark yellow to white, to avoid an additional heating by the solar radiation.

The instrument is operating in two wavelength regions simultaneously by two inbuilt independent spectral radiometers, namely in the UVB from 280 to 320 nm and the UVA from 320 to 400 nm. Both radiometers are supplied with array detectors, which are a 32 channel photon counting Multi Channel Plade (MCP) for the UVB and a 256 channel Photo Diode Array for the UVA. A complete spectrum is obtained each few seconds (1 sec for the UVB, 2 to 32 seconds in the UVA dependent on brightness). So the relative spectral distribution of the solar irradiance is affected by the variable atmospheric conditions like cloud, solar zenith angle. The instrument was in operation day and night during the whole cruise from 12 October to 4 November and did never fail. The measured spectra where stored as average values by time interval of five minutes.

The results of this measurement are listed in table 10.1 and displayed in figure 10.1.

Eluv-14 and biometer dose measurements

For direct measurements of the erythemally weighted UV-B irradiances and doses, a UV-B-biometer, type 501 form Solar Light was used and installed nearby the spectrometer. The biometer is a broad band radiometer and was running during the whole cruise. Data were recorded at 5-minutes intervals as averaged value.

The Eluv-14 dosimeter is an electronic personal broad band dosimeter and it is able to measure the erythemally weighted irradiance, too. The data were recorded at a one–minute interval as averaged value. Table 10.1 shows all relevant data of the UV-B measurements during this cruise.

Tab. 10.1: Summary of all UV-B data collected during ANT-XXII/1; 12 October to 4 November 2004

Date	Zenith Time [UTC]	Latitude [deg]	Longitude [deg]	UV-B Dose [J/m^2]	Erythem Dose [J/m^2]	Erythem Dose [MED]	Ozone [DU]	Max.Sun Elevation [°]
12.10.2004	11:26	53.58	8.55	7333.4	247.87	1.180	270	28.7
13.10.2004	11:58	51.27	1.78	7379.0	240.73	1.146	301	30.6
14.10.2004	12:22	49.00	-5.53	11571.4	377.08	1.796	337	32.5
15.10.2004	12:38	44.28	-9.37	8488.4	303.85	1.447	304	36.9
16.10.2004	12:46	39.55	-11.58	19136.9	782.59	3.727	288	41
17.10.2004	12:53	35.58	-13.25	16833.1	712.01	3.391	273	44.8
18.10.2004	12:57	32.37	-14.20	28781.3	1300.05	6.191	264	47.7
19.10.2004	13:02	27.95	-15.30	31847.3	1599.89	7.619	248	51.7
20.10.2004	13:12	22.78	-18.03	37856.4	1974.19	9.401	250	56.6
21.10.2004	13:13	17.05	-18.20	46165.2	2525.51	12.026	255	61
22.10.2004	13:11	11.55	-17.73	42868.6	2339.44	11.140	266	67.1
23.10.2004	13:05	6.37	-16.18	23034.7	1211.20	5.768	260	71.9
24.10.2004	12:52	2.05	-13.05	50463.1	2916.23	13.887	269	76
25.10.2004	12:41	-1.03	-10.30	55718.3	3237.48	15.417	265	78.7
26.10.2004	12:28	-4.93	-7.12	46805.7	2678.68	12.756	270	81.3
27.10.2004	12:18	-8.20	-4.42	56958.2	3290.07	15.667	270	86.2
28.10.2004	12:05	-12.17	-1.10	39009.9	2175.89	10.361	277	88.8
29.10.2004	11:55	-15.00	1.28	37478.4	2076.82	9.890	285	88.6
30.10.2004	11:44	-18.18	4.00	50540.7	2840.52	13.526	282	85.7
31.10.2004	11:34	-21.05	6.50	49334.2	2739.51	13.045	283	83.2
01.11.2004	11:26	-23.33	8.43	53638.5	2933.98	13.971	285	81.3
02.11.2004	11:12	-27.22	11.97	60071.1	3223.32	15.349	293	77.7
03.11.2004	10:58	-31.00	15.50	61945.5	3302.39	15.726	287	75.3

Figure 10.1 shows the UV-B unweighted and erythemally weighted daily UV-B-doses during the cruise.

All measurements were affected by the bad weather conditions. On 23 October 2004 a heavy cloud cover occurred the very low dose for this day (23 kJoul). The maximal dose of 61945 Joul (UV-B) and 3302 Joul (Erythemally weighted = 15.7 MED, Minimal Erythemal Dose) were recorded on 3 November 2004 at sun elevation by 75°. The dose maximum was expected on 28 October 2004 at sun elevation of 88.8°. But the cloud cover on this day reduced the expected dose.

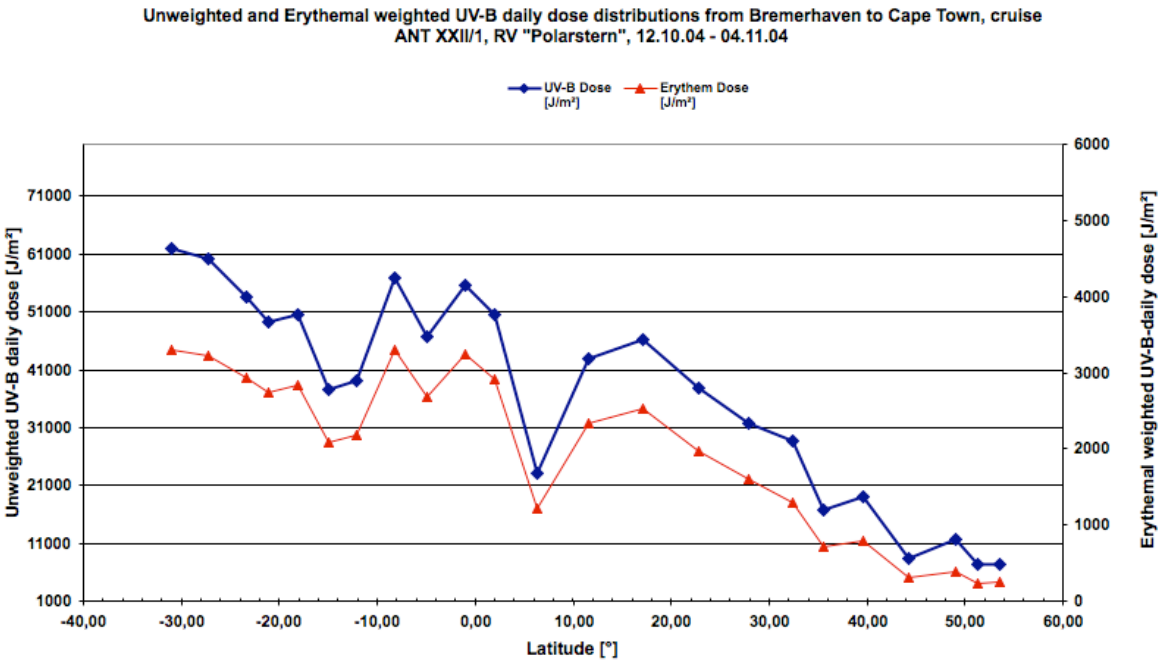

Fig. 10.1: UV-B dose distributions between Bremerhaven and CapeTown during ANT-XXII/1

Ozone distribution

Ozone soundings were not carried out during this cruise, due to a deficit on qualified personnel, who were able to participate on this cruise. Therefore the ozone data from TOMS were inquired from the ozone data centre by AWI and were sent daily to the ship to complete the required data sets.

Total ozone columns are listed in table 10.1. No information about the ozone profile at location was available.

Figure 10.2 shows the preliminary results of the total ozone column distribution. The total ozone column was changing between 350 DU in the north decreasing to 200 DU in the equatorial area and increasing again in the south to 314 DU.

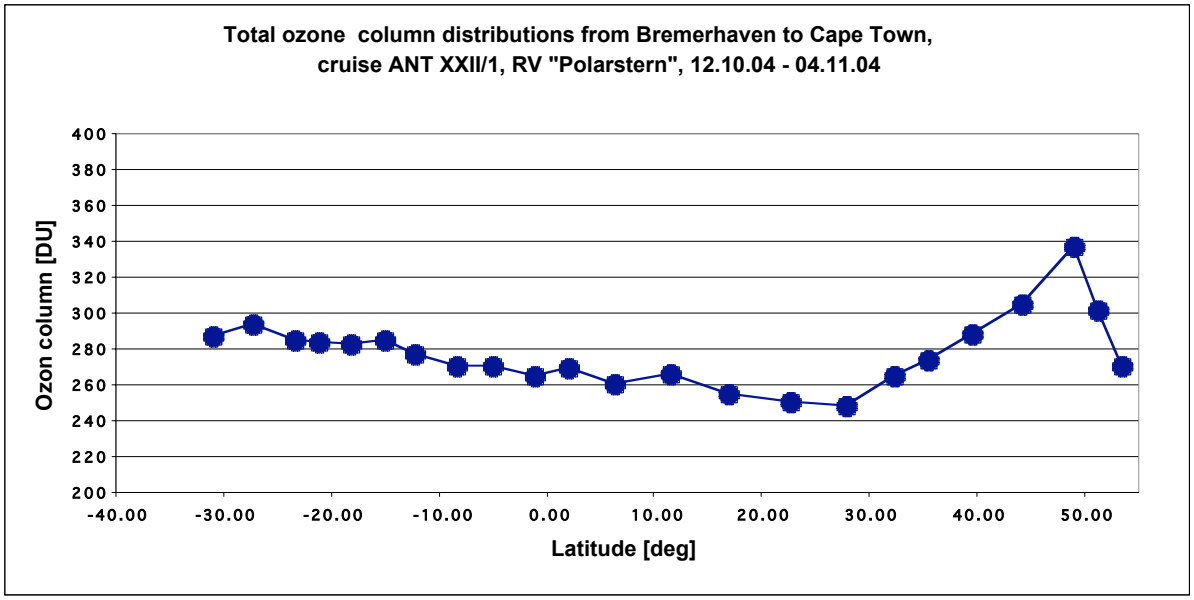

Fig. 10.2: Ozone column distribution between Bremerhaven and Cape Town during ANT-XXII/1

11. METEOROLOGICAL CONDITIONS

Hartmut Sonnabend, Thorsten Truscheit
Deutscher Wetterdienst/DWD Hamburg

As scheduled RV *Polarstern* left the harbour of Bremerhaven on 12 October at 1 p.m. with clear and sunny weather conditions. Soon after having reached the mouth of river Weser and the German Bight, the wind increased rapidly from south-easterly directions, reaching forces up to 7 to 8 Beaufort at times. The reason for this was a relative great difference of air pressure of about 35 hecto Pascal (hPa) between a strong high centred over the Baltic states and a flat low over the English Channel. The development of significant sea however was prevented by the nearby coast-line.

These conditions changed when RV *Polarstern* reached the western part of the English Channel and later on the Gulf of Biscay. Induced by strong westerly to north-westerly winds and gales at the south-western flank of a strong low pressure-system centred over England and Scotland the sea rose up to 6 to 7 meters at times. This made cruising uncomfortable due to heavy pitching of the ship for a while.

After having passed Cape Finisterre, the north-western tip of Spain, weather and sea conditions improved temporarily under the influence of a weak ridge. A Hydrosweep-Station on 17 October near 35°N was carried out without problems.

A new depression, that tracked from the sea-areas southwest of the Acores towards Cape Finisterre, affected RV *Polarstern* from the following night until morning of 18

October with strong southerly to south-westerly winds up to 7 to 8 Beaufort associated with a wave-maximum of 3 to 4 meters.

Approaching the island of Gran Canaria, weather conditions improved quickly. The wind became very light in the lee of the mountains but got a sudden increase near the south-eastern edge of the island. Within a few minutes the wind gusted up to wind force 7 to 8 Beaufort from southwest and calmed down to normal conditions soon after RV *Polarstern* had passed the island.

The trade wind set in after having passed 25°N. With wind forces around 6 Beaufort from northerly to north-north-easterly directions the trade-wind reached his maximum along the coastline of Mauretania. After the very short duration of only two days, the trade wind flow into the circulation of a flat low over the coastal areas west of Cape Verde.

The wind shifted to westerly directions and became very light. The water temperatures along the cruise line of RV *Polarstern* reached 29°C off Cape Verde and rose up to a preliminary maximum of 30.2°C near 10°N. Between 9° and 8°N RV *Polarstern* reached the Intertropical Convergence Zone (ITCZ). Within its northern most convective cloud band some light to moderate rain showers, associated with a short thunderstorm were observed from morning until noon of 23 October. Another water temperature-maximum of 30.4°C was measured at 5.7°N. The second convective cloud band along the latitude of 4°N affected RV *Polarstern* with a short rain shower in the early morning of the following day. This southernmost ITCZ-line marked the change to the South Atlantic trade-wind-sphere. Water temperatures dropped down to 25.0°C at the equator.

Between the large subtropical anticyclone, located along the latitude of around 30°S with a wedge extending towards the sea areas of Ascension Island and a nearly stationary trough along the coasts of Angola and Namibia, the following days the trade wind blew predominantly moderate to fresh from south-easterly directions. Along the heading line of RV *Polarstern* towards 10°S clear and sunny periods changed with cloudy intervals and some light rain showers. South of this line RV *Polarstern* encountered large areas of strati-form low clouds which had formed below the well defined trade wind inversion. For several days overcast to broken cloud conditions predominated, interrupted by only brief intervals of fair weather around noon or in the early afternoon.

After RV *Polarstern* had passed the latitude of 20°S the wind increased gradually up to force 5 to 6 and gusts near 7 Beaufort at times, associated with rough seas around 3 meters. On 2 November, after all, the cloud cover broke up to mainly sunny weather in the lee of Namibia. Sunshine, strong southerly winds with forces around 6 Beaufort and wave heights between 2.5 and 3 meters persisted also through 3 November, the last day at sea of this cruise. In the morning of 4 November 2006 RV *Polarstern* entered the harbour of Cape Town.

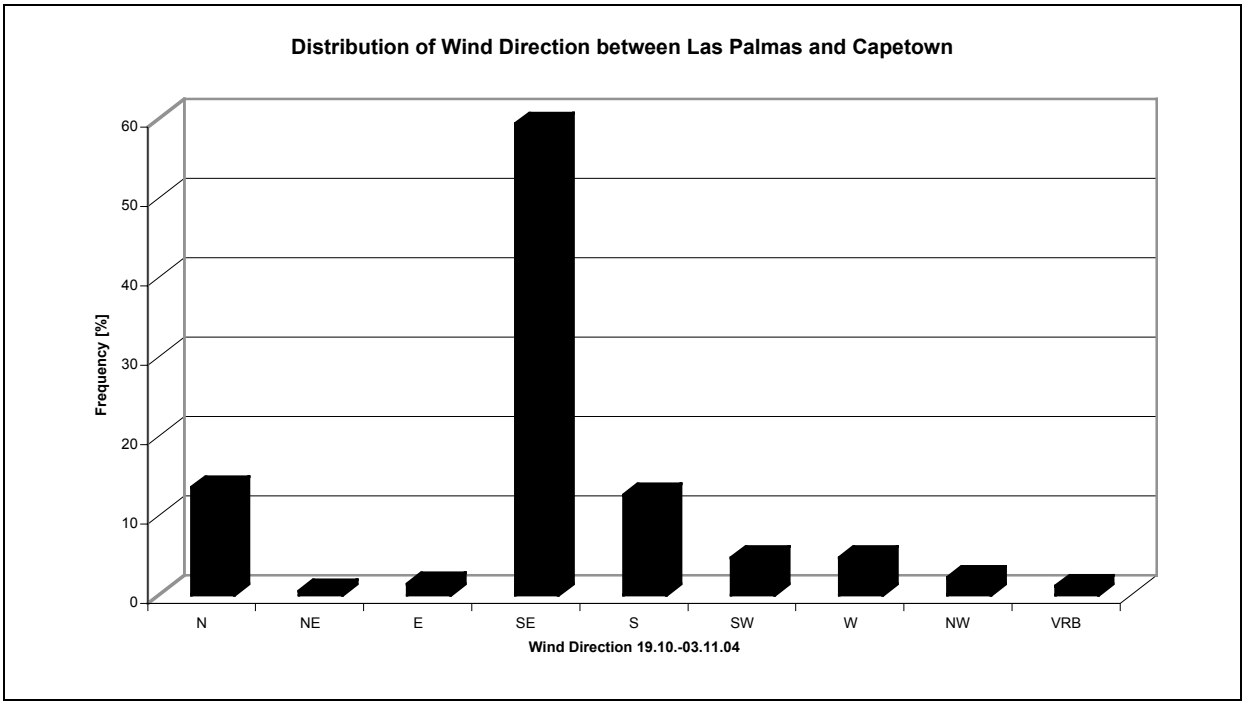

Fig. 11.1:Distribution of wind direction during ANT-XXII/1

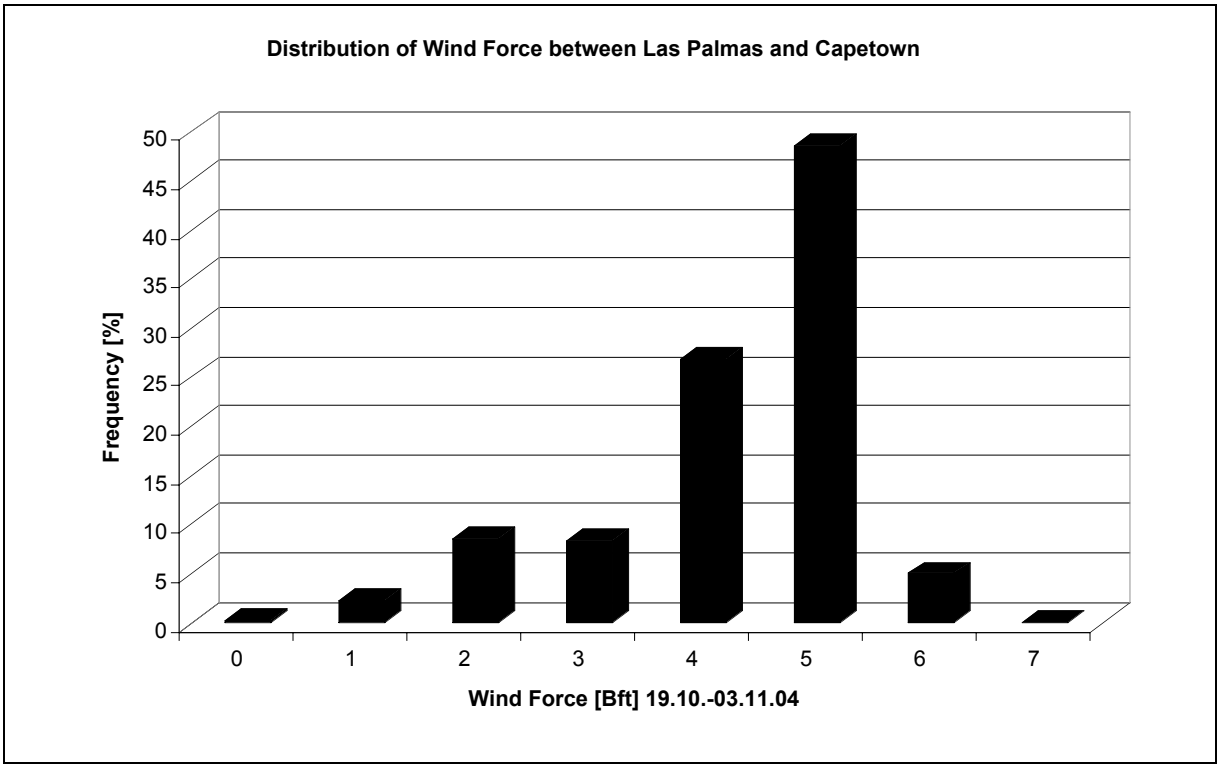

Fig. 11.2: Wind forces distribution during ANT-XXII/1

12. PARTICIPATING INSTITUTES ANT-XXII/1

Atlas Hydrographic	Atlas Hydrographic GmbH Kurfürstenallee 130 28211 Bremen
AWI	Alfred-Wegener-Institut für Polar- und Meeresforschung in der Helmholtz-Gemeinschaft Postfach 120161 27515 Bremerhaven
DWD	Deutscher Wetterdienst Hamburg Abteilung Seeschifffahrt Bernhard-Nocht Str. 76 20359 Hamburg Germany
FIELAX	FIELAX Gesellschaft für wissenschaftliche Datenverarbeitung mbH Schiffer-Str. 10 - 14 27568 Bremerhaven
IfBM	Inst. f. Biogeochemie u. Meereschemie Universität Hamburg Bundesstraße 55 20149 Hamburg
IfM-GEOMAR	Leibniz-Institut für Meereswissenschaften an der Universität Kiel Düsternbrooker Weg 20 24105 Kiel
IUP	Institut für Umweltphysik Universität Heidelberg Im Neuenheimer Feld 229 69120 Heidelberg
LAEISZ	Reederei F. Laeisz Bremerhaven GmbH Brückenstr. 25 27568 Bremerhaven

13. CRUISE PARTICIPANTS

Name	Institute
El Naggar, Saad	AWI
Fiedler, Björn	IfM-GEOMAR
Köhler, Hayo	IfBM
Niederjasper, Fred	AWI
Sinreich, Roman	Uni Heidelberg
Sonnabend, Hartmut	DWD
Spitzy, Alejandro	IfBM
Truscheit, Thorsten	DWD
Ewert, Jörn	Atlas Hydrographic
Kuhn, Gerd	AWI
Niessen, Frank	AWI
Pfeiffenberger, Hans	AWI
Wübber, Chresten	AWI

14. SHIP'S CREW

No.	Name	Rank
01.	Pahl, Uwe	Master
02.	Schwarze, Stefan	1.Offc.
03.	Schulz, Volker	Ch.Eng.
04.	Spielke, Steffen	2.Offc.
05.	Bratz, Herbert	3.Offc.
06.	Koch, Georg	R.Offc.
07.	Erreth, Gyula	1.Eng.
08.	Kotnik, Herbert	2.Eng.
09.	Simon, Wolfgang	2.Eng.
10.	Holtz, Hartmut	Elec.Tech.
11.	Nasis, Ilias	Electron.
12.	Verhoeven, Roger	Electron.
13.	Kahrs, Thomas	Fielax-Elo
14.	Clasen, Burkhard	Boatsw.
15.	Neisner,Winfried	Carpenter
16.	Kreis, Reinhard	A.B.
17.	Schultz, Ottomar	A.B.
18.	Burzan, G.-Ekkehard	A.B.
19.	Schröder, Norbert	A.B.
20.	Moser, Siegfried	A.B.
21.	Pousada Martinez, S.	A.B.
22.	Hartwig-Labahn, A.	A.B.
23.	Niehusen, Arne	Apprent.
24.	Beth, Detlef	Storekeep.
25.	Toeltl, Siegfried	Mot-man
26.	Fritz, Günter	Mot-man
27.	Krösche, Eckard	Mot-man
28.	Dinse, Horst	Mot-man
29.	Scholl, Christoph	Apprent.
30.	Fischer, Matthias	Cook
31.	Tupy,Mario	Cooksmate
32.	Martens, Michael	Cooksmate
33.	Dinse, Petra	1.Stwdess
34.	Schöndorfer	Stwdss/KS
35.	Streit, Christina	2.Stwdess
36.	Schmidt,Maria	2.Stwdess
37.	Schmutzler, Gudrun	2.Stwdess
38.	Tu, Jian Min	2.Steward
39.	Wu, Chi Lung	2.Steward
40.	Yu, Chung Leung	Laundrym.

Additional crew members:

Gerchow, Peter FIELAX
Hoffmann, Mathias FIELAX
Dimmler, Werner FIELAX

ANT-XXII/2

6 November 2004 - 19 January 2005

Cape Town - Cape Town

Ice Station POLarstern (ISPOL)

Fahrtleiter/ Chief Scientist:
Prof. Dr. M. Spindler

Koordinator / Coordinator:
Prof. Dr. P. Lemke

Report compiled by
Dr. G. Dieckmann, Dr. C. Haas and Dr. M. Schröder

CONTENTS

1. FAHRTVERLAUF UND ZUSAMMENFASSUNG

Christian Haas
Alfred Wegener Institute

1. Einleitung und Fahrtverlauf

Das Weddellmeer ist eines der wenigen Gebiete im Südpolarmeer, das ganzjährig von Meereis bedeckt ist. Frühere FS *Polarstern*-Expeditionen haben eine ausgeprägte Schichtung des Eises mit einer hohen Algen-Biomasse in den oberen Schichten gezeigt, die auf die große Rolle des Meereises für die Primärproduktion und den Kohlenstoffkreislauf hinweisen. Im November 2004 fuhr FS *Polarstern* in das Weddellmeer, um die Rolle des Meereises während der Eisdriftstation ISPOL („Ice Station POLarstern“) weiter zu untersuchen. An diesem multidisziplinären Projekt waren führende Wissenschaftler aus acht Ländern beteiligt, mit dem Ziel, unser Verständnis der physikalisch-biologischen Prozesse im Meereis während der frühsommerlichen Schmelzperiode zu verbessern. Das wesentliche Ziel von ISPOL waren meteorologische, glaziologische, biologische, chemische und ozeanographische Messungen auf einer Eisscholle während einer fünfwöchigen Driftstation.

FS *Polarstern* verließ Kapstadt am Abend des 6. November 2004. Bereits am 9. November wurden auf einer Breite von 45°S die ersten Eisberge gesichtet. Am 10. November wurde in der Nähe der Bouvetinsel einem nahenden, schweren Sturm ausgewichen (Kapitel 2.1). Die Eiskante wurde am Abend des 13. November bei ca. 58°S, 15°W erreicht. Schon am nächsten Tag wurde die erste biologische/glaziologische Eisstation durchgeführt (Kapitel 3). Mit weiteren, täglichen Eisstationen bis zum Erreichen der ISPOL-Scholle konnte somit bereits während der Anfahrt ein Profil der Eiseigenschaften quer durchs Weddellmeer vermessen werden. Das Schiff stoppte nur ein einziges Mal bei 65°37.6’S, 36°29.4’W, um eine CTD-Station durchzuführen. Diese Stelle wurde bereits in der Vergangenheit mehrfach untersucht (Kapitel 5.1). Bis zum 22. November waren die Eisverhältnisse einfach, so dass das Schiff gut vorankam. Allerdings zeigten Satelliten-Radardaten, die zusammen mit der Europäischen Raumfahrtagentur ESA und dem Deutschen Zentrum für Luft- und Raumfahrt DLR in Echtzeit am Schiff empfangen wurden, dass im geplanten Untersuchungsgebiet bei 70°S, 55°W sehr schwere Eisbedingungen herrschten. Deshalb wurde eine westlichere Route eingeschlagen, und ein weiter nördlich liegendes Gebiet angesteuert. Am 25. November begann per Hubschrauber die Suche nach einer geeigneten Eisscholle. Bei zahlreichen Landungen wurden Dickenbohrungen durchgeführt, die allesamt sehr dickes Eis zeigten. Deshalb wurde die Suche zwei weitere Tage lang fortgesetzt. Erst als das Schiff in dem dicken Eis kaum mehr vorankam, wurde schließlich eine Scholle ausgewählt. Am 27. November wurde Dicke und Art der Scholle an mehreren Stellen von einem internationalen Team untersucht, und man war sich einig, die ideale Scholle gefunden zu haben (Abb. 1.2).

In den nächsten fünf Wochen war das Schiff fest mit der Scholle verankert, um biologische, chemische, glaziologische, meteorologische und ozeanographische Messungen in der Luft, dem Eis, und um Wasser durchzuführen. Während dieser

Zeit driftete die Eisscholle 98 km nach Norden (Abb. 1.1 und Kapitel 5.3). Eisdickenmessungen zeigten, dass das Untersuchungsgebiet im Wesentlichen aus zwei unterschiedlichen Eisregimen bestand: zwei bis vier Meter dickes zweijähriges Eis mit einer bis zu einem Meter dicken Schneeauflage im Westen und Osten, und dazwischen ein sich nord-süd erstreckendes Band dünnerem einjährigen Eises. Aus Satellitenbildern wurde geschlossen, dass dieses Eis aus einer Polynja vor dem Ronne-Schelfeis kam, und seit März 2004 fast 1000 km in das ISPOL-Untersuchungsgebiet gedriftet ist.

Trotz der frühsommerlichen Bedingungen und der niedrigen Breite von 67°30'S nahm die Eis- und Schneedicke im Untersuchungszeitraum nur um 20 bis 30 Zentimeter ab. Dies lag an den geringen atmosphärischen und ozeanischen Wärmeflüssen von wenigen Watt pro Quadratmeter, die nur zu einer geringen Erwärmung des Eises auf -2 bis -1°C führten. Dadurch erhöhte sich allerdings die Porosität des Eises erheblich, so dass der Austausch klimarelevanter Gase wie Kohlendioxid (CO_2) und Dimethyl-Sulfid (DMS) zwischen Ozean und Atmosphäre stark zunahm, sogar ohne stark erhöhtes Algenwachstum im Eis. Das beobachtete Algenwachstum reichte allerdings aus, um als Futter für große Krillschwärme unter dem Eis zu dienen. Die großen Mengen Krill führten zu einem ständigen Fluss gelösten und partikulären Kohlenstoffs in die Wassersäule.

Messungen der Temperatur- und Salzschichtung im Wasser wurden mit einer neuentwickelten Hubschrauber-CTD-Sonde durchgeführt. Die Messungen zeigten, dass das Bodenwasser im Umkreis von 60 Nautischen Meilen um FS *Polarstern* herum 0.5° C kälter war als bei der 1992 im selben Gebiet durchgeführten russisch/amerikanischen *Ice-Station-Weddell ISW-1*. Spurenstoffuntersuchungen konnten erstmals zeigen, dass dieses Bodenwasser vom benachbarten Larsen-C Eisschelf stammte und während eines sporadischen Ereignisses den Kontinentalhang hinabgeflossen ist. Während der Drift nahm der Salzgehalt der Deckschicht nur geringfügig ab, was auf laterales Schmelzen von Eisschollen und Eisbruchstücken in Rinnen offenen Wassers zurückzuführen ist.

Während der Drift zerbrach die ISPOL-Scholle zweimal, am 2. und 25. Dezember. Die Arbeiten wurden dadurch jedoch kaum behindert. Leider musste FS *Polarstern* schon am 2. Januar 2005 die Eisscholle verlassen. Nach drei Tagen schwerer Eisfahrt in zweijährigem Eis erreichte FS *Polarstern* die Eiskante am frühen Morgen des 5. Januars bei ca. 65°S und 54.8°W. Wegen dichten Nebels und zahlreichen Eisbergen war die Fahrt jedoch weiterhin schwierig. Am 9. Januar wurde Grytviken auf Südgeorgien für ein paar Stunden angesteuert. ANT-XXII/2 endete am 19. Januar in Kapstadt.

ISPOL/ANT-XXII/2 wurde von Gerhard Dieckmann, Christian Haas, Hartmut Hellmer und Mike Schröder vom AWI koordiniert. Der Fahrtleiter war Professor Michael Spindler vom Institut für Polarökologie in Kiel (IPOE). Berichte, Daten und wissenschaftliche Veröffentlichungen von ISPOL werden auf der Internetseite http://www.ispol.de gesammelt und zur Verfügung gestellt.

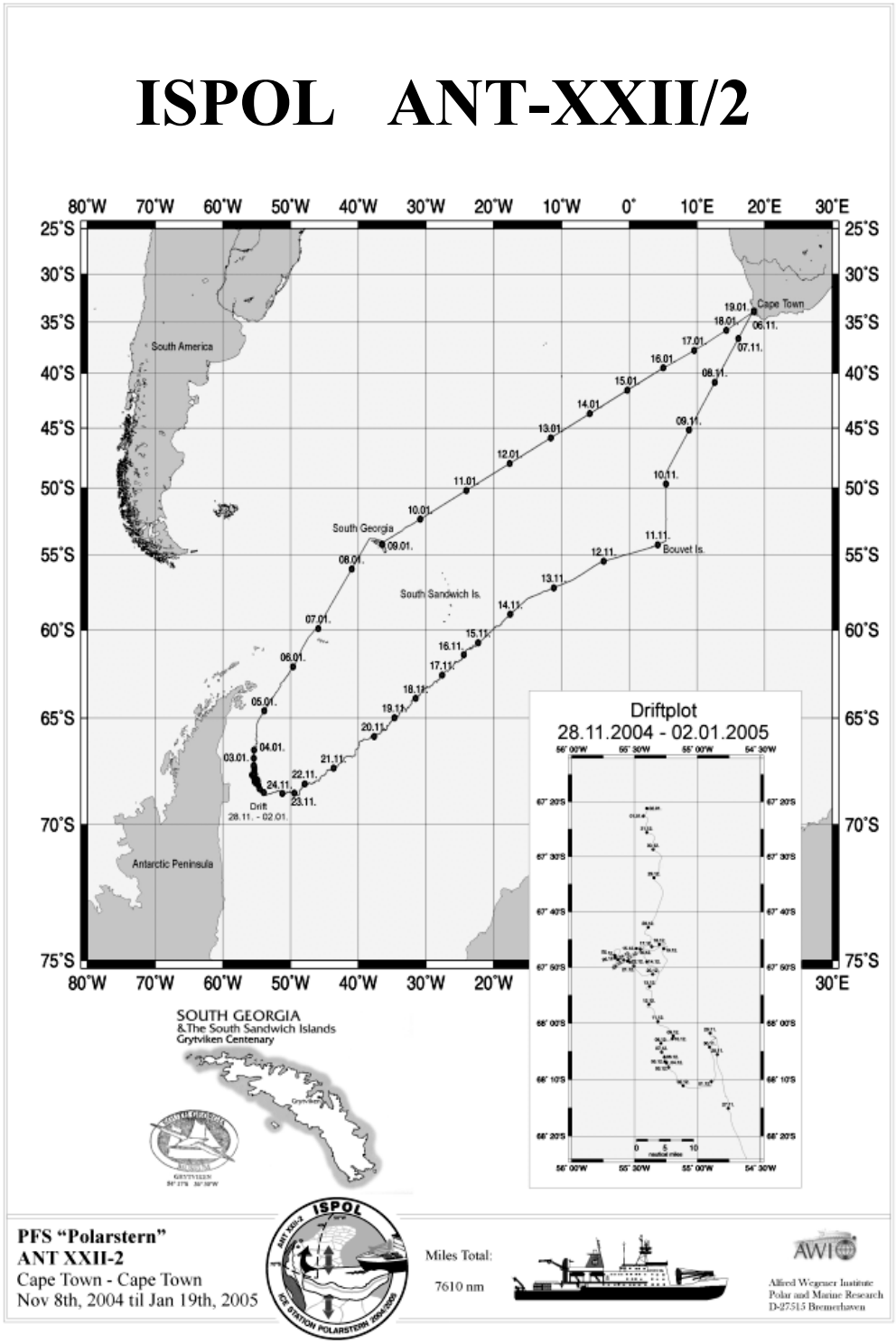

Abb. 1.1: Karte des Südatlantiks und des Weddellmeeres mit der Polarstern Fahrtroute während ANT-XXII/2 und der ISPOL-Drift
Fig. 1.1: Map of the South Atlantic Ocean and Weddell Sea, showing the ANT-XXII/2 cruise track and ISPOL drift

CRUISE NARRATIVE AND SUMMARY

The western Weddell Sea is one of the few regions of the Southern Ocean covered by perennial sea ice. Earlier RV *Polarstern* expeditions have shown a strong layering of the ice with high algal standing stocks, suggesting that the ice plays an important role for primary production and the carbon cycle (Fig. 1.1). In November 2004, RV *Polarstern* headed towards the Weddell Sea to conduct the Ice Station POLarstern (ISPOL) experiment. This multidisciplinary project involved leading scientists from eight countries to improve our understanding of physical-biological processes during the sea ice melting season. The main task of ISPOL were atmospheric, glaciological, biological, chemical, and oceanographic observations on an ice floe during a five week long drift station.

RV *Polarstern* left Cape Town in the evening of 6 November 2004. First icebergs were already sighted at approximately 45°S, on 9 November. A severe storm system close to Bouvet Island was circumvented by a small detour in the vicinity of the island on 10 November (Section 2.1). The ice edge was reached in the evening of 13 November at approximately 58°S 15°W. The first biology/geophysics ice station was already performed on the next day (Section 3), and continued once every day until the station floe was reached. The only other scientific station before the main ice station work was a CTD cast at 65°37,6‘S 36°29,4‘W, a location which has been studied during numerous earlier cruises as well (Section 5.1). Ice conditions were mostly favourable, and the ship made good progress until 22 November. Satellite SAR imagery provided by the European Space Agency (ESA) and German Aerospace Center (DLR) revealed severe ice in the originally planned study region at 70°S 55°W. Therefore a more westerly route was chosen. On 25 November search for the station floe commenced by helicopter. Ice thickness measurements were carried out on several floes, all showing very thick ice. Therefore, the search continued for 2 more days. Only when the ship made hardly any more progress in the very thick ice regime, an ice floe was finally chosen. On 27 November an international team sampled the ice thickness at several places and finally agreed that this was a good floe (Fig. 1.2).

For the following five weeks the ship was anchored to the floe to conduct biological, chemical, glaciological, meteorological, and oceanographic measurements in the air, ice, and water. During the experiment, the floe drifted 98 kilometers to the north (Fig. 1.1 and Section 5.3). Ice thickness measurements showed the presence of two major ice regimes in the study region: two to four meter thick second year ice to the west and east covered by up to one meter of snow, and a south-north extending band of thinner first-year ice in between. Satellite imagery revealed that this ice originated from the Ronne polynya, and has drifted almost 1000 kilometres into the study region.

Despite spring/summer conditions and the high southern latitude of 67°30'S, ice and snow thickness only decreased by 20 to 30 centimetres. Low atmospheric and oceanic heat fluxes of a few Watts per square meter lead to warming of the ice to –2 to –1°C, resulting in increases of ice porosity. Chemical measurements showed that this increased the exchange of climatically relevant gases like carbon dioxide (CO_2) and dimethyl-sulfide (DMS) between ocean and atmosphere, even at low increases of algal growth. However, increased algal growth did support large swarms of krill feeding under the ice, and resulted in a continuous flux of dissolved and particulate carbon into the water.

Observations of vertical temperature and salinity distributions in the water column were performed by means of a new CTD probe deployable by helicopter. Within a region of 60 nautical miles around the RV *Polarstern* drift track, the bottom water was 0.5°C colder than observed during the similar Russian-American drift experiment ISW-1 in 1992. Tracer analysis showed for the first time that this water originated from the neighbouring Larsen-C Ice Shelf, and has flown down the continental slope in a sporadic event. During the drift period, surface water salinity decreased only slightly, mainly due to lateral melting of ice floes and brash ice in leads.

The station floe fractured twice during the observation period, on 2 December and 25 December, but with little consequences for the scientific programme. Unfortunately, the long-term RV *Polarstern* schedule required a completion of the study on 2 January 2005.

After 3 more days of heavy ice breaking in the outflow regime of old ice, RV *Polarstern* reached the ice edge in the early morning of 5 January at approximately 65°S and 54.8°W. Navigation was still difficult, as there was dense fog and many icebergs. On 9 January *Grytviken* on the island of South Georgia was visited for a few hours. ANT-XXII/2 ended in the late morning of 19 January in Cape Town.

ISPOL/ANT-XXII/2 was coordinated by Gerhard Dieckmann, Christian Haas, Hartmut Hellmer, and Mike Schroeder from the Alfred Wegener Institute. The cruise leader was Professor Michael Spindler from Institute for Polar Ecology, Kiel (IPOE). A web site has been established at http://www.ispol.de, serving as the main communication platform after the cruise, and as a joint site for the collection of data and results.

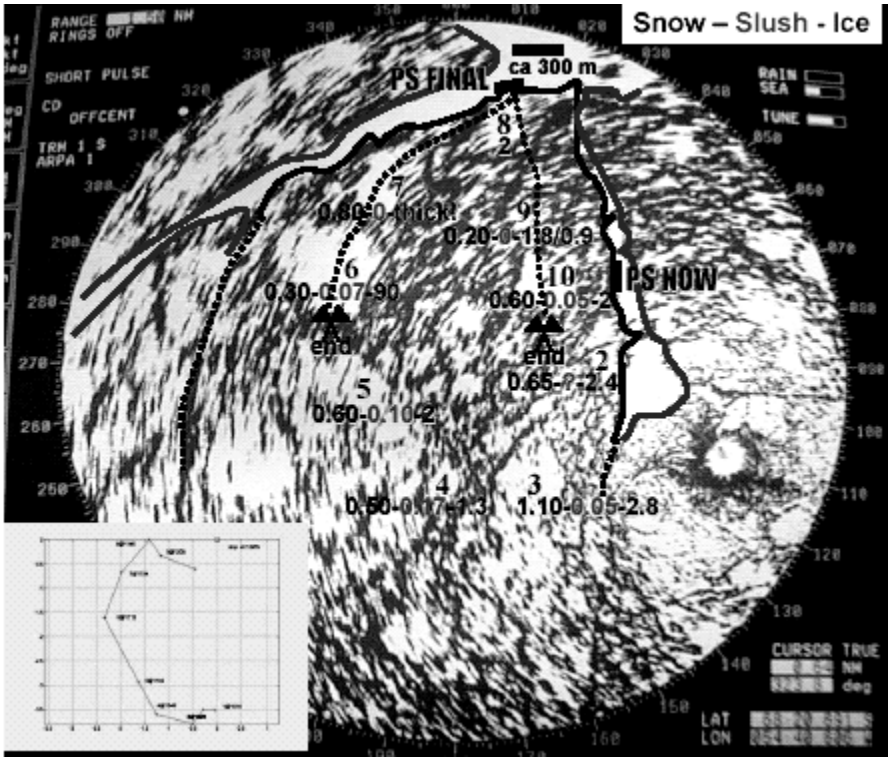

Abb. 1.2: Schiffs-Radarbild der ISPOL-Scholle am 27. November 2004. Die Zahlen zeigen die Ergebnisse der Erkundungs-Eisdickenbohrungen prominenter Flächen ebenen Eises, die als wesentliche Untersuchungsgebiete ausgewählt wurden.
Fig. 1.2: Radar screen shot of the ISPOL station floe on 27 November 2004. Numbers show the results of reconnaissance drill-hole measurements of prominent level ice areas which were chosen as the main sampling sites.

2. METEOROLOGY

2.1 General weather conditions during ANT-XXII/2

Karl-Heinz Bock, Klaus Buldt (not on board), Rüdiger Hartig
Deutscher Wetterdienst, Hamburg

RV *Polarstern* left Cape Town on the evening of 6 November, 2004 sailing southwest, bound to the Antarctic. The cruise started at fair skies and fresh westerly breeze. These conditions occurred in the transition zone between weakening subtropical high and strengthening zonal west drift. On 9 November a line of instability crossed RV *Polarstern*, increasing the wind to “near gale” from northeast. Around 45°S the first iceberg was observed and the temperature dropped to 4°C.

As the numerical forecast showed the development of a violent storm crossing the route on 12 November (Fig. 2.1), the course was altered to south and southwest. Due to this change RV *Polarstern* avoided contact with the “hurricane like winds”.

Fig. 2.1: NOAA AVHRR visible channel image of 12 November showing development of strong cyclone in the planned cruise track of RV Polarstern

RV Polarstern reached the sea ice edge on 14 November, still north of 60°S. In the vicinity of a high pressure system over Scotia Sea moderate westerly winds prevailed until 18 November, while several Weddell Sea depressions sent their clouds temporarily into the working area. The first intensive cyclogenesis occurred west of the Antarctic Peninsula on 18 November. A secondary low developed the following night, moved eastward and intensified. It hit the *RV Polarstern* on 19 and 20 November and with southwest “near gale” to “gale” and gusts up to 50 kn.

The general atmospheric circulation with shallow depressions west of the Antarctic Peninsula and small scale secondary lows east of the Antarctic Peninsula continued until 28 November. During this period a moderate to fresh breeze from south and southeast prevailed. The flight conditions were more or less bad, due to overcast skies, occasional snowfall and moderate contrast.

RV Polarstern reached the ISPOL drift station at approx. 68°S 50°W on 27 November. From that day on until 2 January the vessel drifted, attached to an ice floe chosen for the scientific work, across the Weddell Sea.

At the end of November a high pressure ridge, extending from the Falklands/Malvinas into the Weddell Sea, determined the weather. For two days there were nearly sky clear conditions, although the maximum air pressure reached only 1007 hPa in the ISPOL area. December started with cyclonic activity. A passing cold front terminated the high pressure influence. On the following days several small scale depressions developed at the tip of the Antarctic Peninsula and moved humid and mild maritime air into the ISPOL region. Thus, low stratus, occasional snow and temperatures between –3° C und 0° C prevailed. Caused by weak pressure gradients around the Antarctic Peninsula, the wind had been below force 4 Bft for nearly 3 weeks. The radio soundings confirmed weak to moderate winds up to high levels. From mid of December high pressure, extending from the continent to the Weddell Sea and the Antarctic Peninsula, ruled the weather again. In dry air multiple long-distance flights were carried out. Even in this dry air, low stratus and shallow fog occurred twice surprisingly.

The next major development of a cyclone started on 22 December in the western parts of the Drake Passage. Weather stations on King George Island observed wind from northeast with “gale” force, while in the ISPOL area wind reached only force 4-5 Bft from east. Precipitation during this period was mainly bound to the western and north-western slopes of the Antarctic Peninsula. In the ISPOL area it was remarkably low, only 5.8 mm of precipitation were observed during the drift period between 27 November 2004 and 2 January 2005 with the onboard instrumentation.

A secondary low located at the tip on the Antarctic Peninsula on 26 December intensified to a well developed cyclone on 27 and 28 December. It turned the wind flow to northwest and north, adding wet unstable air and causing intensification into a storm cyclone centred over the central Weddell Sea. The storm turned the wind to west, later to southwest and south with average force of 7 Bft and gusts of 8 Bft in the ISPOL working area. When the frontal zone passed by freezing rain occurred for a short period. Unsettled weather ruled the following days. Poor visibility and friendly periods with sufficient flight conditions changed more or less daily. An analysis of the conditions of changing visibility is displayed in figures 2.5 and 2.6.

Dense sea ice with numerous high ridges delayed the cruise towards South Georgia. Reaching the ice-free waters on 4/5 January visibility deteriorated rapidly and “coldwater fog” formed. This is explained by condensation in humid air, coming in from the Drake Passage and cooled down by the cold sea water (-1 to –1.5°C) near South Georgia. With rising water temperatures to the north, visibility increased again. Two cold fronts, combined with showers and reduced visibility, crossed *RV Polarstern* on its northbound course.

The return journey from South Georgia to Cape Town started on 9 January with north-westerly winds force 5 to 7 Bft and mostly cloudy skies. On 11 January another storm cyclone developed near 60°S 15°W. It moved eastward and the pressure in its centre dropped to 956 hPa. At the same time a subtropic high ruled north of 40°S. Both systems produced a pressure gradient greater 50 hPa between 40°S and 60°S. So the wind reached force 8-9 Bft with gusts force 10 Bft on 12 January. The very next day the wind decreased to force 6 Bft. South of 60°S the storm cyclone intensified again and the pressure dropped to 944 hPa on 15 January. The attached frontal system reached far north into the cruise track of *RV Polarstern* and brought two days of dense clouds, poor visibility and periods of fog. Conditions increased on 16 January again. Fair weather prevailed for the rest of the journey, due to a stationary high pressure ridge over the eastern Atlantic.

a)

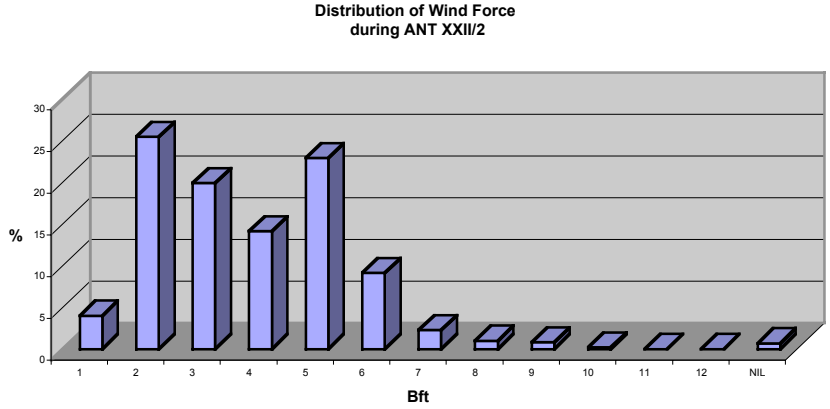

b)

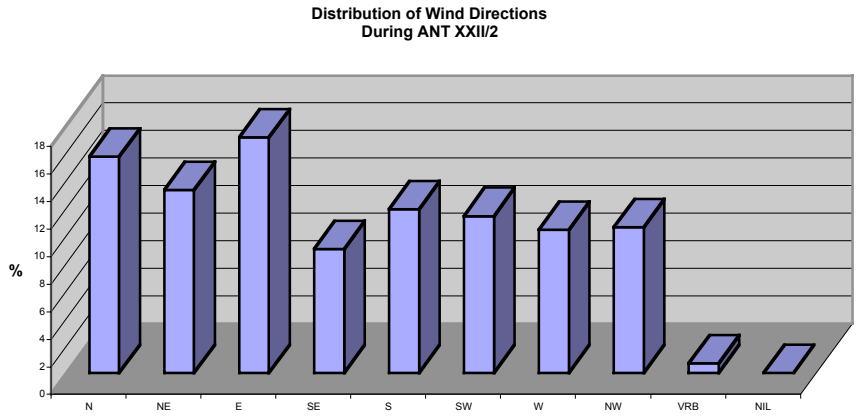

Fig. 2.2: Frequency distributions of wind speed (a) and direction (b) during ANT-XXII/2, including the transit and ISPOL drift periods, measured by the met station on board RV Polarstern

The wind conditions are displayed in figures 2.2 and 2.3 and the precipitation in figure 2.4.

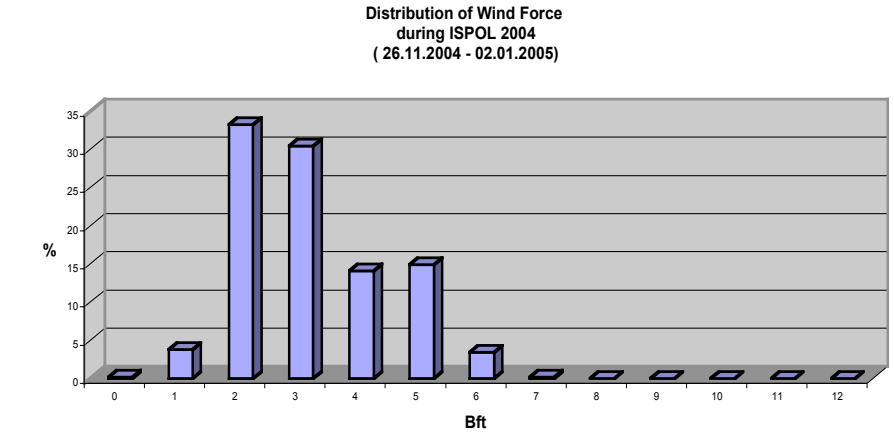

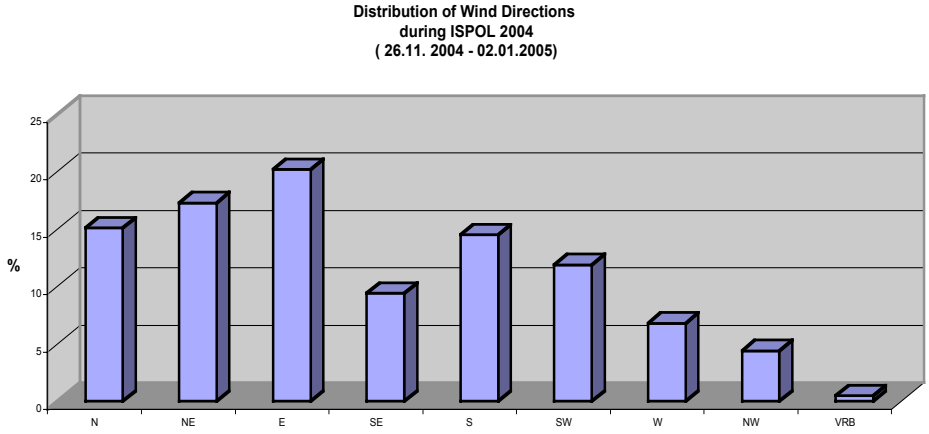

Fig. 2.3: Frequency distributions of wind speed (a) and direction (b) during the ISPOL drift period, measured by the met station on board RV Polarstern

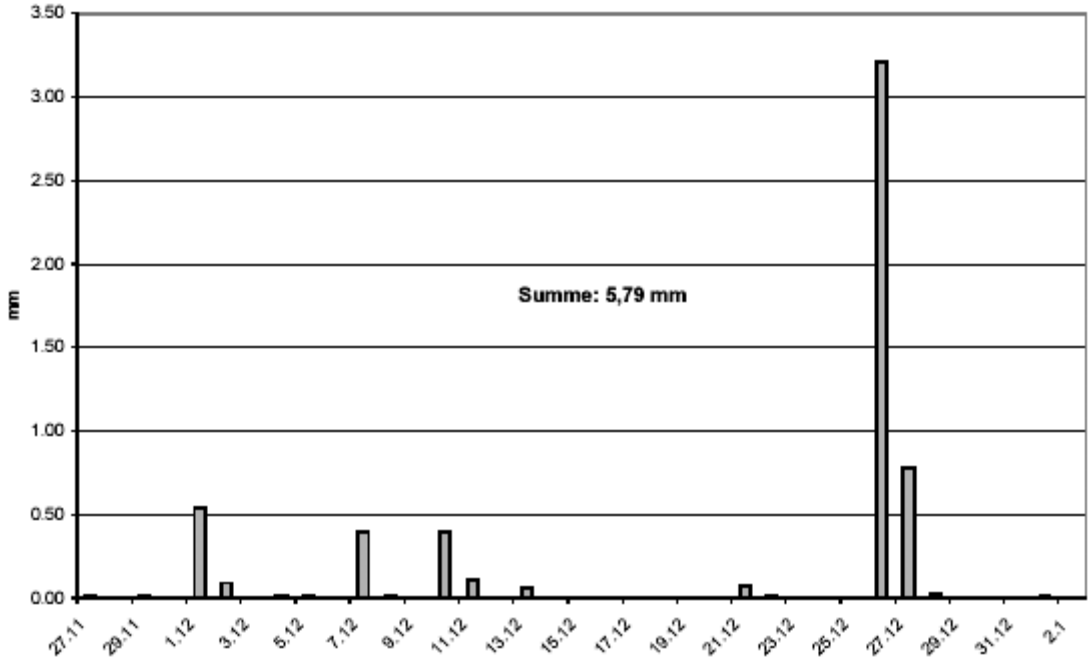

Fig. 2.4: Daily precipitation during ISPOL, measured by the met station on board RV Polarstern

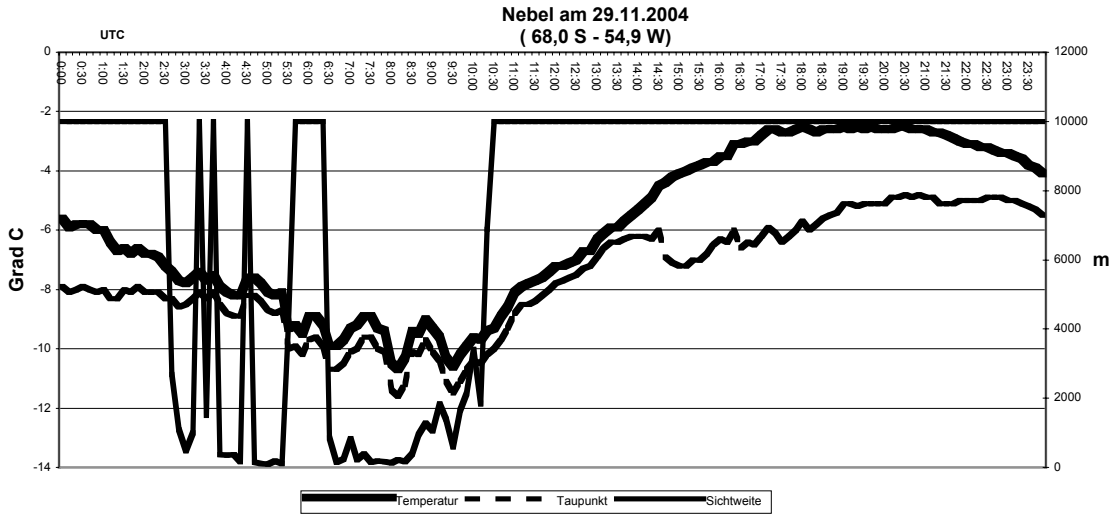

Fig. 2.5: Visibility, air temperature, and dew point during a fog event on 18 December causing major restrictions for airborne operations

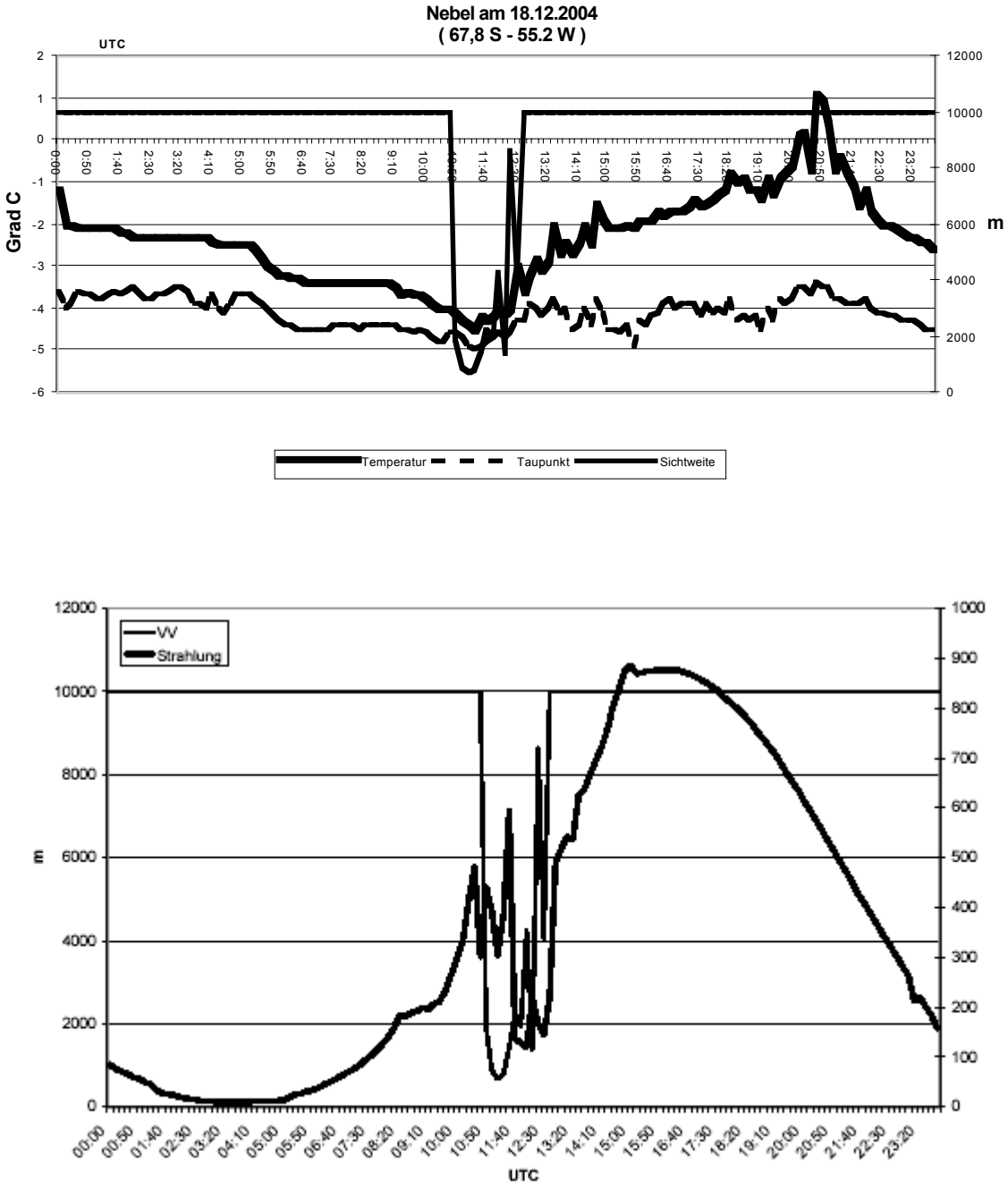

Fig. 2.6: Visibility, air temperature, dew point, and global radiation during a fog event on 18 December causing major restrictions for airborne operations

2.2 Meteorological conditions and surface fluxes and energy balance during ISPOL

Jouko Launiainen, Milla Johansson, Pekka Kosloff — Finnish Institute of Marine Research, Helsinki

2.2.1 Introduction and objectives

The FIMR group carried out measurements and studies of air-ice interaction during ISPOL. Those studies covered three main objectives as follows. The first was concerned with the air and ice/snow heat balance controlling the melting and freezing of snow and ice. The heat balance is composed from the shortwave and longwave (thermal) radiation balance, and the turbulent fluxes of sensible and latent heat. The second objective was related to the studies of wind and air-ice interaction in the turbulent atmospheric boundary layer and questions how those act as the driving force to the movement of sea ice. The third one was related to the albedo and irradiation (light) to snow and ice. The latter one is important also to biological processes because of light conditions affect, e.g. growth of sea ice algae and biota. Additionally, we participated in the international ISPOL ice drifter buoy array study.

In the measurements meteorological profile mast and air-ice turbulence masts, radiation stations and drifting satellite buoys were used. Some of the stations transmitted the data to the ship by cable, others by radio, and, the drifting buoys transmitted the data by the satellite system of cls. Argos.

2.2.2 Meteorological conditions

From late November 2004 up to early January 2005, the overall and synoptic meteorological conditions in the western Weddell Sea and ISPOL area were gentle. After the strong wind of the mean wind up to 23 m/s during the deep CTD- station (RV *Polarstern* 67-5) on 20 November 2004 in the northern central Weddell Sea any deep lows with high winds didn't occur in the western and south-western Weddell Sea and ISPOL area. On the eastern side of the Antarctic Peninsula and the Bellingshausen Sea large and deep lows used to exist frequently (data and information from the forecasts from ECMWF and the meteorological office of the Deutscher Wetterdienst onboard RV *Polarstern*). Just a couple of deep lows twisted from north via Drake Passage to the western Weddell, as they sometimes do. Accordingly, except a few days of moderate wind speed in the beginning and later December 2004, the surface wind velocity stayed as rather low of 2 to 6 m/s during the ISPOL ice camp period (Fig. 2.7a). Most frequently, the winds were from north to east (Fig. 2.7b), but they were strongest and warmest from northwest to north. The cold wind came over the high concentration sea ice fields in east or from the continent in south and southwest. From the west directly from the nearest Peninsula the winds were very few. The air temperature did not go below – 5°C, except in a few cases of cold advection and cases of surface inversion generated by radiation cooling in clear and calm nights. Generally, the air temperature used to stay just a few degrees below zero (Fig. 2.7c). Actually, the first week in December 2004 was the warmest in the period, daytime temperature around zero, and the daily variation in the air temperature above the ice and snow was of the order of 2°C or less.

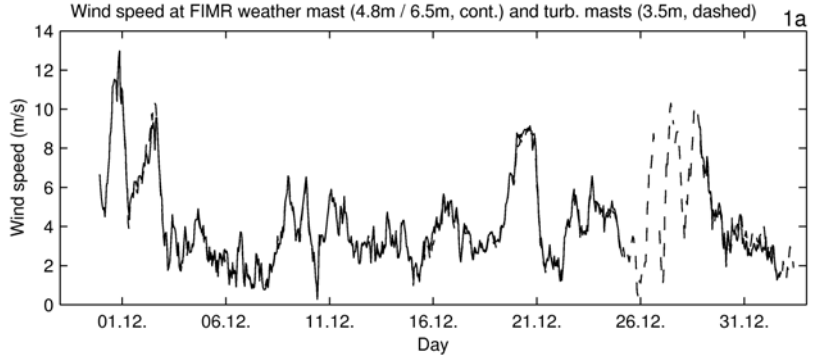

Fig. 2.7a: Wind speed during the ISPOL ice station (various FIMR stations of 3.5-6.5 m height)

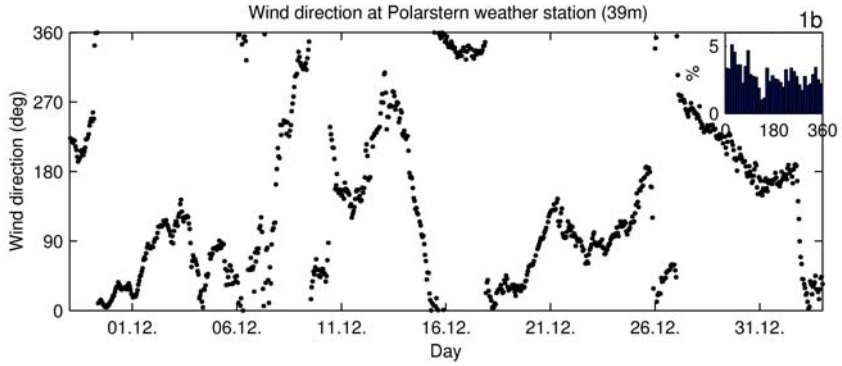

Fig. 2.7b: Wind direction during the ISPOL ice station (at RV Polarstern at 39 m)

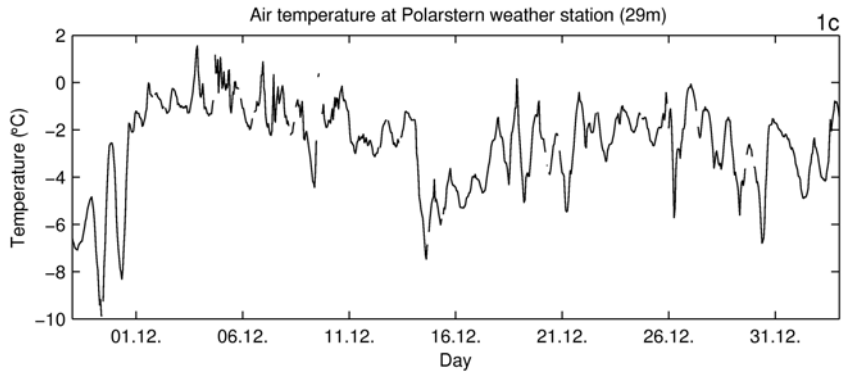

Fig. 2.7c: Air temperature during the ISPOL ice station (at RV Polarstern at 29 m)

2.2.3 Measurements

The main measurements consisted of a 10 m meteorological mast, two air-ice turbulence masts, two sets of all-components radiation measuring equipments, and three satellite drifting buoys and some other measurements completing the snow/ice studies. The observation quantities and methods are given in table 2.1. The measurement sites are given in the ISPOL station map. The ISPOL floe breakup on early 25 December faulted the meteorological mast. Additionally, one sonic anemometer and one of the radiation stations had to finish their functioning and another set of radiation stations was moved. All the times are given in UTC.

Table 2.1: Observations made in the FIMR surface fluxes and air-ice interaction studies

QUANTITY / METHOD	PARAMETERS	PERIOD	SAMPLING/ REGISTRAT -ION RATE	NOTES
				For sites, see the ISPOL-station map
Radiation station 1	All component short- and long-wave radiation	28 Nov - 25 Dec 2004	1 min.	Eppley PSP-sensors for short-wave (down/up), Eppley PIR for long-wave (down/up)
Radiation station 2	All component short- and long-wave radiation	1 Dec - 4 Dec 2004 17 Dec 2004 - 2 Jan 2005	1 min.	Kipp & Zonen pyranometers (CM1) and pyrgeometers (CG 1/2) 1 - 4. Dec 2004 K&Z-station in site of Radiometer station 1
Weather mast	Wind and air temp profile	29 Nov - 25 Dec 2004 28 Dec 2004 - 1 Jan 2005	10 min.	10 m high: 5 wind-, 3 temp-, 1 moist 6,5 m high: 3 wind-, 3 temp-, 1moist
Sonic anemometer 1 (Atm turb1)	Momentum and sensible heath flux air-ice turbulence characteristics	30 Nov – 25 Dec 2004	20 Hz (10 min)	Metek – USA1 in 3.6 m, rawdata + 10 min averages
Sonic anemometer 2 (Atm turb2)	Momentum and sensible heath flux air-ice turbulence	6 Dec –17 Dec 2004 18 Dec 2004 – 2 Jan 2005	20 Hz (10 min)	On buoy 52292 floe, 5-8 nm from ship On ISPOL floe (Metek – USA1, in 3.5 m)
Satellite drifters:				
ID 1154	GPS, air press, air temp, hull temp.	28 Nov 2004 -	1 h	Remained in the ISPOL area
ID 5892	GPS, air press, air temp, hull temp.	29 Nov 2004 -	1 h	Recovered and remained in the ISPOL floe on 2. Jan. 2005
ID 52292	GPS, air press, air temp, hull temp	4 Dec – 31 Dec 2004	1 h	Vast (1.5x2.5 nm) highly ridged (up to 3 m), thick (1.5 to 3...m) floe. Fluxes and air-ice turb measured on the flow
Snow density		1 Dec 2004 – 1 Jan 2005		
In-ice temperature	10 vert sensors, 2 sets			time series
Meteor. soundings	Wind, air temp, humidity			6 soundings from above sea ice

2.2.4 Preliminary results

2.2.4.1 Radiation

The time series of the global (shortwave) radiation is given in figure 2.8a. The highest (hourly) radiation exceeded 900 W/m^2, but during even the cloudy days the daytime highest shortwave radiation exceeded 400 – 500 W/m^2. In the time of just mid-summer any (clear sky) time trend cannot be detected or expected. Additionally, in the cooler latter half of the ISPOL period the incoming shortwave radiation was not lower than in the warmer first one.

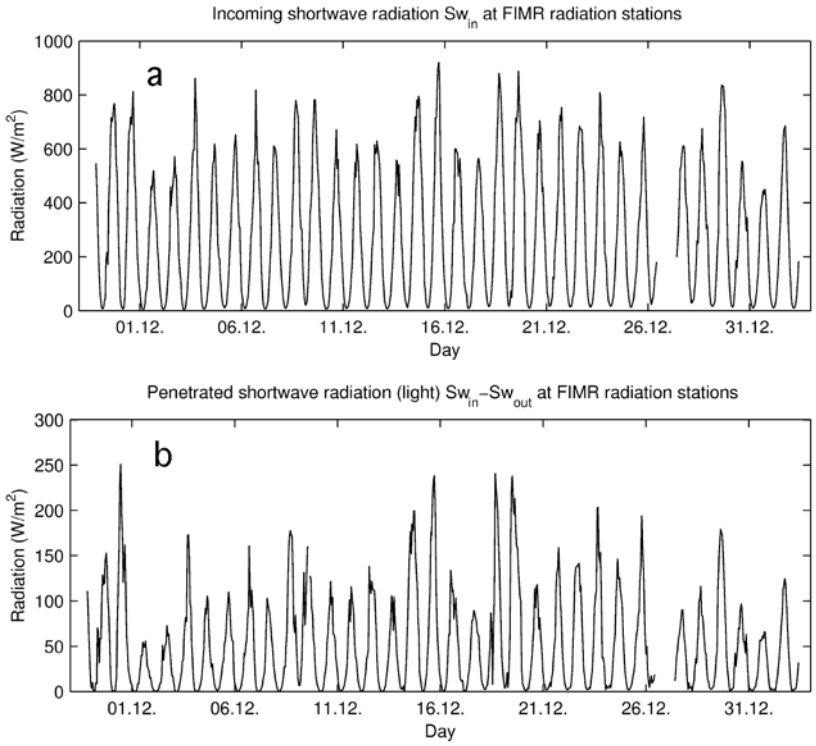

Fig. 2.8a: Global incoming radiation (W/m^2) at FIMR radiation stations during ISPOL
Fig. 2.8b: Shortwave radiation penetrated into snow and ice

The time development of the albedo is given in figure 2.9. The overall time development indicates a slightly decreasing trend. During 17 to 25 December 2004, the time series of the albedo in the two FIMR measuring sites overlap and were only very slightly different from each other. This was the case although e.g. the snow thickness in the sites was different (of 0.6 m and 0.15 m) and visually the snow surface in the places was somewhat different. In figure 2.9a the albedo is calculated for “significant” global radiation as the “effective” albedo, whereas figure 2.9b gives the albedo accompanied with all the hourly radiation fluxes. In the average, in the ISPOL period the albedo was gradually decreasing, from about 0.9 to 0.8 in our sites up to the period of 26 December. After this the station was moved in a new place and there the albedo was higher again. The small albedo decrease is reflected as a gradual progress of summer during ISPOL. Main reason of the small albedo was in the smooth clean snow and low air temperatures and occasional snowing and windblown snow whitening during the latter ISPOL period. We could not detect any diurnal albedo variation. Most probably, this was because of just a few days of clear sky and most of the global radiation was of diffuse radiation.

The time series of the amount of shortwave radiation penetrated into snow and ice is given in figure 2.8b, calculated as subtraction of the up-welling radiation from the down-welling one. The daily sums of the penetrated radiation in MJ/m^2 are given in table 2.2. Strictly, the results represent the FIMR measurement sites, but are appropriate as comparing the relative mutual time (e.g. daily) variations, as seen from the point of view of heat balance or light portions penetrated through the surface.

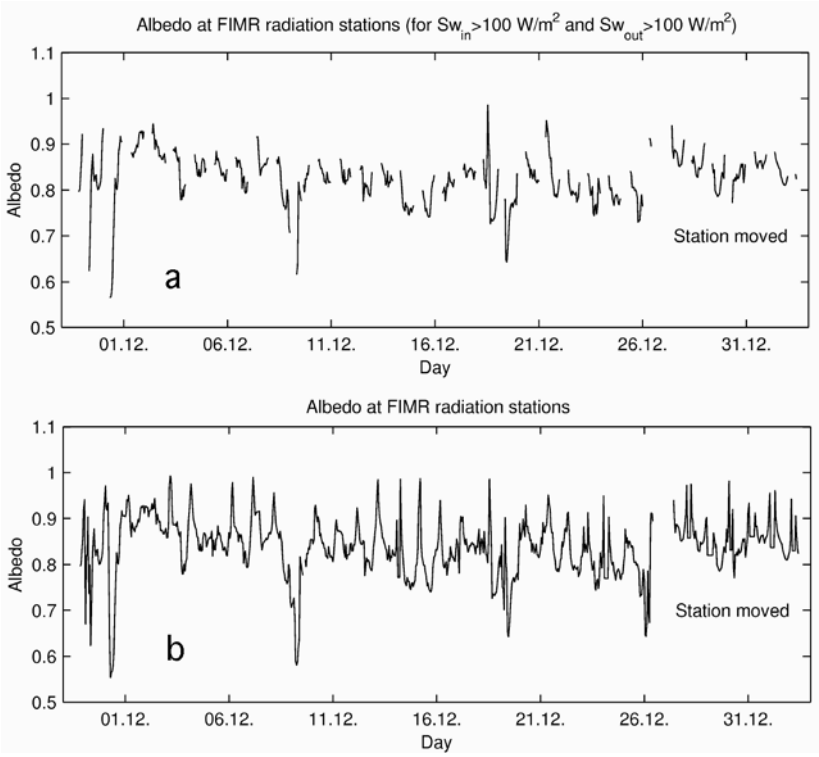

Fig. 2.9: Albedo at the FIMR radiation stations
Fig. 2.9a gives the "effective" albedo for the hours of pronounced daily radiation, and Fig. 2.9b indicates the all-hour albedo.

The longwave radiation emitted by the snow/ice surface, and the one emitted back from the sky and clouds (i.e. up-welling and down-welling thermal radiation) and the radiation balance are given in figure 2.10. Variability in up-welling radiation is small and due to small diurnal surface temperature variations. Down-welling radiation increases with clouds and warm atmosphere and is more variable than the earth surface emitted one.

At an average, the longwave radiation balance was negative by -10 to -15 W/m^2, but less negative during the warm first ISPOL week. However, during clear sky nights and days, the longwave radiation balances used to be negative up to -80 to -90 W/m^2.

The accumulate daily net radiation balance, composed from short- and longwave radiation is given as MJ/day in table 2.2.

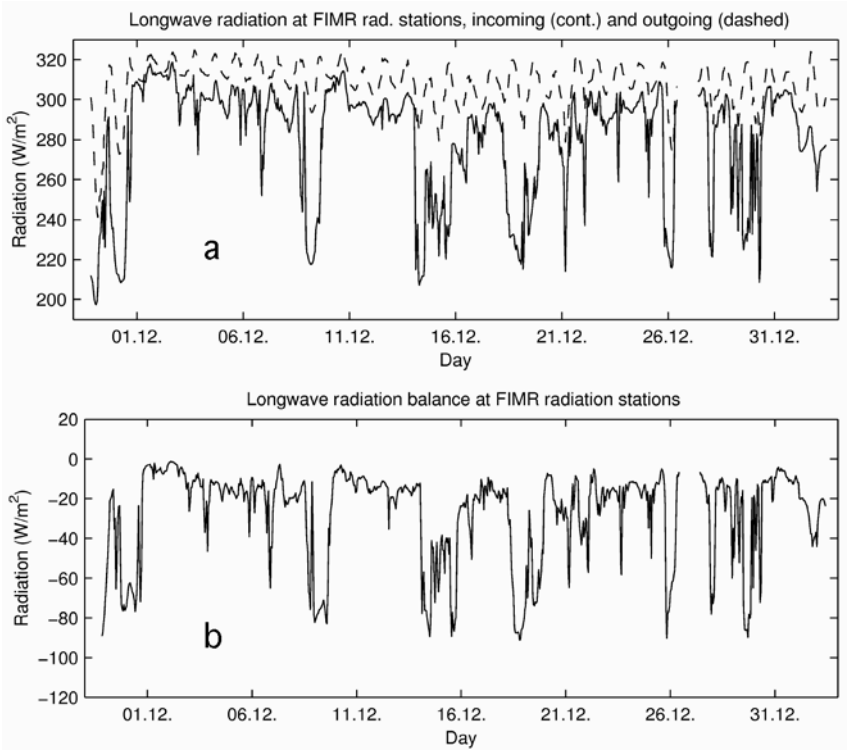

Fig. 2.10a: Longwave radiation upwards by snow/ice surface (upper smooth graph) and down-welling longwave radiation from clouds and sky (lower graph)
Fig. 2.10b: Longwave radiation balance in W/m^2

2.2.4.2 Turbulent fluxes of sensible and latent heat

The sensible heat flux between the air and snow/ice surface was measured by the eddy correlation method as $H = \rho c_p \overline{\Theta' w'}$ where the heat transfer is carried out by turbulent fluctuations of temperature (Θ') and vertical velocity (w'). Two sonic anemometers (Metek-USA1) were gathering the data. The time series composed from the measurements at various sites and overlapping periods show rather comparable results and time history and the fluxes are given in figure 2.11a. Except of some cases of warm air advection, the sensible heat flux used to be from the snow and ice to the air. In the calm and warm first week, the sensible heat flux and its diurnal variation were weak, but the fluxes and variations increased later. However, the flux from the snow and ice used to be two times larger in magnitude than that from air to snow and ice. Especially during the latter part of the period H had a diurnal cycle and the daily maximum was reached around noon local time. The overall mean sensible heat flux for the ISPOL period was -5.9 W/m^2.

Table 2.2: The penetrated shortwave flux (Sw), total radiation balance (Sw + Lw) and net surface heat balance (H_{net}), given as daily accumulate sums

Day	Sw (MJ/m^2)	Sw + Lw (MJ/m^2)	H_{net} (MJ/m^2)	Day	Sw (MJ/m^2)	Sw + Lw (MJ/m^2)	H_{net} (MJ/m^2)
29.11.	5.45	1.44	-	16.12.	4.49	2.43	-0.2
30.11.	6.92	2.91	-	17.12.	3.58	2.11	0.6
1.12.	1.88	1.43	0.7	18.12.	6.70	1.48	0.6
2.12.	2.30	1.75	0.9	19.12.	8.53	3.71	2.6
3.12.	4.37	2.88	2.5	20.12.	3.93	2.25	-0.1
4.12.	2.99	1.76	0.7	21.12.	4.34	1.77	0.8
5.12.	3.55	2.07	1.4	22.12.	5.25	3.50	1.9
6.12.	4.08	2.06	1.3	23.12.	5.31	3.64	2.3
7.12.	3.04	1.68	1.2	24.12.	4.82	3.50	2.3
8.12.	5.72	2.83	2.1	25.12.	5.16	2.55	(1.2)
9.12.	6.27	1.51	0.8	26.12.	(3.30)	-	(-1.2)
10.12.	3.59	2.84	2.0	27.12.	3.01	-	(-1.2)
11.12.	3.45	2.35	0.6	28.12.	3.60	1.48	(-1.0)
12.12.	4.48	3.00	1.3	29.12.	5.92	1.68	-0.7
13.12.	3.30	2.00	0.4	30.12.	3.51	1.70	0.3
14.12.	7.62	2.25	-0.1	31.12.	2.48	1.76	0.9
15.12.	6.97	2.51	0.1	1.1.	4.01	1.65	-

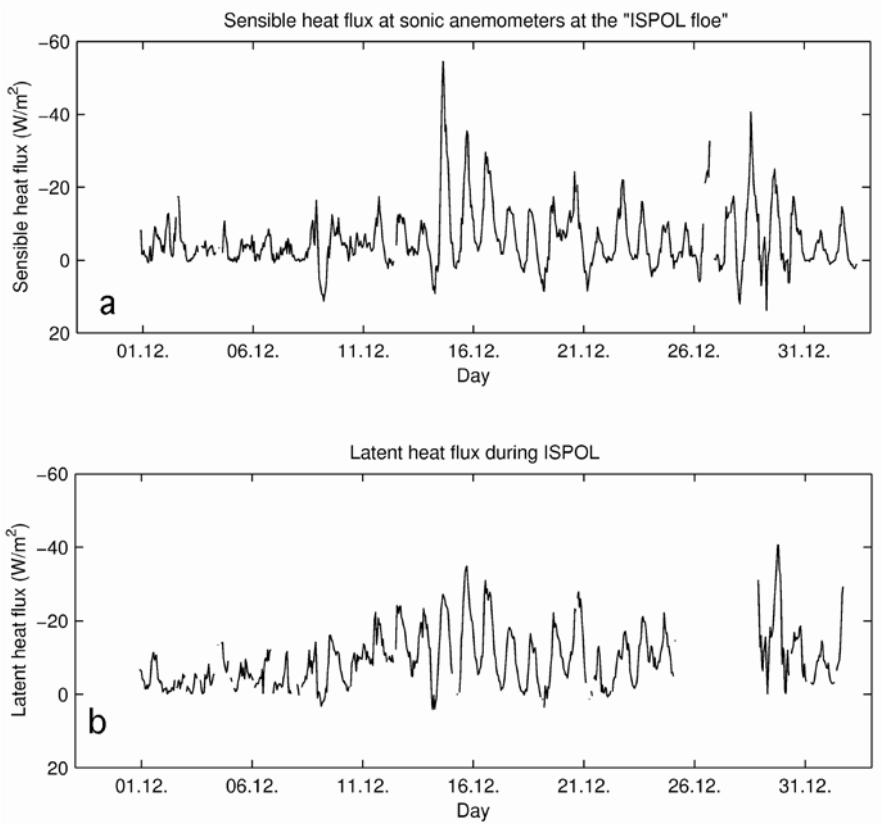

Fig. 2.11a: Sensible heat flux derived from the sonic anemometers for various FIMR measuring sites
Fig. 2.11b: Latent heat flux during ISPOL

As to determination of latent heat flux (the heat flux connected with evaporation), the task for ISPOL study turned out to be somehow tricky and challenging. It was not possible to apply the eddy correlation method to measure water vapour flux (nor was there any relevancy for it in freezing conditions and because power would be needed for heating and ventilation of equipment over ice floe etc.) In practice, accordingly, it is relevant to use the so-called bulk aerodynamic formula to calculate the latent heat flux as

$$L E = L \rho C_E (q_s - q_z) V_z$$

where V_z denotes wind speed, and $q_s - q_z$ is the difference in specific humidity between the surface and the atmosphere, and ρ is the air density, and L is the latent heat of fusion.

C_E is the turbulent bulk transfer coefficient, a site dependent coefficient and dependent on thermal air-ice stratification. The neutral transfer coefficient was calculated according to the theory of Andreas (1987), from the basis of the turbulence measurements and drag coefficient, the latter discussed in section 2.2.4.4. The stratification was taken into account using well-recognized universal functions.

Determination of an accurate snow/ice surface temperature for air-ice exchange estimations turned out to be difficult and not any trivial. The real surface (skin) boundary temperature in conditions of large radiation is not possible to measure accurately using any ordinary temperature probes. For the latent heat calculations the surface temperature is crucial because it defines $q_s(T_s)$. As the surface temperature, we planned to use the radiometric surface temperature calculated from the flux of outgoing longwave radiation by using the universal law of thermal radiation. Still, in the coδnditions of very high shortwave radiation and low wind speed, this turned out to be liable to serious errors as well, as discussed in section 4.6 below. Finally, however, we could use the information from the meteorological mast and turbulence mast and find a rather accurate way to calculate the surface temperature and latent heat flux, and finally, close the surface heat balance. Shortly, calculation of the surface temperature is as follows.

From the two sonic anemometers, we had an accurate estimate of the sensible heat flux H and, from the meteorological mast we had an accurate air temperature (T_z) and wind profile. Using the so-called Monin-Obukhov turbulence similarity theory and the universal functions accompanied we could construct “back” the temperature profile from air-to-surface as $T_s = T_s(z, H, V(z))$. The latent heat flux could then be calculated using this “synthetic” surface temperature. In practice, the calculation of the surface temperature and fluxes were computed as an iterative solution, based on the algorithm of turbulent surface flux calculation by Launiainen and Vihma (1990).

The time series of the latent heat is given in figure 2.11b. The results show the latent heat flux to have been larger than the sensible heat flux and indicate the latent heat flux to have been (towards the summer) generally increasing in magnitude. The overall mean was -10.0 W/m^2 and the flux had an apparent diurnal variation. The Bowen ratio ($Bo = H/LE$) was 0.5 typically.

2.2.4.3 Heat balance

From the various components, the net surface heat balance is calculated as

Surface heat balance = Radiation balance + Turbulent fluxes (of sensible & latent heat)

The daily accumulate net heat balance is given in figure 2.12 and in numerical form in table 2.2.

As to be seen from figure 2.12, the mean heat balance was positive especially during the first warm period. The overall mean surface heat balance for the ISPOL period was 0.81 MJ/m^{2}day corresponding to a flux of 9.4 W/m^2. The accumulated surface heat balance for the whole period was 25.2 MJ/m^2. In terms of heat for bulk melting, this corresponds to a melting of thickness of approx. 8 cm of ice (of 0 ‰) or 25 cm of snow. Figure 2.12 shows that the surface gained heat for melting in the beginning of ISPOL and during the week before Christmas, whereas the middle and end of the period was of time of no melting or refreezing. On the other hand, any specific amount of melting cannot be defined from the air-ice heat balance only. For study of melting (refreezing as well) a more complete physical approach is needed. This is because in these conditions the shortwave radiation is the heat source for heating and melting of ice. Roughly taking, decay of shortwave radiation due to absorption is exponential. Accordingly, resulting heating and melting happens as a process in an ice column and not always just as a bulk interface-melting, but in slightly deeper and as a rather complicated process. Later on when the surface is getting less transparent, all the processes affect the very surface mostly. For the complete sea ice thermodynamics study, the heat flux from below, the ocean-ice heat flux time series is needed also.

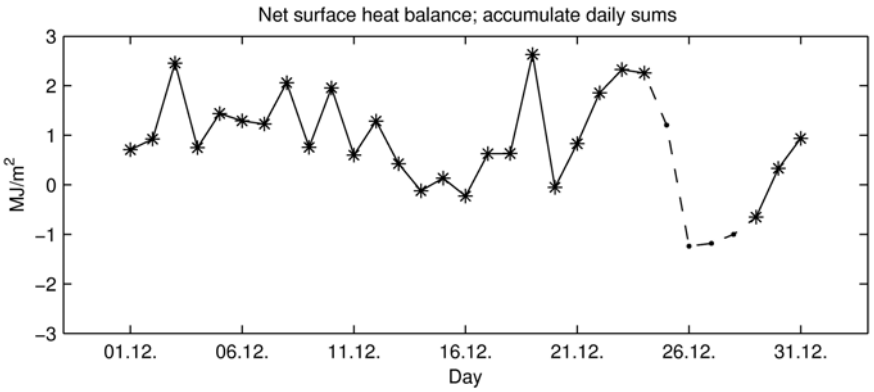

Fig. 2.12: Accumulate daily net surface heat balance (MJ/m^2)

For investigation of the ISPOL sea ice thermodynamics, i.e. melting and freezing and time development of in-ice temperatures the coupled FIMR air-ice-ocean thermodynamic process model will be used.

In terms of thermodynamics and surface heat balance we may find the seasonal progress towards the summer during ISPOL to have been rather gradual. This was mostly because the albedo in this high sea ice concentration area stayed as large, and, due to gentle weather conditions with only a few storms and advection.

2.2.4.4 Momentum flux and wind drag coefficient

The sonic anemometers gathered data on momentum flux and turbulence and stratification characteristics. The wind force per unit area i.e. momentum flux, defined as the covariance of the turbulent horizontal (*u'*) and vertical (*v'*) fluctuations, is for practical applications parameterized as $\tau = \rho\overline{u'w'} = \rho C_D V_z^2$ where V_z is the wind velocity and C_D is the drag coefficient. The sonic anemometer yields data on the drag coefficient in conditions under the air-ice stratification conditions prevailed. Using the universal functions based on the Monin-Obukhov similarity theory the drag coefficient was corrected by an iteration process to represent the neutral stratification and a 10 m wind observation level (C_{DN10}). The drag coefficient, with respect to floe related wind direction, is given for the various measuring sites in figure 2.13.

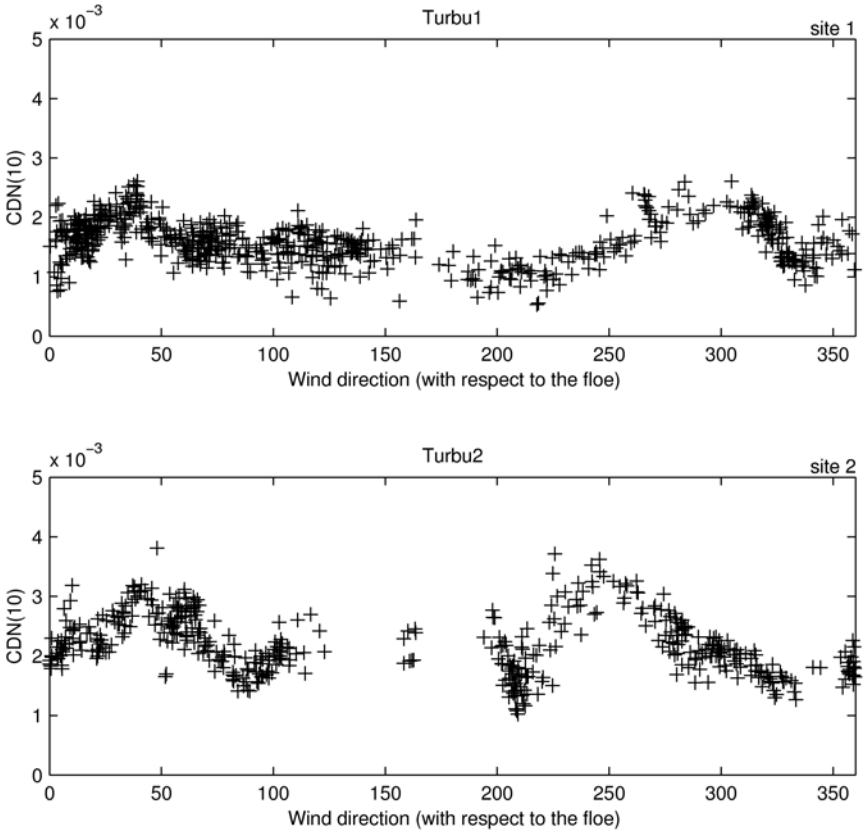

Fig. 2.13a: Neutral drag coefficient C_{DN10} *versus wind direction for FIMR sites 1 and 2*

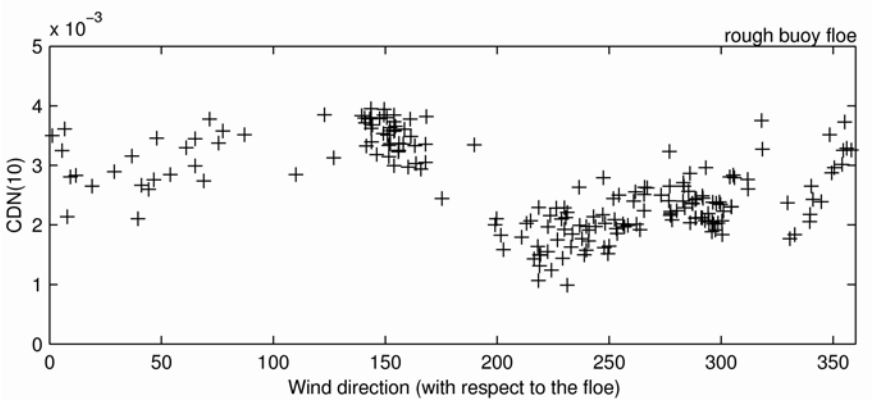

Fig. 2.13b: Neutral drag coefficient C_{DN10} versus wind direction for the rough buoy floe

The results show the drag coefficient to be rather large and dependent on wind direction in the ISPOL area. The latter means merely existence of geometric roughness elements such as ridges and ice blocks upwind. C_{DN10} use to vary from 1 x 10^{-3} up to almost 4 x 10^{-3}. The lowermost value represents a smooth surface and, the rough buoy floe having ridges up to over 3 m represents the highest drag coefficient. At the ISPOL floe sites the drag coefficient of up to 2 – 3 x 10^{-3} seems to be rather frequent. For no one of the sites, a wind dependency of the drag coefficient was observed. As to quantify the drag coefficient to the on-site geometric roughness, our data does not allow any very good approach so far. A distribution (directional) is known just as semi-quantitative terms based on surface photography and compass based directional visual mapping. Actually, in ordinary tools a strict roughness mapping is very difficult to be made, because of visual white out and no photo contrast etc. From helicopter-borne altitude measurements carried out by AWI we hope to get some further insight.

The above preliminary drag coefficient results suggest the over-ice wind drag coefficient in the Western Weddell Sea to be rather large, larger than used in many meso-scale or global models.

In addition to the drag coefficient and turbulent fluxes, other air-ice interaction quantities such as intensity of turbulence and fluctuation spectra etc. will be evaluated. In addition, the universal functions and especially that of wind speed will be studied using the turbulence and profile meteorological mast data.

2.2.4.5 Derivation of snow and ice surface temperature in conditions exposed to large shortwave radiation

In practice, a surface temperature measurement representing the real surface temperature (air-surface interacting skin) can only be determined by applying radiation methods. Because of daylight radiation penetration into snow and ice (and air bubbles etc. in snow) even a smallest mechanic sensor tends to absorb radiation and give erroneous readings. About this we have got several experience from ISPOL. Accordingly, from the radiation measurements the temperature can be calculated using the universal law of radiation of $R_l = \varepsilon\sigma T^4$. Equipment manufacturers use to give formulae for correcting and compensating errors for sensor temperature. However, under conditions of large incoming radiation derivation of the surface

temperature from the measured radiation flux is still not any trivial to do. The background and reasoning reads as follows:

From the down-looking pyrgeometer, the radiometric surface temperature is calculated. However, in those conditions of very high shortwave (solar) radiation, and low wind speed, the dome of the pyrgeometer (longwave sensor) tends to be heated excessively and the accuracy of the surface temperature derived from the longwave radiation flux is poor. The heating gives an excess in the measured radiation flux, and, the surface temperature calculated is too large: it tends to be above zero by up to +2°C and erroneous. Figure 2.14 gives the surface temperature calculated from the radiation measurements. Even during nights in summertime in very high latitudes the equipment (it's vertical parts) is heated by the radiation and the night-time surface temperature estimate may be erroneous. The longwave flux correction and its diurnal variation is unknown, strictly. The radiation equipment factories could give just a hint about a correction which is not specific/accurate enough to give the correct (i.e. below or up-to-zero) snow surface temperature. At present, it is unknown if one can find such a specific final correction.

The arguments from which we know the radiation derived measurement surface temperature is incorrect in very high shortwave radiation and low wind conditions is based on the heat flux results from the two FIMR turbulence masts. The flux together with the simultaneous meteorological mast air temperature (several sensors mutually comparing each other) defines the "correct" air-snow temperature difference as the precondition for the flux measured. Accordingly, the incorrect surface temperature derived from the radiation flux suggested a good air-snow temperature difference even for cases when the turbulence masts indicated a zero heat flux, and hence, a zero air-ice temperature difference.

For ISPOL study, we were lucky to have an accurate sensible heat flux from the sonic, and air temperature and wind data from the profile mast. Based on those measurements we could construct a rather accurate surface temperature as a “synthetic” surface temperature (cf. section 2.2.4.2) using the Monin-Obukhov boundary layer similarity theory. The corrected surface temperature is given in figure 2.14.

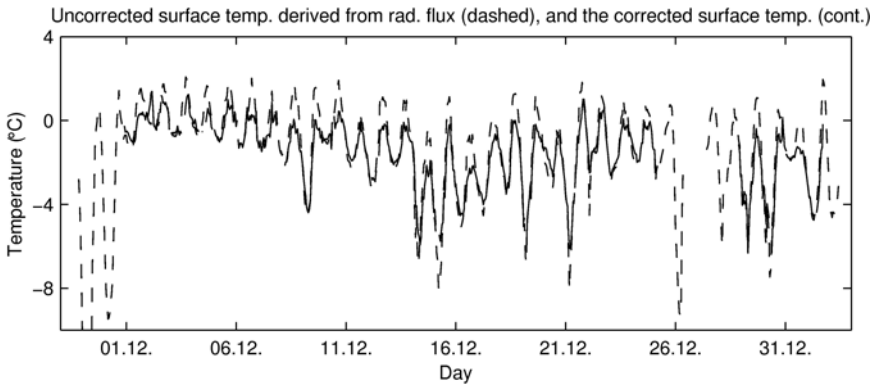

Fig. 2.14: Surface temperature derived from the longwave radiation (broken) and the corrected surface temperature based on the measured heat flux and air temperature and wind profile (continuous)

Finally, we may notice that both the short-and longwave radiation fluxes under the highest radiation fluxes tend to be in error of overestimation of 1.5 to 2 %. (The magnitude found out from the temperature error investigation.) However, in the short- and longwave radiation balance the final error is insignificant, the errors then balancing each other. Still, the above small flux error is enough to make the surface and air-ice temperature estimation inaccurate.

2.2.4.6 Other measurements and studies

Satellite buoys

Totally, 3 FIMR buoys were deployed in the buoy array of the international (AWI, AAD, IARC, FIMR) sea ice drift and deformation ice buoy project. The FIMR buoys had sensors for position (GPS), air pressure, air temperature and buoy hull temperature. Two buoys (Id's 1154 and 52292) were deployed in the main buoy array, and one (5892) buoy 54 nm north from the main array. On the buoy floe of 52292, an air-ice turbulence measuring sonic anemometer was functioning in 6 December – 17 December 2004. In the end of the expedition, buoy 1154 was left in the area and 5892 was redeployed on the ISPOL floe.

An animation of the buoy trajectories of the ISPOL buoys was made (and available). The animation contains the past-ISPOL trajectories of the buoys left in the area. The buoy data is being used for meso-scale sea ice drift and deformation and air-ice-sea interaction studies, and, comparison and verification of Antarctic and Southern Ocean meteorological (esp. ECMWF) and marine models.

A set of meteorological balloon soundings were launched from over the sea ice. Those completed with the surface observations and ship's routine aerological sounding data are goaled for a mesoscale atmospheric boundary layer study and modeling in co-operation with the Finnish Meteorological Institute (FMI).

2.2.5. Concluding remark

As the general conclusion in terms of the thermodynamics and surface heat balance we may find the seasonal progress towards the summer during ISPOL to have been rather gradual. This was mostly because the albedo in this high sea ice concentration area used to stay as large, and due to gentle weather conditions with only a few storms and advection heating. The above results put us forward a question whether the ISPOL period was an exception or was it a period and case study that might represent the summer season development in the area more generally. The latter would mean that in the deep western Weddell Sea the summer melting tends to be rather gradual generally, and the sea ice will be exposed to summer and melting not before it drifts to north enough, up to latitudes of 66° to 65° or so. In the southern part, a thick snow cover and surface refreezing and frequent snowing may keep the albedo as high enough to prevent a pronounced melting and progress of summer. However, in terms of heat balance and thermodynamics, as well as in sea ice dynamics the area is too few investigated so far.

Acknowledgement
We appreciate and thank the Alfred Wegener Institute for Polar and Marine Research for the excellent working conditions and successful expedition onboard RV *Polarstern*. We would like to particularly thank the chief scientist, Professor Dr. Michael Spindler, and the ship master, Captain Uwe Pahl, for their crucial efforts making this successful expedition come true. We express our thanks to all of the crew and the scientific colleagues of the international expedition for the cooperation and help and for the working atmosphere which was exemplarily good throughout the expedition.

References

Andreas, E. L. 1987: A theory for the scalar roughness and the scalar transfer coefficients over snow and sea ice", *Boundary-LayerMeteorol*. 38, 159-184.

Launiainen, J.and T. Vihma 1990: Derivation of turbulent surface fluxes - an iterative flux-profile method allowing arbitrary observing heights. - *Environmental Software* 5, 1-15.

3. SEA ICE AND GEOPHYSICS

3.1 ASPECT ice observations, aerial photography, buoy array, and DC conductivity measurements

Antony Worby
Australian Antarctic Division, Kingston

3.1.1 ASPECT ice observations on transect from ice edge to ice station

Hourly ice observations were made from the ship's bridge. The observations recorded the concentration, thickness, snow cover, floe size and topography of the pack ice along the ship's path and will contribute to the Antarctic Sea Ice Processes and Climate (ASPeCt) data base. The data from ISPOL will be the 85th voyage added to the data base, which now provides circumpolar sea ice data in all seasons. The data show two distinct sea ice regimes along the transect into the ice, separated by an area of lower ice concentration between approximately 40-45ºW (Fig. 3.1). The thicker multi-year ice was found to the west of 68°S 45ºW as shown in figure 3.2.

Volunteers from numerous scientific groups onboard assisted with the observations, which are available to all ISPOL participants on the intranet. At the time of each observation three photographs were also taken (looking to port, ahead and starboard) and Sascha Willmes produced a html document which presents these images together with the hourly data. The observations were continued after we had left the ice station on 2 January, heading north to the ice edge.

3.1.2 Drifting buoy programme

Drifting buoys were deployed in an array to monitor the drift and deformation of the pack ice. A total of 23 buoys were contributed from Germany (AWI), Australia (AAD), Finland (FIMR) and the US (IARC). The buoys were deployed in a triangular grid SW of the ship, 70 km along each side (see Fig. 3.3). Most of the buoys transmitted their position via system ARGOS, while 6 of them had only onboard data storage. A number of buoys also had air pressure and temperature sensors. Most of the buoys were recovered at the end of the voyage, except for three which marked the corners of the array and one to mark the location of the ISPOL ice floe.

The ice drifts with velocities between 0 to 0.6 knots, driven by the wind and ocean currents. However, the ice drift is not uniform, and therefore there are locations where ice floes diverge, generating open water leads in between, and other regions where the ice converges, leading to ice deformation and subsequent thickening. Observation and computer simulations of these processes are essential for an understanding and prediction of sea ice in future climate scenarios, and for its role in the freshwater balance and exchanges with the atmosphere. By observing the relative differences between the motion of those buoys, the strain rates and deformation of the ice pack can be measured, which in conjunction with high resolution satellite data will be used to validate models of sea ice dynamics.

Preliminary results show a significant difference between the drift of the western and eastern buoys. In the west the buoys have slowly moved southward during the 1 month observation period, while the eastern buoys have moved northward by about 20 km, indicating a shear zone between the central Weddell Sea and the ice on the continental shelf close to the Antarctic Peninsula.

3.1.3 Aerial photography

The objective of the aerial photography programme is to record changes in sea ice properties throughout the experiment, in particular, changes in floe size and the distribution of ice types, which are related to the drift/deformation observed from the buoy array. The photographs were taken along the 3 sides of the buoy array from an altitude of 5000 ft. We flew on 10 occasions, but due to persistent cloud only 3 of these were complete. We also had equipment problems on one flight. A summary of flight activities is in table 3.1 and the ISPOL floe is shown in figure 3.5 (photo taken on Christmas Day, 2004).

The photographs were taken with a Nikon D1x (6 mega pixel) digital camera, and have a ground size of approx 1.2 x 1.0 km with a resolution of approximately 35 cm. The grey scale and colour histograms are used to determine the fraction of different ice types. At the time of writing it is clear that over the course of the experiment there was a significant decrease in mean floe size, although some vast floes (>5 km across) were still present. This was also noticed in the vicinity of the ship and on our own floe. There was not much change in open water fraction, however we observed a big increase in the amount of brash ice between the floes which became increasingly brown with time as well as a significant increase in areas of surface flooding. The relative percentages of the different ice types and changes in floe size distribution will be quantified when the images are completely analysed. However it is clear that dynamics plays a key role in deforming the ice, and that ridges collapse into newly formed leads during periods of divergence. The high productivity in the leads causes these brash areas to turn brown which has a positive feedback on ice decay because of the enhanced albedo effect.

Table 3.1: Dates of aerial photography flights and success (or otherwise) along each flight leg

Flight	Date	Leg 1	Leg 2	Leg 3	Comments
1	-				There is no flight 1
2	16/11				Test flight
3	29/11	Part	Full	Full	First flight over array
4	8/12	Part	Full	Part	Cloud over much of Legs 1 and 3
5	9/12	Full	Full	Full	Happy about that ☺
6	19/12	Part	None	None	Cloud, shutter problem, camera problem
7	21/12	None	None	None	Aborted due to cloud
8	25/12	Full	Part	Part	Cloud in SW
9	29/12	Full	None	None	Patchy cloud on Leg 1. Too cloudy further south
10	1/1/05	Full	Full	Full	High cloud, very bright, poor ground contrast

3.1.4 DC Conductivity Measurements and Sea ice structure and properties

Time series measurements were made at Site 9 of the electrical conductivity of the sea ice. Over the month of December we saw a significant increase in conductivity, consistent with other observations from core data showing increasing ice temperature and porosity.

Oxygen isotope samples were taken from the time series cores at the ice station, and numerous other cores from the surrounding area. The samples will be analysed in Hobart and the data will be used in conjunction with other core data to determine the changes within the sea ice system throughout of the experiment. This is a collaborative effort with other groups on the cruise.

Acknowledgements and thanks
Field personnel assisting with this project were Carl Hoffman (Australia) and Adrienne Tivy (US), both providing invaluable support. Sincere thanks to the Captain, crew, chief scientist and all colleagues onboard for support throughout the programme. Particular thanks to the helicopter crew whose efforts were instrumental to the success of the drifting buoy and aerial photography programmes.

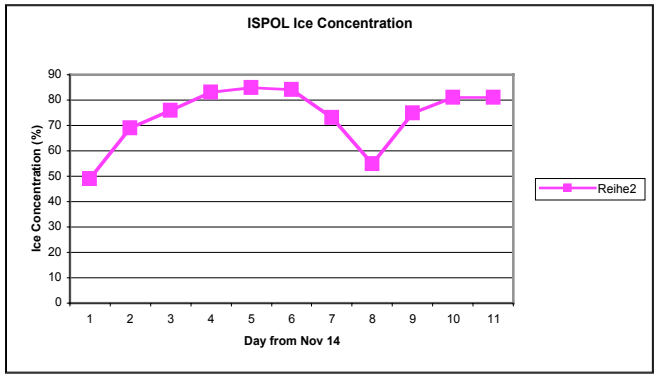

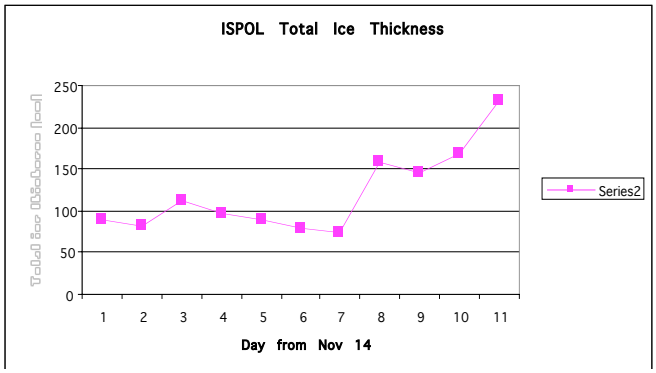

Fig. 3.1 and 3.2: Ice concentration and total ice thickness (excluding the open water fraction) along the transect from the ice edge to the ISPOL floe location

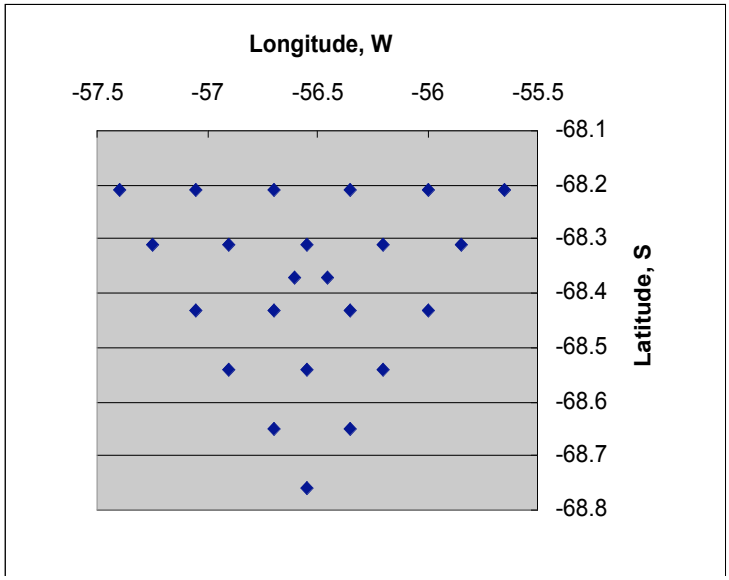

Fig. 3.3: Initial deployment locations of the 23 buoys in the drifting buoy array

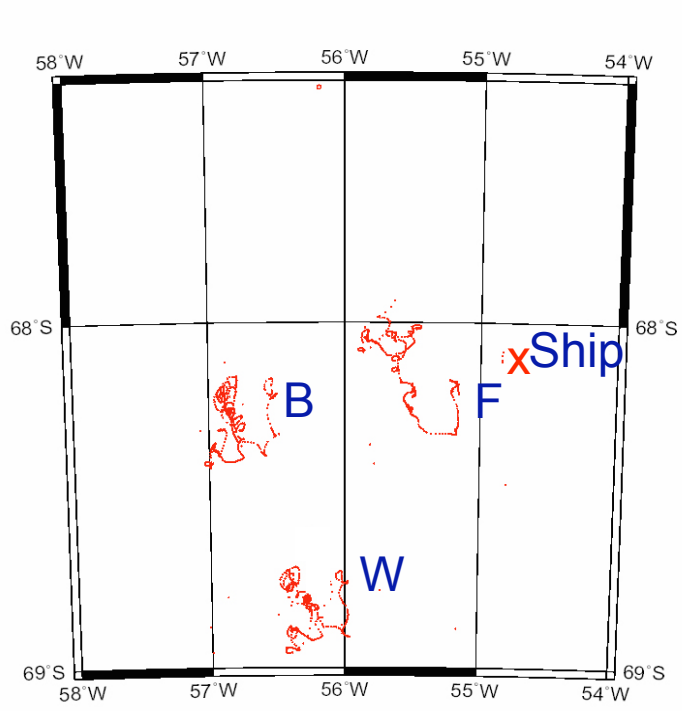

Fig. 3.4: Drift tracks of the three corners of the array (data from A unavailable). The buoy deployment location is nearest to the letter denoting the Site ID.

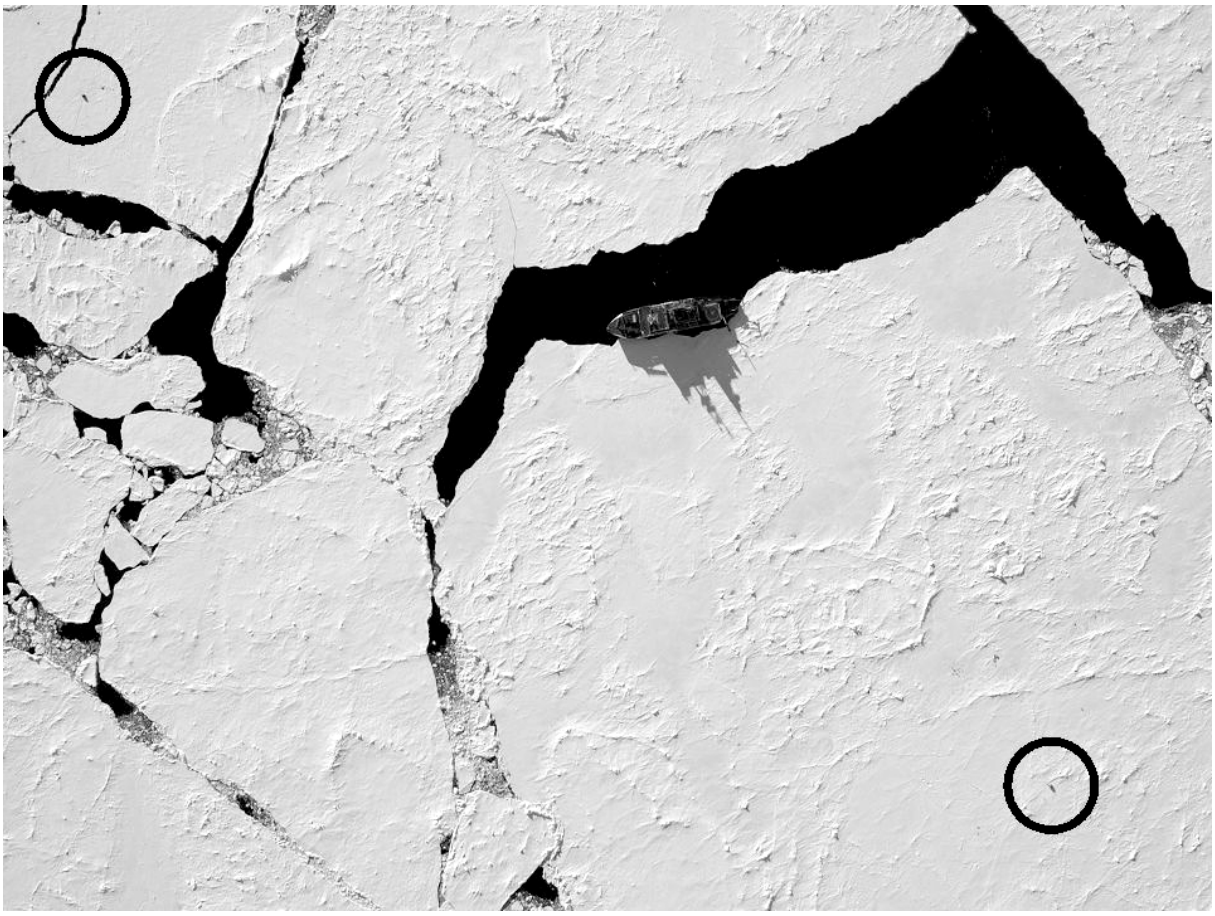

Fig. 3.5: An aerial photograph of the ISPOL ice station, taken at 2200Z on Christmas Day, 2004. The locations of the two apple huts are marked, and various other experimental sites can also be seen.

3.2 Changes of sea ice physical properties during the onset of melt

Christian Haas[1)], Marcel Nicolaus[1)], Anja Batzke[1)], Sascha Willmes[2)], John Lobach[3)]

[1)] Alfred Wegener Institute, Bremerhaven
[2)] Universität Trier
[3)]Ferry Dynamics Inc. Mississauga, Canada

3.2.1 Introduction

The German sea ice geophysical programme focused on three main objectives which were however closely related to each other: Snow melt and superimposed ice formation, changes of ice thickness, and satellite observations of surface changes. In order to address these topics, a wide range of *in-situ* measurements of snow and ice properties and of the surface energy balance were carried out. In addition, we have performed airborne ice thickness measurements and we have obtained near-real-time satellite imagery, either directly received on board or processed and transmitted from Europe.

The project was partially funded by two DFG projects: *„Beobachtung und Modellierung der Aufeisbildung auf sommerlichem antarktischem Meereis“* and *„Beobachtung des Beginns und der Länge der sommerlichen Schmelzperiode auf antarktischem Meereis mit Hilfe passiver und aktiver Fernerkundungsverfahren“.*

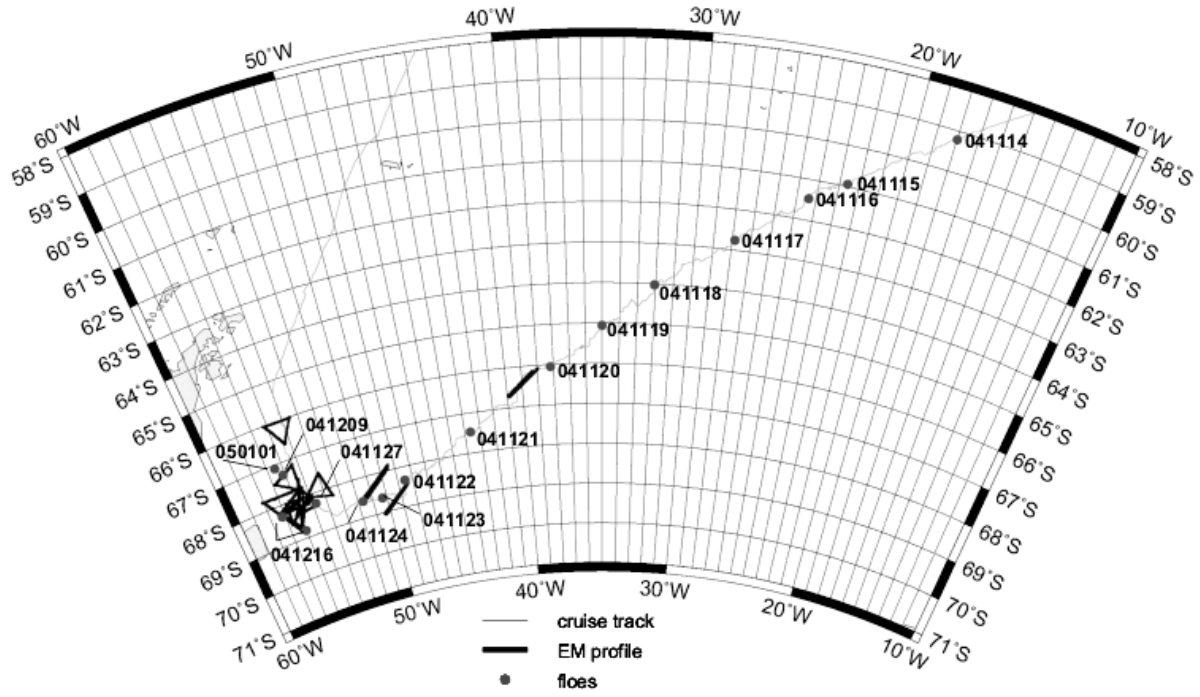

Fig. 3.6: Map of ice floes sampled during the transect between the ice edge and the ISPOL floe. Tracks of all HEM flights are also shown.

Nov. 13, 2004 Dec. 30, 2004

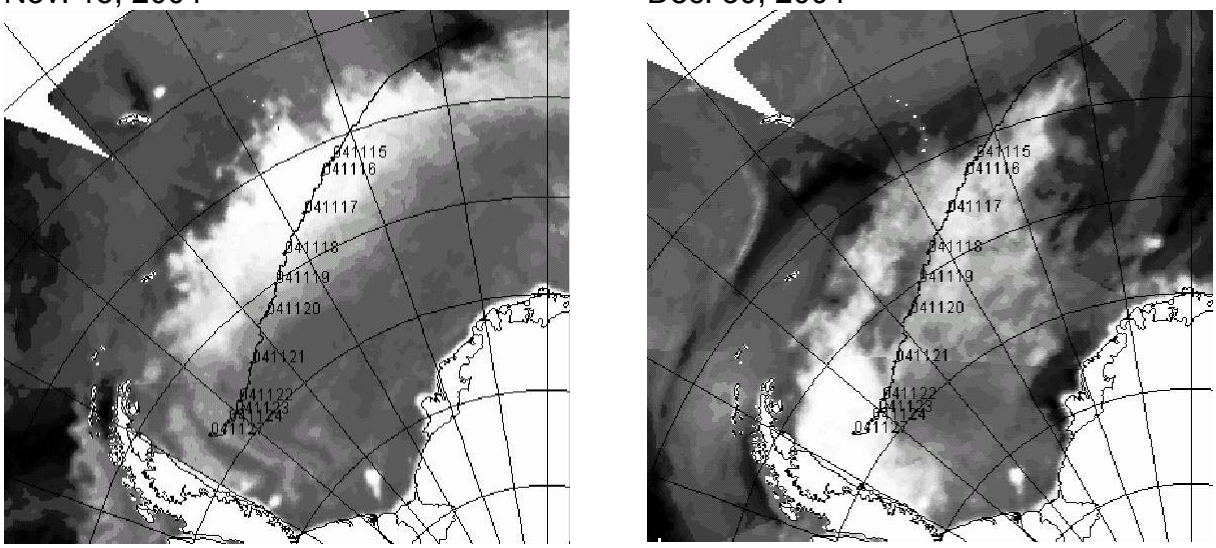

Fig. 3.7: Typical radar backscatter maps obtained by Seawinds/QuickScat, showing ice conditions at the beginning of the ISPOL transect (left) and at the end of the ISPOL drift (right), as well as the dates and locations of ice floes sampled during the transect. Bright grey shades correspond to high radar backscatter. Images were supplied daily by Leif Toudal, DTU, Denmark.

3.2.2.1 Ice thickness and general ice conditions

3.2.2.1.1 Continuous ship-based along track measurements using RV Polarstern' SIMS

Between 15 and 27 November ship-based along track ice thickness measurements were performed using RV *Polarstern'*s Sea Ice Monitoring System SIMS. This is based on electromagnetic induction sounding of sea ice thickness, using a Geonics EM31 instrument and a laser distance meter. Measurements were taken with 10 Hz for the laser data and 1 Hz for the EM data.

Figure 3.8 shows results of a SIMS calibration performed on 16 November by rising and lowering the SIMS slowly above some open water. The resulting thick curve allows computation of the SIMS height above the water surface or ice underside. Subtraction of the laser height above the ice surface yields total (ice plus snow) thickness. Figure 3.8 shows that the calibration curves falls well within other curves obtained on earlier RV *Polarstern* cruises. The variability can be explained by different instrument tilts and different seawater conductivities. However, the figure also shows that the accuracy of ice thickness retrievals is probably not better than 0.2 m.

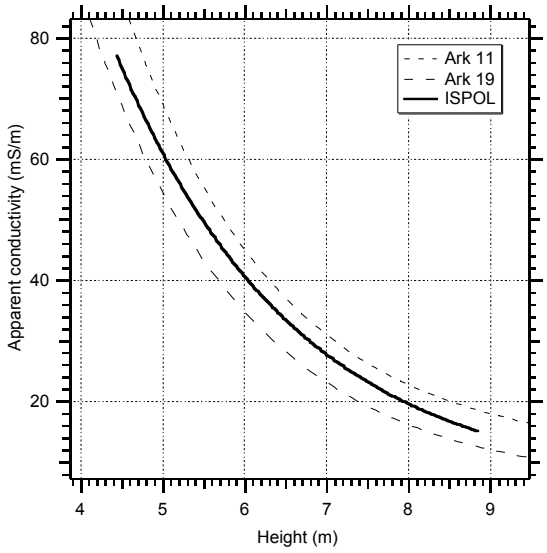

Fig. 3.8: SIMS calibration curve obtained on 16 November and compared with data from earlier RV Polarstern cruises

The thickness distribution along the cruise track is shown in figure 3.9. Mean ice thicknesses have been computed both for all data for a spatial interval of 1 degree longitude, and for data with ice thicknesses larger than 0.3 m only to exclude open water measurements leading to thinner estimates (Fig. 3.9a). It can be seen that the mean ice thickness amounted to 1.0 – 1.2 m between 23 and 40°W, and was larger than 1.5 m west of about 45°W, in good agreement with visual ice observations (Section 3.1.1). The thickness increase at 45°W is probably due to increasing amounts of second year ice, although on the backscatter map in figure 3.7 second year ice is only clearly visible west of 50°W. However, airborne measurements also indicated the presence of ice typically thicker than 2 m even between 40 and 41°W (Fig. 3.10), in agreement with the SIMS data. There was also thicker ice upon entry into the pack ice between 20 and 23°W, which considerably slowed down the ship.

The large ice thickness probably indicates the presence of second year ice in the outflowing branch of the Weddell Gyre.

Note that between 23° and 45°W between the ice floes the ship encountered very much open water which allowed good progress towards the ISPOL floe.

Figure 3.9b shows ice thickness histograms for 1 degree longitude intervals, for ice thicknesses greater than 0.3 m, i.e. excluding open water. As in figure 3.9a, increasing amounts of thick ice can be seen west of 40°W, with typical thicknesses as high as 2 m, and in agreement with the airborne measurements (Section 3.2.2.1.2).

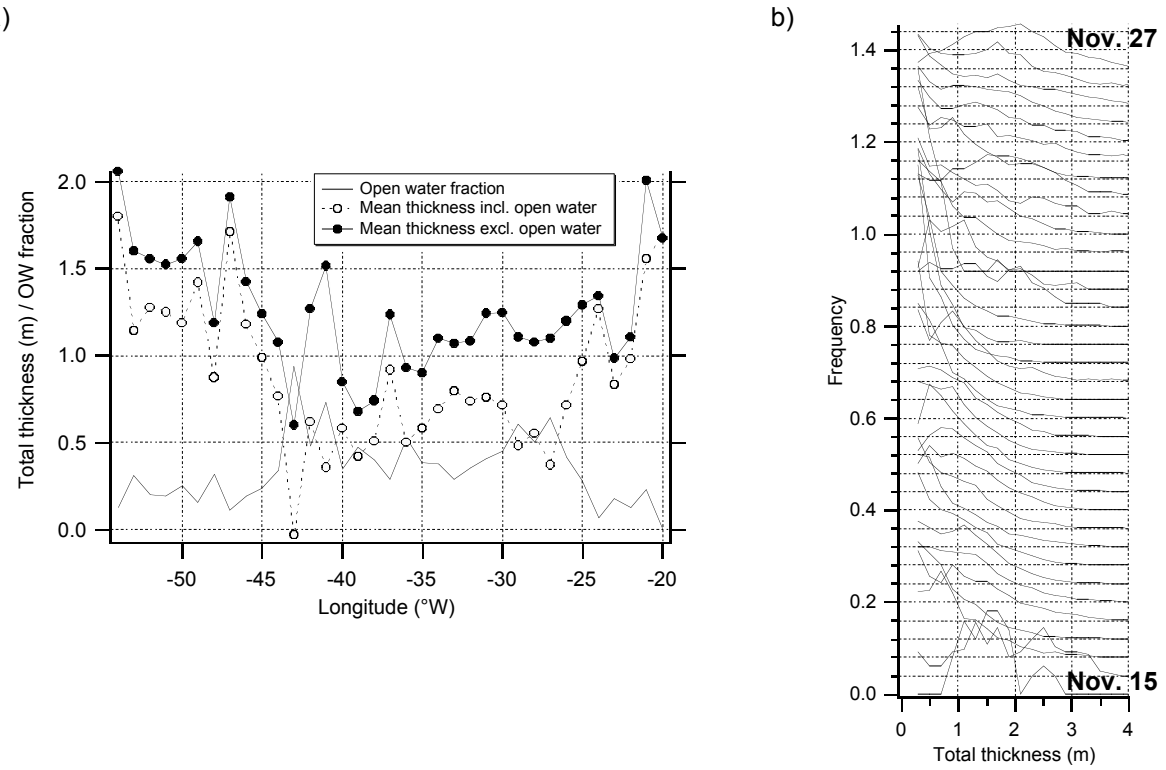

Fig. 3.9: a) Ice thickness (including and excluding open water for computation of the mean) and open water fraction along the cruise track from -20°W (right) to -55°W (left). b) Corresponding thickness histograms for 1 degree longitude bins. Histograms are only displayed for ice thicknesses greater than 0.3 m, and are offset by 0.04 each for better clarity.

3.2.2.1.2 Helicopter-borne ice thickness profiling

Helicopter-borne thickness surveys have been performed with a towed EM ice thickness sensor (EM-Bird). The bird is 3.5 m long, has a diameter of 35 cm, and weighs around 100 kg. It was towed 20 m below the helicopter, at an operation altitude of 10 to 15 m above the ice surface with 70 - 80 kn. The bird operates at 3.68 and 112 kHz, with coil spacings of 2.77 and 2.05 m, respectively. During the transect take-off and landing were conducted from the helicopter deck, whereas it had to be performed from the ice during the ice station due to varying wind directions. Every 20 nautical miles, the helicopter ascended to an altitude of >400 ft to allow for internal

calibration and nulling of the bird. Geo-referenced digital still photographs were taken to document general ice conditions. Subsequently they were included into an html linked map projection allowing for easy geocoded image browsing. All bird flights were also used by the Alterra-group (Hauke Flores, see Section 4.13) for counting inventories of penguins, seals and wales, as required by the German Environmental Agency. On seven flights, a DGPS reference station was deployed on the ISPOL floe. With this, and with the birds DGPS antenna and laser profiler, the elevation of the snow surface above the water level can be measured. Comparison of surface elevation with ice thickness is required for ice thickness retrieval from satellite altimetry missions like ICESat and CryoSat.

A summary of HEM flights is given in table 3.2, all flight tracks are shown in figure 3.6.

Table 3.2: Summary of HEM thickness surveys (Fig. 3.6). Geographical positions are approximate locations of furthest distance to ship. * marks flights with DGPS/laser profiling of sea ice surface elevation.

Flight No.	Date	Latitude °S	Longitude °W	Length nm	Comment
1	20.11.2004	-66.4	-40	120	Transect
2	22.11.2004	-68.8	-49.5	120	Transect
3	24.11.2004	-68.2	-50.5	120	Transect
4	27.11.2004	-68	-55	5	Grid survey of ISPOL floe
5	29.11.2004	-68.3	-56.5	100	Bird flight 30 miles west and south of ship
6	30.11.2004	-68.2	-55.5	30	Aborted due to bad weather
7	09.12.2004	-68.6	-56.5	140*	Buoy triangle. Last leg aborted
8	09.12.2004	-67.6	-54	120*	Flight to NE, across prominent vast floes
9	14.12.2004	-68.3	-55.5	120*	Flight to S
10	14.12.2004	-67.2	-55.5	120*	Flight to N. Rubble fields in the NW
11	15.12.2004	-67.7	-58	160*	Flight to W, into high SAR backscatter; includes northern leg of buoy triangle (F-A)
12	18.12.2004	-68.5	-56.25	150*	Buoy triangle & three overflights of ISPOL floe
13	23.12.2004	-68	-55	20	Laser surface-roughness profiling of FIMR buoy 52292
14	29.12.2004	-68.6	-56.3	160*	Buoy triangle
15	01.01.2005	-67.5	-55.5	10	Two profiles of ISPOL floe
16	04.01.2005	-66.1	-55.5	120	MIZ and former Larsen polynya ice

On the transect, three flights have been carried out with a total length of 360 nautical miles (see map in Fig. 3.6). Each flight extended 60 nautical miles away from the ship, towards the main steaming direction of 233°. The return flight was performed 5 nautical miles away from and parallel to the outward leg to allow for the study of spatial variability of the derived ice thickness distributions.

Only a few sections of the flights were processed on board. Figure 3.10 shows a thickness distribution obtained at 66.6°S, between 40 and 41°W. Large amounts of open water can be seen, as well as prominent modes at 1.15 and 2.15 m. While the former represents typical first year ice thicknesses, the latter indicates that there was also thick second year ice in the study region. This and the large amount of open water is in good agreement with the results of the SIMS measurements (Section 3.2.2.1.1) and visual observations (Section 3.1.1).

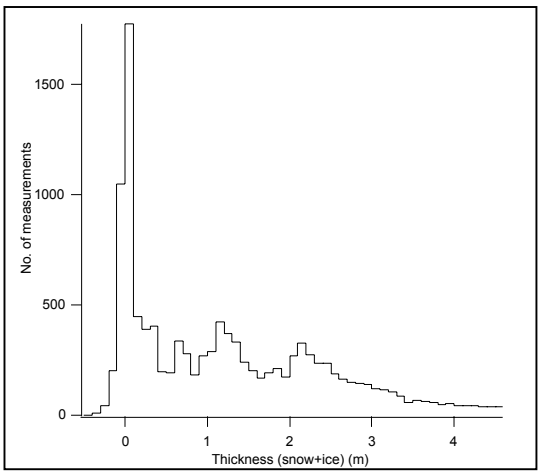

Fig. 3.10: Sea ice thickness histogram obtained by helicopter-borne EM sounding on 20 November at about 66.6°S and between 40 and 41°W (see Map in Fig. 3.6)

3.2.2.2 Ice core and snow properties

Between 14 and 27 November daily snow and sea ice measurements were performed by means of helicopter floe hopping (locations see map in Fig. 3.6). All measurements were performed jointly with biological and biogeochemical studies (Section 4). Floes were chosen to be representative (size, thickness, ridging) for the actual region. Typical floe diameters ranged from 300 m to 5000 m. On all floes an ice patch with a level as homogeneous as possible was selected for sampling to reduce the influence of ridges. Ice cores were drilled on all floe stations except on 23.11.04. On all floes, snow properties as well as ice salinity and texture profiles were analysed, whereas ice temperature profiles were obtained only every 2 days. Ice cores were processed on board in a -25°C cold lab container. Texture was determined by means of ice thick sections analysed in polarized light.

Figure 3.11 shows mean and modal snow thickness obtained along 50 m profiles with a measurement spacing of 1 m. Like with ice thickness (Fig. 3.9) a marked increase from between 0.13 and 0.30 m to between 0.33 and 1.21 m can be seen at about 40°W (20 November) indicating the transition to predominantly second year ice, or less melting.

Salinity and texture profiles of all cores obtained on the transect are shown in figure 3.12. Most profiles exhibited a C-shape, although top salinities were usually much lower than typical for young first year ice. Overall, mean salinities were relatively small, ranging between 3.0 to 4.8 ppt. This might be mainly due to desalination of the upper ice layers during the preceding spring warming, which had already commenced before our study period as can clearly be seen with ice temperatures as

well (Fig. 3.13). Mean salinities also decrease towards the Southwest, indicating increasing amounts of second year ice along the cruise track.

In total, ice cores consisted of 24 % orbicular granular, 25 % mixed, and 48 % columnar ice, quite typical for this region of the Weddell Sea. The large amount of columnar ice also points to the prevalence of congelation ice growth under a closed ice cover and far away from the influence of open ocean swell and turbulence.

Core 041122TEX11 consisted of 3 % platelet ice at a depth of 1.50 to 1.85 m, embedded between granular and columnar ice. This indicates that this floe originated from or passed the large ice shelves along the southeastern Weddell Sea coast, and the underlying ice provides an estimate for ice growth during the drift to the sampling location of 0.35 m (columnar ice).

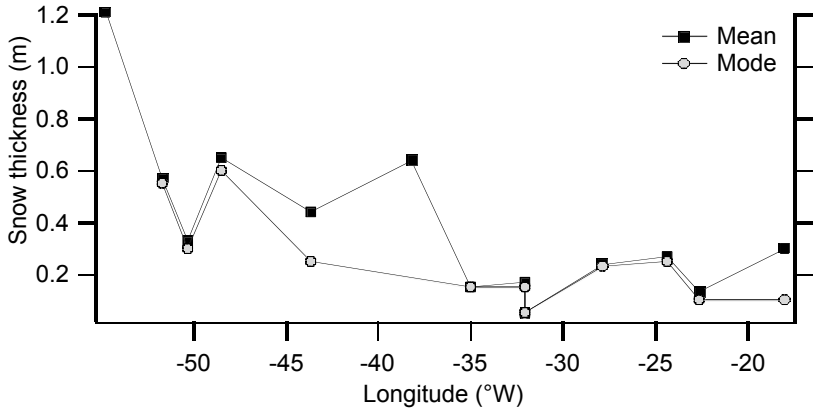

Fig. 3.11: Mean and modal snow thickness across the Weddell Sea, obtained from 50 m profiles (1 m point spacing) along the ships transect to the ISPOL floe

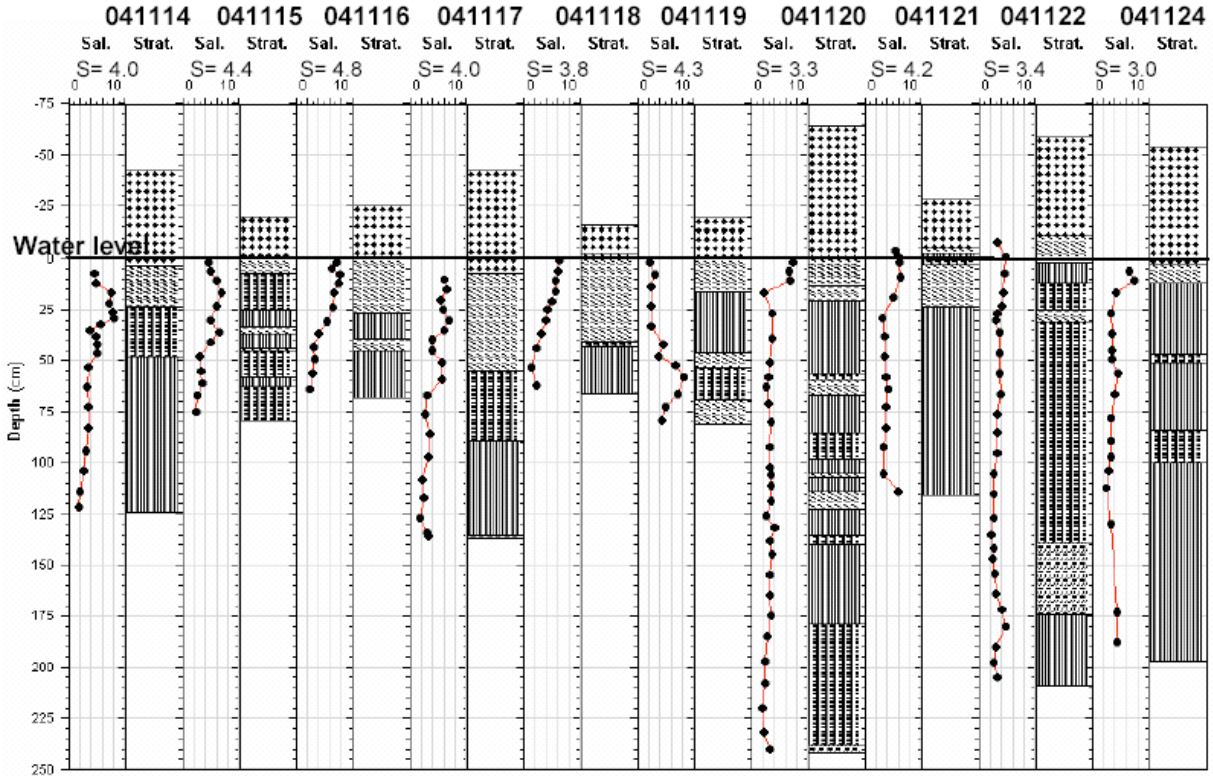

Fig. 3.12: Salinity and texture profiles with respect to their elevation below water level along the ships transect to the ISPOL floe, from east (left) to west (right). Mean salinities are shown in the top. Note the decreasing mean salinity and increasing thickness towards the west (right).

Snow and ice temperature profiles indicate that summer warming had already progressed upon our arrival at the ice edge, as most snow and ice temperatures ranged between 0 and -2°C (Fig. 3.13). Note that the snow in the early stations was warmer than later in the southwest, which points to progressed snow metamorphosis which is also responsible for increased radar backscatter in that region. Warmer snow was also accompanied by a more widespread occurrence of multiple ice layers in that region. However, temperatures at the snow/ice interface were too low to allow for substantial formation of superimposed ice.

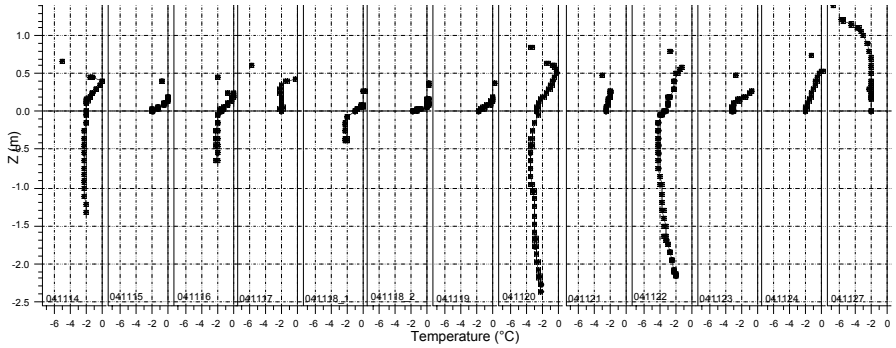

Fig. 3.13: Ice (5) and snow temperature profiles obtained during the transect to the ISPOL floe. Z = 0 m refers to the snow/ice-interface. The topmost temperature measurement in each panel indicates air temperature.

3.2.3 Measurements and results from ISPOL station

3.2.3.1 Ice thickness and ice types

3.2.3.1.1 Overview over ISPOL region

The scatterometer image in figure 3.7a) and the SAR image in figure 3.14 show three characteristic bands of sea ice with different radar backscatter extending from South to North: Along the Antarctic Peninsula, a bright band extended eastward to about 57°W. East of this, a darker band is visible, extending to about 55.5°W, where another bright sea ice zone begins. Interpretation of scatterometer imagery throughout the preceding winter revealed that the dark sea ice band actually represented first year ice formed in a prominent polynya off the Ronne Ice Shelf from March 2004 onwards, which was subsequently advected northward into our study region. To the west of this band, the high backscatter ice represents older and heavily deformed ice of probably second year origin, which might have drifted much slower than the less confined ice to the east, or which might even partially have recirculated from the North by currents on the Weddell Sea continental shelf. The bright ice in the east of our study region represents second-year ice, which has survived the 2003/2004 summer in the southern Weddell Sea. The differences between the latter two ice regimes was also visible from the distribution of snow thickness, which was measured during the deployment of drifting buoys spawning almost all three ice regimes (Section 3.1.2). For the first year ice, they ranged between 0.3 to 0.4 m around the southernmost buoys, whereas typical snow thickness on second year ice ranged between 0.6 and 1.2 m. Unfortunately, there are probably no snow measurements from the highly deformed ice in the West.

The different ice regimes are most clearly distinguishable by means of the helicopter-borne thickness measurements (see Section 3.2.2.1.2 for a general description). 5 flights were performed to characterize the large scale ice conditions in the study region, extending north, east, south, southwest, and west of the ISPOL floe (see maps in Figs 3.6 and 3.14). Figure 3.15 shows thickness distributions of three flight sections typical for the different ice regimes. In agreement with drill-hole observations

of snow and ice thickness at numerous locations (see below), the mode of the first year ice thickness distributions results from 1.6 to 1.8 m of ice and 0.3 to 0.4 m of snow. The second year ice is characterized by modal ice thicknesses of 1.6 to 2.5 m, with modal snow thicknesses of 0.6 to 1.2 m.

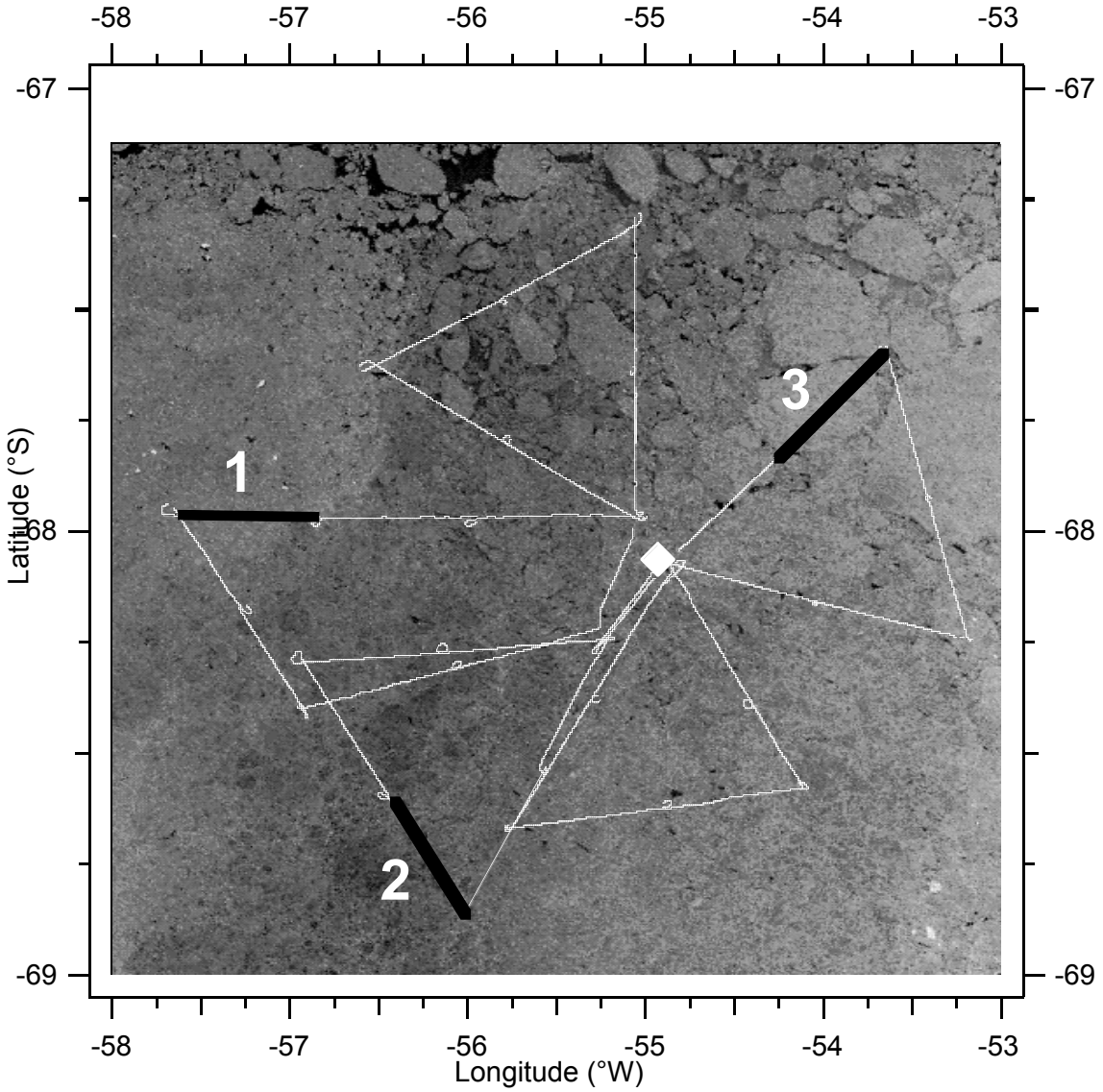

Fig. 3.14: Envisat SAR image of the ISPOL study region, acquired on 30 November 2004. At least three different ice regimes can be distinguished in the west, middle and east of the image based on different radar backscatter. The white diamond shows the location of the ISPOL floe on the same day, and white lines show HEM flight tracks which were drift corrected. Ice thickness distributions for the black sections are shown in figure 3.15.

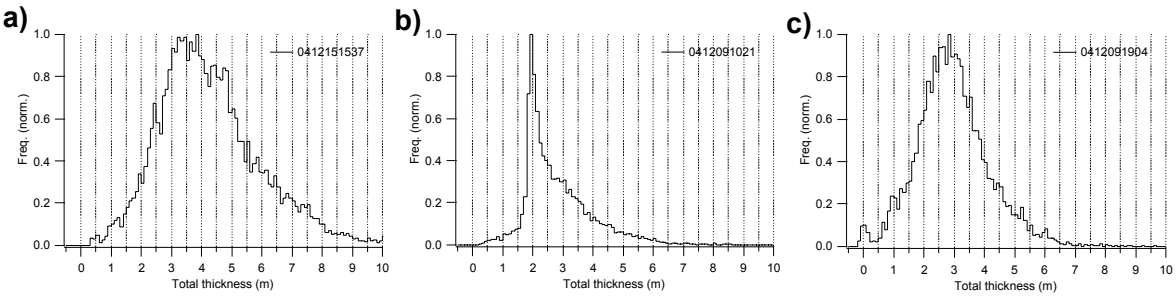

Fig. 3.15: Thickness distributions obtained by HEM surveying along sections 1 (a), 2 (b), and 3 (c) of the profiles shown in figure 3.14. Modes of the distributions represent very thick deformed ice in the West (a), first year ice with 0.3-0.4 m snow cover (b), and a mixture of first year ice and predominantly second year ice with snow thicknesses between 0.6 and 1.2 m (c).

3.2.3.1.2 Ice and snow thickness changes on ISPOL floe

On 27 November a survey of the ISPOL floe was performed with the EM Bird, flying densely spaced profiles across the floe. As this was the first day at the floe, it was still approximately 10x10 km^2 large. The obtained thickness distribution (Fig. 3.16) resembles the thickness distribution of predominantly second year ice very well (Fig. 3.15). In fact, the reconnaissance drill-hole measurements performed during the selection of the floe provide a confirmation for the predominantly second year origin of the floe, and a validation of the derived thickness distribution (see horizontal bars in Fig. 3.16). The mode at 1.05 m represents the locally formed first year ice which was mainly present at sampling sites 6 (bio coring) and 9 (Belgian site). The mode at 0 m ice thickness shows that in the beginning of the ISPOL drift our floe was surrounded by considerable amounts of open leads, mainly in the East.

Figure 3.16 also shows the corresponding thickness distribution obtained by pulling the EM31 thickness sounder along the skidoo tracks connecting sampling sites 7, 6, and 5 as well as 8 and 9. The thin ice of sites 6 and 9, as well as the thick ice of 5, 7 and 8 are well visible and agree well with the airborne thickness distribution. However, there is some disagreement of 0.2 m between the modal thickness of the thin ice obtained from the air and from the ground. This is probably due to the occurrence of widespread flooding at least on site 6, which was the largest thin ice site and contributed most of the data. While the effect of flooding was accounted for in the calibration of the ground measurements, the airborne measurements assume negligible ice conductivity, and therefore underestimate the thickness of flooded ice.

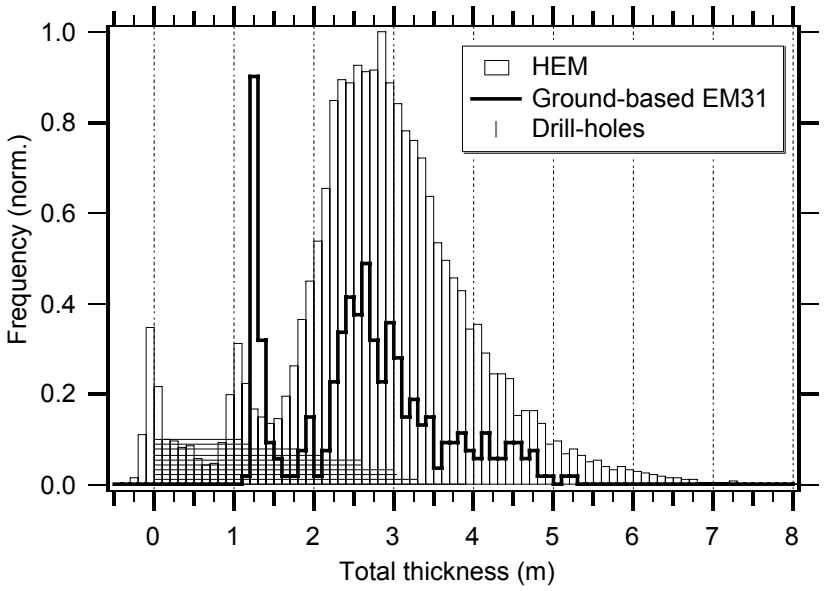

Fig. 3.16: Ice thickness distribution of the original ISPOL floe, obtained by HEM surveying on 27 November (bars) and by ground-based EM sounding along the skidoo track across sampling sites 7, 6, 5, and 8, 9. Horizontal lines show the results of 10 drill-hole measurements performed by the international floe reconnaissance team.

Due to repeated floe breakup, it was difficult to maintain the same ground-based thickness profiles for repeated observations of ice thinning. Only the old skidoo track between the former floe edge between sites 9 and 10 and the new floe edge between 9 and 8 could be repeatedly surveyed four times. Figure 3.17 compares the thickness distributions obtained along this 660 m long profile between 4 and 30 December. Unfortunately, due to the small sample size the histograms can only be displayed with 0.2 m bins. The figure shows that there was hardly any observable thinning of the thin ice, although there are increasing amounts of ice in the 1.0-1.2 m range, which are absent during the first measurement. There is a stronger decrease of about 0.4 m of the mode of the thick ice. However, dedicated careful measurements performed repeatedly at the same site to observe changes of ice conductivity revealed a strong increase of ice conductivity, which alone could account for the observed thinning. Therefore, our data presented in figure 3.17 suggest that the overall thinning was probably not larger than 0.2 m, with most of it due to the thinning of snow (Fig. 3.19).

We have also tried to measure ice thickness changes at dedicated ice mass balance stations, by means of heated wires frozen vertically into the ice. However, unfortunately there were several problems related to superimposed ice formation and melting around the former drill-hole and heated wire which prohibit proper analysis of those measurements. Although the mass balance stations were deployed to avoid major disturbances of the natural processes affecting ice melting, even the installations of those sensors caused already a too strong disturbance. This was also due to the timing of the experiment, when the summer warming had already commenced before arrival at the ISPOL floe.

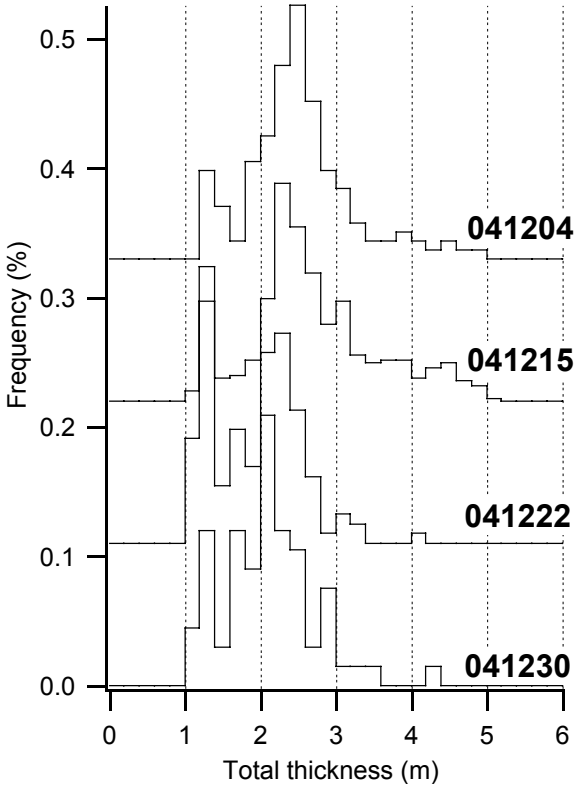

Fig. 3.17: Ice thickness distributions obtained from repeated ground-based EM profiling along the old skidoo track on Floe 9

On 17 December snow thickness was profiled along the skidoo track between RV *Polarstern* and the floe edge between Floes 9 and 10. 107 measurements with a point spacing of about 10 m were performed. The mean thickness was 0.6 m, and the resulting thickness distribution showed a broad mode between 0.2 and 0.5 m, as well as between 0.7 and 0.8 m (Fig. 3.18). This thickness distribution resembles well the occurrence of thinner snow on the first-year ice and thick snow on second year ice.

Repeated snow thickness measurements were also performed along the same 50 m profiles (1 m spacing) on sites 5, 6, 8, 9, and at the northernmost buoy about 30 nm north of ISPOL floe. Mean ice and snow thicknesses indicated that these sites were representative for first and second year ice in the whole region. Snow thickness measurements on site 6 were slightly biased by repeated crack formation across the profile, and the subsequent movement of the profile to some other location. The results shown in figure 3.19 show a general thinning of snow over the observation period at all sites. However, the thinning was less than 0.2 m at all sites. Note that 20 cm of ice thinning can supply enough melt water for the formation of 6 cm of superimposed ice or ice layers, if increases in ice density are neglected.

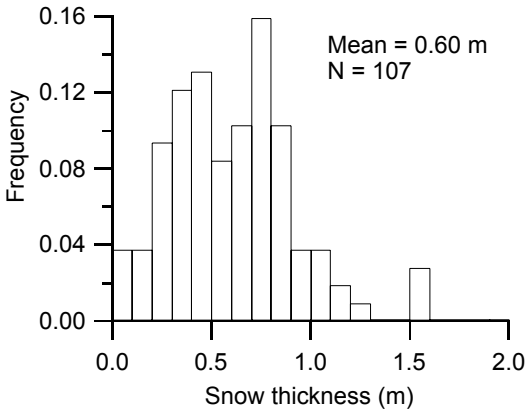

Fig. 3.18: Snow thickness distribution along the skidoo track between RV Polarstern and the floe edge between sites 9 and 10, obtained on 17 December

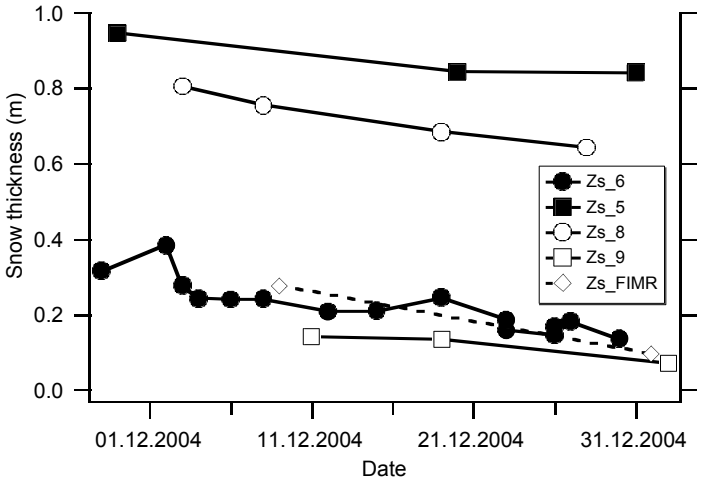

Fig. 3.19: Mean snow thickness observed and its decrease during the ISPOL study period determined along 50 m profiles on different sampling sites

3.2.3.2. Surface energy balance

The main objective for continuous measurements of the surface energy balance is to quantify the amount of energy which enters the snow-sea ice system. This energy forces changes of snow surface properties as wetness, grain size and stratigraphic features and controls heat fluxes within snow and sea ice.

To measure these atmospheric boundary conditions a radiation and weather station was set up on the floe as summarized in table 3.3. Radiation sensors were installed 1 m above snow surface to measure long- and shortwave radiation (incoming and outgoing). Additionally, air temperature, wind velocity and relative humidity were measured 2 m above snow surface to determine turbulent heat fluxes. These fluxes were computed using an algorithm by Launiainen (1995), whereas positive signed

fluxes are directed downward. All sensors were sampled in 10 s intervals and averaged 5 min means in the field.

The recorded data from all three places are well comparable, because the snow cover underneath and around all three sites of the station was of very similar thickness and stratigraphy. Furthermore the sites were chosen to be on thinner sea ice and snow cover than similar stations of the FIMR, hence comparisons of different snow and sea ice effects may be performed later on.

During the observation period melt processes at the base of the station's poles lead to a tilting of the whole station and effecting especially the radiation measurements. Therefore the station was re-levelled several times, which will be corrected during further data processing.

Table 3.3: Registration times and set-up positions of the radiation and weather station. Interruptions from a continuously registration result from the break-up of the floe.

Start of registration			**End of registration**			**Position**
Date	**DOY**	**Time**	**Day**	**DOY**	**Time**	
29.11.04	334	16:45	02.12.04	337	15:10	Patch 6, close to Patch 5
03.12.04	338	15:30	25.12.04	360	15:25	Patch 6, close to Patch 7
27.12.04	362	14:50	01.01.05	001	21:10	Patch 9

The most important time series, surface energy balance and (wavelength integrated) albedo, are presented in figure 3.20 as full resolution raw data (only obvious outliers were filtered out) and daily means. To exclude hours of low sun elevation, which lead to an artificially amplified diurnal cycle, daily mean values of albedo are only computed from 6 hours around highest sun elevation. Means of the energy balance, in contrast, include full (24h/day) data to consider natural variations due to sun elevation. Mean values are only computed for days with full data coverage.

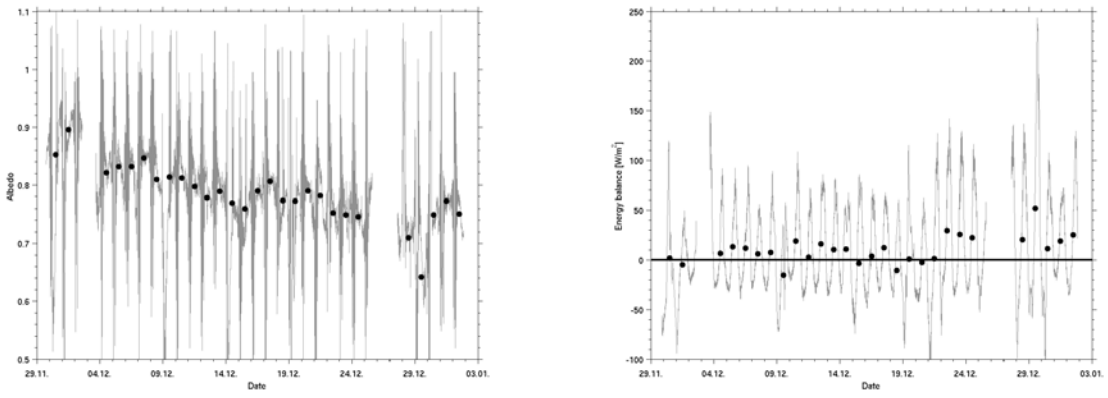

Fig. 3.20: Albedo (left) and Surface energy balance (right) measured on Patch 6 until 25 December and on Patch 9 from 27 December onwards. Full resolution time series and daily means are presented as grey lines and black dots, respectively.

During the entire observation period a steady decrease of albedo from 0.90 at the beginning of the observation period to 0.75 at its end was recorded (Fig. 3.20). This decrease was only interrupted by some events of new snow fall as on 16, 21 and 26 December. The minimum albedo of 0.64 on 29 December is probably an artefact, because on this day the station was significantly tilted - even after being re-levelled twice. Mean albedo over the whole registration period was 0.786.

Related to the decrease in albedo the total amount of absorbed shortwave radiation increased with time. Parallel longwave radiation balance and turbulent heat fluxes depended on overall weather conditions and did not show any trend. Hence the total surface energy balance, computed from the sum of shortwave and longwave radiation balances as well as turbulent heat fluxes, increased form daily means of ~0 W/m^2 to >20 W/m^2 with an overall mean of 10.66 W/m^2, equalizing 0.92 MJ/m^2 (Fig. 3.20). Diurnal variations range from 150 W/m^2 on mainly overcast days to <300W/m^2 on clear sky days. But the radiation balance was negative during hours of low sun elevation all over the observation period, and on some clear sky days even the daily mean showed a heat flux out of the snow cover to the atmosphere.

These considerations of snow-atmosphere interactions partly explain the daily refreezing of near surface snow layers and give reasons why the 0° C isotherm did not reach the snow / ice interface (see Chapter 3.2.3.4.1). It is expected that the mean energy entry into the snow needs to be significantly higher to allow the formation of thicker layers of superimposed ice.

Further data processing will aim to a final balance of the surface energy for the whole ISPOL time span (including days with partial data coverage). This will include further measurements as available from RV *Polarstern*'s radiation and meteorological sensors and additional comparisons with FIMR datasets (see chapter 2.2).

3.2.3.3 In-situ spectral albedo measurements

Spectral albedo measurements were performed in order to observe the evolution of snow cover in terms of its reflection properties during the ISPOL drift. This was done by using a *Spectron Engineering* SE590 portable data-logging spectroradiometer. The instrument measures a continuous spectrum in 256 bands in the wavelength region 400 to 1069 nm. Spectral albedo was determined by recording cosine corrected sky and ground spectra and calculating their ratio. This setup was successfully tested during several campaigns in the Arctic.

However, severe problems showed up during the ISPOL experiment. Ground and sky spectra were observed over different snow thicknesses, under different light conditions, at different daytimes and the instrument was tested with reflecting materials other than snow. But with snow, EACH of the recorded datasets ended up in albedo values larger than one.

This effect also showed up in the time series of albedo recorded on two weather stations on the ISPOL floe where, however, this was limited to daytimes with low solar elevation.

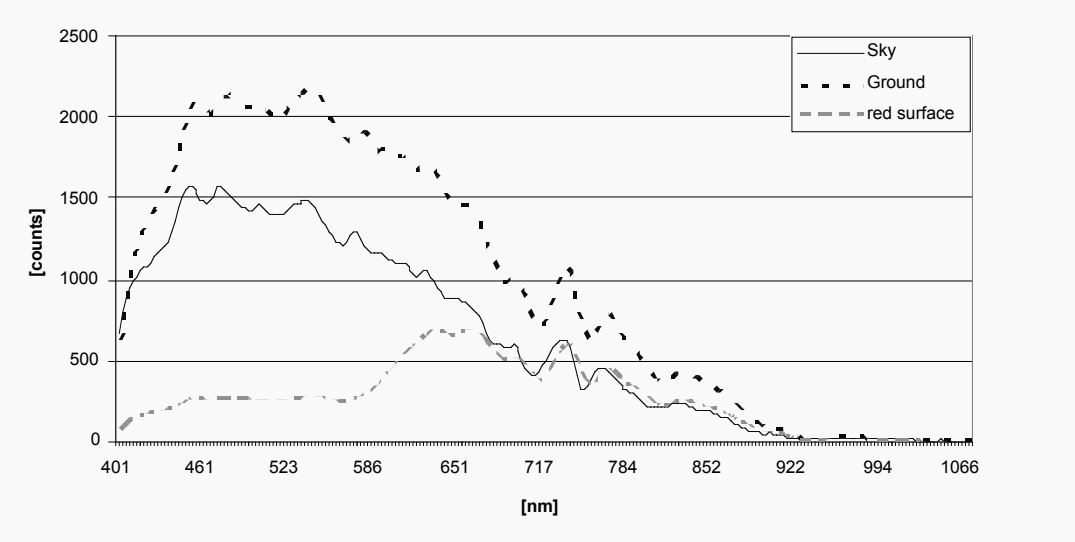

Fig. 3.21: Cosine corrected spectral response [counts] from sky, snow surface and a red surface, acquired on the ISPOL floe, 2 December 2004, 10:30 a.m.

Figure 3.21 gives an impression of the phenomenon mentioned above. Ground measurements reach values that are up to two times larger than the corresponding sky values. The shape of the spectra is very similar as one should expect from a snow surface with an albedo that is almost constant up to at least 700 nm.

The lower curve represents a red surface that was scanned to test the instrument. It is - at least in the visible wavelength region - far below the sky value with a peak in the red, as expected.

After a lot of testing and discussing, the measurements were finally stopped at the end of December since no change in this problem could be observed. Multiple reflection effects were discussed as being the reason for the snow spectra that were much too high compared to the sky values. This discussion has not come to an end yet.

3.2.3.4 Ice core and snow properties

3.2.3.4.1 Temporal evolution of snow temperature, density, wetness and salinity

Daily measurements of vertical snow temperature profiles were performed during the whole ISPOL drift period. The measurements were carried out with a hand-held PT100 thermometer stuck into the vertical walls of snow pits, which were excavated on different locations for each measurement to avoid disturbances of the temperature fields. We consider manual measurements as the only means to obtain accurate temperature measurements in spring and summer, because fixed thermistor strings cause melting by radiation absorption, and therefore lead to wrong measurement results.

Several spots with different snow thicknesses were chosen, mostly close to the snow thickness monitoring sites (Section 3.2.3.1.2). Therefore, characteristic differences of the snow temperature evolution between thin and thick snow could be studied.

For more than a week measurements were performed every three hours throughout the day in the beginning of the drift station in order to investigate the amplitude of the diurnal snow temperature cycle and the time of its maximum. The results showed the maximum surface temperatures at around 17:00 UTC (13:00 LT), and the minimum at around 8:00 UTC (4:00 LT).

Figure 3.22 gives an example for the temperature evolution of the snow cover for sites 8 and 6 with each measurement performed at 17:00 UTC ± 2 hours. Like in figure 3.19 the decrease of 0.15 to 0.20 m in mean snow thickness can be seen at both sites. At both sites, warming was quite strong in the beginning with rather little change afterwards, except for the last two days. The zero degree isotherm moved only very slowly downwards to the snow/ice interface which showed only a slow warming and was never at 0°C during the observation period.

On most snow pits, we have also determined vertical profiles of dielectric snow properties by means of a snow fork (manufactured by TOIKKA, Finland), which can be converted to snow wetness and density. Increases of snow wetness are shown in figure 3.30. Density estimates will be compared with densities determined by volumetric density measurements. In general, we will investigate if there were any changes in the density profiles due to melt-freeze cycles and meltwater percolation.

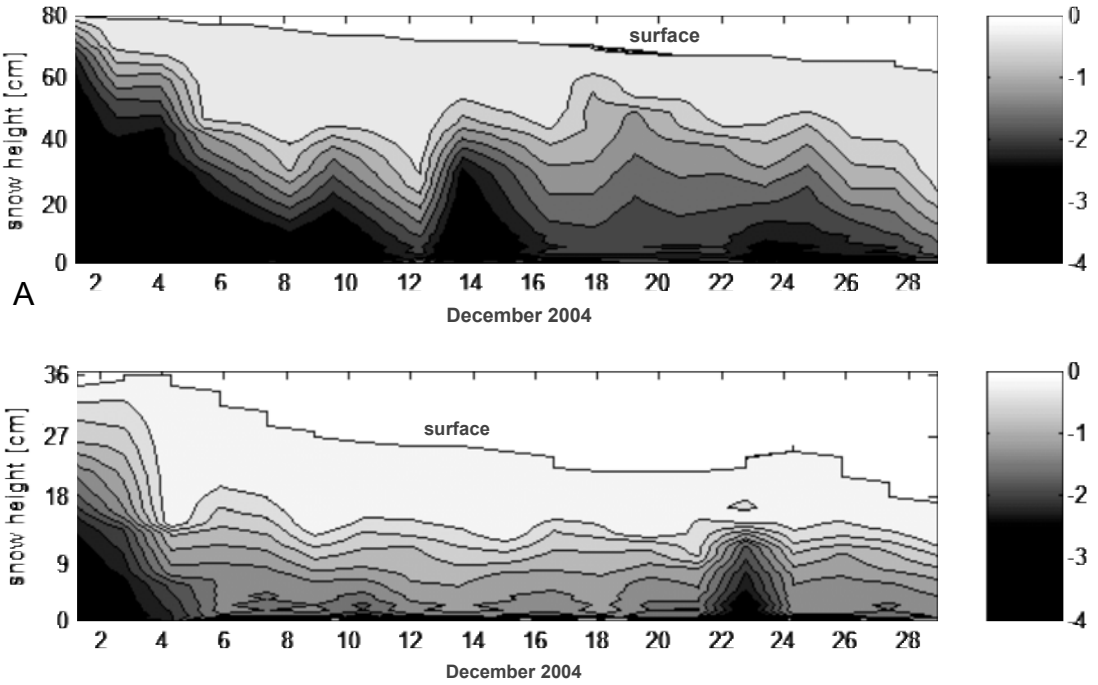

Fig. 3.22: Evolution of 17:00 (UTC) snow temperatures on the ISPOL floe in thick snow (A, patch 8) and thin snow (B, patch 6). December 2004. The upper line marks the development of snow surface height.

3.2.3.4.2 Texture, salinity, $\delta^{18}O$, and temperature of different ice types and sampling sites

During transect and drift stratigraphy analyses were performed on 74 sea ice and surface cores. The processing consisted of thin and thick sections, sampling for tomographic analyses as well as salinity measurements and $\delta^{18}O$ sampling. $\delta^{18}O$ measurements will be performed by A. Worby in Hobart, Australia, once samples have been shipped to their laboratories. Time series (TS11) cores, drilled on the Bio Site, were processed as shown in figure 3.23, whereas slight deviations from the scheme depended on core properties.

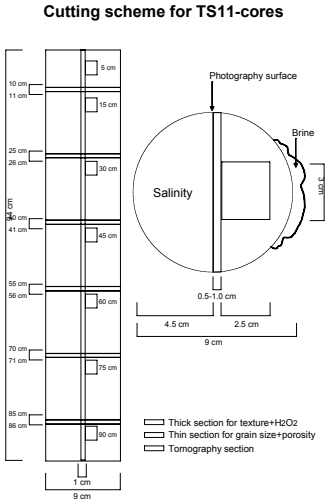

Fig. 3.23: Cutting scheme for time series cores

In addition to texture analyses for all the biological time series ice cores, we have also observed temporal changes of salinity and temperature at a number of other places which represented different ice types than the thin first year ice at the biological time series site. Note that the thick ice was most abundant in the study region and on the ISPOL floe (Figs. 3.15 and 3.16). Texture and salinity profiles as well as snow thickness and properties point to the first year origin of the thick ice at site 9, where the sediment trap and optodes were also installed (Fig. 3.24). All these properties were strikingly similar to an ice core drilled at the southernmost buoy site "Whiskey" at about 68°50'S (Fig. 3.6). The first-year origin of that site also follows from the ice thickness distribution obtained there (Fig. 3.15), and from the temporal development of scatterometer signatures before the cruise (Fig. 3.7). Ice cores and snow thickness from sites 5 and 8 indicate the second year nature of those floe sections (Fig. 3.24). Note that the snow thickness at both sites was very large, and that the freeboard lower than -0.15 m. Upon drilling, water came up through the holes for more than a week, flooding large areas around the drill-holes. This showed that the ice was quite impermeable in the beginning, and that negative freeboard is not necessarily accompanied by flooding, although there was a 5-10 cm thick slush layer present at the snow ice interface.

Figure 3.24 also shows the warming and desalination of the thick ice between the beginning and end of ISPOL. Although from visual inspection it was clear that the upper ice layers became very porous towards the end of the drift, this is not reflected in calculations of brine volume from temperature and salinity. Therefore we believe that the decrease of bulk salinity in the upper layers is rather an artefact due to brine loss during sampling of the porous ice than a real fact.

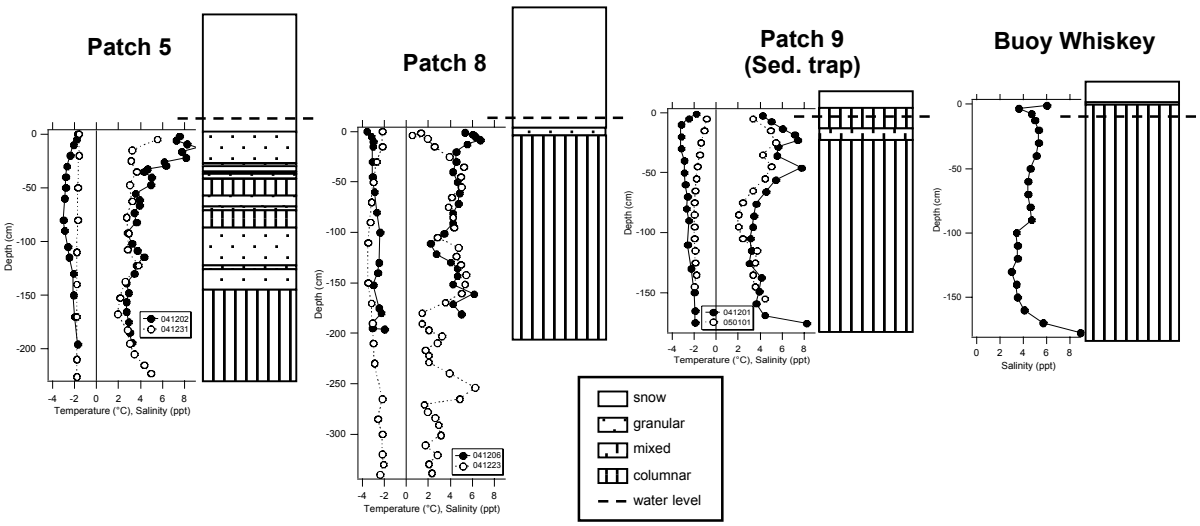

Fig. 3.24: Texture, salinity, and temperature profiles of thick ice in the ISPOL region. For three cores, also the salinity and temperature changes to the end of the study are shown.

3.2.3.4.3 Superimposed ice formation

First formation of superimposed ice was observed on Patch 6 on 11 December 2004. But the distribution was horizontally discontinuous and heterogeneous on a scale of decimetres and thicknesses amounted to a few centimetres only. The first observation of superimposed ice was somehow surprising, because it formed without the 0°C isotherm reaching the snow ice interface. This means, that fresh water ice layers (in the snow) and superimposed ice formed due to other processes than liquid melt water percolation.

During the drift the amount of superimposed ice increased, but it was very difficult to quantify the findings, because thickness and distribution remained very patchy until leaving the floe. Nevertheless, ice layers were frequently observed above opening gaps, probably composed of snow ice mixed with snow melt water. Larger grained ice lenses occurred however in the bottommost snow layers. A sequence of such a layering is shown in figure 3.25, where snow ice with salinities of 4.2 (bottom) to 0.0 (top) underlies an ice layer with grain sizes of up to 10 mm. More detailed analysis will be performed later on, using $\delta^{18}O$ measurements to distinguish atmospheric and oceanic contributions to the total ice mass.

Additionally to the observations on our floe surface cores were drilled twice on a more northern floe hosting a FIMR buoy and another floes near the ice edge (see

Fig. 3.6). On these two more northern floes superimposed ice formation was already much more developed, because those floes had experienced more summer-like weather conditions. The FIMR floe surface consisted of a 4 cm thick layer of superimposed ice with 3 cm highly metamorphic snow on top, floating on a 13 cm thick gap layer. Grain sizes range from 2 mm to 10 mm as shown in figure 3.25. On these floes the ice layers were even much more consolidated than comparable layers on the ISPOL floe.

a) b)

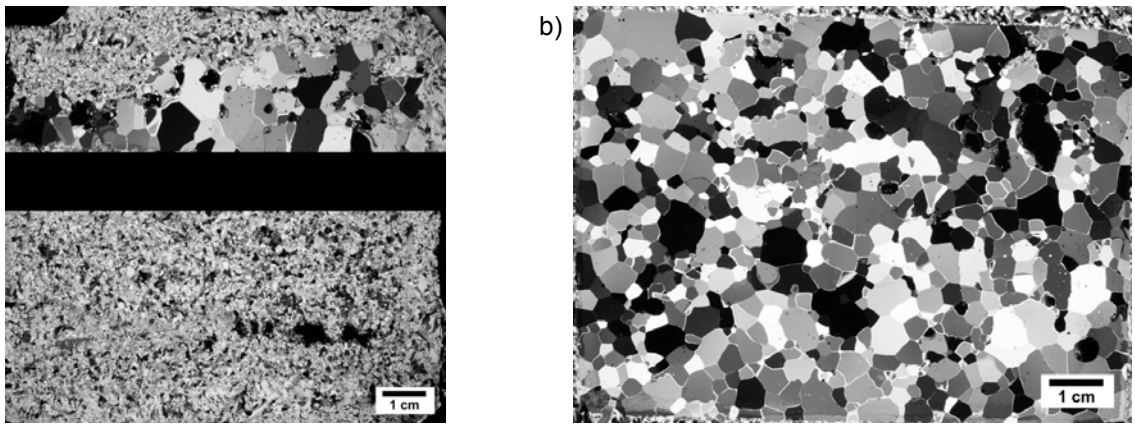

Fig. 3.25 left: Vertical thin section of a surface core from Patch 9 on 01.01.05. The section consists of an upper ice layer with grain sizes up to 10 mm and a lower small (ca. 3 mm) grained part. The middle section was of very loose grains and hence lost during thin section preparation. Right: Horizontal thin section of superimposed ice layer from FIMR buoy floe on 1 January 2005.

Figure 3.26 gives an example for the planed detailed superimposed ice grain size analyses. Single grains can be detected by digital image processing and histograms of grain sizes will be computed to describe superimposed ice formation processes. Grain sizes of samples taken near the ice edge raised up to 178 mm^2 (approx. diam. 15 mm) with a mean grain size of 33 mm^2 (approx. diam. 6,5 mm).

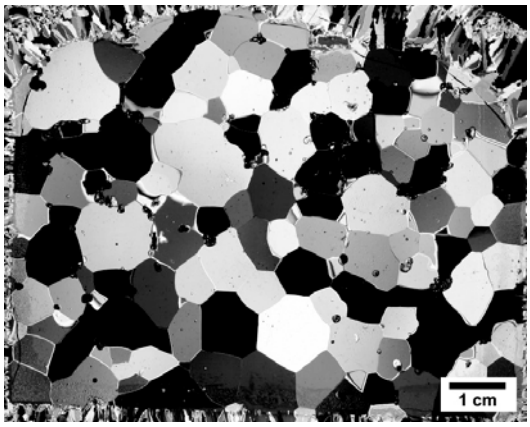

Fig. 3.26a: Horizontal thin section of super-imposed ice from a floe at the ice edge on 4 January 2005

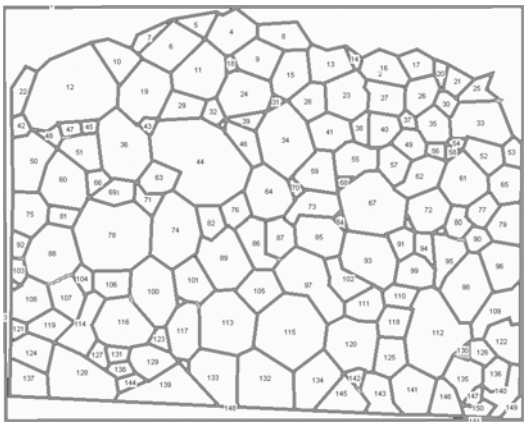

Fig. 3.26b: Analyzed ice grains

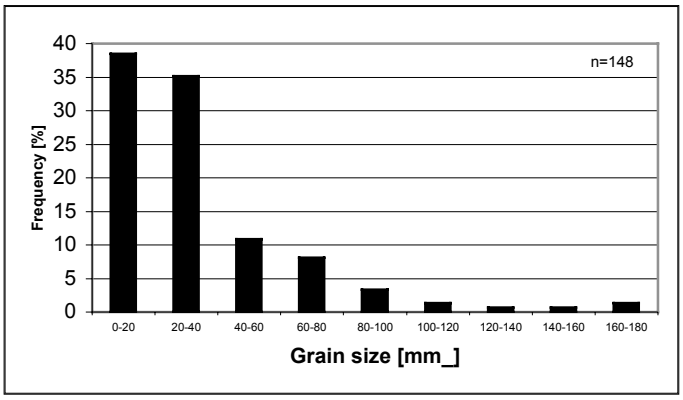

Fig. 3.26c:. Statistical mean grain size analysis of the section shown in Fig. 3.26b

3.2.3.4.4 Tracer studies of snow meltwater percolation

Two different fluorescent colour tracers were used to study melt water percolation to and permeability of ice layers, especially superimposed ice layers. Both tracers are commonly used in hydrologic experiments and were already used for melt water flux analysis in Arctic sea ice melt ponds. Some first experiments were performed using Uranin, but due to a relatively rapid decay under solar irradiation their results are difficult to analyze and hence they are not presented here. Therefore Sulforhodamine (SR) was used on 7 tracer-field and 4 local-injection experiments. Additional tracer study set-ups were tested (e.g. horizontal injections into distinct horizontal snow layers), but they did not show clear results, because it was not possible to identify the original injection point afterwards.

The tracer-field experiments were performed to study melt water percolation from the snow surface to deeper snow layers. Therefore 250 ml of a 100 mg/l solution of SR were sprayed homogenously over a 1 m by 1 m snow surface (see photo in Fig. 3.27), whereas the tracer solution was cooled to below 2°C before injection to avoid artificial local melt processes as far as possible. As control measurements showed, with this method only the uppermost 1 cm to 2 cm were initially affected by colour tracers. Afterwards surface cores (snow + uppermost ice layers) were drilled or sawn to analyze the vertical distribution of tracer particles with a spatial resolution of 1 cm to 2 cm and a temporal resolution between 3 hours and 2 days.

The second type of experiments differed only in the way of injecting the tracer itself. Here 2 ml of 100 mg/l SR solution were injected directly on top of an already existing layer of superimposed ice. This was performed by drilling vertically from the snow surface to the ice layer and afterwards injecting the SR with a pipette at the bottom end of the drill hole. This method allows analysis of the melt water permeability of the underlying superimposed ice and furthermore it is possible to investigate superimposed ice formation processes in more detail. Analyzing radial tracer concentrations from the point of injection to the sides showed horizontal melt water fluxes are negligible on level sea ice.

Further applications of this method might enable a quantification of the importance of both formation processes of superimposed ice: settling of existing ice layers and refreezing of percolated melt water.

A first result, showing how melt water fluxes can be detected with this method is presented in figure 3.27. The figure shows a time series of relative tracer concentrations progressing through a 35 cm thick snow cover (on Patch 9). The surface injection took place on 28 December 2004 at 14:30, whereas analyses were performed 5 and 78 hours later. After 5 hours, the tracer had progressed downwards only by about 10 cm. However, after 78 hours almost all tracer solution had percolated to an ice layer at a height of 10 cm above the snow/ice-interface. Detailed results and interpretations of these tracer experiments are not yet available, because they need to be related to small scale variations of snow stratigraphy and meteorological events.

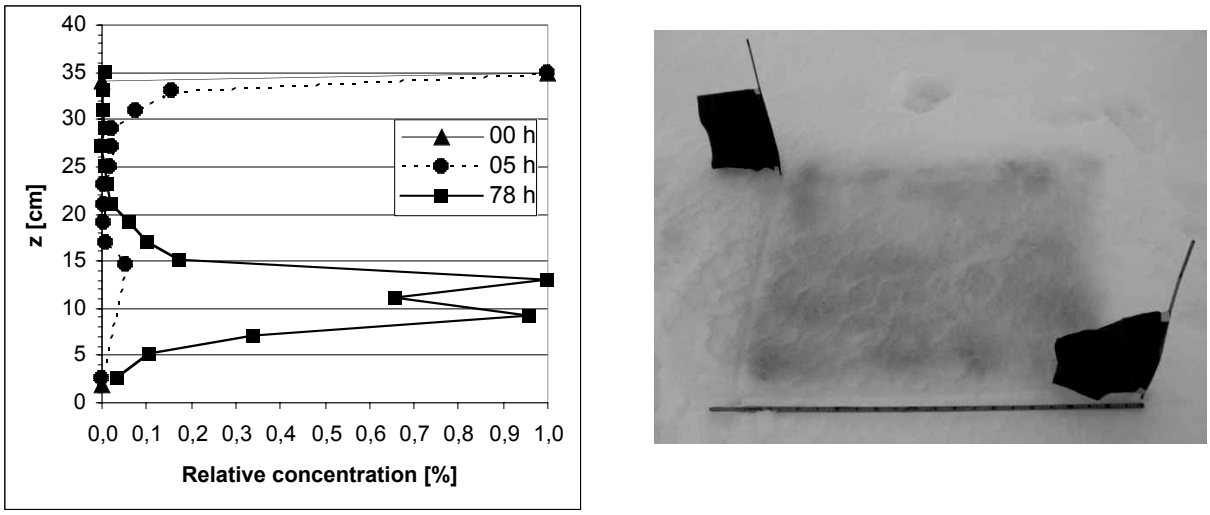

Fig. 3.27: Temporal evolution of relative Sulforhodamine concentrations (left) at a tracer field as shown on the right

3.2.3.5 Satellite remote sensing

3.2.3.5.1 AVHRR – visible and near infrared reflectivity

RV *Polarstern* receives several images a day from the *Advanced Very High Resolution Radiometer* (AVHRR) – sensor on the NOAA polar orbiting satellites. These images are transferred real time in *High Resolution Picture Transmission* (HRPT) format with a spatial resolution of 1.1 km by 1.1 km in either 5 or 6 channels covering the visible (red), near and thermal infrared wavelength regions. These images are mainly used for meteorological forecasts and navigation.

During the ISPOL cruise information from the AVHRR channels 1 (580 – 680 nm) and 2 (725 – 1100 nm) was collected to observe the sea ice cover in the Weddell Sea and perform studies on the spectral development of the snow/sea ice surface on the ISPOL floe and the surrounding areas.

One important limitation is to be made when it comes to the use of AVHRR imagery and visible/near infrared satellite images in general, which is that – because of the disturbing influence of cloud cover – one is dependant on clear sky conditions for the analyses. There is also an effect of water vapour in the air column that cannot always be neglected.

One main objective was to derive changes in surface properties from surface reflectivity.

The *Normalized Difference Snow/Ice Index* (NDSII) (De Abreu and LeDrew, 1997) is a suitable tool for this task. It is based on the reflection difference of channel 1 and 2 (ch1-ch2), normalized by their sum (ch1+ch2).

Considering a strong decrease of reflection in the near infrared with the presence of liquid water in the upper snow column with a coincident unchanged reflection in the visible, the index values should increase with increasing snow wetness. Previous studies used this method to derive the time of snow melt onset by isolating the day with the strongest index increase.

Apart from the amount of liquid water, grain size and density are the variables with the strongest influence on the index value.

The NDSII was used in two ways. First, its temporal development was observed by following drifting floes or buoy positions (“floe tracking”). Second, the index was plotted for larger areas to get an impression of its spatial distribution and, in consequence, the spatial distribution of surface properties (“index mapping”).

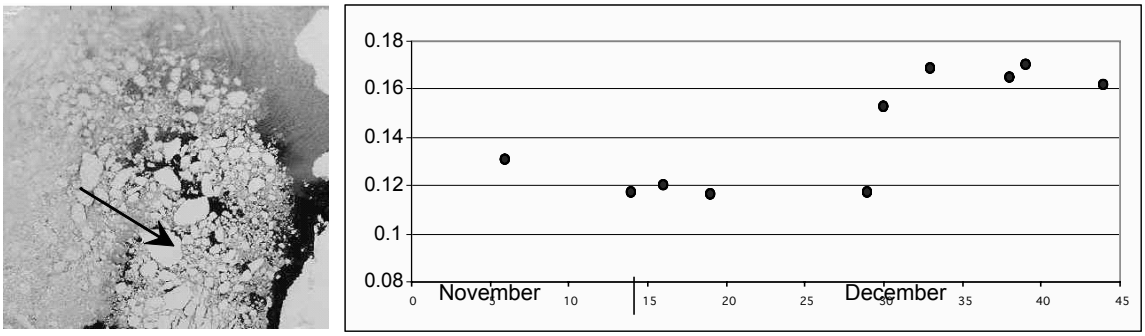

Fig. 3.28: Development of NDSII values for a large floe in the southern Weddell Sea for clear sky events in the time period 15 November 2004 to 31 December 2004

Figure 3.28 gives an example for the NDSII development of a floe in the southern Weddell Sea. It shows an abrupt increase of NDSII values in the middle of December. This obvious change suggests an event that is affecting the surface properties, i.e. a melt event. Figure 3.29 shows the temporal development of the calculated index at the ISPOL position. Unfortunately, rare clear sky conditions for the observed time period prevented us from more clearly identifying the temporal

change. Nevertheless, also here a strong increase of NDSII values can be seen around the middle of December.

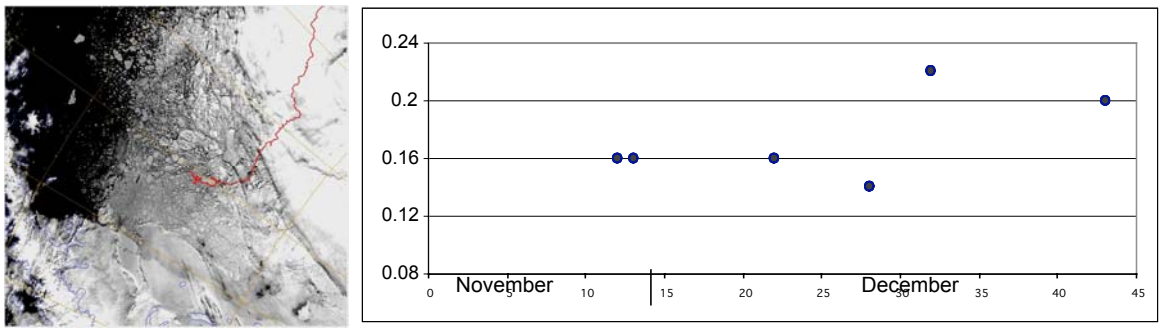

Fig. 3.29: Development of NDSII values for the ISPOL floe for clear sky events in the time period 15 November 2004 to 31 December 2004

This curve can now be compared with the wetness measurements that were taken several times a day in different snow depths across the ISPOL floe. Figure 3.30 shows a coincident increase of surface snow wetness beginning around the middle of December.

These measurements were taken at various locations along a profile on the ISPOL floe.

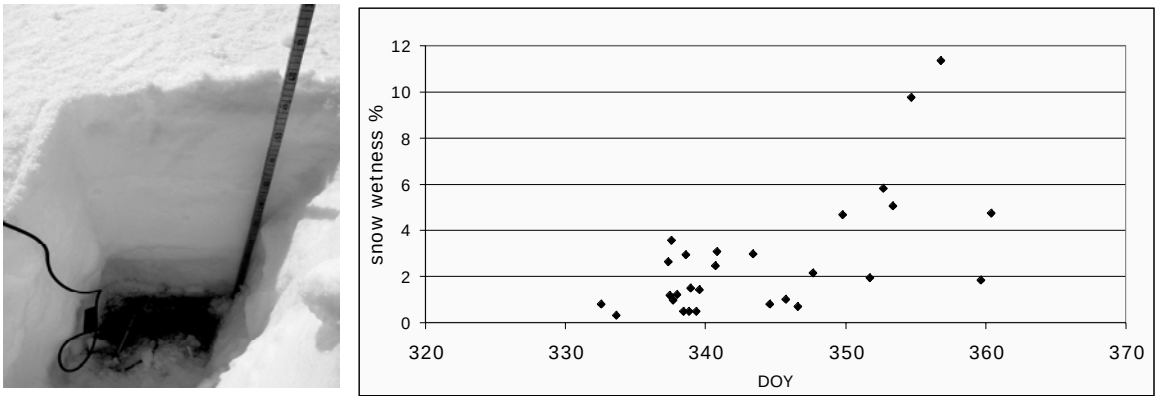

Fig. 3.30: Development of surface snow wetness values for the ISPOL floe at patch 6, where average snow depth was app. 20 cm

With all the ground data that were obtained during the 2 weeks of steaming through the ice to the final ISPOL floe and the following 5 weeks drift, a huge data base is now available for the validation of satellite data for this region in this time of the year. Another application for the NDSII is the monitoring of its spatial distribution to get an overview about surface properties.

For this purpose, the index was calculated for each pixel and mapped in a new image. Figure 3.31 gives an example for the result of this application.

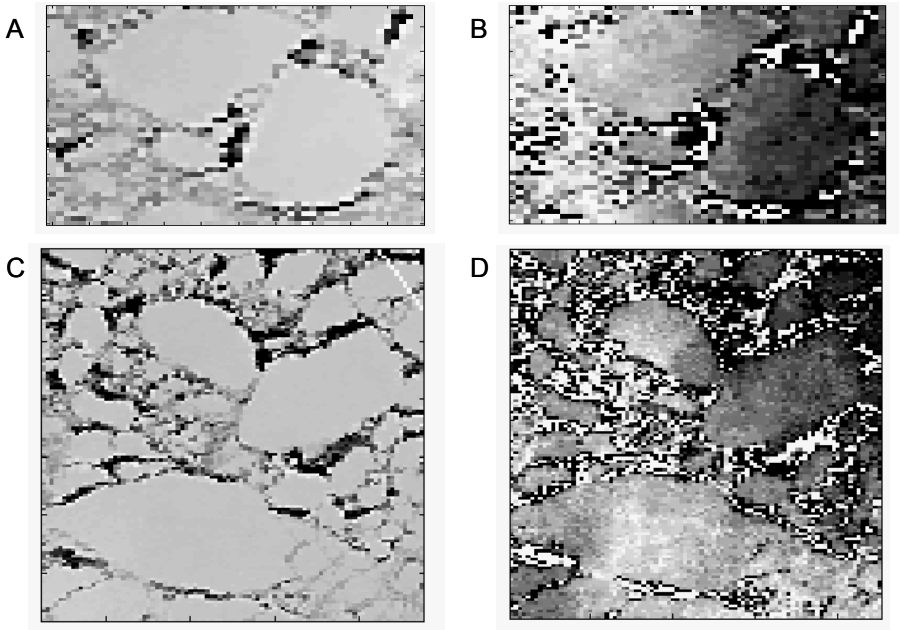

Fig. 3.31: Images of floes in the Weddell Sea from AVHRR channel 2 (near infrared, fig. A and C) and the corresponding images of the NDSII values (Fig. B and D)

It can be seen from figure 3.31 that in the NDSII images spatial features become visible that were not apparent in the channel 2 images. Light areas in these images mark high index values.

These images were used to choose interesting spots to be sampled by helicopter and to obtain coincident in situ measurements. Unfortunately, a combination of poor clear sky conditions, helicopter availability and big distance from the ship to the floes led to only very little validation data for the spatial NDSII variability during the ISPOL cruise.

3.2.3.5.2 SSM/I brightness temperatures

During the course of the ISPOL drift station, up to four real time satellite images a day were received from the DMSP (*Defense Meteorological Satellite Program*) – satellites. One sensor of those carried by the DMSP - platforms is the Special Sensor Microwave Imager (SSM/I). It records the earth's microwave emission in 7 channels ranging from 19 to 85 GHz each (except from the 22 GHz) as vertically and horizontally polarized radiation. The spatial resolution is approximatly 25 km by 25 km for the 19, 22 and 35 GHz channels, and 12.5 km by 12.5 km for the 85 GHz channels.

The *Sea Space* Satellite Image Receiving facility on board RV *Polarstern* automatically dumps only the SSM/I products total ice concentration, multi year ice concentration and first year ice concentration. Therefore, in order to receive also the

single channels' raw data and thereby obtain a basis for further analyses, computing routines were adjusted.

This made the raw information on the brightness temperatures available for the time period 10 December 2004 to 5 January, 2005.

The preliminary results presented here are based on this data set, which consists of mostly two passes a day – one in the morning and another one in the evening – giving useful coverage of the ISPOL area and the rest of the Weddell Sea.

Development of brightness temperatures during the ISPOL drift
Figure 3.32 shows the development of brightness temperatures (Tb) for the area of the ISPOL station. The 3 channels giving highest contrasts are plotted for the pixel containing the drift station. No obvious trends are detectable for either channel. Remarkable is the strong diurnal cycle which can be identified for the days when both - morning and evening passes - were obtained, esp. in the time period from 21 December until 25 December with Tb being higher in the evening than in the morning.

Furthermore, the evening values of 37 GHz brightness temperatures are remarkably higher than the 85 GHz values whereas the morning values turn out to be similar or even lower.

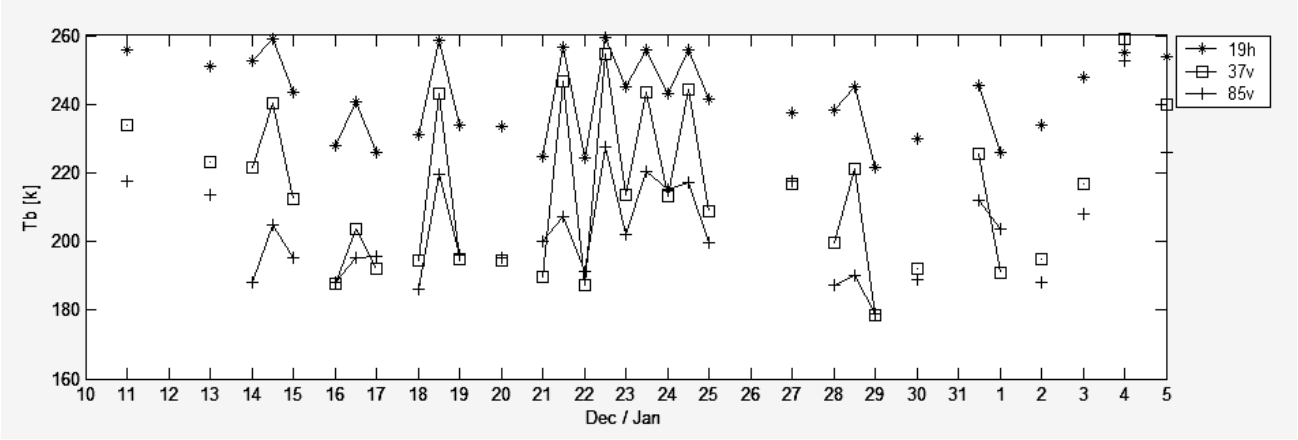

Fig. 3.32: Development of SSM/I brightness temperatures [Kelvin] around the ISPOL station from 10 December 2004 until 5 January 2005

The 19 GHz channel shows almost constantly the highest values compared to the 37 GHz and 85 GHz channels which is typical for the north-western Weddell Sea region that is characterized by high multiyear sea ice concentrations. In the eastern Weddell Sea, where first year ice is predominant this relation is reversed, and 37 GHz values are higher than 19 GHz values. Furthermore, figure 3.33 shows a clear flattening of the brightness temperature curves in this region for the investigated channels. Apart from this, the diurnal cycle in all channels is less pronounced or not present at all.

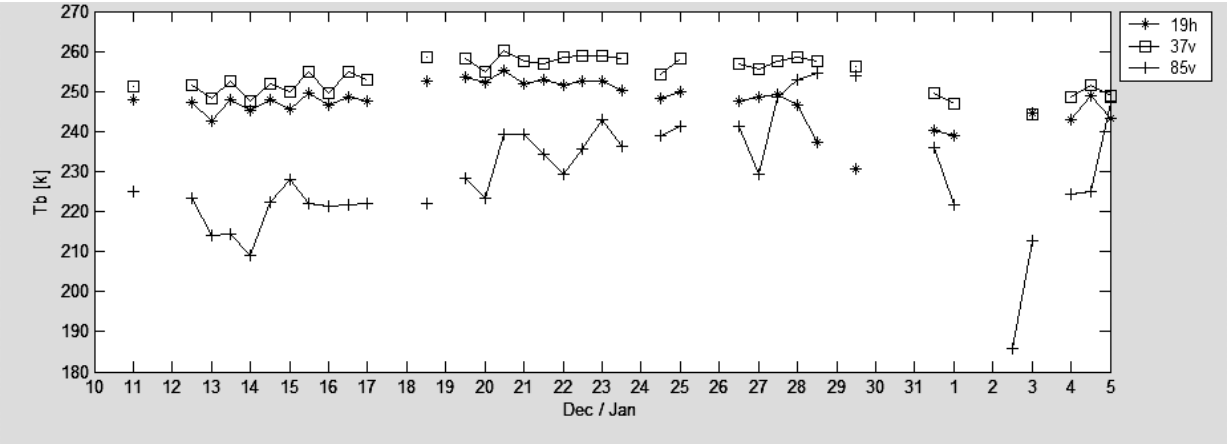

Fig. 3.33: Development of SSM/I brightness temperatures [Kelvin] for a pixel in the central Weddell Sea

Figure 3.34 underlines the presence of a distinct diurnal cycle of brightness temperatures in the north-western Weddell Sea. The distribution of brightness temperatures in the morning of 23 December is characterized by a warm band parallel to the Larsen ice shelf and cold areas around, in the evening this cold area turns very warm and extends like a plume to the west and is limited by a cold ellipsoid area in the south.

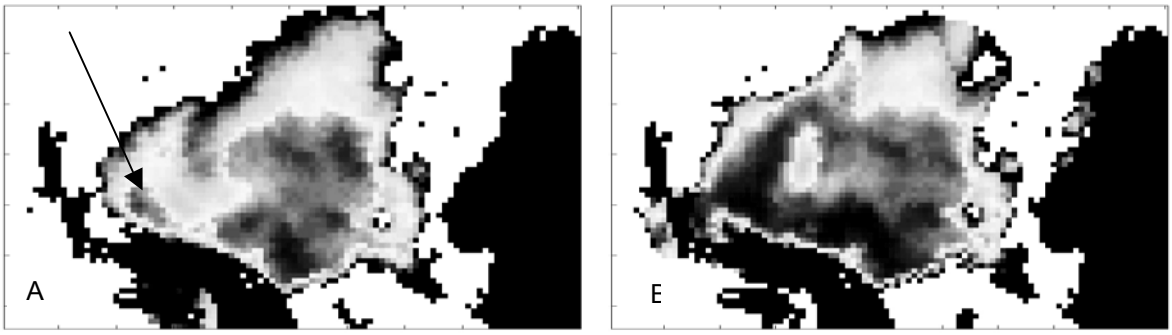

Fig. 3.34: Brightness temperatures in the Weddell Sea (dark=warm, bright=cold) as observed from the SSM/I at 19 GHz (horiz. Pol.) at 23 December 2004, 7:43 (A) and 23:11 UTC (B). Approximated position of RV Polarstern is marked with an arrow in figure A.

A similar change from the morning to the late evening is observed in all the other available passes, only the shape of the warming up area west of the Larsen Ice Shelf varies from day to day. In some cases it becomes very obvious that this shape clearly follows cloud patterns as recorded by the AVHRR so that a difference in atmospheric longwave radiation is suggested as being the cause for the diurnal changes in this area. With this, longwave energy input to the surface would be largest during daytime when clouds are present, warming up the surface in the time between morning and evening.

The mean strength of the diurnal cycle as expressed by the mean difference in brightness temperatures between morning and late evening for the time period 10 December 2004 to 5 January 2005 is revealed in figure 3.35. Again, the north-western part of the Weddell Sea is clearly an area of enhanced surface variation within one day.

Remarkable is also the difference in location of the maxima of the mean change of brightness temperatures between the channels 19 GHz hor. polarized (Fig. 3.35A) and 37 GHz vert. polarized (Fig. 3.35B). The strongest diurnal cycle for the former is found to be parallel to the Larsen Ice Shelf with another maximum parallel to the northern ice edge, whereas for the latter the values are strongest to the northeast of Larsen, gradually decreasing towards East.

The emphasized values close to shelf breaks (coastal polynyas) and the ice edge suggest an influence of open water to this effect.

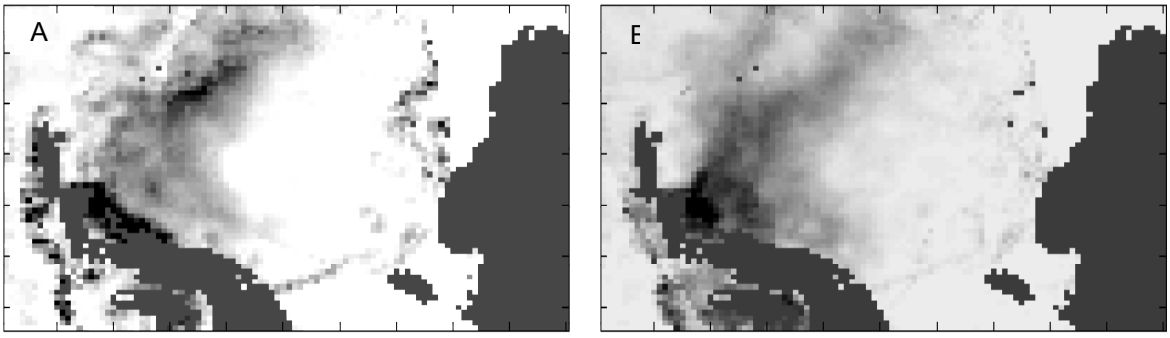

Fig. 3.35: Strength of diurnal cycle of brightness temperatures as an average of the time period 10 December 2004 to 5 January 2005 for 19 GHz hor. pol. (A) and 37 GHv vert. pol (B)

Apart from the SSM/I, the DMSP – satellites carry an optical line scanner (OLS) to record reflected sunlight in the red and near infrared wavelength regions. These data provide with 500 m by 500 m higher spatial resolution than AVHRR images but are less suitable for snow studies since the low radiometric resolution of only 6 bit (AVHRR: 10 bit) leads to over saturation effects very quickly.

Processing of OLS data was taken into account but finally skipped because of the even better availability of AVHRR images and the AVHHR's spatial resolution of approximately 1.1 km by 1.1 km is considered to be sufficient for the observation of melt.

3.2.3.5.3 SAR radar backscatter

A range of Synthetic Aperture Radar (SAR) from Envisat, ERS, and Radarsat images have been acquired over the ISPOL study region. Imagery was used for near-real-time navigation support, and for supporting the selection of the ISPOL study region as well as for the design and interpretation of HEM thickness measurements during the expedition.

Envisat imagery was obtained through a peer-reviewed CAT 1 proposal with the European Space Agency (ESA): “Usage of SAR imagery for ice navigation and observations of sea ice dynamics and surface properties and processes in the Weddell Sea”. Wide Swath Mode (WSM) images in HH-polarization were acquired during the background mission, i.e. whenever Envisat passed our Region of Interest and when there was no acquisition order of higher priority at the same time. WSM images have a coverage of 400x400 km^2. All images were archived on ESAs html- and ftp-rolling archive in near real-time. We have set up an automatic procedure in Bremerhaven to look for new images on the web server every hour, download the imagery, geocode and enhance them, and email them as small jpg files (about 1 MB) to the ship. On board, jpg images were imported into the ships TeraScan system, geocoded, and combined with geographical information of the ship and of helicopter flights.

After some initial technical problems at ESAs web sites, the procedure worked very well towards the end (Fig. 3.36). In total, 40 Envisat WSM images have been acquired and were readily processed and sent to the ship at AWI 5.5 hours later on average. However, on board they were on average only received 10.2 hours after the satellite overpass, a limit mainly caused by the low frequency of email exchange between the ship and the AWI. However, transmission times reduced considerably in the second half of ISPOL, and the record minimum was actually 0.85 and 1.63 hours on 29 December (Fig. 3.36). Figure 3.37 shows an image of the ISPOL floe.

ERS-2 SAR images have also been acquired through the same CAT 1 proposal as above. Acquisition programming required much more care as the size of ERS images is only 100x100 km^2. All acquisitions have been received at the German Receiving Station O’Higgins on the Antarctic Peninsula, which was operated throughout the season by Deutsches Zentrum für Luft- und Raumfahrt DLR. In total, 17 GEC images have been processed and sent by email to the ship approximately 1 day after the satellite overpass. Unfortunately, only 6 images cover the ISPOL floe.

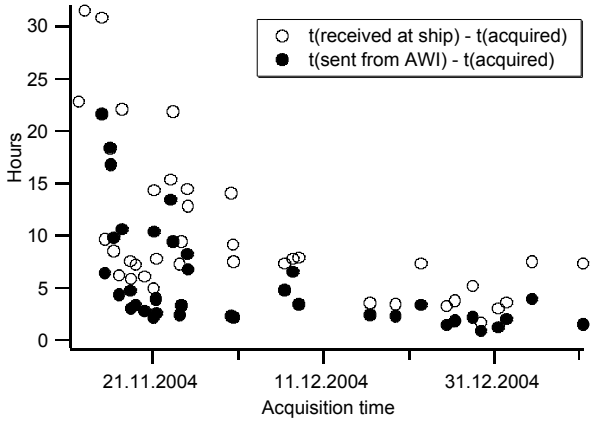

Fig. 3.36: Time between satellite overpass over Polarstern and sending Envisat WSM SAR images from AWI and receiving them on board

Acquisition of 17 Radarsat SNB SAR images with a coverage of 300x300 km^2 has been purchased from Radarsat International in Canada. Data were only processed off-line for analysis after the cruise. However, about one week after acquisition they have been downloaded to the AWI, and processed in the same manner as the Envisat images. As they are easy to calibrate, they will be analysed for temporal changes of ice surface signatures as well as for ice motion studies.

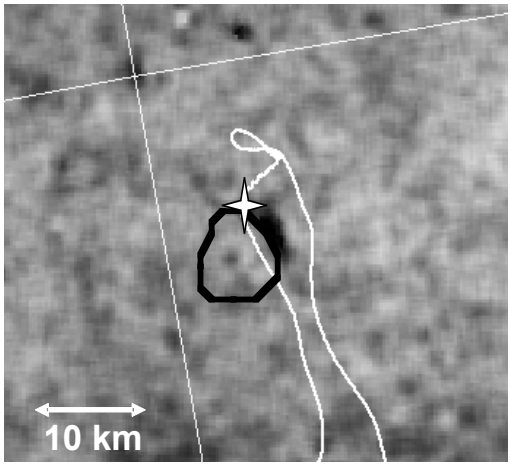

Fig. 3.37: Envisat SAR image of 30 November 2004, of the ISPOL floe. The approximate boundary of the floe and location of the ship are outlined by the black polygon and the white star. The white line shows the ships drift track before and after the satellite overpass.

3.2.3.5.3.1 Observation of changes in iceberg backscatter and associated surface properties

The coverage of Envisat WSM SAR images was large enough to map both the ISPOL study region as well as parts of the Antarctic Peninsula. At the northern tip of the Larsen-C Ice Shelf two prominent icebergs possessed high backscatter in early December (Fig. 3.38). On 28 December backscatter of the southern iceberg had drastically decreased due to snow melt and wetting, as have parts of the Ice Shelf itself. After 4 January 2005, both icebergs had become dark in the SAR image.

On 2 January a helicopter flight was performed to both icebergs for visual observations of their height, surface roughness and snow properties, as well as for temperature measurements of the upper 0.8 m of snow. Both icebergs were approximately 30-40 m high, and had a very smooth and level surface. The snow consisted of alternating layers of coarse snow with 2-4 mm grain size (5-6 cm thick) and 3-4 cm thick soft ice. Snow thickness was larger than 1 m. However, the temperature of the dark iceberg was 0°C down to a depth of 0.55 m, and decreased only to -0.1°C at 0.75 m depth. In contrast, the snow of the bright iceberg was much colder, with temperatures of 0°C only down to 0.2 m, and a temperature of -1.4°C at a depth of 0.7 m. It is clear that the backscatter differences were due to differences of the warming rate of both icebergs, which resulted in much stronger melting and wetting of snow in the dark iceberg. As the bright iceberg has also become dark on 4 January this shows that there is a threshold of melting snow thickness of about 0.2-0.4 m for snow becoming absorptive for C-Band radar waves. This has major implications for sea ice SAR signatures as well.

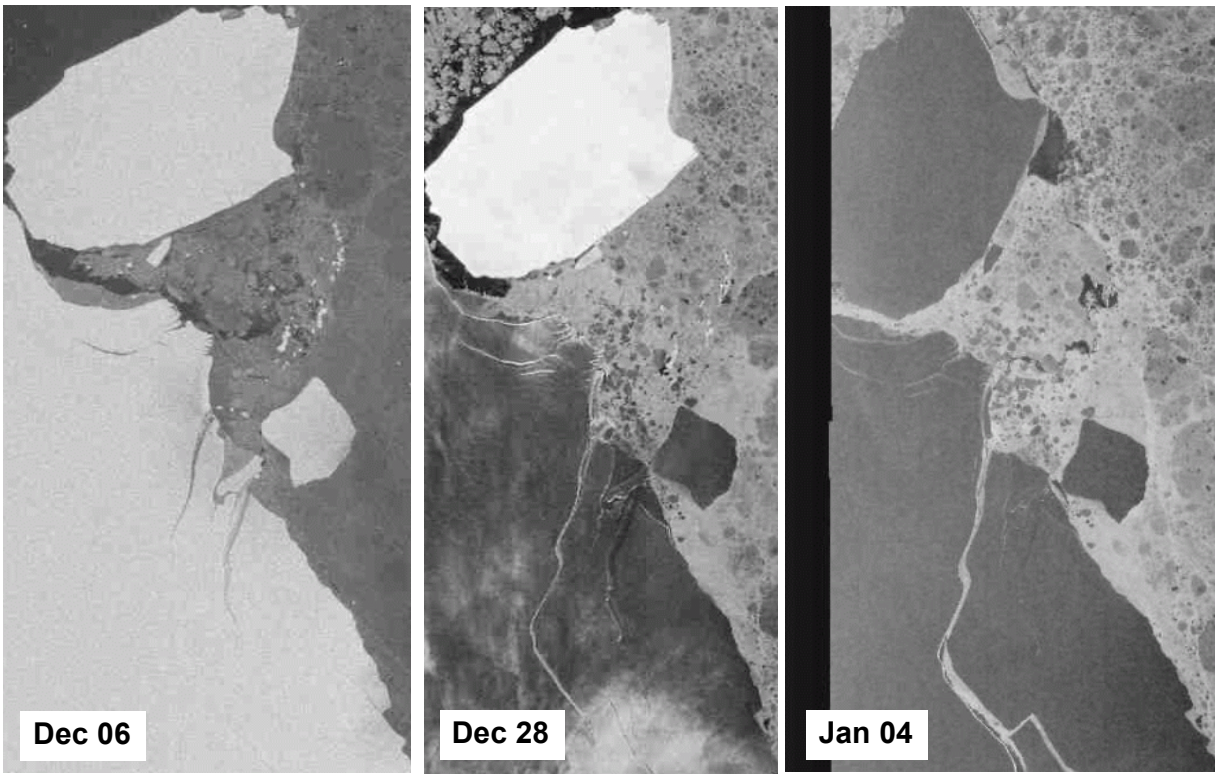

Fig. 3.38: Envisat WSM HH-pol SAR images of two icebergs in front of the northern tip of the Larsen-C Ice Shelf

3.2.3.5.4 Scatterometer

SeaWinds/Quickscat scatterometer images of the Weddell Sea have been emailed daily by Leif Toudal from the Danish Technical University as background information on ice conditions and changes of radar signatures (Fig. 3.7). They could be watched comfortably in the DTU sea ice browser, a mini-GIS allowing to easily overlay. Comparison with weather conditions and snow properties around the ship revealed that the Ku-band backscatter of those radar images is very sensitive to changes in snow temperatures and wetness. For dry snow, backscatter increases more strongly than C-band radar signals with the occurrence of ice layers in the snow. Due to their sensitivity to changing snow surface properties, the spatial variability of backscatter changes was also related to similar changes in the passive microwave data (Section 3.2.3.5.2).

4. BIOLOGY AND GEOCHEMISTRY

4.1 Deuterated tracers for DMS dynamics in Weddell Sea ice

John W.H. Dacey[1)], Jacqueline Stefels[2)]

[1)] Woods Hole Oceanographic Institution, Woods Hole, USA
[2)] University of Groningen, Haren, The Netherlands

Progress in understanding biosphere-climate interactions is significantly hindered by the difficulty of accurately constraining, parameterizing, or validating models of dimethylsulfide. More is known about the fate of DMS once it reaches the atmosphere than is known about the dynamics of DMS in the surface water. The production and consumption of DMS and DMSP are governed by complex chemical and biological interactions such as nutrient availability, primary production, senescence of DMSP-producing phytoplankton, zooplankton grazing, and bacterial degradation.

A growing body of evidence indicates that in typical marine systems DMS turns over rapidly through a variety of production and consumption processes. The key precursor of DMS is DMSP, a sulfonium compound produced by algae. A significant fraction of this DMSP decomposes to form DMS, most likely by passing through a pool of soluble (extracellular) DMSP. DMS itself is oxidized photochemically and biologically, and it also escapes from surface waters to the atmosphere. One major oxidation product is DMSO, a compound which has only recently begun to draw serious attention in oceanographic research. The range of simultaneously possible transformation pathways makes tracers an ideal tool for following the kinetics of these processes.

Kiene and co-workers have pioneered the use of ^{35}S (radioactive) tracers to investigate turnover. This method has high sensitivity and can be very useful in characterizing the product pools, but it requires extremely high specific activities for the radiotracer because background concentrations of DMS and DMSP are so low in seawater. Also, this radiological tracer method does not allow the simultaneous tracing of multiple pools of DMSP and DMS pools in the same sample.

This project is an early attempt to measure the build-up and turnover of DMS and its main precursor DMSP in seawater using stable isotope tracers. The unique combination of tracers we have been developing allows the simultaneous tracing of turnover in three DMS-relevant pools in the same sample (Fig. 4.1). With suitable tracers we can measure the rates of several processes in one incubation flask. All DMS derivatives were converted to DMS and analyzed for isotopic composition by Proton Transfer Reaction Mass Spectrometer (PTR/MS) described more fully in section 4.2.

DMSP synthesis: Since all of the hydrogen atoms in photosynthetic plants are derived from H_2O, we can use D_2O to trace the *de novo* synthesis of DMSP. Tracer is measured by hydrolyzing cellular DMSP in base and looking for the increase in deuteration of the resulting DMS. Singly-deuterated (D1) DMSP is most probable product of the tracer, with decreasing probabilities of occurrence for D2 and D3 deuteration.

Turnover of extra-cellular DMSP: It is generally held that in seawater most DMS formation occurs by enzymatic conversion of extra-cellular DMSP. We can trace this process by adding deuterated DMSP to samples and sythesizing them. Decomposition of the labelled DMSP by the elimination reaction of this tracer yields D6-DMS. Loss of tracer without appearance in the DMS pool indicates some other pathway of DMSP decomposition.

Turnover of DMSO: We used D-6 DMSO to investigate the turnover of DMSO. Our preliminary results suggest that DMSO turnover is very low.

Turnover of DMS: Since the above methods impact the pools of DMS with mass 63, 68, and somewhat 64, we chose a D3-DMS (mass 65) for monitoring the DMS pool. Loss of D3-DMS is an indication of DMS turnover when, perhaps, the concentration of bulk DMS may not be changing, as in figure 4.2. Simultaneously we can measure the appearance of D3-DMS in other pools, like dimethylsulfoxide.

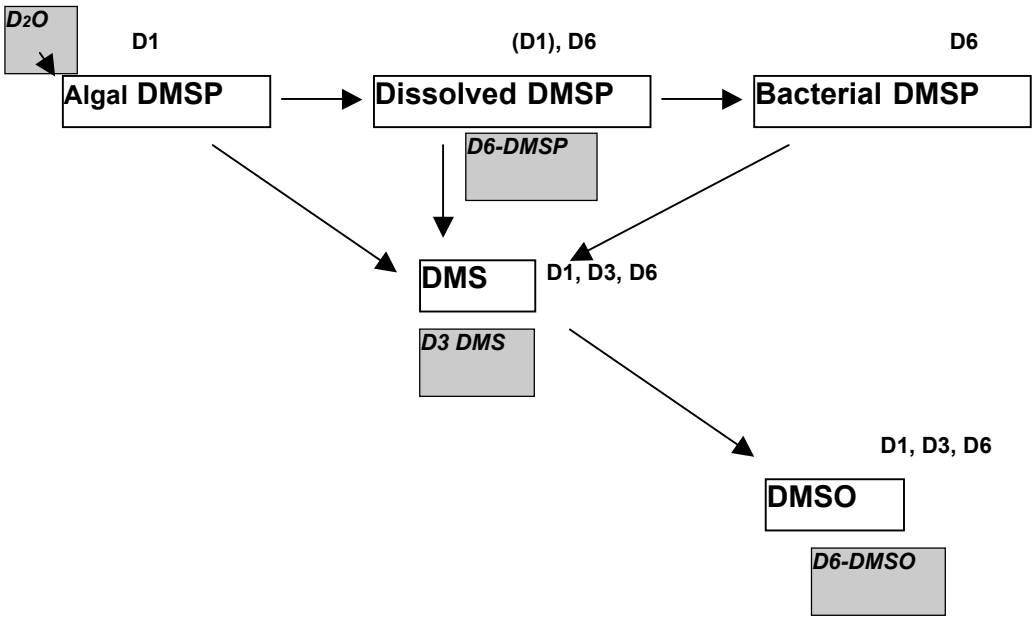

Fig. 4.1: Turnover of DMSP, DMS and DMSO. Blank boxes show relevant pools, shaded boxes show which tracers we add, and the small letters outside the boxes indicate where we might expect to find which tracer.

DMSP is formed by certain species of phytoplankton and can reach very high intracellular concentrations (>100 mmol/L). Addition of D_2O (the deuterated analogue of H_2O) to the sample serves as a tracer for *de novo* DMSP production. Some of this DMSP decomposes directly to DMS inside phytoplankton, but most DMS formation appears to result from the enzymatic decomposition of dissolved DMSP. Dissolved

DMSP (in 10's and 100's of nmol/L in ice floe samples) is cleaved to form DMS (typically <300 nmol/L), is consumed biologically to form other products, or is taken up by plankton as DMSP. Addition of D-6 DMSP provides a powerful tracer for measuring the turnover of the DMSP pool and aids in detecting some of its major products. DMS is consumed by biological and chemical oxidation processes (in addition to the flux to the atmosphere). Simultaneous addition of D-3 DMS traces the turnover of DMS independently of DMSP.

We conducted several experiments using combinations of these tracers. We used D_2O and D3-DMS in all tracer experiments, and used D6-DMSP or D6-DMSO in other experiments. Experiments focused on the effects of light and nutrients on the dynamics of DMSP, DMS, and DMSO.

Here we present some preliminary findings from a 24-hour experiment to demonstrate the practicality of this procedure. Figure 4.2 shows the incorporation of D_2O into DMSP, indicating production of new DMSP by phytoplankton. Figure 4.3 shows a slight decrease in D-3 DMS, suggesting a slow turnover of this pool in the incubations.

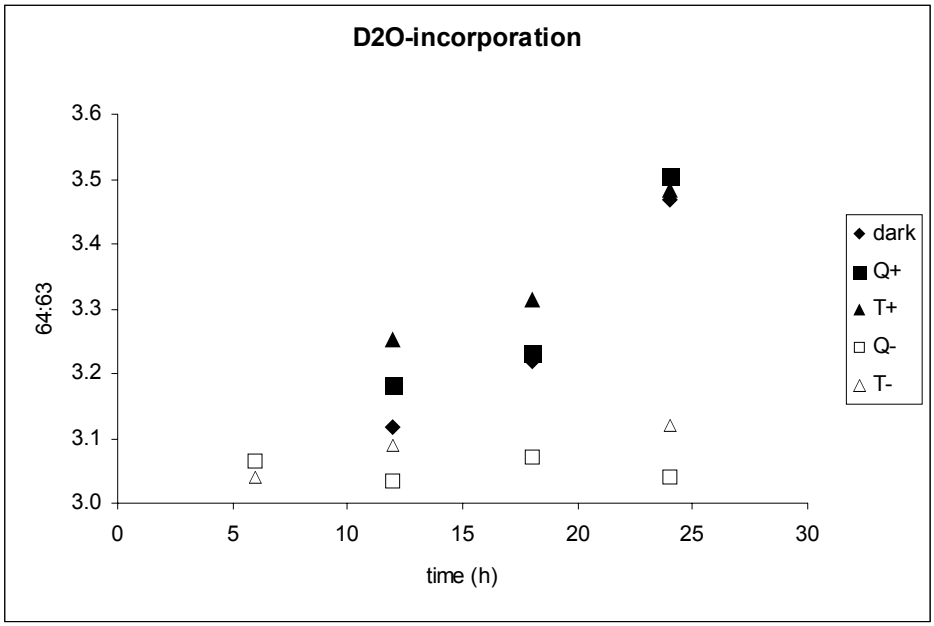

Fig. 4.2: Deuterated DMSP accumulates in all bottles treated with D_2O. Incubations were conducted in Quartz (Q) and Teflon (T) bottles, with D_2O (+) added or not (-).

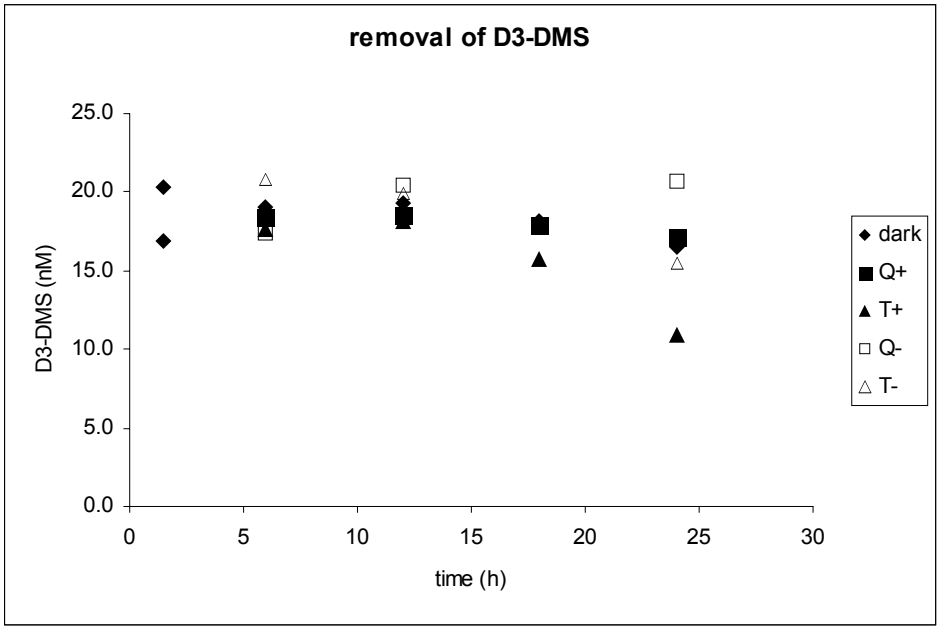

Fig. 4.3: D3-DMS shows a slight decline while the bulk DMS pool showed no change.

The addition of D6-DMSP aids in quantifying the turnover of the DMSP pool. The loss of D6-DMSP (Fig. 4.4) from the overall DMSP pool can be used to estimate DMSP turnover in a pool, which remains relatively unchanged throughout the experiment. The concomitant rise in D6-DMS (Fig. 4.5) indicates that after 24 hours about half of the consumed DMSP is present as DMS.

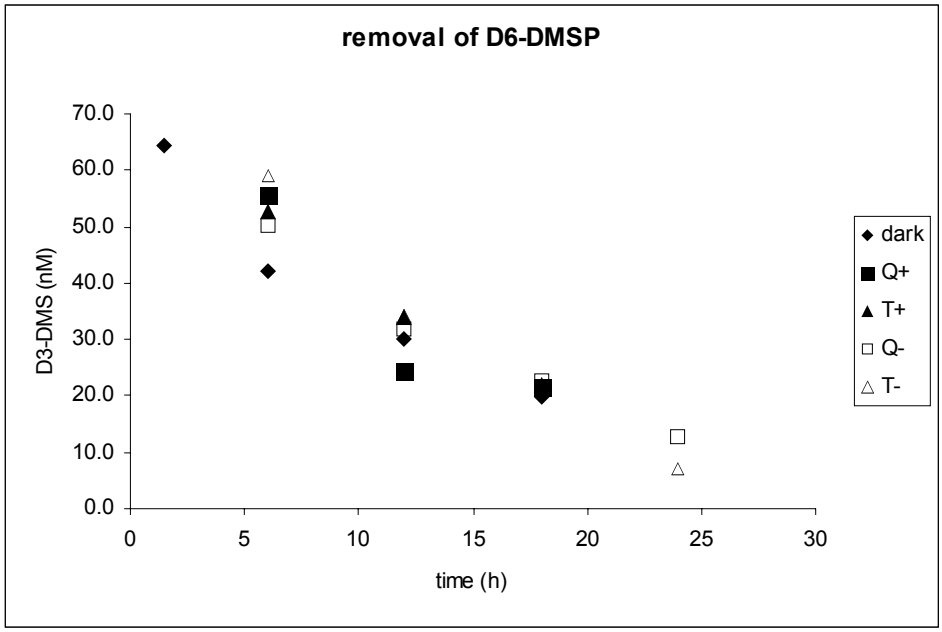

Fig. 4.4: Disappearance of D6-DMSP from the DMSP pool. During the same time interval, unlabeled DMSP dropped by no more than 30 % in any bottle.

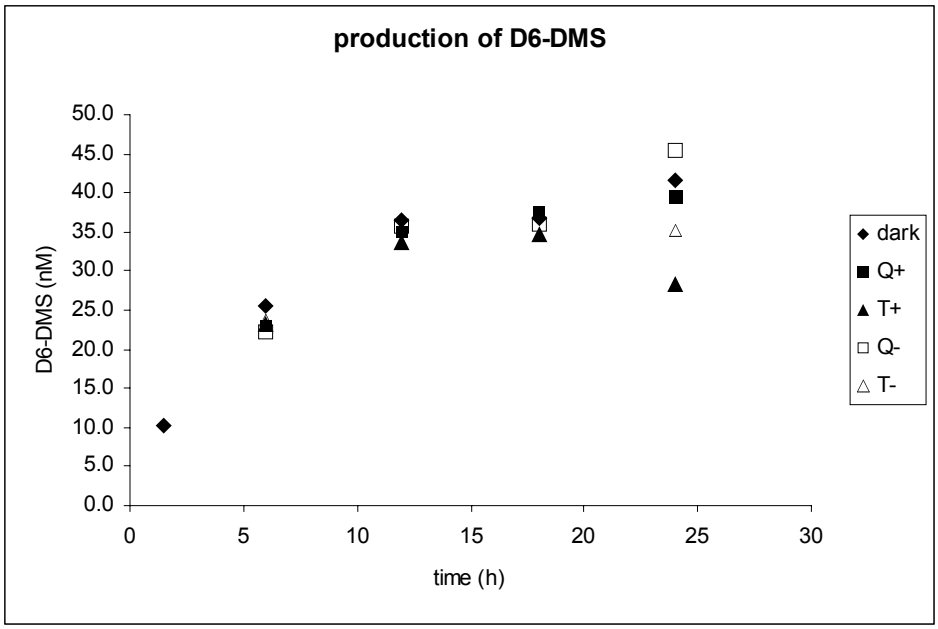

Fig. 4.5: Increasing concentrations of D6-DMS indicate the decomposition of DMSP. The increase in D6-DMS is almost as large as the drop in D6-DMSP [Fig. 4.4], indicating that a major part of the DMSP decomposition is to DMS.

4.2 The dynamics of dimethylsulphide and related compounds in sea ice

Jacqueline Stefels[1)],
John Dacey[2)],
Jean-Louis Tison[3)],

[1)] University of Groningen, Haren, The Netherlands
[2)] Woods Hole Oceanographic Institution, Woods Hole, USA
[3)] Université Libre de Bruxelles, Bruxelles, Belgium

4.2.1 Introduction

From open-ocean research we know that dimethylsulphide (DMS) is a biogenic gas that for 95 % is produced in the marine environment and that accounts for 50 to 60 % of the total natural sulphur emission. Through its atmospheric oxidation products, DMS affects the radiative properties of skies and clouds. An important role of DMS in climate regulation could be that it might be able to counterbalance the greenhouse effect of CO_2 through biogenic feedback processes. Recent model calculations have shown that, especially in the Southern Hemisphere where antropogenic sulphate emission is low, DMS plays a major role (70 %) in the production of atmospheric sulphate. These model calculations use a global DMS database as input, but in fact this database suffers from a severe lack of data from the Antarctic region. Moreover, there are no data at all on DMS in sea ice, although there is reason to believe that this is substantial. Up until now, only analyses on dimethylsulphoniopropionate (DMSP), the algal precursor of DMS, have been performed in ice and were found to be orders of magnitude higher than in the surrounding waters.

The aim of this project was to study the spatial and temporal variability of DMS and DMSP in sea ice cores.

4.2.2 Methods

Ice cores were obtained from the transect coming inward to the ISPOL-station (courtesy C. Haas et al.) and from the time series measurements: both from field # 6 (M. Steffens et al.) and from field # 9 (J-L Tison et al.). In total 18 cores were analysed for DMS and DMSP in depth intervals of 5 or 10 cm. A major effort was put into the development of a new method to analyse DMS in the ice. Both dry crushing and melting of ice was explored. In addition, samples for algal pigment analyses were taken from the melted cores. Data will later be combined with biotic and abiotic parameters taken by others.

The dry crushing involved deep freezing of the ice cores, cutting ice blocks with a volume of approximately 20 ml, crushing the ice in a cold stainless steel vessel under vigorous shaking and sweeping the gas phase from the crusher vessel directly into the mass spectrometer using high purity air at a flow rate of 150 ml/min. The analysis of DMS by the mass spectrometer took approx. 10 minutes after which the ice powder inside the vessel was quantitatively collected. About 10 ml of the ice powder was used for further DMSP analysis: the powder was collected in crimp seal vials, NaOH was added and left to react for 24 hours, after which the DMSP could be analysed in the form of DMS. By then, the sample had melted and the DMS was purged out of the liquid with 150 ml/min air and directly analysed by the mass spectrometer.

The melting of ice was done in 1L buckets. To the 5 cm slices of ice (approx. 250 ml) high-salinity filtered deep sea water with a negligible concentration of DMS and DMSP was added. At the beginning of the melting procedure deuterated isotopes of DMS and DMSP were added in order to be able to follow the losses of these compounds during the melting process with the mass spectrometer.

The mass spectrometer used in this project was a proton-reaction-transfer mass spectrometer (ptr-ms). This technique allows the direct measurement of DMS at sub-ppb levels, every second. This means that no concentration step is needed, like in the conventional gas chromatographic method that uses a purge-and-trap. The mass spectrometer also allows the parallel analysis of a variety of different masses of the same compound. In this way, we were able to analyse not only the natural abundance of the stable isotopes of DMS, but also to analyse the artificially deuterated DMS. Since different levels of deuteration were used for the DMS tracer and for the DMSP tracer, both compounds could be followed individually (see also chapter 4.1)

4.2.3 Preliminary results

Figure 4.6 clearly shows that melting of ice can severely change the ratio of DMS versus DMSP. The conversion of DMSP into DMS presumably takes place after the algal cells inside the ice collapse during the melting procedure. In viable cells, DMSP is most probably located in another compartment of the cell than the cleavage enzyme that converts DMSP into DMS. The enzyme can be either from bacterial or from algal origin, but the high rates of conversion we observed during the melting suggests that the majority of the lyase enzyme was of algal origin.

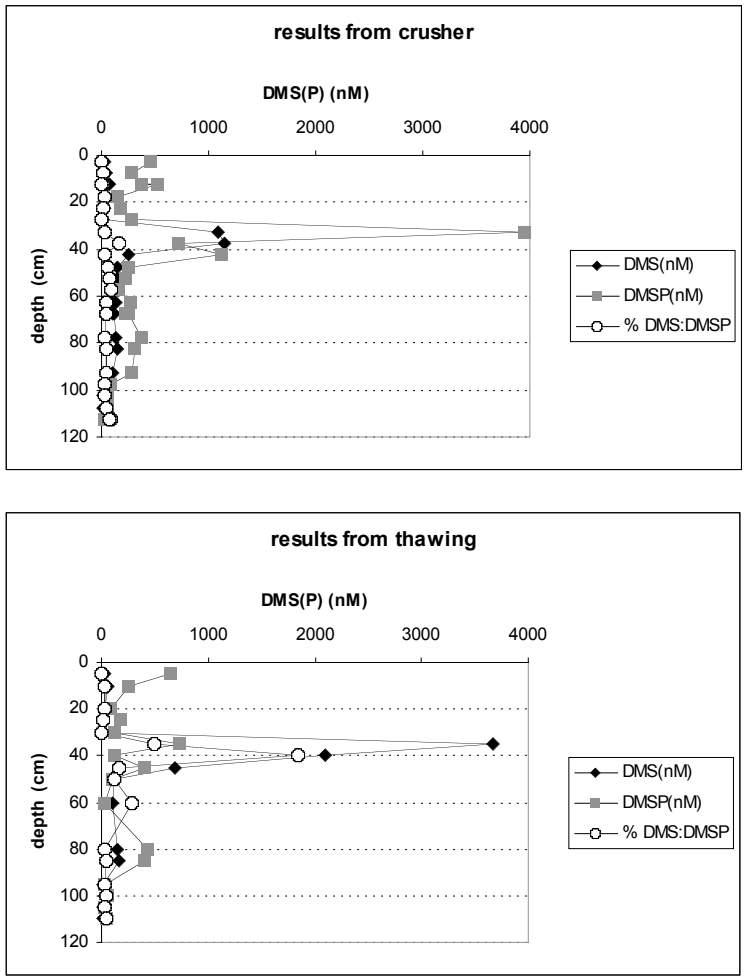

Fig. 4.6: DMS and DMSP in a profile of ice core # 041114-TR-21, taken during the transect on 14 November 2004

Figure 4.7 shows ice profiles from both field #6 and #9 from the first station of the time series sampling. Although both sites consist of first-year ice, there are some differences in the distribution of DMS and DMSP. The profile from field #9 shows a clear internal community, next to the upper and bottom community that are also observed in the core from field #6. Data from the subsequent stations will reveal how these communities developed in time and how this related to other parameters and to changes in ice structure.

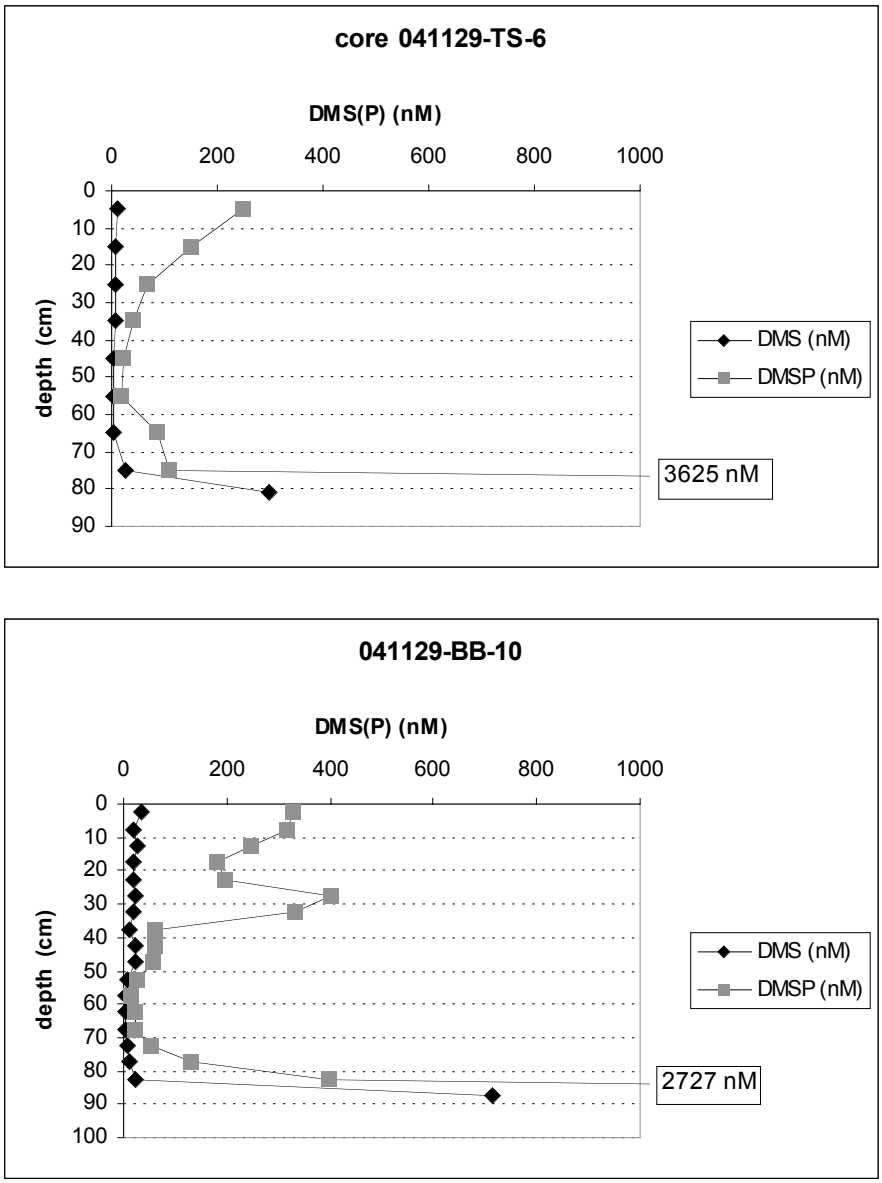

Fig. 4.7: Depth profiles of DMS and DMSP of ice cores from the first time series station. Core 041129-TS-6 originates from field #6; core 041129-BB-10 originates from field #9.

A further evaluation of the data, including calculations of the conversion of DMS and DMSP isotopes, will give us insight into the preferred method for an accurate analysis of both DMS and DMSP in ice cores.

In addition to the ice core analyses, brines and water from just under the floe of field #9 were analysed for DMS and DMSP during the time series stations. The full dataset is not yet available, but from the first 4 stations a modest increase of DMS and DMSP in the underlying water can be observed, which might be related with the opening of brine channels during the ice melt and subsequent release of high amounts of DMS and DMSP to the water.

4.3 Sequestration of carbon by "pumping" microbial reworked dissolved organic matter to the abyssal ocean

Thorsten Dittmar[1)], Boris Koch[2)] Stathis Papadimitriou[3)] and David N. Thomas[3)]

[1)] Florida State University, Tallahassee, USA
[2)] Alfred Wegener Institute, Bremerhaven
[3)] School of Ocean Sciences, Anglesey, UK

4.3.1 Introduction

Dissolved organic matter (DOM) in the oceans contains about the same amount of carbon as the global biomass or atmospheric CO_2 and exhibits an average age of several thousand years. Source, diagenesis and preservation mechanisms of DOM remain elemental questions in contemporary marine sciences and represent a missing link in models of global elemental cycles. The polar oceans are probably a primary source of DOM to the deep ocean because these regions are the only places where surface waters efficiently convect down to the oceans' bottom. Deep-water formation is directly linked to sea-ice formation, when salt is rejected and dense brine-enriched waters penetrate the deep ocean. Sea ice is one of the most productive marine environments, and DOM concentrations in the brine are among the highest measured in marine waters. The biogeochemistry of sea ice is widely unknown and it is not clear whether sea-ice DOM is persistent enough to survive downward convection.

Broad significance is expected by answering the question: "Do ice-covered oceans act as a DOM pump to the abyssal ocean and so sequester carbon from active cycles?"

By combining several molecular tracer techniques we will be able to quantify the concentration of ice-algal derived DOM in the different water masses and along diagenetic pathways on a large scale in the Weddell Sea.

4.3.2 Material and Methods

Approx. 200 experimental and *in situ* samples were taken on the cruise from different sources, including detailed CTD-profiles from surface to bottom, ice, brine, and gap waters. In order to determine DOM fluxes from sea ice to the water column and from surface water to the deeper Weddell Sea, a molecular fingerprinting approach will be applied. All samples will be analysed on land for total dissolved carbon (DOC) and nitrogen (DON), and molecular components of DOM. For further molecular characterisation via mass spectrometry and nuclear magnetic resonance, DOM was extracted via a solid phase adsorption technique out of almost 4000 l of approx. 100 seawater, brine, ice core and experimental samples. Analyses of nutrients, UV/Vis-absorbance spectra and oxygen concentration of all samples were performed onboard. These data gave first hints on the origin and diagenetic state of the water masses during ISPOL.

In addition to *in situ* sampling, four degradation experiments were performed in order to study the impact of solar radiation on DOM in sea ice brine. Several other groups during ISPOL participated on these experiments (Harri Kuosa: species composition,

Birte Gerdes: bacterial activity, Jaqueline Stefels: DMS, Andreas Krell: H_2O_2, Rupert Krapp: light profiles, Gerhard Dieckmann: pigments). For the experiments sterile-filtered (0.2μm) and unfiltered brine and gap water samples were put into quartz bottles and placed in different depths under snow and on the snow surface. Samples were taken as soon as 6 hours after the incubations started until up to 16 days.

4.3.3 Preliminary results

Warm Deep Water (WDW) was characterised by the highest temperatures (~0.5°C, ~600 m, Fig. 4.8) and represented the oldest water mass being transported southwards from the Antarctic Circumpolar Current. The mineralization of sinking organic particles in the history of this water mass caused strong nutrient accumulation and oxygen depletion in WDW. The nutrient maximum (~1200 m) is significantly deeper than the temperature maximum of the WDW (~600 m). Hence mixing of WDW with surface and bottom water alone cannot explain the nutrient profiles in the water column. The nutrient increase was rather caused by mineralization of sinking particles. The increasing silicate/nitrate-ratio with water depth reflects the slower mineralization rates of silicate compared to nitrate. Bottom water was the densest water with lowest temperatures (-1.7°C) and the highest salinity (34.6). Contrary to WDW it was characterised by low nutrient content and high oxygen concentration, indicating the formation of fresh bottom water from biologically active surface water within relatively short periods of time. This could be a first indication for DOM being transported from surface into bottom waters.

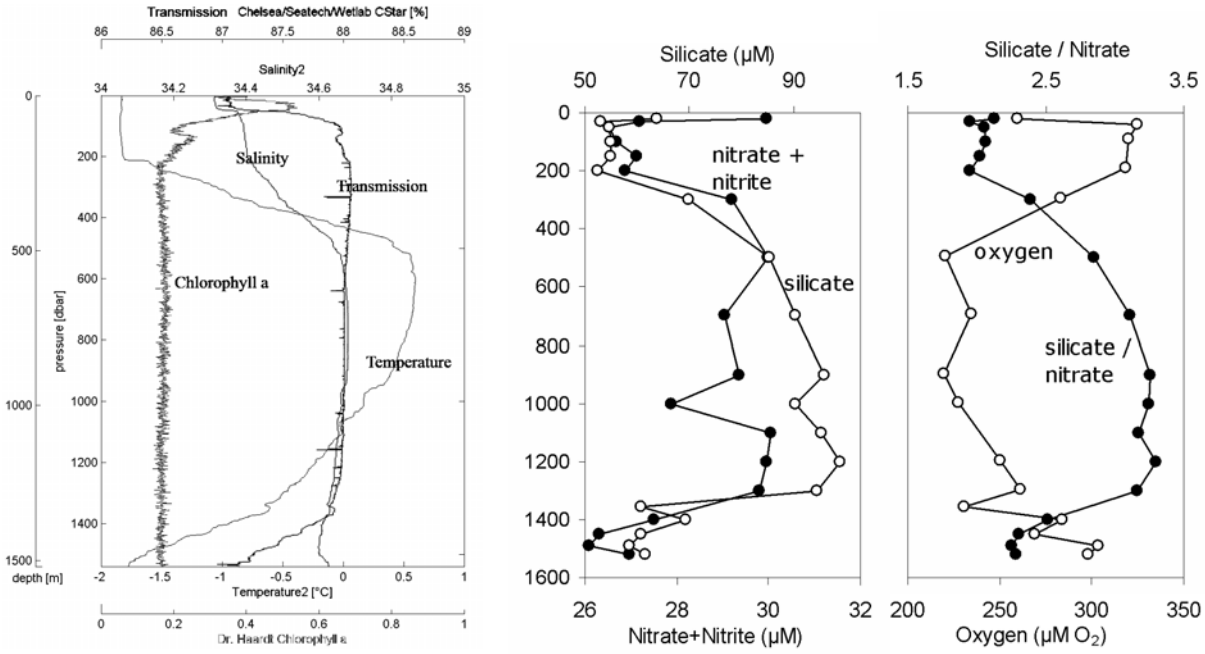

Fig. 4.8: CTD-station (ISPOL PS67/006-131) with nutrient and oxygen profiles (CTD data by M. Schröder et al.)

None of the photodegradation experiments caused a significant change in nutrient concentrations, indicating the absence of significant organic matter mineralization by light. However, chlorophyll *a* concentrations and phytoplankton abundances in the unfiltered samples sharply dropped after few hours in the bottles placed on the snow surface (data from G. Dieckmann and H. Kuosa). For samples buried under snow (15 cm) these changes were more gradual. UV/VIS-absorbance measurements (CDOM) showed considerable molecular changes of DOM. The absorbance of UV-active compounds strongly decreased depending on the amount of radiation received (Fig. 4.9). The dark control showed no significant changes in the absorbance-spectra.

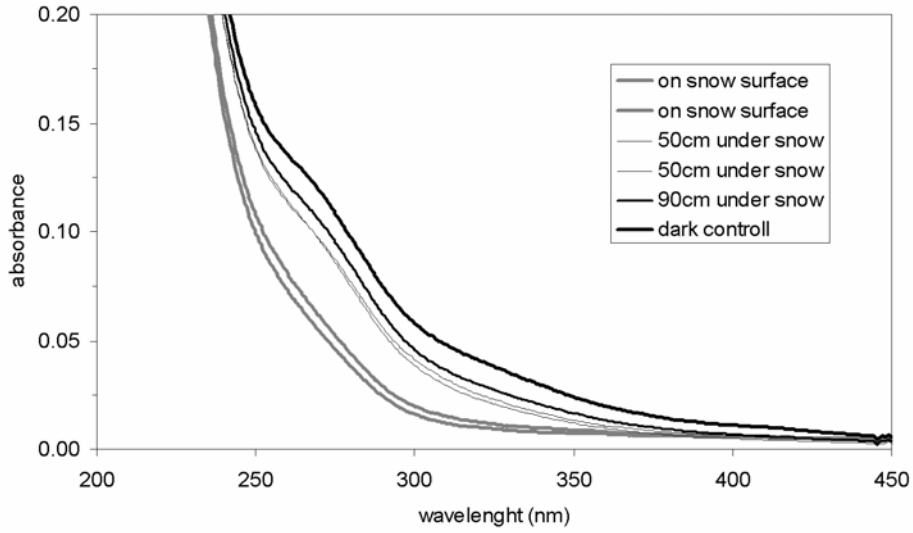

Figure 4.9: UV-absorbance spectra of sterile-filtered (0.2μm) brine samples buried in quartz bottles in different snow depths for 16 days

4.3.4 Future analysis

All samples will be analysed for DOC, DON, amino acid enantiomers and molecular size distribution. Selected samples will be analysed with various techniques for in-depth molecular characterisation. A special focus will be on Fourier transform ion cyclotron resonance mass spectrometry (FTICR-MS), which is a highly promising new technique for the development of new molecular tracers, and nuclear magnetic resonance spectroscopy (NMR).

Besides indicating the source of DOM, these molecular tracer techniques will give hints to the source of bottom water, i.e. whether bottom water in the Western Weddell Sea is derived from sea-ice or shelf-ice areas. The results from this molecular fingerprinting will be integrated into physical models of regional and global ocean circulation, in order to obtain a detailed and quantitative biogeochemical model for DOM cycling in the ice-covered regions of the world oceans and beyond.

Surface water from the ISPOL cruise will be used as an inoculum for a long-term (1 year) microbial degradation experiment. We hypothesise that the refractory

chemical structure of mature bulk marine DOM is largely independent of the source, and controlled by marine microbes. For this purpose, DOM formed by microbes from different substrates will be characterised on the molecular level.

4.4 Biogeochemistry of subsurface lead water in pack ice

Hendrik Zemmelink[1)], Stathys Papadimitriou[2)], David Neville Thomas[2)], Andreas Wisotzki[3)], Annette Scheltz[4)], Leah Houghton[5)], John Dacey[5)]

[1)] University of East Anglia, Norwich, UK
[2)] School of Ocean Sciences, Anglesey, UK
[3)] Alfred Wegener Institute, Bremerhaven
[4)] Institut für Polorökologie, Kiel
[5)] Woods Hole Oceanographic Institution, Woods Hole, USA

4.4.1 Introduction

Sea ice research over the past decades has resulted in detailed studies of biogeochemistry and the ecology of sea ice organisms that thrives on the ice surfaces, in brines and in open water surrounding ice floes. Because of the profound effect of freezing and thawing on water chemistry, considerable attention has also been focused on the water column beneath the sea ice. Conventional techniques such as CTD casts with niskin bottles are usually used to study the water column. The disadvantage of this technique is that sampling starts at some depth from the water surface and that it spans a considerable depth range, thereby only providing information on bulk water mixing and circulation. Hence, such techniques cannot be used to study near-surface processes that might be relevant for nutrient transport and exchange of gases to the atmosphere.

For instance the understanding of factors that regulate the near surface concentration of DMS (and of any other gas) in time and space is a significant and specific problem that hampers an accurate quantification of the sea to air flux. In addition, the microbial communities and chemical processes (e.g. the loss of DMS through photolysis) are affected by chemical and physical dynamics of the surface layer and by meteorological forcing such as total solar radiation, UV intensity (and spectrum), and wind speed. Studies performed in coastal seas indicate that the surface microlayer contains elevated levels of nutrients and bacteria compared to underlying bulk water. Such studies also show that horizontal and vertical distribution of bacteria may be dependent on spreading rates of surfactants, wind induced surface drift and mixing rather than on bulk water circulation.

It is likely that lead water surrounding ice flows is stratified due to the accumulation of (fresh) melt water in the surface. Melting processes at the ice edge will influence the distribution of nutrients and organisms and result in different biogeochemical characteristics of surface waters compared to deeper water. Here we present preliminary results from a study of the distribution of major nutrients and sulfur compounds in near-surface water between floes.

4.4.2 Methods

Two studies were preformed in two leads. The first lead was sampled from year day 345 through 359 (10 December– 24 December), the second from year day 362 through 001 (27 December - 01 January). Both leads were sampled after a period of elevated wind speeds during which waves mixed the upper water column. Samples were taken at 0.002 m, 0.1 m, 0.25 m, 1 m, and 4 m by suspending sampling inlets from a small catamaran and by pulling water into a syringe with subsequent collection into vials and flasks for later analysis. Water was collected for analysis of DMS, DMSP, DMSO, Chl-a, salinity, PO_4, Si, NO_x, and NH_4. In addition samples were taken for analysis of DIC, CDOM, nitrogen isotopes, amino-acids, and phytoplankton and bacterial counts. The latter parameters will be analyzed later and are not presented in this report. In total two liters of water were collected from each depth.

4.4.3 Results

Data obtained from the two leads are presented in figures 4.10 - 4.16 A for the first lead and figures 4.10 - 4.16 B for the second. The width of the first lead varied between 1 meter and 50 meters due to relative motion of adjacent floes, the width of the second lead remained constant throughout the study and was about 10 meters. During both studies the water column appeared to be well mixed at the first sampling day, which was caused by the elevated wind speed and short breaking waves during the prevailing days. No profiles were observed during such conditions but stratification rapidly occurred when breaking waves subsided and enhanced when time progressed. Salinity (Fig. 4.10) at the sea surface dropped from 34 to 28.6 during the first period and even more during the second while water below 0.1 meter remained at a salinity around 34.3. Chlorophyll concentrations (Fig. 4.11) increased during calmer conditions but this stratification of chlorophyll was not as pronounced as that of the other compounds. Nutrients showed depletion at 0.002 m during the time series (Figs. 4.12-4.14). This indicates an enhanced biological activity in the top water layer as compared to deeper layers. Analysis of DIC and nitrogen isotopes will allow us to distinguish between biological and photochemical production processes and dilution of melt water.

The biogenically produced sulfur compound DMSP increased rapidly during the study periods (Fig. 4.15), but might not only originate from enhanced local production but also from the melting ice that contains high amounts of this compound. DMSP is the precursor of the volatile DMS that is formed after chemical or biological conversion of DMSP. Similar to DMSP, DMS appears to accumulate towards the sea surface (Fig. 4.16) where it is subject to outgassing to the atmosphere or photochemical oxidation to DMSO. DMSO concentrations were only measured in the second study and exhibited, as the other major sulfur compounds, an increase towards the water surface (Fig. 4.17). DMSO may be produced *in-situ* by photochemical oxidation of DMS, but as with DMSP, DMSO may also originate from melting ice that contains high DMSO concentrations.

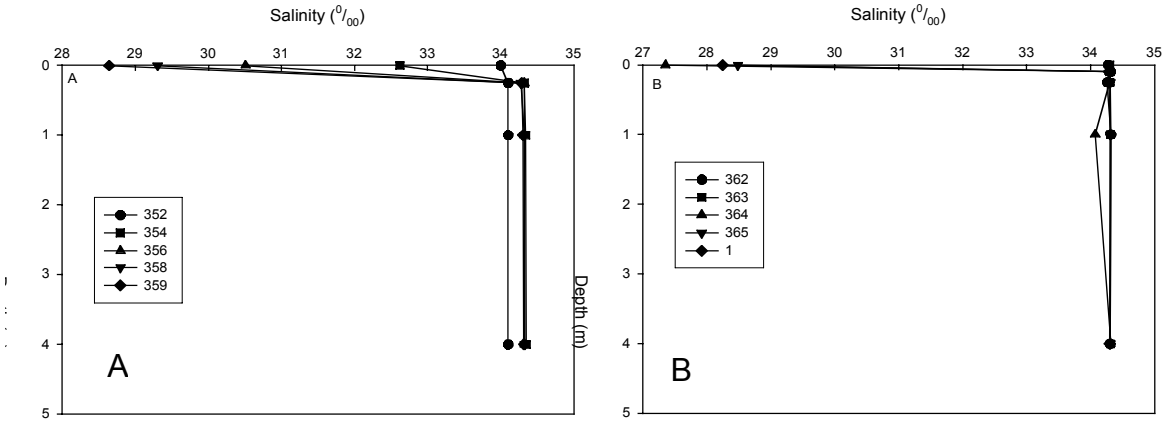

Fig. 4.10: Salinity

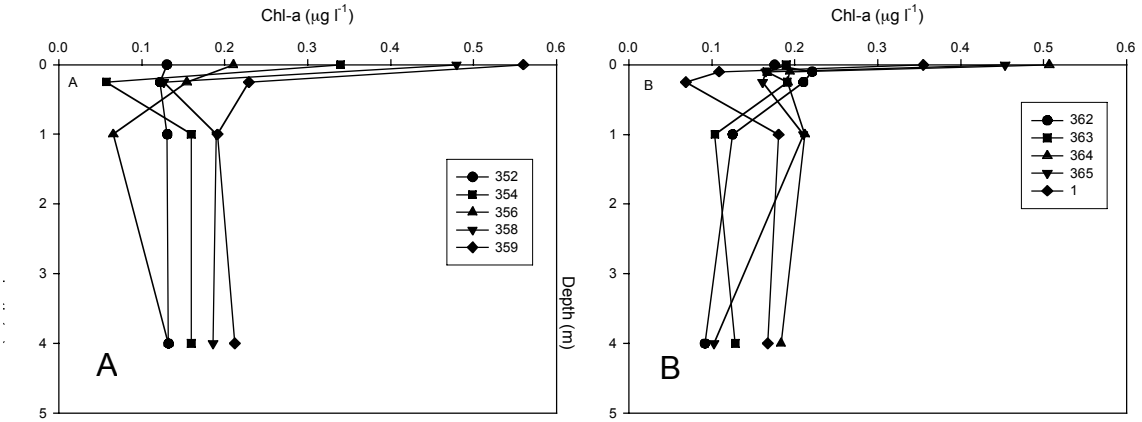

Fig. 4.11: Chlorophyll-a

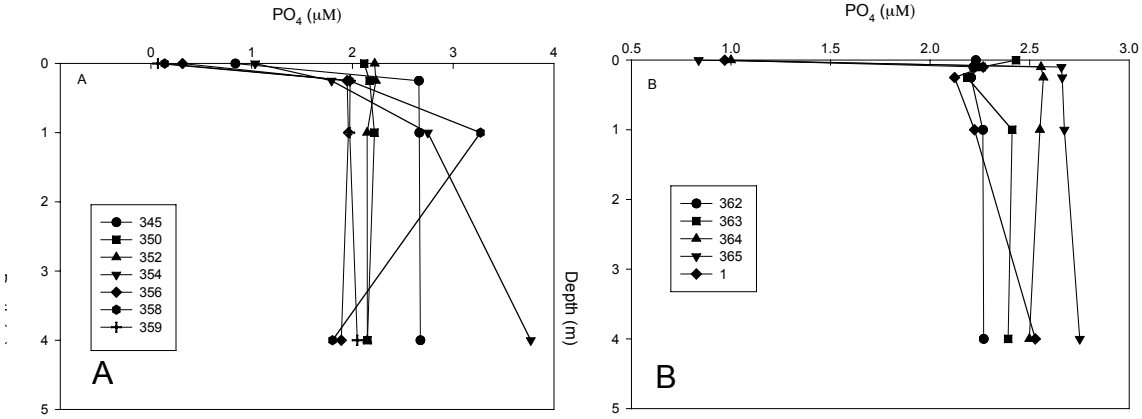

Fig. 4.12: Phosphate

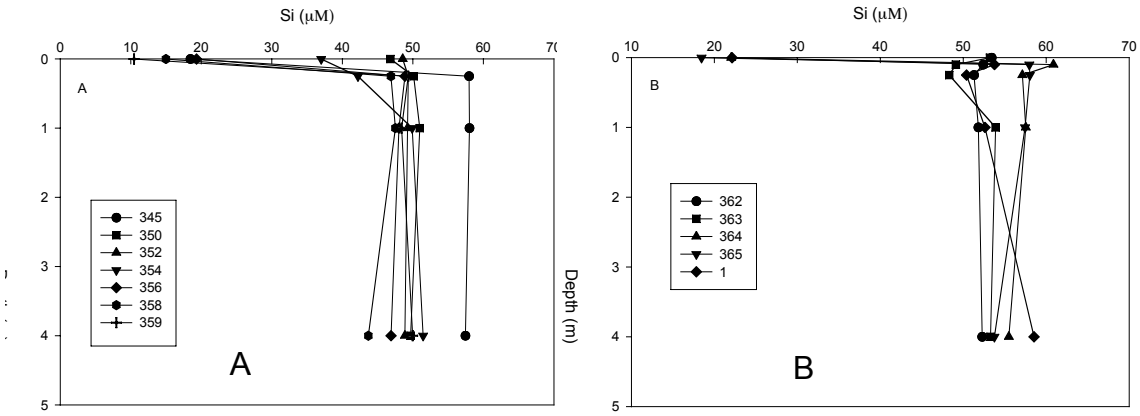

Fig. 4.13: Silicate

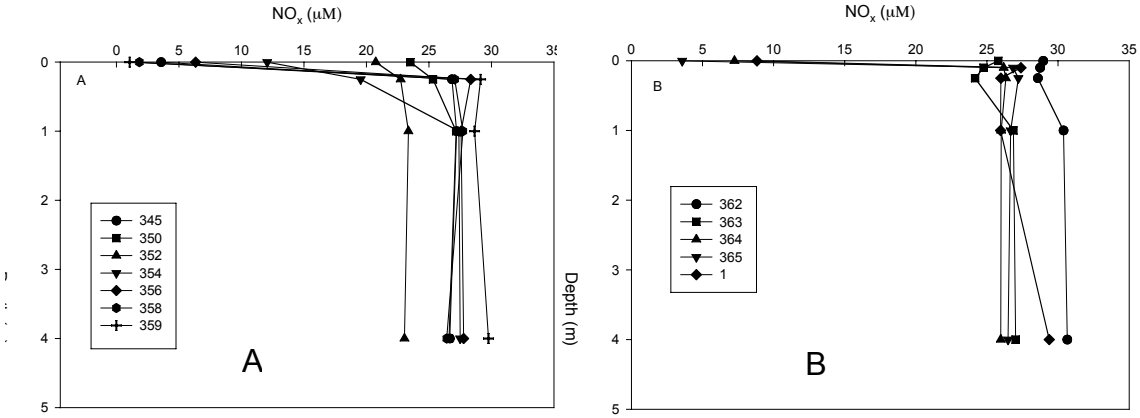

Fig. 4.14: NO_x (total nitrate and nitrite)

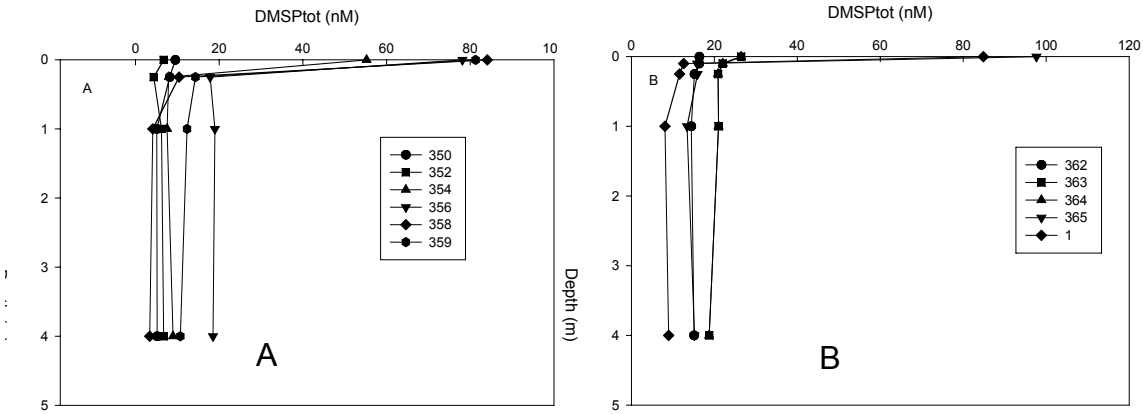

Fig. 4.15: Total dissolved and particulate dimethyl sulfoniopropionate (DMSPtot)

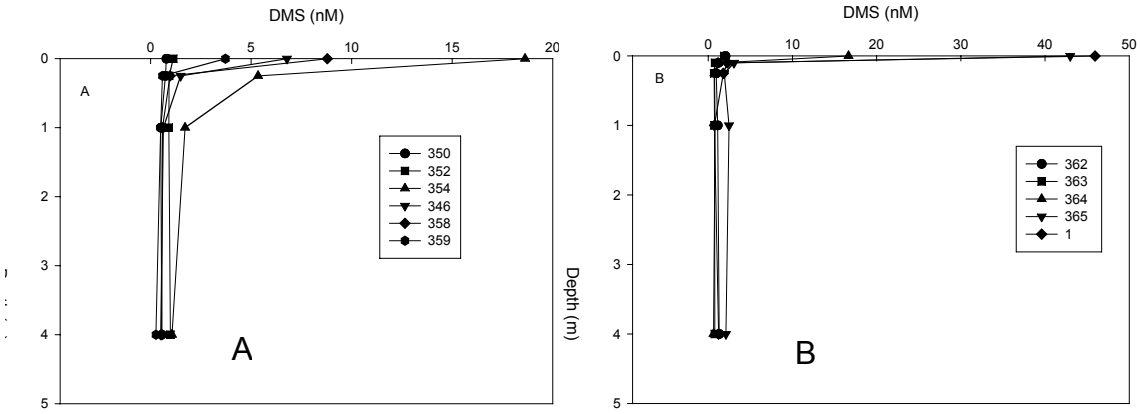

Fig. 4.16: Dimethyl sulfide (DMS)

Fig. 4.17: Total Dimethyl sulfoxide (DMSOtot)

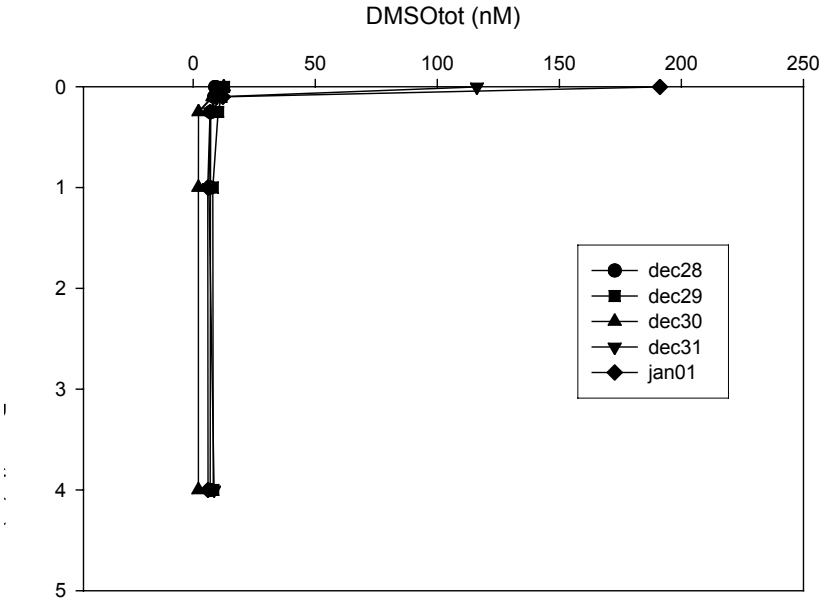

Figures 4.10 through 4.17 present depth profiles (m) of salinity (‰), Chlorophyll-a ($\mu g\ l^{-1}$), PO_4, Si, NO_x, NH_4 (μM), DMSP, DMS, and DMSO (nM) respectively. Figures A represent data from the first lead, sampled from year day 345 – 359. Figures B represent data from the second lead that was sampled from year day 362 – 001.

4.5 Inorganic nutrients and dissolved organic matter in sea ice and seawater

David Neville Thomas, Stathys Papadimitriou — School of Ocean Sciences, Anglesey, UK

4.5.1 Aims

Our aim has been to document temporal and spatial changes in biogeochemical processes in sea ice during late spring and early summer. Our specific objectives are the following: *i)* to make an extensive characterization of the temporal and spatial variability in the physical-chemical environment experienced by sea ice communities, *ii)* to investigate the nature and role of dissolved organic matter in sea ice, *iii)* to determine the role of UV and non-UV photo-oxidation of DOM on ammonium and/or urea production and subsequent nitrite/nitrate production, *iv)* to investigate biological processes in relation with the physical-chemical environment during the transition from winter to spring/early summer, *v)* to investigate the influence of major grazers on biogeochemical processes in sea ice, and *vi)* to investigate the habitat range of the foraminifera *Neogloboquadrina pachyderma*, using stable carbon and oxygen isotopes in its shell for environmental reconstruction.

4.5.2 Sampling

Extensive sampling took place at the drift ice station, Ice Station *RV Polarstern* (ISPOL), in the Western Weddell Sea between 27/11/04 and 2/1/05. Samples were taken from: *i)* sectioned ice cores in collaboration with Haas et al., Dieckmann et al. and Steffens et al. for bulk ice measurements both during the transect from the ice edge to the final position at ISPOL and the ISPOL floe, *ii)* sectioned ice cores from the ISPOL floe for centrifuged ice and brine measurements in collaboration with Dieckmann et al., *ii)* sackholes drilled in sea ice, *iii)* gap and slush layers, as well as leads in collaboration Zemmelink et al., around the ice floe, *iv)* under-ice water from diving operations, and *v)* seawater from 21 CTD stations during the drift in collaboration with T. Dittmar and B. Koch. Further sampling was generated by a number of experiments designed to investigate the contribution of photo-oxidation to DOM dynamics in sea ice (*in situ* incubations), as well as of major sea ice grazers, *i.e.*, sea ice dwelling and pelagic copepod species, flat worms and jelly fish (laboratory-controlled incubations) in collaboration with Schiel et al.

The collected samples were analyzed in the chemistry laboratory onboard for the major dissolved inorganic nutrients, nitrate plus nitrite ([NO_x]), phosphate ([P]) and silicate ([Si]) with standard colourimetric methodology using a LACHAT Autoanalyzer. Analyses of dissolved organic nitrogen ([DON] were also conducted onboard after in-line chemical and UV oxidation of the samples followed by colourimetry on the LACHAT Autoanalyzer. Further onboard measurements include: salinity, temperature, ammonium ($\left[NH_4^+\right]$), using fluorimetry, dissolved oxygen by Winkler titration, pH using standard glass electrodes calibrated with NBS standards, total alkalinity by Gran titration, and coloured dissolved organic matter (C-DOM) spectra in the visible and UV light ranges. The determination of the following parameters will be

conducted in the home laboratories: dissolved organic carbon (DOC), urea, dissolved inorganic carbon (DIC) and its stable isotopic composition (δ^{13}C-DIC), elemental and stable isotopic composition of carbon and nitrogen (POC, PON, δ^{13}C-POC, δ^{15}N-PON) in particles isolated from bulk ice, brines and seawater by gentle vacuum filtration, stable isotopic composition of dissolved nitrate plus nitrate (δ^{15}N-NO_x), the stable isotopic composition of oxygen (δ^{18}O) in bulk sea ice, sackhole brines, snow, seawater, and foraminiferan shells, and the stable isotopic composition of carbon and nitrogen in foraminiferan cytoplasm and copepods. Further characterization of sea ice DOM on the molecular level will also be conducted in collaboration with G. Underwood at the University of Essex, UK.

4.5.3 Preliminary results

4.5.3.1 Dissolved nutrient content of bulk sea ice

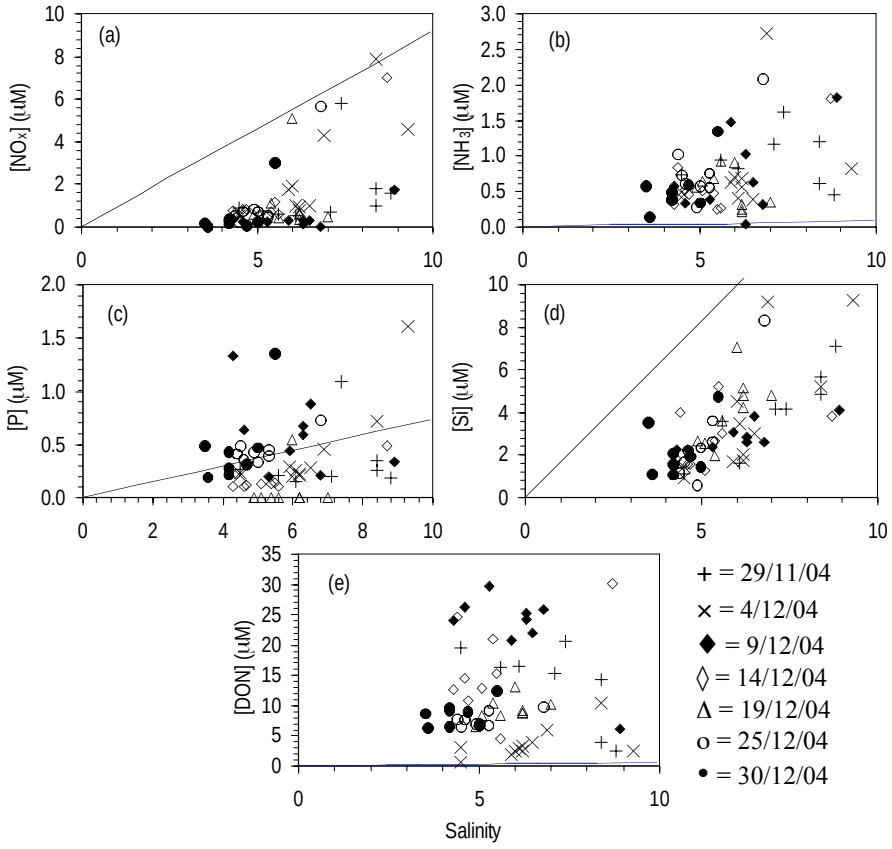

Fig. 4.18: Inorganic nutrients and dissolved organic nitrogen (DON) vs. bulk ice salinity in ice core sections from site 6 on the ISPOL floe: a) dissolved nitrate plus nitrite (NO_x), b) dissolved ammonium (NH_3), c) dissolved phosphate (P), d) dissolved silicate (Si), and e) DON. The solid line represents dilution by ice of the composition of contemporaneous seawater measured during the cruise.

Measurements taken from a number of cores collected between the 29/11 and 30/12/04 showed low concentrations of dissolved nitrate plus nitrite (hereafter,

nitrate; concentration range: 0 – 9 μM) and silicate (0.5 – 9 μM) in bulk ice, which exhibited L-shaped profiles with depth in the ice. Maximum values of dissolved nitrate and silicate were invariably measured in the bottommost 5 cm of the ice cores. Comparison with a simple dilution line of contemporaneous seawater concentrations showed that dissolved nitrate and silicate were mostly depleted in the bulk ice (Figs. 4.18a and 4.18d). The concentration of dissolved phosphate was variable and ranged from very low to elevated concentrations (0 – 1.5 μM) relative to contemporaneous seawater depending on core (Fig. 4.18c), while dissolved ammonium (0 – 2.5 μM) and DON (0.5 – 30 μM) were considerably elevated in the bulk ice (Figs. 4.18b and 4.18e).

4.5.3.2 Chlorophyll, dissolved oxygen, pH, dissolved carbon dioxide, and nutrients in sea ice brine and gap layer waters

Chemical measurements were conducted in sea ice brine collected from sackholes. The temperature of the sackhole brines ranged from -3.4 to -2.1 ^{o}C, while their salinity ranged from 39.6 to 63.2. The brines exhibited a large concentration range of dissolved oxygen (O_2), from 220 to 625 μM (Fig. 4.19a), while the chlorophyll concentration ranged from 0.6 to 2.2 μg L^{-1} (Fig. 4.19b). The concentration of dissolved carbon dioxide (CO_2(aq)) ranged from 1.4 to 6.0 μM and was much less than the value calculated for brines at equilibrium with the atmosphere at *in-situ* temperature and salinity (Fig. 4.19c), while the in-situ pH (reported on the seawater scale) ranged from 8.3 to 9.0 (Fig. 4.19d).

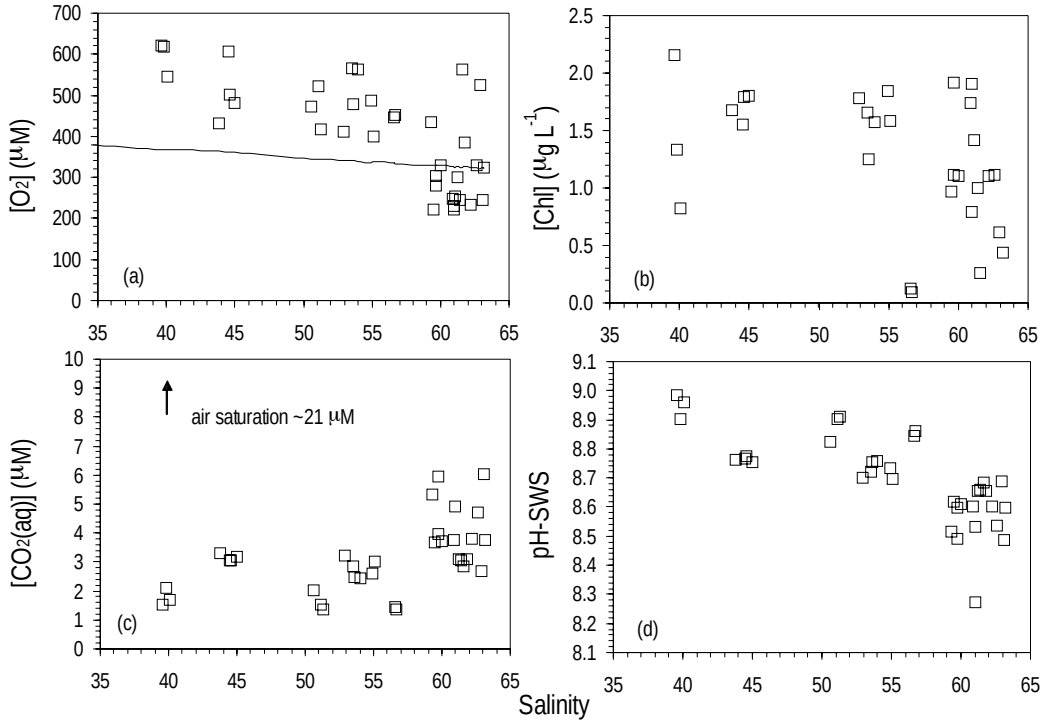

Fig. 4.19: a) The concentration of dissolved oxygen (O_2), b) chlorophyll (Chl), c) dissolved carbon dioxide (CO_2(aq), and d) in-situ pH on the seawater scale (pH-SWS) vs. salinity in sackhole brines drilled in sea ice. The straight line in (a) represents the O_2 concentration at in-situ temperature and salinity at equilibrium with air (air saturation).

The concentration of dissolved nutrients in sackhole brines exhibited similar depletion and enrichment patterns relative to the contemporaneous seawater composition to the bulk ice described earlier (i.e., Figs 4.18a to 4.18e). Specifically, dissolved nitrate ranged from 0.1 to 3.2 μM and was depleted by comparison with a conservative behaviour during brine formation by freezing of contemporaneous seawater (Fig. 4.20a). Dissolved phosphate (Fig. 4.20c) and silicate (Fig. 4.20d) ranged from 0.4 to 4.3 μM and from 4.2 to 84.1 μM, respectively, and appeared to be similarly depleted in the sackhole brines relative to a conservative concentration during the freezing of contemporaneous seawater. In contrast, dissolved ammonium (Fig. 4.20b) and organic nitrogen (Fig. 4.20e), which ranged from 0.2 to 2.5 μM and from 7.7 to 26.4 μM, respectively, appeared to be considerably enriched in the brines relative to contemporaneous seawater composition.

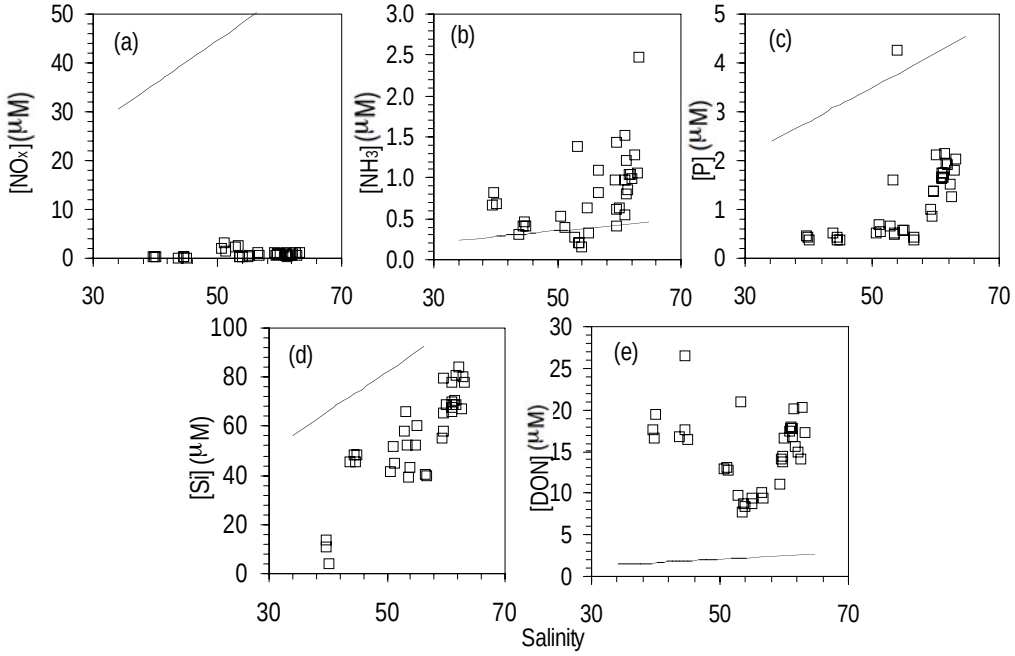

Fig. 4.20: Inorganic nutrients and dissolved organic carbon (DON) vs. brine salinity in sackhole brines from the ISPOL floe: a) dissolved nitrate plus nitrite (NO_x), b) dissolved ammonium (NH_3), c) dissolved phosphate (P), d) dissolved silicate (Si), and e) DON. The solid line represents conservative behaviour of the solutes during brine formation by expulsion of sea salts from the ice matrix.

Chemical measurements were conducted in water collected from a thin gap layer formed in a surface depression of the ISPOL floe. The gap feature was sampled daily over a period of seven days.

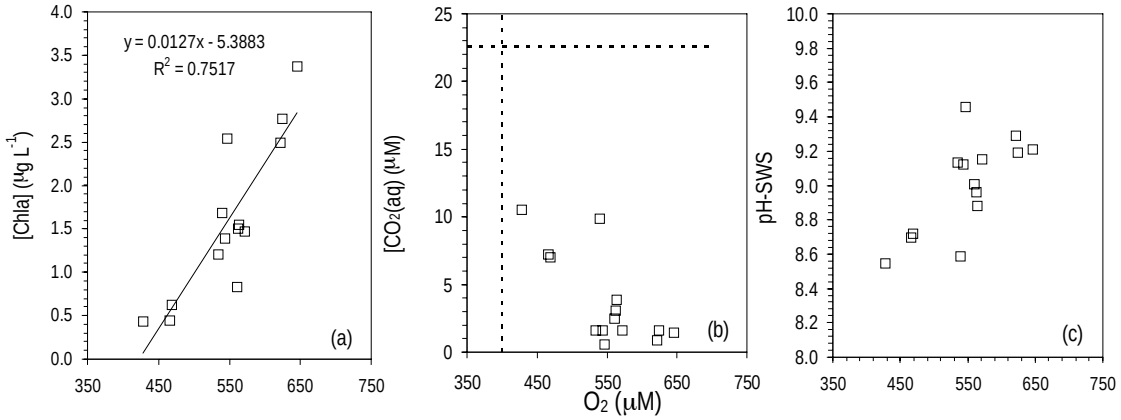

Fig. 4.21: a) Chlorophyll (Chl), b) dissolved carbon dioxide (CO_2(aq)), and c) in-situ pH-SWS vs. dissolved O_2 in the waters of a thin gap layer in the surface of the ISPOL floe. The solid line and equation in (a) represent the linear regression fit to the observations. The horizontal and vertical dashed lines in (b) indicate the %air saturation concentrations of CO_2(aq) and O_2, respectively, at in-situ temperature and salinity.

The temperature and the salinity of the water ranged from -1.7 to -0.8 ^oC and from 22.4 to 30.9, respectively. The water exhibited a moderate range of elevated O_2 concentrations, from 428 to 646 μM (Fig. 4.21), while the chlorophyll concentration ranged from 0.2 to 3.4 μg L^{-1} (Fig. 4.21a). The concentrations of O_2 and chlorophyll were positively correlated suggesting the influence of autotrophic biological activity (Fig. 4.21a). Additional evidence for the influence of biological activity on the chemical characteristics of the gap waters is provided by the CO_2(aq) and pH-SWS measurements. Specifically, the concentration of CO_2(aq) was very low, ranging from 0.6 to 10.5 μM (Fig. 4.21b), while the in-situ pH-SWS was amongst the highest measured on the ISPOL floe, ranging from 8.5 to 9.5 (Fig. 4.21c). Both very low CO_2(aq) concentrations and high pH-SWS were concurrent with high O_2 concentrations.

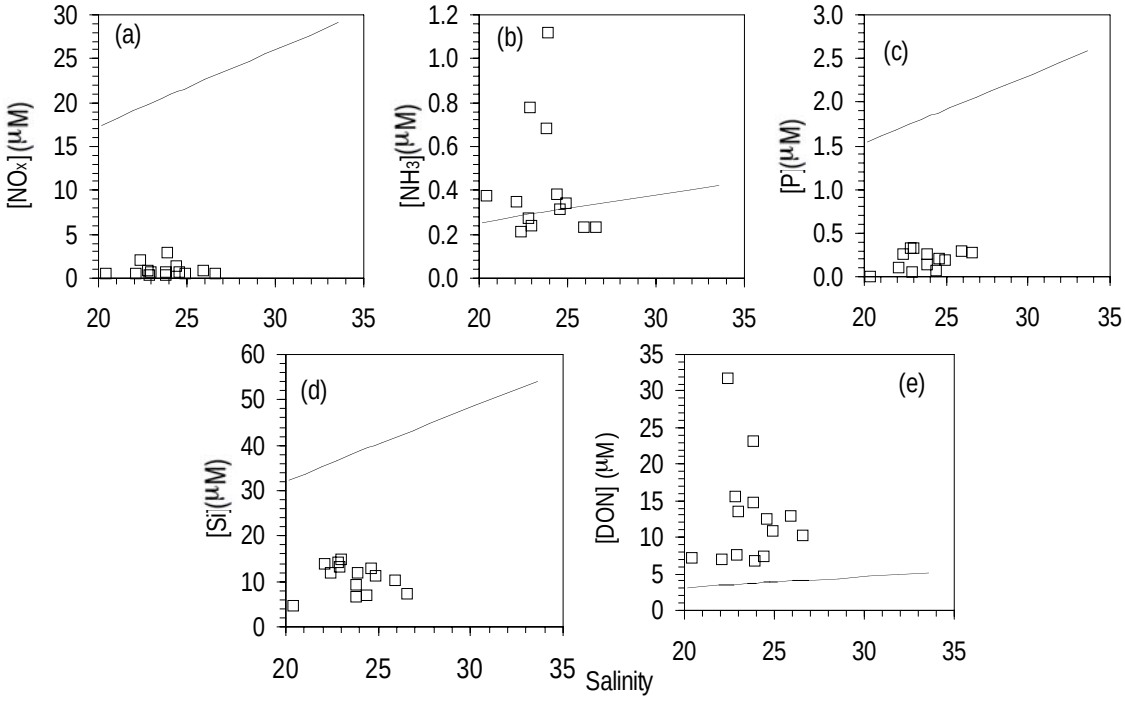

Fig. 4.22: Inorganic nutrients and dissolved organic carbon (DON) vs. salinity in the waters collected from a thin gap layer in the surface of the ISPOL floe: a) dissolved nitrate plus nitrite (NO_x), b) dissolved ammonium (NH_3), c) dissolved phosphate (P), d) dissolved silicate (Si), and e) DON. The solid line represents the concentration which can be expected from the gap waters originating in contemporaneous seawater diluted to the observed range of gap water salinity.

The dissolved inorganic nutrient concentrations in the gap water were typically very low (Fig. 4.22), following closely the trends seen in bulk ice cores and sackholes elsewhere on the flow (Fig. 4.18 and Fig. 4.20). Dissolved nitrate (concentration range: 0.3 – 2.9 µM), phosphate (0 – 0.3 µM) and silicate (5 – 15 µM) were all considerably lower than what can be expected from the gap waters originating in contemporaneous seawater diluted to the observed range of gap water salinity. Together with the trends seen in O_2, CO_2(aq), pH and Chlorophyll, these observations can be associated with autotrophic biological activity on the surface of the floe. In contrast, the concentrations of dissolved ammonium and DON were relatively elevated in the gap water (Fig. 4.22b and Fig. 4.22e).

4.5.3.3 Photo-oxidation of sea ice dissolved organic matter and the effect of major grazers on dissolved nutrient dynamics in sea ice

The preliminary results of the effect of light on the sea ice dynamics of dissolved organic matter (DOM) and inorganic nutrients are discussed in Dittmar and Koch, while the preliminary results of the effect of respiration, excretion and ingestion of sea ice zooplankton on the dynamics of dissolved nutrients and oxygen are presented in Schiel et al.

4.6 Carbon, iron and sulphur dynamics and interactions with biological activity and physical processes during sea ice melting

The SIBClim ISPOL team
Jeroen de Jong[1)], Bruno Delille[2)], Delphine Lannuzel[1)], Jean-Louis Tison[1)]

[1)]Université Libre de Bruxelles, Bruxelles, Belgium
[2)]Université de Liège, Liège, Belgium

4.6.1 General context

This field project comes in support of a long-term research programme aiming to assess to which extent ice-covered polar oceans contribute to biogeochemical processes regulating the Earth's climate. The programme involves a multidisciplinary consortium combining the expertise of glaciologists, biologists, geochemists and ecosystems-modelers of the Université Libre de Bruxelles (ULB, Belgium).

The main goal of the project is to study, understand and quantify the physical and biogeochemical processes associated with the sea ice biota that govern the emissions of marine gases of climatic significance. These processes are indeed presently unknown and therefore not integrated into Oceanic Biogeochemical Climate Models (OBCMs). In this context, particular attention is paid to carbon dioxide (CO_2) and Dimethyl Sulphide (DMS), both actively involved in the sea ice microbial metabolism. It has now been demonstrated that iron can play a crucial role in controlling phytoplanktonic productivity and the biological carbon pump in the Southern Ocean. Thus the work programme focuses also on the biogeochemical cycle of iron (origin, availability and fate) in the sea ice environment.

Modelling efforts involve the development of a new sea ice biogeochemical model (SIMCO). Its parameterization will rely on the results obtained during process studies such as ISPOL.

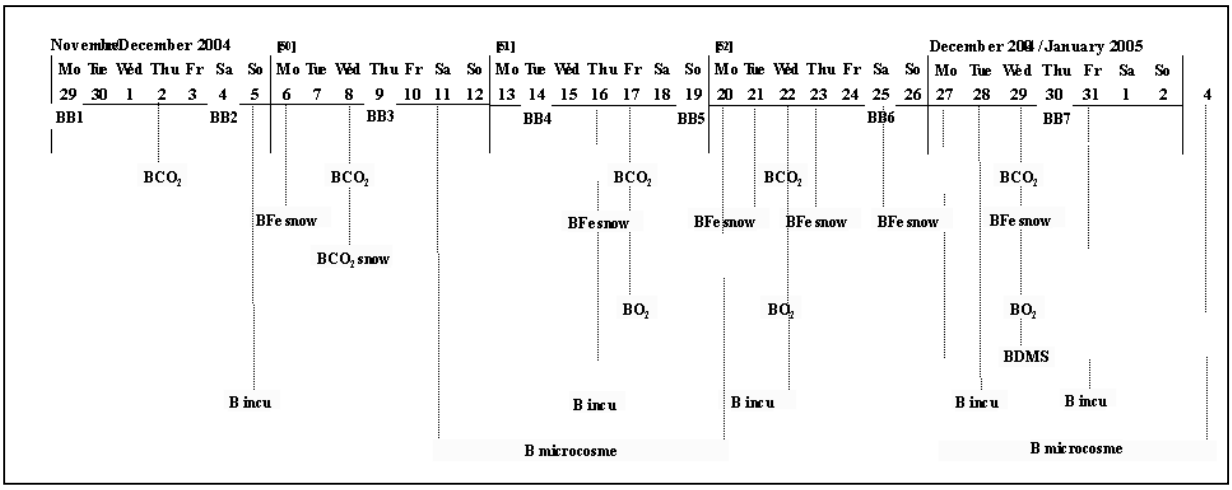

Fig. 4.23: Time chart of our activities during the ISPOL cruise

4.6.2 Field activities and shipboard laboratory work

Deciphering the complex biogeochemical processes governing the iron, carbon and sulphur cycle in sea ice has to rely on an integrated approach providing the best characterization of the sea ice environment during the time sequence involved. Therefore, sea ice sampling and measurements activities have addressed a whole set of physico-chemical and biological parameters both in the ice itself, in the sea water below, in the snow above and in the atmosphere. Further work involved ^{14}C / ^{55}Fe incubation experiments (3), both “in-situ” and in a ship-based incubator, and microcosms experiments (2) on bottom algae-rich ice samples.

Figure 4.23 is a time chart summarizing our activities during the ISPOL cruise. Figure 4.24 lists the set of parameters measured for each of the field sites. Sample aliquots were taken for nutrients, iron, Chl a, algae speciation, bacterial stock, protozoan biomass, viruses, TEP, viability and DGGE measurements during the microcosme experiments and for ^{14}C and ^{55}Fe during the incubation experiments. As a whole, 98 ice cores have been extracted, 165 brine sack holes were drilled, about 160 samples were processed for biological and nutrients measurements and 450 for iron, 100 CO_2 fluxes were measured and 680 DMS ice crushings carried out.

Figure 4.25 locates our main working areas listed in figure 1 and 2, on a floe map from 29 December 2004 (McPhee, personal communication). The “BB Time series” and “BIron Snow” were located inside the “Clean Site” perimeter, The “BCO_2 Time series” at the “B CO_2” site, the “BO_2” at the “Optodes” site and the “BDMS” at the “Tomato 1” site.

Taking the opportunity of a long cruise track from Cape Town to our study floe in the Western Weddell Sea and return, “underway” continuous pCO_2 measurements were performed, and complemented by discrete Chl a and oxygen measurements in areas of interest.

	BB Time series	BCO_2 Time series	BIron Snow	BCO_2 Snow	BO_2	BDMS
Texture	●	●			●	●
Fabrics	●	●			●	●
Bulk salinity	●	●			●	●
Water stable isotopes	●	●				●
Gas composition (O_2, $C0_2$, N_2, Ar, DMS)	●	●			●	●
Total Gas	●	●			●	●
Particulate material (Fe including isotopes, Al, Biogenic Si, POC, DMSP)			●			
Filtrate (Na^+, K^+, Ca^{2+},Mg^{2+}, δFe, Fe^{3+}, Cl^-,$SO4^{2-}$, NO_3^-, NH_4^+,PO_4^{3-}, H_4SiO_4, DOC, DON, BSi)	●		●			
Carbonate equilibrium (ice and brine pCO_2, CO_2 fluxes, $CaCO_3$, T_{alk}, pH, O_2)	●	●		●	●	●
Microbial Communities (stock, viablity, biodiversity)	●	●			●	●

Fig. 4.24: Summary of the set of parameters measured at each field location

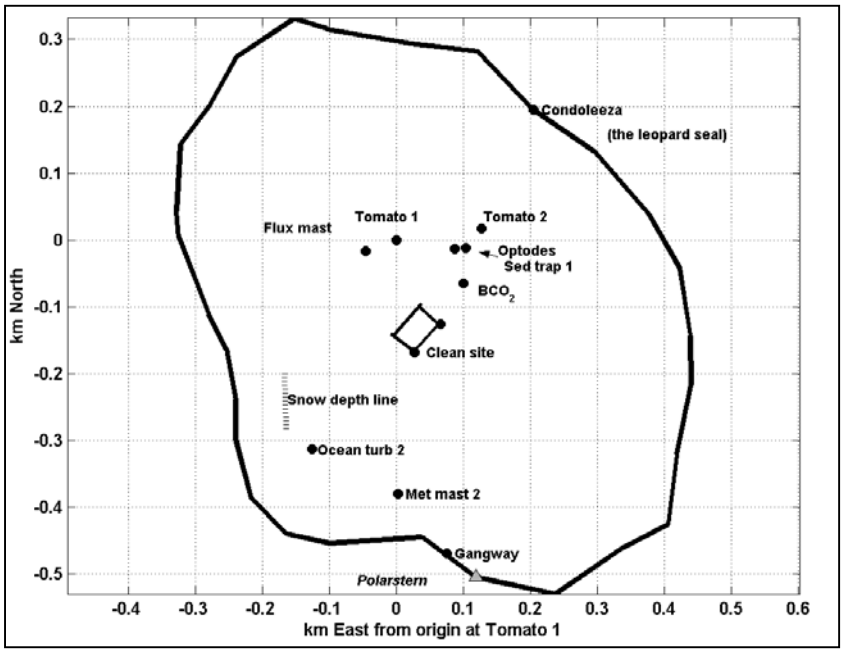

Fig. 4.25: Location map of our study sites on the floe (courtesy Miles McPhee)

4.6.3 Preliminary Results

A fair amount of ice core, water and filter samples is still to be processed in the home laboratories. We will therefore focus, in this section, on the already available preliminary data sets at the “Clean Site” location (Fig. 4.25) and from the “underway” measurements. DMS (P) measurements where performed in collaboration with J. Stefels and will therefore not be discussed in this report.

4.6.4 Underway pCO_2

Bruno Delille
Université de Liège, Liège, Belgium

Measurements of pCO_2 was carried out from the RV Polarstern sea water system inlet at a depth of 11 meters, using an equilibrator (Frankignoulle et al., 2001) coupled to an infrared gas analyzer (IRGA, Li-Cor® 6262). Water temperature *in situ* and at the outlet of the equilibrator were temperature-corrected and simultaneously measured using Li-Cor® sensors.

Figure 4.26 plots the underway pCO_2 measurements along the ISPOL cruise track. The atmospheric value is about 374 ppmV. The water concentrations are close to equilibrium on the way in, until a first localized pCO_2 low (down to nearly 300 ppmV) is observed entering the ice edge. From the edge onwards, all the values, as we travelled into the pack ice and stayed at the ice floe, are generally oversaturated. On the way out, strong undersaturation occurs as the ice edge is crossed. It remains a general feature of the crossing to South Georgia, demonstrating the clear impact of water mass properties driven by the proximity of land (tip of the Peninsula, islands) on the primary production in these areas in summer.

Figure 4.27 shows an interesting plot of the pCO_2 vs. the salinity in the surface water in the Marginal Ice Zone Area, both on the way in (open circles) and on the way out (dots). There is a sharp contrast in the dynamics of these two parameters depending on the location and the time of the year. On the way in, a clear pattern emerges from more saline oversaturated waters to less saline undersaturated waters, with a plateau at atmospheric values for intermediate salinities. On the way out, undersaturation is much stronger, and the pCO_2/salinity relationship breaks down. Future developments will aim at relating these contrasted spatial behaviour to physico-chemical evolution of the sea ice cover and bloom development in the sea ice and in the water column respectively, in the light of the ISPOL findings described below.

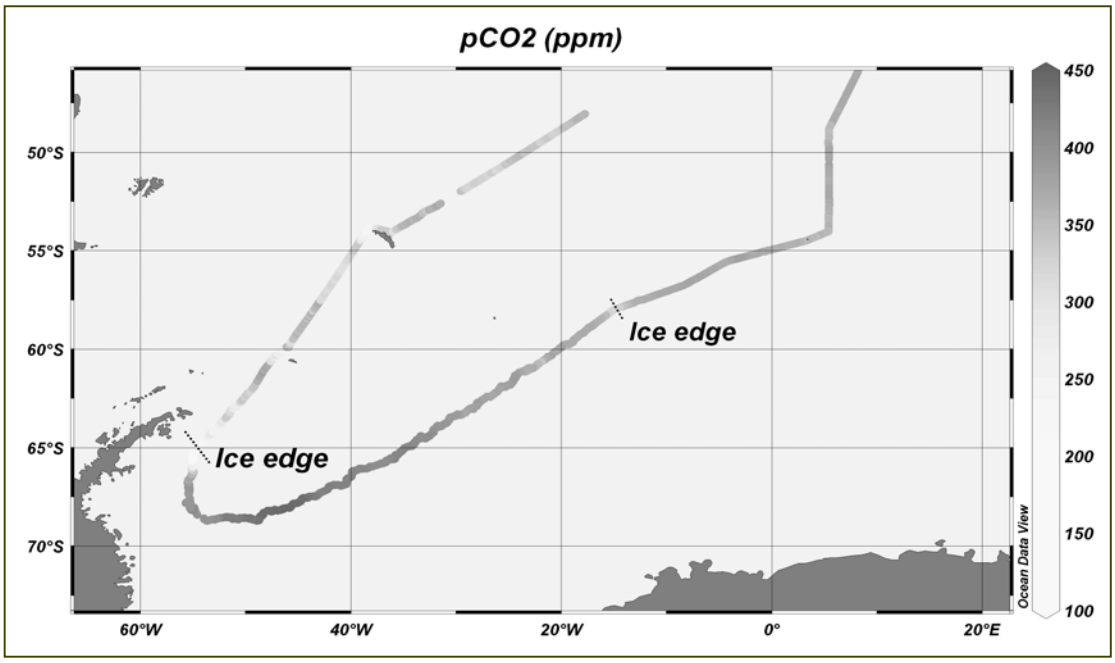

Fig. 4.26: Underway pCO_2 measurements during the ISPOL cruise

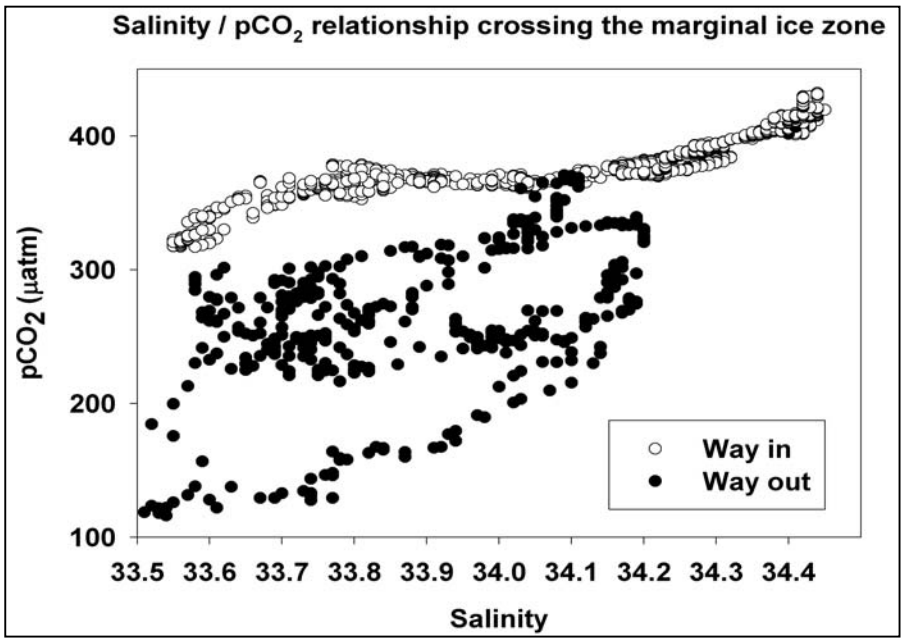

Fig. 4.27: Salinity / pCO_2 relationship crossing the marginal ice zone on the way in (open circles) and on the way out (dots)

4.6.5 Physical properties of ice, brine and sea water at the BB Time series site

Bruno Delille[1)], [1)]Université de Liège, Liège, Belgium
Jean Louis Tison[12] [2)]Université Libre de Bruxelles, Bruxelles, Belgium

Thin section profiles from the ice cores will be produced back in the home laboratory. In the meantime, we have recorded a rough visual description of a representative core from each of the 7 stations at the BB-Time series location (Figure 4.28).

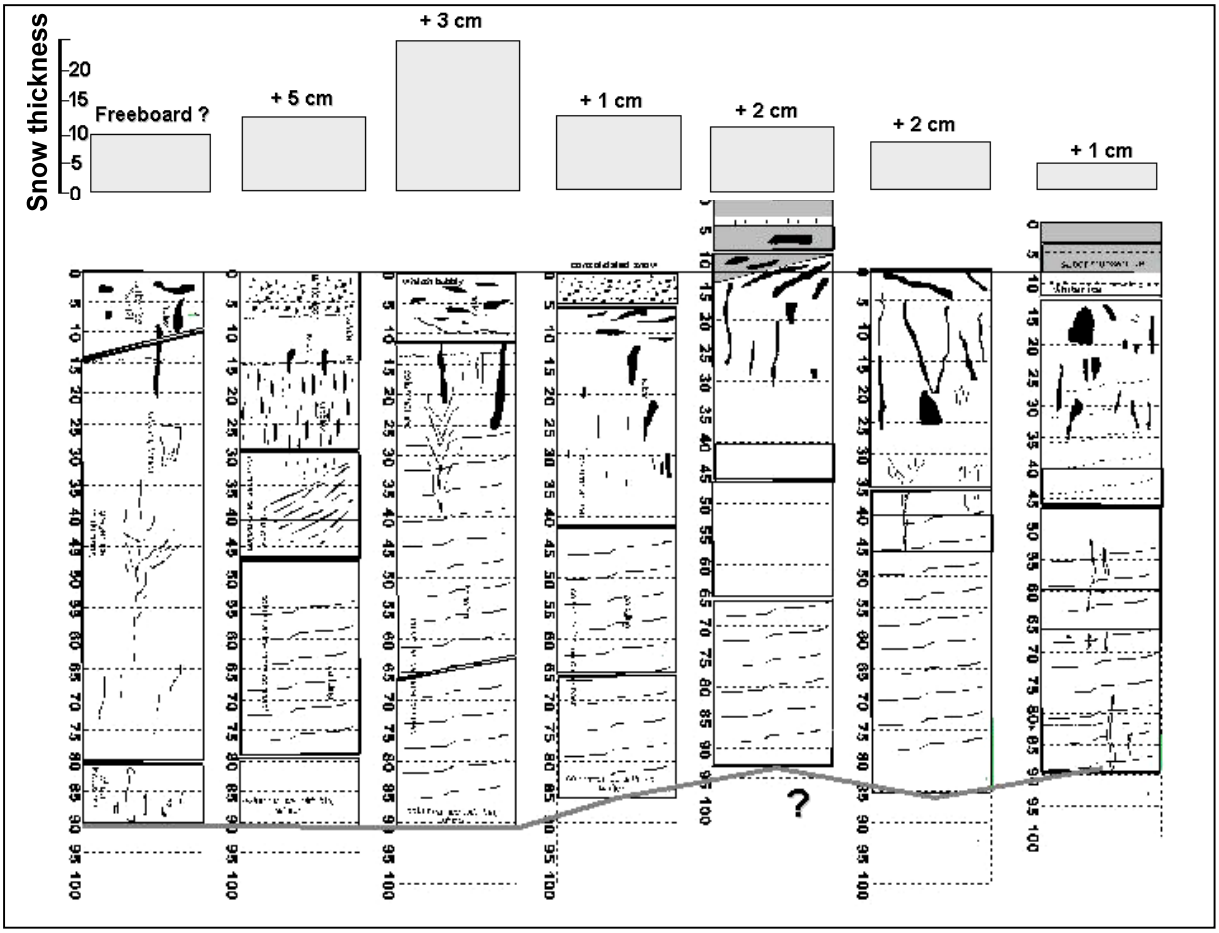

Fig. 4.28: Freeboard, snow thickness and ice texture at the 7 BB-Time series stations. Light grey area is snow, dark grey areas is superimposed ice. Black areas and sub-vertical or oblique features are voids and brine channels, sub-horizontal linear features suggests banding in the columnar ice. The lower thick line traces the hypothesized bottom of the ice cover.

The main recognizable features are:

a) positive freeboard throughout the experiment
b) limited snow thickness (as compared to most of the floe), decreasing towards the end of the experiment
c) increasing porosity in the top third of the core in the course of the experiment
d) widening brine channels at the bottom of the core towards the end of the experiment

e) potential, but limited, bottom melting of the core of the order of 5 to 10 cm, compatible with the low oceanic heat fluxes measurements (Miles McPhee, personal communication)
f) general development of a superimposed ice layer at the surface of the flow, becomes evident in the last two stations.

Figure 4.29 shows the temperature profile measured *in-situ* on one of the ice cores from each of the BB- time series stations, directly after extraction, with a calibrated TESTO thermometer probe (± 0.1℃) inserted in the ice core at regular intervals.

The profiles show a typical transition process of summer warming in the upper half of the core. Bottom temperatures only increase in the second half of the experiment, concomitant to the observed slight bottom melting in figure 4.28

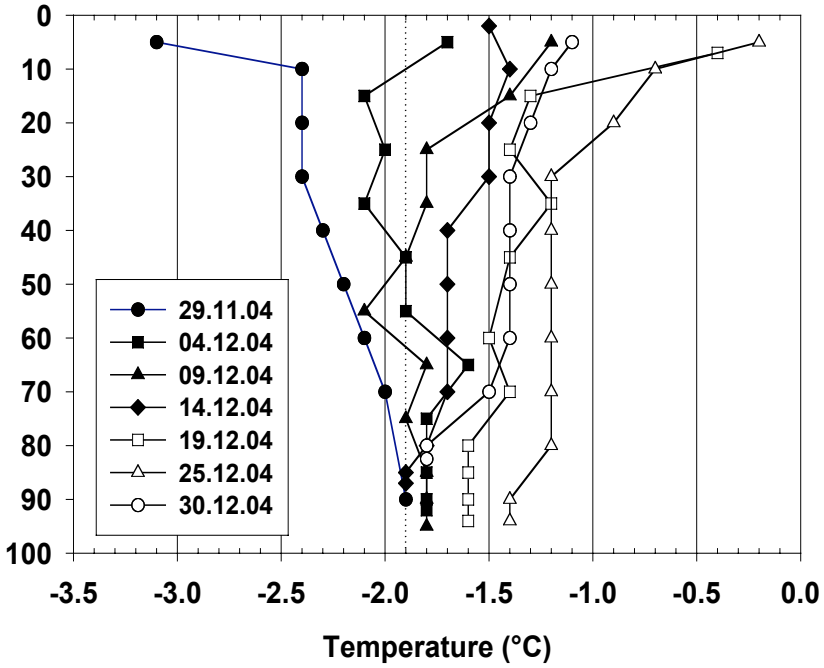

Fig. 4.29: Temperature profile for the seven stations of he BB-Time series

Figure 4.30 presents the salinity profiles for the same seven time series stations. In order to limit brine drainage the ice cores have been deep-frozen in the field, immediately after sampling, by storage into an insulated box filled with cooling bags at -35°C. Bulk salinity has been determined on melted 5 cm ice slices (portable salinity meter, ± 0.1), previously decontaminated from the outer 2 cm layer by sawing in a -25°C reefer container. Starting with the “classical” C-shape profile in accordance with the initial incorporation and brine drainage processes in the sea ice cover, an unusual Z-shaped profile develops with time, in parallel to the increasing porosity observed in the upper third of the core during visual inspection (Fig. 4.28). Very low salinities are measured in the bulk ice, down to a few per mil. This trend is indeed confirmed by the salinity measurements performed on brine waters collected in two sack holes of respectively 20 and 60 centimetres depth at each station (Fig. 4.31).

Whilst the first two stations of the time series indicate an expected (given the relatively lower ice temperature) higher salinity of the brine with respect to sea water at both depths, an inversion occurs from the third station on, with increasing dilution of the brines with time. This “stratification” of the brine “water table” should have important implications for the rate of exchanges of nutrients and dissolved gases, between the sea ice cover and the sea water below, and, therefore on the dynamics of the biological processes occurring in the sea ice. It is not clear yet, which process(es) is(are) responsible for this intense desalination of the upper sea ice layer. Melting of the brine channels walls under the gradually warming regime and transfer downwards is one potential process, although this transfer should be quickly inhibited once the brine stratification occurs. Contribution of melted snow to the upper brine layer is another option. It should however be kept in mind that the salinity

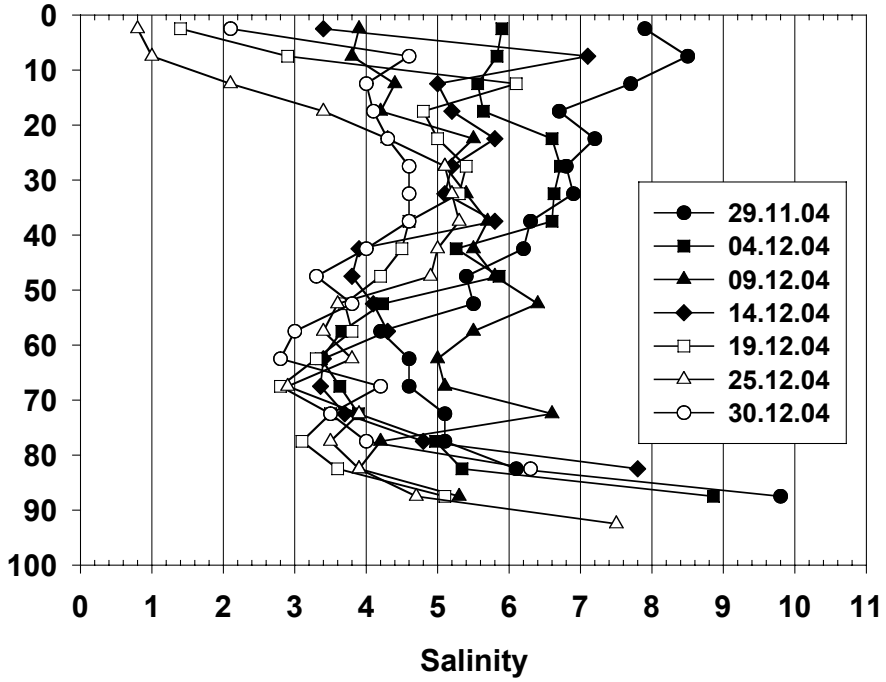

Fig. 4.30: Bulk ice salinity profiles for the seven BB-Time series stations

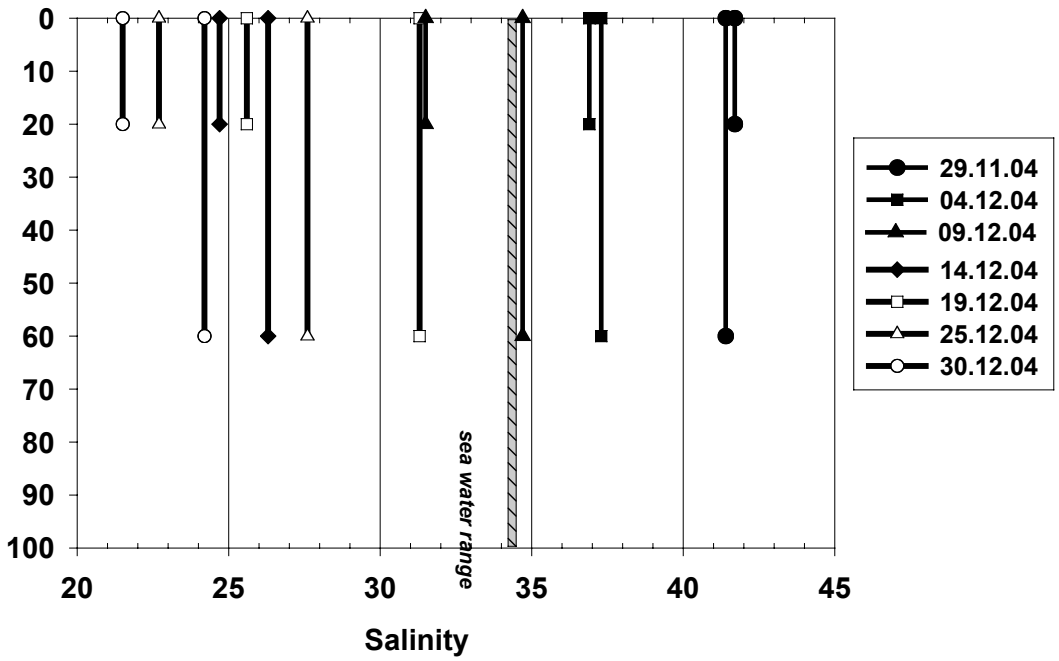

Fig. 4.31: Brine salinities in sack holes at 20 cm and 60 cm depth at each of the BB-Time series stations

measurements in the ice could have been biased by brine drainage on sampling, in this warm highly porous ice. Further arguments are expected to be found, once theoretical brine volumes and brine salinities will be calculated and compared to the observed ones, and in the light of the stable isotopes measurements in the collected brines (tracing of a more negative snow component or input of less negative melted ice from the brine walls).

Figure 4.32 plots the time evolution of brine salinities in ice and sea water salinities down to 30 meters. Samples were collected using a peristaltic pump (Masterflex® - Environmental Sampler), lowered in the brine sack holes (20 and 60 cm) and in the water column (interface, 1 m, 30 m). A clear change of regime occurs between stations 2 (4 December 2004) and 3 (9 December 2004). Initially higher brine densities trigger convection in the brine channels, resulting in salt fluxes at the ice ocean interface. Once brines density become lower than that of sea water, convection stops and exchanges across the interface are probably reduced to (much slower) diffusion processes.

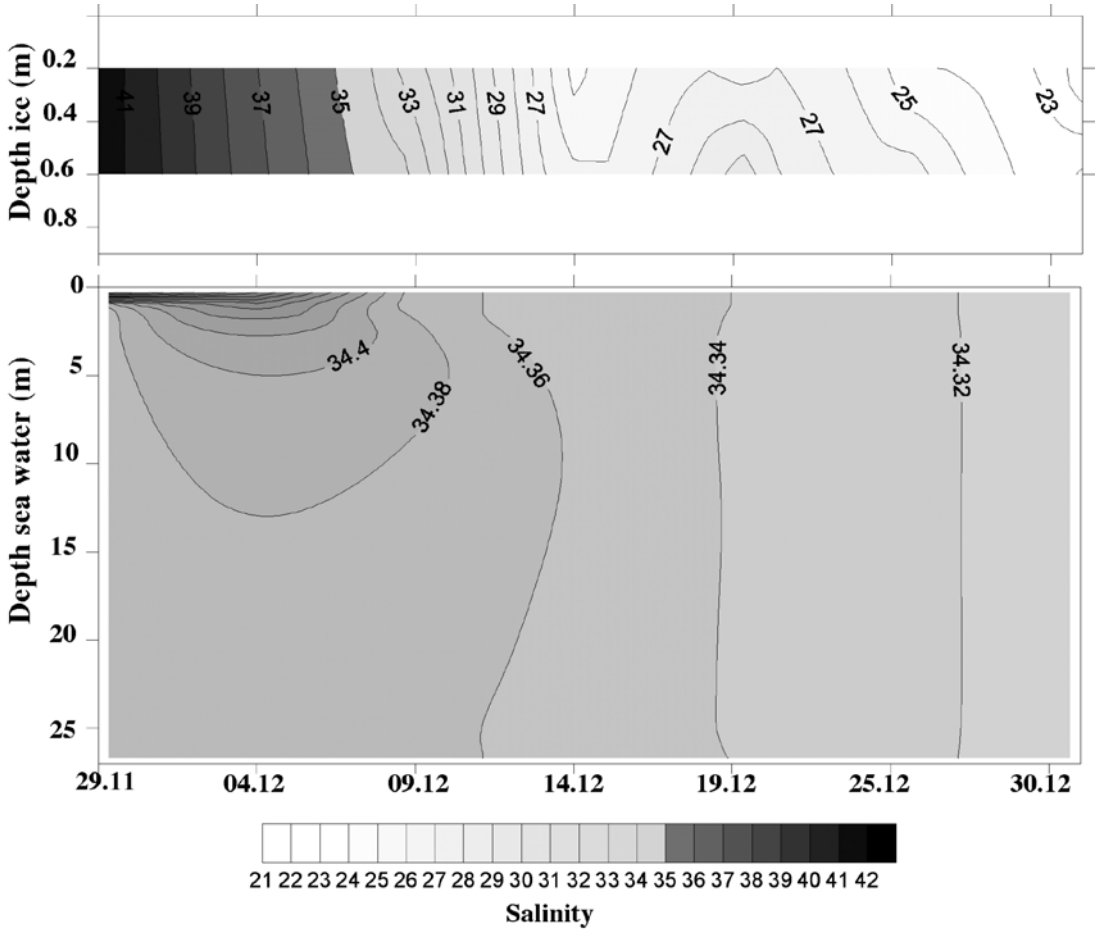

Fig. 4.32: Time evolution of the brine salinities in the ice (20 cm, 60 cm) and in the water column (interface, 1 meter, 30 meters) at the BB-time series site

4.6.6 PCO_2 in brines and water and CO_2 fluxes at the ice-atmosphere interface

Bruno Delille
Université de Liège, Liège, Belgium

Sampling of ice brine was conducted by drilling sackholes through the surface of the ice sheet at 20, 40, 60 and 80 cm depth. The brine from adjacent brine channel and pockets was allowed to seep into the sackhole as it has been reported to be the best current method to conduct brine chemistry studies (Papadimitriou *et al.*, 2004). Water was pumped from the hole and supplied to the pCO_2 measurement device using the peristaltic pump. The same peristaltic pump was used to collect the water samples down to 30 meters under the ice sheet (@ respectively 0, 1, 2, 4, 9, 14, 19, 24 and 29 meters). Measurements of pCO_2 were carried out using an equilibrator (Membrana® Liqui-cell) coupled to an infrared gas analyzer (IRGA, Li-Cor® 6262). Seawater flows into the equilibrator (2 L min^{-1}) from the top of the tube and a closed air loop (2 L min^{-1}) ensured circulation through the equilibrator and the IRGA. *In-situ* water temperature and at the outlet of the equilibrator were measured simultaneously using Li-Cor® sensors.Temperature corrections has been applied assuming that the relation from Copin et al. (Copin-Montégut, 1988) is valid at low temperature and high

salinity. The IRGA was calibrated soon after return to the ship while the analyser was still cold with air standards with nominal mixing ratios of 0.350 ppmV of CO_2. The equilibration time of the system was less than 3 min. The system was kept running twice this time before recording and averaging the values given by the IRGA and temperature sensors over a 30 s period by the data logger Li-Cor® 1400. All the devices (except the peristaltic pump) were enclosed into an insulated trunk (slightly warmed to keep the temperature inside above 0°C) containing a 12V battery as power source.

Figure 4.33 plots the time evolution of the pCO_2 in the ice brines and in the underlying water at the BB time series site during the whole of the experiment. The most striking feature is certainly the overall strong undersaturation of the sea ice cover, with values ranging between 28 and 135 ppmV, as opposed to both the atmospheric value of 374 ppmV and the sea water range of values from 368 to 400 ppmV. Within their range, the sea ice values most probably reflect the balance between CO_2 pumping through primary production of the sympagic organisms on the one hand, and, on the other hand, replenishment through brine convection with the underlying water and diffusion processes both at the ice-sea and at the air-ice interface.

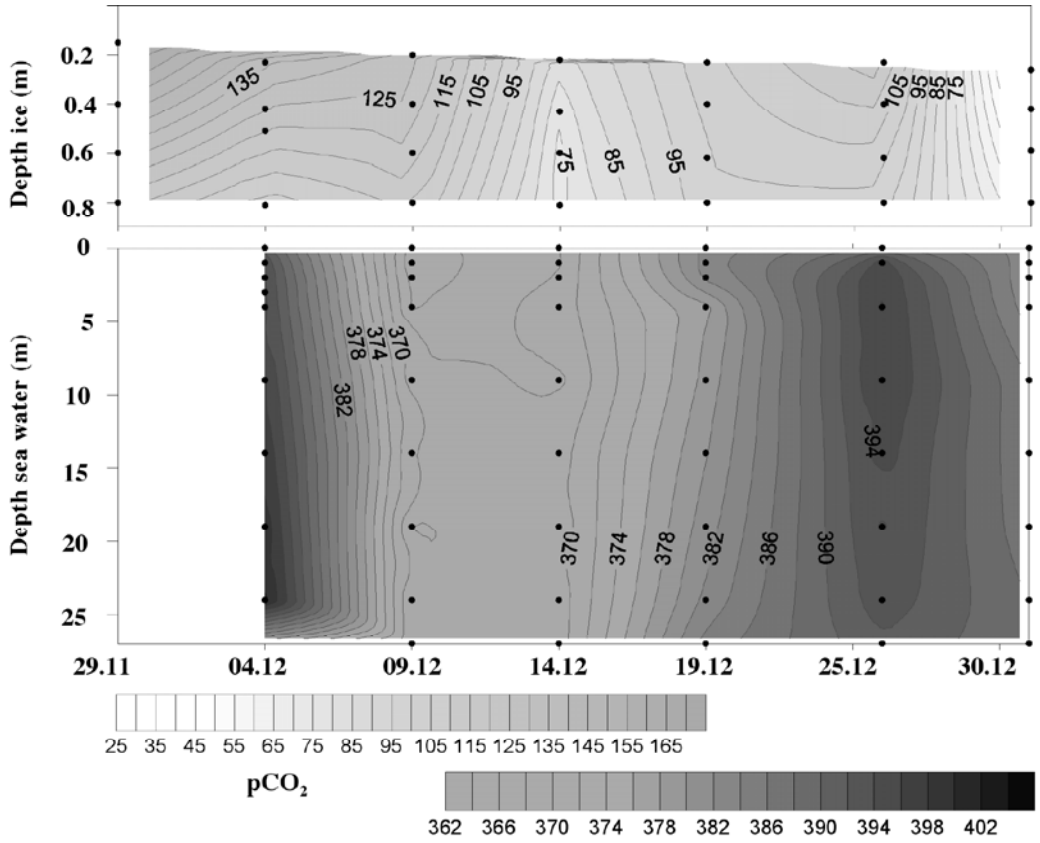

Fig. 4.33: Time evolution of the pCO_2 in the brines and the underlying sea water column at the BB-Time series site . Note that the (strongest) ice-atmosphere and ice-ocean interface gradients are not represented for the sake of clarity. Direct profiles comparison between ice and water through time is probably not pertinent given the decoupling due to ice drifting at the ocean surface.

Although the biologic component of this very dynamic system is not yet known, there are some clues already available on the physical controls of convection and diffusion processes. The stratification of the “brine water table” between the second (4 December 2004) and the third (9 December 2004) station (see above) coincides with an increased depletion of the CO_2 in the sea ice brines with a minimum close to the bottom of the sea ice cover, suggesting that the shut down of brine convection considerably slows down the physico-chemical compensation processes at the ice-ocean interface. Further rising of the pCO_2 in the brines could then reflect the exhaustion of the nutrients and subsequent decrease of biological activity. On the other hand, the sudden revival of CO_2 drawdown (to its record minimal values) at the end of the experiment, this time with minimal values at the ice-atmosphere interface, can also find its origin in the physical processes occuring there, as is shown in the CO_2 flux measurements below.

The air-ice CO_2 fluxes were measured with the chamber method. The accumulation chamber (West system ®) is a metal cylinder closed at the top (internal diameter 20 cm; internal height 9,7 cm) equipped with a mixing device which speed can be set up to 110 rpm. Rubber lips surrounded by a serrated edge metallic ring ensures an air-tight connection between the base of the chamber and the ice. The chamber is connected to a closed loop with the air pump (3 L min^{-1}) and the IRGA. The measurements of pCO_2 in the chamber are recorded every 30 s during 5 minutes. The flux was computed from the slope of the linear regression of pCO_2 against time (r^2 usually > 0.99) according to Frankignoulle (1988). The uncertainty of the flux computation due to the standard error on the regress in slope is on average ±3 %.Figure 4.34 shows the time evolution of the CO_2 fluxes at the ice-atmosphere interface both at the BB and the BCO_2 sites. In both cases it is clear that the undersaturation in the sea ice cover induces active fluxes from the atmosphere, the ice acting as a sink. At both sites, for the area where both data sets were available, the maximum fluxes occur where the undersaturation in the ice is the strongest. However, at site BB, initial measurements at the ice surface for the last two stations gave no measurable fluxes. A more careful examination of the ice at the interface revealed the existence of a relatively thick layer (5 to 6 cm) of superimposed ice. Significant fluxes were measured again after mechanically removing the ice crust (Fig. 4.34, top right). The observed fluxes were equivalent or higher than those calculated on our “way in” into the MIZ, but 2 to 5 times less than those calculated on our “way out”.

Finally, although the comparison is hazardous given the potential decoupling of the sea ice cover with regard to the underlying water mass, it is interesting to note, in Figure 4.33, that the brine convection processes occurring during the period where primary production has already started could result in pCO_2 undersaturation events in the water column below.

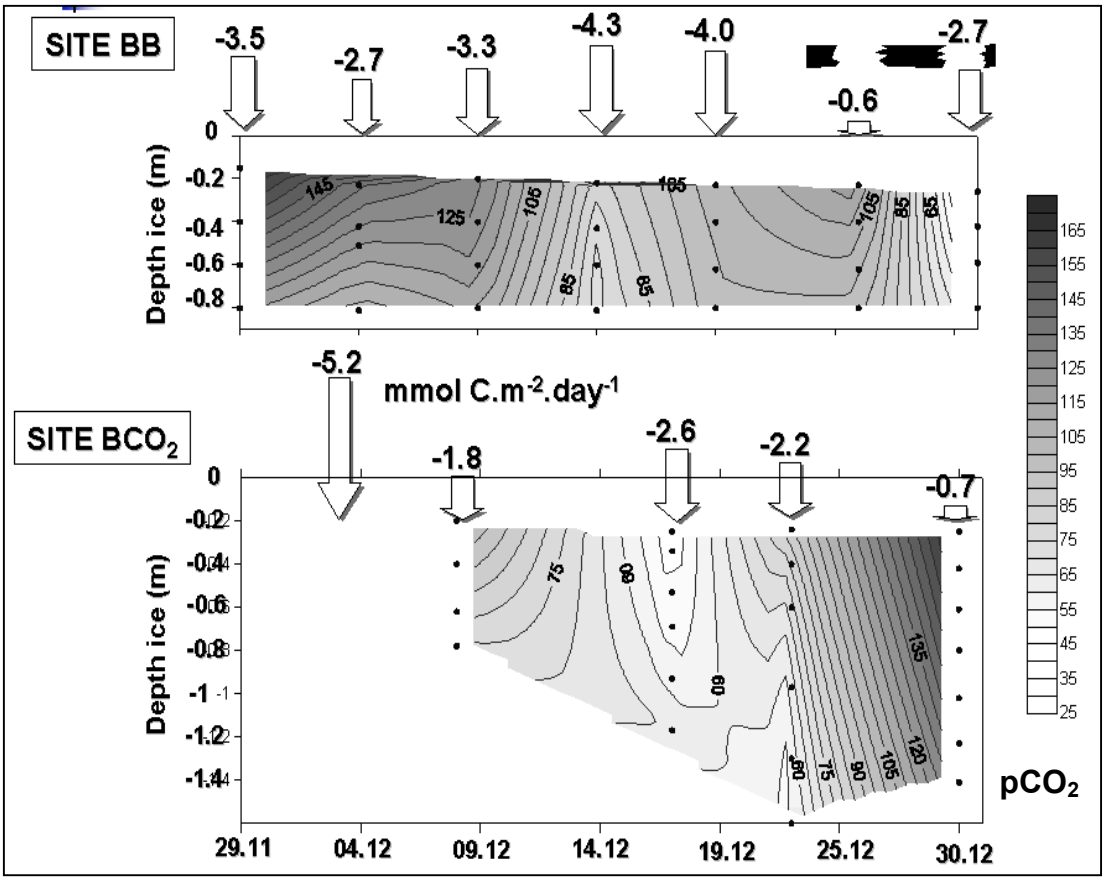

Fig. 4.34: CO_2 fluxes at sites BB and BCO_2, expressed in mmol C m^{-2} day^{-1}. For the last two BB stations no fluxes were observed before mechanically breaking the superimposed ice layer at the surface. No brine pCO_2 profile is available for site BCO_2 in the beginning of the experiment.

4.6.7 Iron concentrations and isotopic composition in snow, sea ice, brine and sea water

Delphine Lannuzel, Johannes de Jong — Université Libre de Bruxelles, Bruxelles, Belgium

Samples of snow, brine (collected at 20 cm and 60 cm deep), seawater (interface, 1 m and 30 m deep) and sea ice (4 sections chosen in function of the texture and presence of micro-organisms) were collected upwind under trace metal clean conditions. Great attention was paid to prevent contamination: the whole team was wearing clean garments over warm clothes, and items dedicated to sample collection and storage were acid-cleaned and wrapped in plastic bags. First, snow was collected with PE shovels, then, seawater and brine were pumped using a peristaltic pump, and sea ice was sampled using an electro-polished stainless-steel corer. Cores retrieved for Fe study were stored in acid-cleaned plastic bags until further processing.

The sea ice core was set in a polyethylene lathe inside a class-100 laminar flow bench in a clean container. Using Ti chisels the potentially contaminated outer few mm of the core were removed mechanically and 6 cm sections were cut. Brine, snow and seawater were treated on board as well. Total Dissolvable Fe (TDFe, unfiltered) and Dissolved Fe (DFe, filtered on 0.2µm Nuclepore filters) were acidified to pH≈1.8 (HNO_3 14N, Ultrex JT Backer). Filtrates and filters dedicated to Fe speciation and particulate Fe (PFe) determination were stored frozen once processed. DFe samples were analysed onboard by Flow Injection Analysis (FIA).

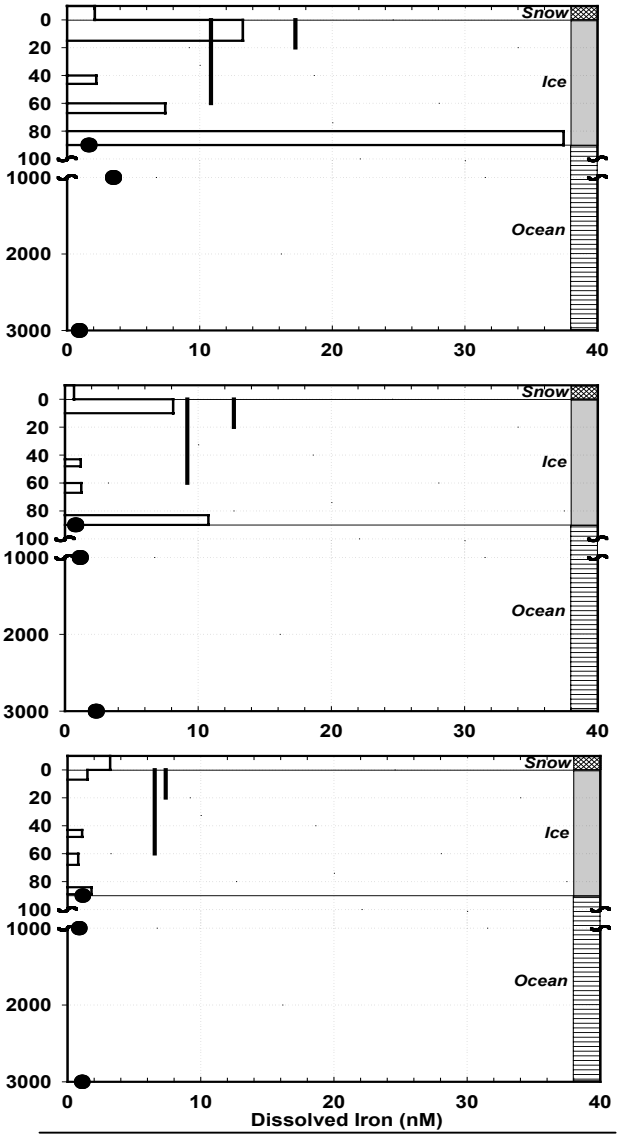

Fig. 4.35: Dissolved iron in snow and ice (bar graphs), brines (vertical lines) and underlying sea water (dots) from three stations of the BB time series

The measurement of Fe by FIA is based on the chemiluminescent reaction between luminol and O_2 catalysed by Fe-ions. The light emitted during this reaction at

pH=10.1 is detected by a photon counter. The resulting signal is proportional to the amount of Fe present in the sample. Our instrument (FeLume, Waterville Analytical, USA) detects dissolved Fe(II) and does not require any pre-concentration step. This system is an adaptation from O'Sullivan *et al.* (1995) and Bowie *et al.* (1998). In order to measure Fe(II+III), a reducing agent (Na_2SO_3) is added to the sample. To avoid contamination, Na_2SO_3 is purified on two sequential Si-8HQ columns prior to its addition to the analyte. The instrument is calibrated by the method of standard additions (3 additions of fresh Fe(II) per sample). Each standard addition is measured in triplicate using peak area integrations. One analytical run is achieved within 45 min and requires 60 ml of sample.

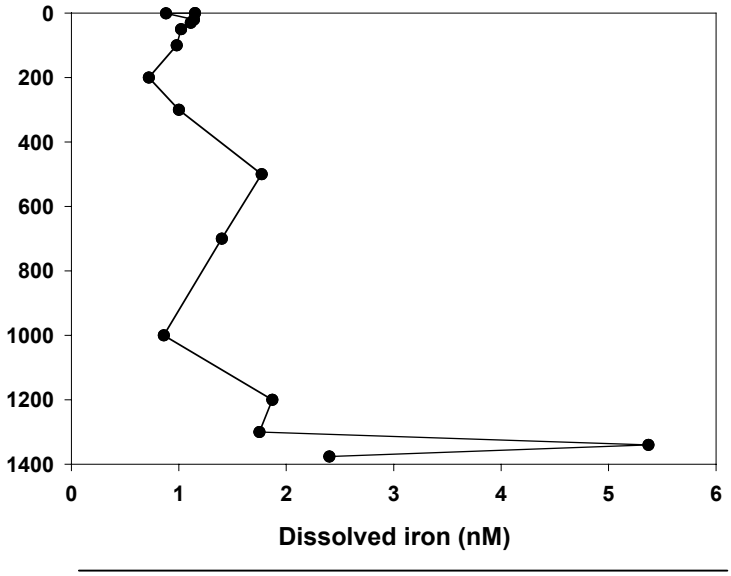

Fig. 4.36: Iron vertical profile in the water column below the ice floe at 67°22.2' S and 55°24.8' W

Figure 4.35 shows dissolved iron concentrations in snow and ice (bar graphs), brines (vertical lines) and underlying sea water (dots) from three stations of the BB time series. The most striking feature is certainly that sea ice concentrations can be up to an order of magnitude higher than those measured in the underlying sea water. It is worth noting, however, that the sea water concentrations are somewhat in the higher range of those described in previous studies (often sub-nanomolar), possibly due to the proximity of the continental shelf. The water depth was around 1400 m only, and a vertical profile (Fig. 4.36) exhibited dissolved iron concentrations of between 1 nM (surface) and 5 nM (sea floor). The other main characteristic is the overall decrease of the dissolved iron concentration at all depths in the course of time. The final concentrations in the ice reach levels similar to those observed in the water column below. Snow concentration are in the lower range of the sea ice values, with a somewhat higher level in the fresh snow layer collected on the 30 December. Further investigations in the home laboratory of the iron particulate fraction and of iron isotopic compositions (Nu Plasma Multicollector Plasma Source Mass Spectrometer)

in the various media, will potentially allow us to distinguish biological processes and input from external iron sources. Comparison with the textural properties of the ice cores (snow ice vs. frazil ice vs. columnar ice) could also gives us some complementary information on the iron pathways in the atmosphere-snow-sea ice-ocean system.

4.6.8 References

Bowie A. R., Achterberg E. P., Mantoura R. F. C., Worsfold P. J., Anal. Chim. Acta 361 (1998) 189-200.

Copin-Montégut C. (1988). A new formula for the effect of temperature on the partial pressure of carbon dioxide in seawater. *Marine Chemistry*, **25**, 29-37.

Frankignoulle M. (1988). Field measurements of air-sea CO_2 exchange. *Limnology and Oceanography*, **33**, 313-322.

O'Sullivan D. W., Hanson Jr. A. K., Kester D. R. Mar. Chem. 49 (1995) 65-77.

Papadimitriou S., H.Kennedy, G.Kattner, G.S.Dieckmann and D.N.Thomas (2004). Experimental evidence for carbonate precipitation and CO2 degassing during sea ice formation. *Geochimica et cosmochimica acta*, **68**, 1749-1761.

4.6.9 Acknowledgments

Our warmest thanks go to the crew of the RV *Polarstern* for their concern, availability, efficiency and creativity. We would also like to thank the Alfred Wegener Institute and our German colleagues for inviting us on the ISPOL endeavour. This project has been funded by the Communauté Française de Belgique (ARC contract # 2/07 287) and by the Belgian Federal Science Policy Office (contract EV/12/7E).

4.7 Sea ice biology

Saskia Brandt[1)], Rainer Kiko[2)], Rupert Krapp[2)], Jan Michels[1)], Stathys Papadimitriou[3)], Annette Scheltz[2)], Henrike Schünemann[2)], Matthias Steffens[2)], Sigrid Schiel[1)], David Neville Thomas[3)]

[1)]Alfred Wegener Institute, Bremerhaven
[2)]Institute for Polar Ecology (IPÖ), Kiel
[3)]School of Ocean Sciences, Anglesey, UK

4.7.1 Time series study

In order to determine temporal changes of the sea-ice habitat and the under-ice habitat during the transition between winter and summer, chemical, physical and biological properties were investigated in a time series study ("TS") during the expedition ANT-XXII/2. For this purpose, an undisturbed sampling site of 12 x 12 m, chosen at the beginning of the ice station, was sampled every 5 to 6 days in a fixed sampling design (Fig. 4.37).

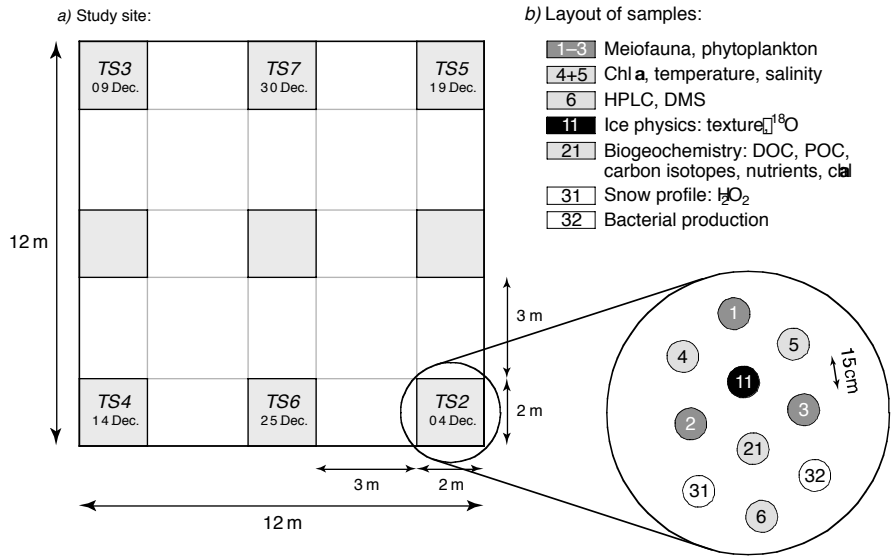

Fig. 4.37: Sampling scheme of the study site (a) and the layout of samples (b) of the time series (TS) study. Station TS 1 was taken at a location different from that of succeeding TS stations.

Since many institutions contributed to this interdisciplinary study, the working groups present their contributions separately in the present report. Investigations, which were conducted by the sea-ice groups of the Institute for Polar Ecology and the Alfred Wegener Institute during this temporal study included measurements of ice thickness, ice temperature, bulk salinity, chlorophyll *a* concentration (chl *a*) as well as the determination of abundance and distribution of sympagic meiofauna organisms. Small-scale distributions of abiotic (temperature, chl *a* concentration, salinity) and biotic properties (abundance and distribution of zooplankton organisms) of the under-ice habitat were investigated by use of an under-ice video system and an under-ice pump system.

4.7.2 Sea ice habitat

Annette Scheltz[1)], Sigrid Schiel[2)], Henrike Schünemann[1)], Matthias Steffens[1)]

[1)]Institute for Polar Ecology (IPÖ), Kiel
[2)]Alfred Wegener Institute, Bremerhaven

All ice cores taken at the same sampling day were drilled within an area of 2 x 2 m to minimize spatial heterogeneity (Fig. 4.37). Ice thickness was determined as the mean length of all drilled cores, whereas ice temperature was measured at only one core. Ice temperature was measured immediately after drilling with a Testotherm 720 thermometer inside small holes, drilled into the core at 5 cm intervals. Chlorophyll *a* concentration and bulk salinity were determined for three cores (Fig. 4.37). After drilling, the ice cores were cut into 1–10 cm segments, placed into cleaned polyethylene-boxes and melted onboard at 4 °C in the dark. Once melted, bulk salinity was measured with a WTW 190 conductometer. Based on ice temperature and bulk salinity measurements, brine salinity was calculated as a function of ice temperature, and brine volume was calculated as a function of bulk ice salinity and ice temperature.

For the determination of chlorophyll *a* concentrations the melted ice samples were filtered onto Whatman GF/F filters, extracted in 90 % acetone, homogenized and analyzed fluorometrically with a Turner Designs 10-AU digital fluorometer. Detection limit of this method is 0.1 µg chl *a* l^{-1}. Meiofaunal investigations were conducted on three cores (Fig. 4.37). After cutting in 5–10 cm, all segments were melted in the dark at 4 °C in addition of 0.2 µm filtered deep-seawater to avoid osmotic stress. Once melted, all samples were concentrated over a 20 µm gauze and the samples of two cores were fixed for later analyses with buffered formaldehyde (1 % final concentration). The samples of the third core were sorted out under a stereo microscope (10–50 fold magnification) onboard.

4.7.2.1 Results

Ice temperature

Ice-core temperatures measured at the first four stations (TS 1 to TS 4) were mostly between -2.0 and -2.5°C (Fig. 4.38). From station TS 5 to TS 7 temperatures increased in the upper part of the ice cores reaching a maximum value of -1.1°C at the topmost ice segments (TS 7). Ice-core temperatures at the ice-water interface were rather constant during the course of the study ranging from -2.2°C (TS 4) to -1.9°C (TS 6 and TS 7).

Bulk salinity

Bulk salinities measured in ice cores taken during the time series study ranged between 3.3 and 11.6 (Fig. 4.38). Salinity profiles for stations TS 1 to TS 4 were of similar shape, with bulk salinities of 5–8 within the uppermost 50 cm of the core and values of 3–5 between 50 and 70 cm depth. Below that depth, salinities did gradually increase towards the bottom of the ice cores reaching maximum values of ~11 at the lowermost segment.

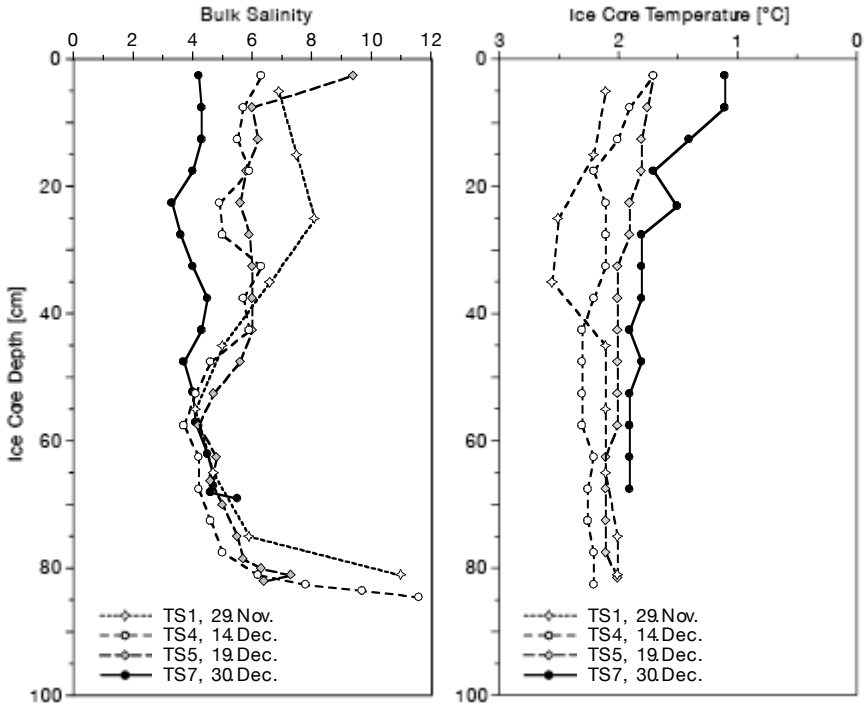

Fig. 4.38: Vertical profiles of bulk salinity and ice core temperature of four selected time series stations (TS 1, TS 4, TS 5 and TS 7)

Bulk salinities measured at station TS 5 were comparable to previous stations except for an abrupt salinity increase at the topmost section and a reduced salinity at the bottom of the ice core (Fig. 4.38). The last two stations of the time series study (TS 6 and TS 7) were characterised by a drop in bulk salinity values to ~4 for the upper 50 cm and further reduced salinities at the bottom of the ice cores.

Ice thickness

Thickness of ice cores taken during the time series study varied between 67 and 94 cm (Fig. 4.39). Within ice cores of the same sampling day thickness variability was generally ≤8 cm. Ice cores of station TS 1 (which were taken at a location different from that of succeeding TS stations) were lower in thickness (median: 82.3 cm) than cores of the following two stations (TS 2 and TS 3, medians: 90.5 and 92 cm, respectively).

Compared to stations TS 2 and TS 3, ice-core thicknesses of stations TS 4 and TS 5 (medians: 84.0 and 82.5 cm, respectively) were on average 8 cm lower. At the last two stations of the time series study (TS 6 and TS 7) ice cores were on average ~11 cm shorter than cores from stations TS 4 and TS 5 (Fig. 4.39).

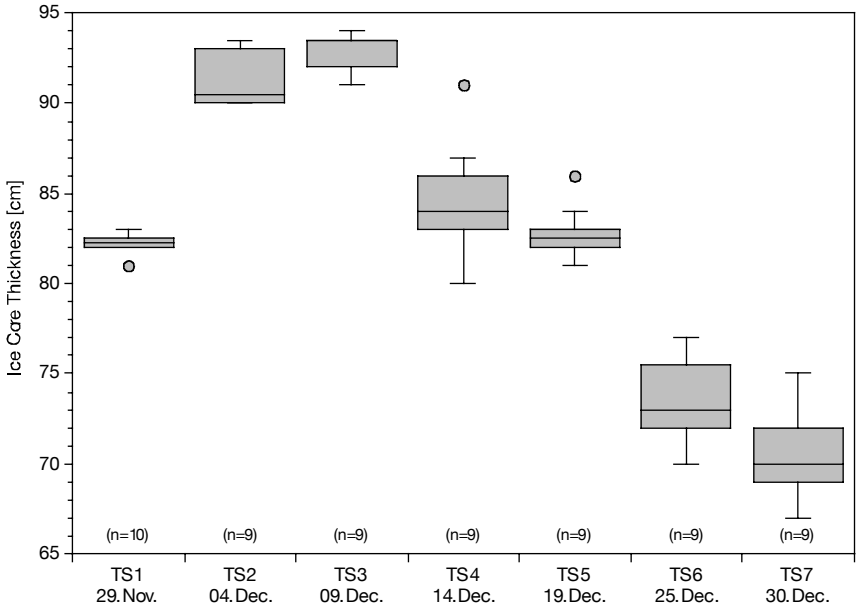

Fig. 4.39: Ice core thickness of all stations sampled during the time series study. Box plots show the total data range, the 25–75 % quartile range and the median. Outliers are marked as single data points.

Chlorophyll a

Time series cores analysed for chl *a* concentration revealed a pronounced bottom assemblage with mean chl *a* concentrations being one order of magnitude higher at the bottom decimetre than in any other segment of the core (Fig. 4.40). During the first four stations (TS 1 to TS 4) chl *a* concentrations within the upper 70 cm of the ice cores generally did not exceed 2.5 µg l^{-1}. Mean chl *a* concentrations at the bottom decimetre of the ice ranged from 34.6 to 38.8 µg l^{-1} and a maximum value of 262 µg l^{-1} was recorded at the lowermost centimetre of station TS 4.

While chl *a* concentrations in the centre part of ice cores from stations TS 5 to TS 7 were not particularly different from previous stations, mean concentrations at the bottom decimetre were considerably lower (17.3–20.3 µg l^{-1}) and chl *a* values at the lowermost centimetre were only about half of what was measured at the first four stations (Fig. 4.40).

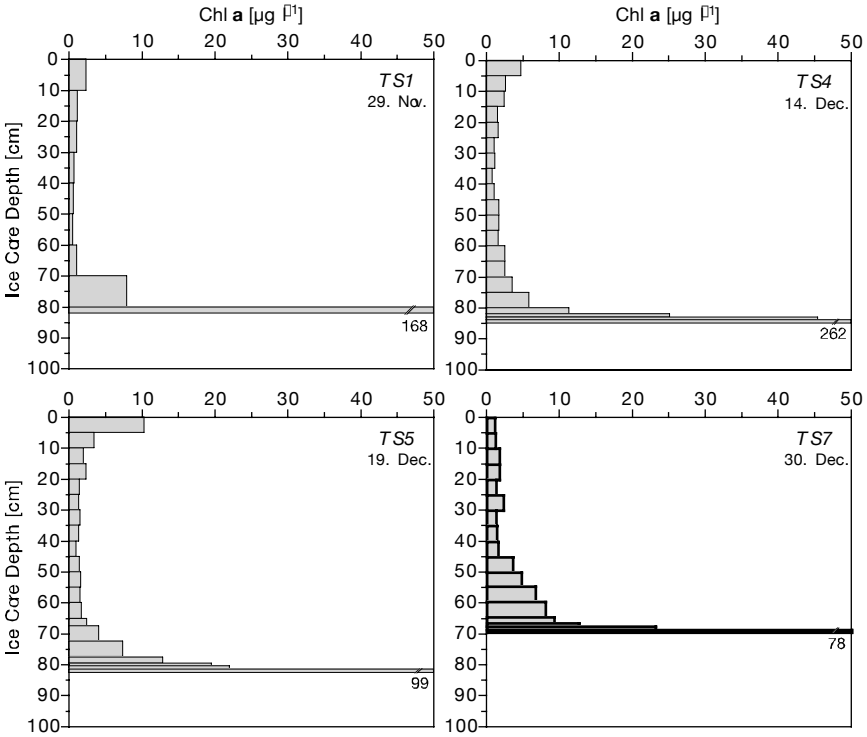

Fig. 4.40: Vertical distribution of chlorophyll a concentrations at stations TS 1, TS 4, TS 5 and TS 7 during the time series study

Sympagic meiofauna

In the beginning of the time series study the occurrence of sympagic turbellarians and copepods was almost restricted to the lowermost part of the ice (Fig. 4.41). With the exception of single specimens, found in the upper part of the ice, organisms concentrated near the ice-water interface. Abundances of turbellarians ranged between 363 (TS 1) and 1075 individuals l^{-1} (TS 2) within the lowermost ice segments and decreased with time. However, starting from the fifth sampling day (19 December), turbellarians and copepods were also found in high abundances in the uppermost part of the ice, more pronounced in turbellarians (Fig. 4.42).

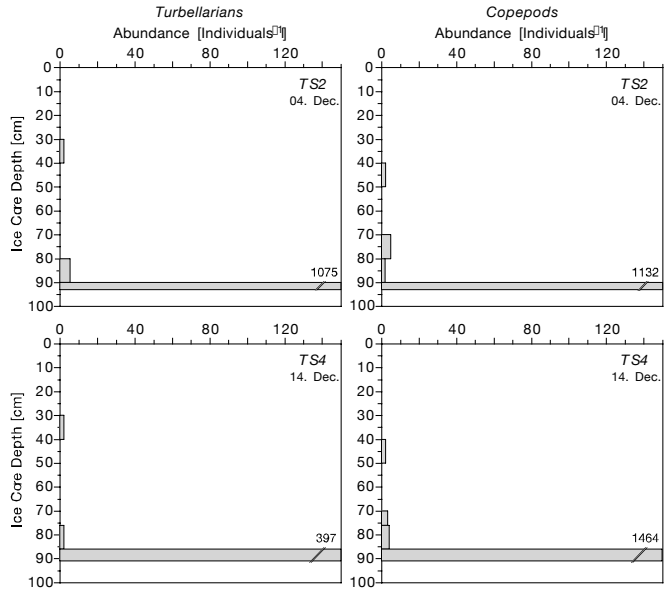

Fig. 4.41: Vertical distribution and abundance of sympagic turbellarians and copepods at stations TS 2 and TS 4 during the time series study

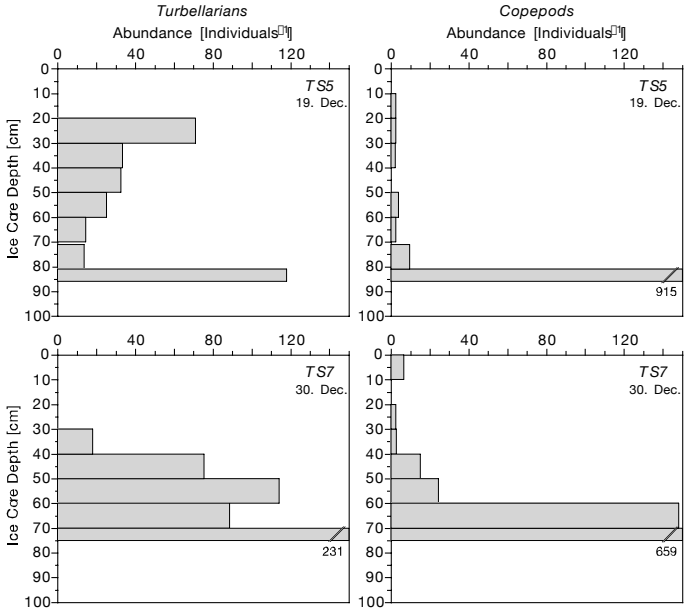

Fig. 4.42: Vertical distribution and abundance of sympagic turbellarians and copepods at stations TS 5 and TS 7 during the time series study

4.7.2.2 Discussion

During the first four stations of the time series study chl *a* concentrations increased in the inner part of the ice as well as at the ice underside (Fig. 4.39). Beginning with station TS 5, considerably reduced chl *a* concentrations were observed at the lowermost two centimetres of the ice which may be attributed to melting at the ice underside and, as a result, algae being washed out to the water column. This is corroborated by the marked drop in bottom-ice salinity at station TS 5 as compared to the preceding stations (Fig. 4.38).

The uppermost 5-cm segment at station TS 5 showed an abrupt increase in salinity (Fig. 4.38) that corresponded to a double-fold increase in chl *a* concentration within the same segment. This observation could indicate flooding of the uppermost part of the ice by seawater providing favourable conditions for algal growth or may simply be the effect of small-scale spatial heterogeneity.

A significant drop in ice-core thickness was recorded between stations TS 3 and TS 4 as well as between TS 5 and TS 6 (Fig. 4.39). Although the thinning of ice cores during the course of the study may be partly attributed to melting, it is unlikely that the ice floe was ablated by as much as 11 cm between two subsequent stations. Thus, it is assumed that the observed reduction in ice-core thickness represents the result of the combined effects of melting and spatial thickness variability.

In the beginning of the time series study the distribution of chlorophyll *a* concentration and sympagic turbellarians showed a pronounced correspondence. Highest values for both were found in the lowermost part of the ice near the water-ice interface. Since sympagic turbellarians most probably use ice algae as main food source their occurrence is distinctively related to high algae biomasses. Although these organisms are characterized by a high degree of body flexibility that facilitates them to penetrate also very narrow passages within the ice, the size of brine channels influences the mobility of these organisms. During the time series study ice structure changed and brine volume increased. Huge bubbles and caves inside the ice were detectable from station TS 5. Due to their high body flexibility turbellarians probably rather than sympagic copepods were able to descend higher into the ice and, thus, use food resources obtained in this upper part. Thereby, the organisms were furthermore able to avoid worsen environmental conditions near the ice-underside, e.g. caused by ongoing melting processes in the beginning of summer.

The results also indicate that total abundances of sympagic turbellarians did not change significantly with time but their distribution changed from an initial accumulation near the ice-underside to an enhanced spatial distribution of organisms during the course of the study.

4.7.3 Under-ice habitat

Annette Scheltz, Rainer Kiko
Institute for Polar Ecology (IPÖ), Kiel

The boundary layer between sea ice and the water column is a unique habitat with special abiotic (e.g. temperature, salinity) and biotic (e.g. food resources) factors, which also vary with season and region. In the Antarctic, studies of this special habitat are still scarce. Until now, krill (*Euphausia superba*) is the best described Antarctic species, which feeds in this habitat mainly during the winter season. Only one Amphipod species (*Eusirus antarcticus*), which lives in this environment, has been recorded until now.

Every five days, starting on 29 November, salinity, temperature and chlorophyll *a* concentrations were measured in the water column beneath the ice. Additionally, on each sampling day the ice underside was recorded with an under-ice video system

for one hour. In order to qualify and quantify the under-ice zooplankton (> 55 µm) an under-ice pump was used sampling water directly beneath the ice and at a depth of 5 m.

4.7.3.1 Results and discussion

It was possible to obtain five data sets at the same position on the one, the other two data sets were taken at different sites, due to ice dynamics, which crushed the first sampling site and made the access to the second site impossible at one occasion.

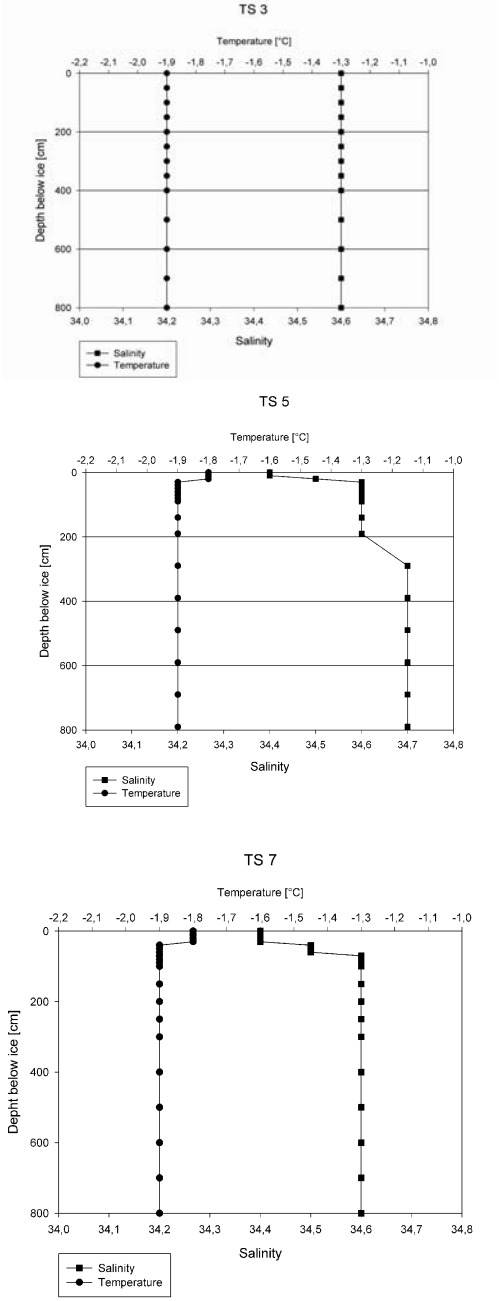

Fig. 4.43: Vertical profiles of salinity and temperature in the under-ice water at stations TS 3, TS 5 and TS 7 during the time series study

Temperature and salinity were measured in the first 8 metres below the ice (Fig. 4.43). During the first three stations, the under-ice water was always at the freezing point (e.g., TS 3) representing winter or early spring conditions. This was accomplished by the under-ice video images, which showed a smooth and level ice under-side.

From 14 December on temperatures in the first few decimetres under the ice rose slightly to -1.8°C and salinities declined to 34.6, indicating that some slight melting took place (e.g., TS 5 and TS 7). At the end of the measurement period also the under-ice video images showed a rougher under-ice surface with holes and depressions indicating melting at the ice-underside. The chlorophyll *a* concentrations slightly increased during the study from values of 0.1 µg/l at the ice underside and 0.1 µg/l five meters below, to concentrations of 0.3 µg/l at the ice underside and 0.2 µg/l five meter below. At one occasion an exceptionally high concentration of 2.3 µg/l was measured at the ice underside. This may be due to melting processes and the release of ice algae into the water column. The overall slight increase in chlorophyll *a* concentrations may indicate the beginning of the ice-algal spring bloom. Analysis of the quantitative under-ice pump samples in the home laboratory will give an insight to the community structure of the under-ice zooplankton but also will reveal if a trend of increasing biomass can also be found in the under-ice fauna.

4.7.4 The Antarctic infiltration layer

Rainer Kiko[1)], Jan Michels[2)] [1)]Institute for Polar Ecology (IPÖ), Kiel
[2)]Alfred Wegener Institute

Ice floes in the Antarctic often carry a large amount of snow, which results in a submerging of the sea-ice due to the weight of the snow. Thus, the snow is infiltrated by seawater, starting from cracks in the ice or directly through the ice if this is porous enough.

The seawater contains nutrients and algae, which find stable and favourable light conditions on top of the sea-ice. Therefore, high primary production can take place in this so-called infiltration or freeboard layer. Infiltration layers were already detectable during the crossing of the Weddell Sea at the beginning of the cruise, indicated by sometimes strongly brownish coloured ice edges.

In order to obtain sympagic copepods (*Drescheriella* spp. and *Stephos longipes*) for experimental studies, sea-ice as well as infiltration layers were probed which partly contained astonishingly high numbers of these copepods. Furthermore, other species like sympagic turbellarians, ctenophores and nudibranchs were found. In order to describe the environmental parameters and to quantify biomass and species composition a patchiness study was performed. At several randomly chosen positions on the floe total snow thickness, thickness of the infiltrated layer, temperature, salinity and chlorophyll *a* concentrations in the infiltration layer were measured. Additionally, quantitative amounts of the infiltration layer were fixed for later analyses of the contained meiofauna. Samples were taken three times every five days to obtain also a temporal resolution. Due to the lack of continuous

accessibility, not all samples could have been taken at the same sampling site as it was planned.

Temperatures within the infiltration layer varied from -2.0°C to -0.9°C with lower values at the beginning of the study (TS 5), and the salinity of the interstitial water ranged from 19.5 to 30.5. Lowest chlorophyll *a* concentrations of 0.7 µg/l were in the same range as those found in the under-ice water, whereas the highest chlorophyll *a*-value of 32.6 µg/l is about tenfold higher than values found in the seawater. Inspection of the samples for retrieval of experimental animals showed, that only the two copepod species mentioned above, one ctenophore species and different turbellarian species dominate the meiofauna of the infiltration layer. Two other copepod species and nudibranchs were only seldom found. Species composition showed a high spatial heterogeneity, especially with respect to the abundances of copepods and turbellarians.

Later analyses of species and stage composition of the taken meiofauna samples and comparison with samples taken from the ice and the under-ice water will show, if the infiltration layer plays an important feeding ground for the sympagic meiofauna.

4.7.5 Experimental and biochemical studies

Saskia Brandt[1)], Rainer Kiko[2)], Jan Michels[1)], Stathys Papadimitriou[3)], Sigried Schiel[1)], Henrike Schünemann[2)], David Neville Thomas[3)]

[1)] Alfred Wegener Institute
[2)] Institute for Polar Ecology (IPÖ), Kiel
[3)] School of Ocean Sciences, Anglesey, UK

4.7.5.1 Objectives

The metazoans in the Antarctic sea ice are dominated by turbellarians and calanoid and harpacticoid copepods. However, there are still great uncertainities concerning their role in energy and particle fluxes within the sea ice and between sea ice and water column as well as their adaptive and survival mechanisms. During ISPOL, experimental studies on feeding, defecation, respiration and excretion activities were carried out with the sea ice associated turbellarians, the dominant copepod species *Stephos longipes* and *Drescheriella* spp*.* and the ctenophore *Callianira antarctica* also found in the sea ice. For a comparison with processes in the water column, experiments were also done with the dominant pelagic copepod species *Calanus propinquus*, *Calanoides acutus* and *Metridia gerlachei*. Additionally studies on biochemical parameters such as lipids, carbon, nitrogen and stable isotopes as well as for amino acids, enzymes, were done for further detailed descriptions of the different life cycle stages and adaptative of the sympagic and pelagic animals encountered.

The studies should highlight to what extent physiological and biochemical mechanisms may differentiate sympagic from the pelagic copepods, and should also elucidate the mechanisms - as well as the limitations - which influence survival in sea ice habitats.

4.7.5.2 Work at sea

For the experimental, biochemical and physiological work, the sea ice meiofauna was obtained from ice cores and slush ice samples. The pelagic animals were caught by means of a Bongo net (100 mesh size) over the upper 200 and 500 m.

Feeding and defecation experiments were run at 0°C in a cooled laboratory container in dim light. The food offered was the natural phytoplankton suspension from the rosette samples of the upper 50 m. The concentrations of chlorophyll *a* were determined at the beginning and end of the experiments and were measured on board. Additional, subsamples for POC analyses and microscopic counting were also taken, the latter for obtaining information on preferential feeding on different size classes. The respective species and size composition will be determined on these preserved samples in the laboratory in Bremerhaven.

Investigations on physiological and biochemical adaptation included physiological rate responses and mechanisms and scopes of osmotic regulation. Experimental work in response to low temperatures and high salinities. concentrated on measuring respiration and excretion rates and has been carried out in a wide range of temperatures (between 0° and –1°C) and salinities (between 22.5 and 65). For measurements of inorganic ions, amino acids and enzyme activity whole animals were frozen at –80°C for later analyse. On board, oxygen, phosphate (PO_4) and nitrogen (NO_2, NO_4, NH_3, DON) values were determined using the Winkler method and an autoanalyzer, respectively.

4.7.5.3 Preliminary results

First results of the experimental work show low filtration and ingestion rates of the pelagic copepods and no clear trend with changing chlorophyll *a* concentrations was observed. This coincided with the feeding behaviour of the early developmental stages (nauplius stage VI and copepodite stages I - IV) of the ice associated copepod *Stephos longipes*. In contrast, the filtration rates of late developmental stages (adults and copepodite stage V) of *S. longipes* and *Drescheriella* spp. decreased with increasing chlorophyll *a* concentrations while ingestion rates increased. The impact of the sea ice copepods on the cryo-pelagic coupling will be calculated on the basis of the obtained results and data on their abundance in the ice.

Excretion rates did not change significantly with increasing salinities and temperature, neither in the sea ice metazoans nor in the pelagic species *Metridia gerlachei*. This result is puzzling since *M. gerlachei* occurs preferentially in mid-water layers and hence, is not exhibited to great changes in their environment.

4.7.6 Molecular-biological studies on sympagic organisms

Rainer Kiko
Institute for Polar Ecology (IPÖ), Kiel

During this cruise samples were taken to analyze adaptations of sympagic species to high salinities and low temperatures with molecular-biological methods.

The transcription of DNA to mRNA is the first step during the synthesis of proteins, which are the main effectors of physiological functions and adaptations. As the protein synthesis is energy demanding, it is very important for the cell to control this first step precisely. Therefore gene expression analysis is one of the first steps to understand physiological adaptation mechanisms on the transcriptional level. It will be searched for transcripts whose proteins are responsible for adaptations to the extreme habitat. Specimens of the copepod species *Drescheriella glacialis* and *Stephos longipes* were isolated mainly from the infiltration layer and incubated subsequently at different temperatures. For both species it was found, that they still actively swim at temperatures as low as -3.1°C and the corresponding salinity of 55. Underneath this temperature their activity strongly declines. Therefore about 1600 specimens per experiment and species were incubated at different salinities and temperatures: 400 specimens at -3.1°C and S = 55, 400 specimens at -1.2°C and S = 55 and 800 specimens at -1.2°C and S = 55 for at least two days.

From these different groups mRNA will be isolated and it will be searched for differentially expressed genes using a molecular-biological technique called “suppression subtractive hybridization”. The group, which encountered high salinities but no low temperatures functions as a control to find genes which are only strongly expressed due to salt stress. Thereafter the differentially expressed transcripts will be furthermore characterised with different molecular-biological methods.

Another side aspect of this project will be the sequence- and expression analysis of sodium potassium ATPase in both sympagic copepod species.

4.7.7 Under-ice amphipods in the Antarctic pack-ice zone

Rupert Krapp
Institute for Polar Ecology (IPÖ), Kiel

The Antarctic under-ice fauna is commonly believed to consist mostly of krill (*Euphausia* spp.) and copepods, while amphipods seem to play a minor role and have only occasionally been reported from the pack ice zone. The aim of the cruise was first of all to verify this assumption, i.e. to check whether there also were any amphipods under the pack ice of the western Weddell Sea, and secondly, whether they could be considered truly sympagic organisms, i.e. that they could be observed living close to and attached to the underside of the ice. Another goal was to measure ultraviolet radiation (UVR) at the sea ice surface and underside in different places to measure the penetration of this potentially harmful radiation under different ice types and thicknesses. This should then be combined with the findings of under-ice fauna sampling to test whether the UV radiation might have an impact on these organisms, or whether the ice provided sufficient cover and protection. Previous studies have indicated that UV can be an important ecological factor even under sea ice, and have pointed to certain pigment compounds, the mycosporine-like amino acids (MAA's) as a possible source of UV protection, since these pigments absorb at different wavelengths in the UV range. So sampled organisms were to be tested for total pigment content as well as MAA content, to address both the aspect of their food selection and possibly also MAA accumulation through intake of MAA-producing microalgae, notably diatoms.

Sampling was mainly based on conventional scuba- and rebreather diving, allowing the deployment of sampling gear and sensors selectively and accurately under the sea ice, as well as visually observing and recording the habitat and its fauna. Rebreather diving was the preferred choice of sampling, since it reduced the amount of disturbing exhaled air to an absolute minimum, while the time the diver could work underwater was greatly prolonged, due to the effective use of the recycled breathing gas. Another sampling method was the deployment of baited traps through core holes in the ice, as well as from the floe edge. A total of six dives were performed, during which two types of amphipods were observed and sampled under the ice. Sampling was performed using a hand-held dip net. These amphipods were identified as truly sympagic organisms, since they could be observed both in the habitat as well as in the aquarium as they were sitting attached to and even crawling into the ice under-surface. Later, samples from the infiltration layer revealed that they also reached this area of the ice floe, either by passing through larger vertical brine channels or by entering this layer horizontally. A first taxonomic analysis revealed that these amphipod types most probably belonged to the family Eusiridae, which matches previous observations of Eusirid species under Antarctic ice, though from other regions.

Another amphipod type was observed in the baited traps several times, where the previously mentioned Eusirid amphipods occurred only once. These amphipods were of a distinctively different type, namely of the family Lysianassidae, but since they were only found in the baited trap deployments and not in the under-ice net samples, it could not be determined whether they could also be considered as sympagic or rather sub-ice fauna. Laboratory observations in cooled aquaria showed no active attachment to the ice, while the previously mentioned Eusirid specimens readily and actively sought the attachment to pieces of ice when being offered this as substrate.

Apart from sampling individuals for total pigment and MAA content, several respiration and feeding experiments were performed, whose results will first be accessible after subsequent laboratory analysis and calculations. Preliminary observations revealed a carnivorous and even cannibalistic feeding mode for the Eusiridae, while data on the diet composition of the Lysianassidae as well as on the uptake of phytoplankton remain to be analysed. If possible, lipid analysis of all amphipod types will also be performed and could give additional information on that subject.

Due to the restricted possibility of sampling, the systematic measurement of UV penetration through the ice was limited to one transect, but more extensive measurements of surface irradiance and snow cover penetration were performed instead. The planned *in-situ* and laboratory experiments with artificial UV irradiance using lamps and the modification of artificial or natural light fields by means of filters had to be abandoned due to insufficient sample amounts.

4.8 Oxygen dynamics in sea ice

Andreas Krell
Alfred Wegener Institute, Bremerhaven

4.8.1 Introduction

Sea-ice algae play a major role as primary producers in polar ecosystems. Especially during late spring and early summer algal biomass accumulates in the sea ice and significantly contributes to primary production. Various techniques have been employed to quantify the photosynthetic activity of these communities, namely modified versions of the C^{14} incubation technique and measurements of net O_2 fluxes over the ice water boundary layer obtained from microelectrode profiles. The aim of this study was to measure oxygen concentrations in sea ice, brine and sea water as a proxy for biological activity. Measurements were carried with two different types of optodes. Mini sensors with a tip diameter of 4 mm for measurements in brine and sea water. Sea ice oxygen values were obtained in situ with the micro sensor having a sensor tip of 140 µm. The measuring principle of the optodes is based on the dynamic quenching of luminescence, i.e. a chemical cocktail, the luminophore is exited by a light flash of a reference LED. In the presence of oxygen the exited luminophore is quenched and hence not emitted back. Thus the luminescence lifetime and intensity can be correlated to the oxygen concentration.

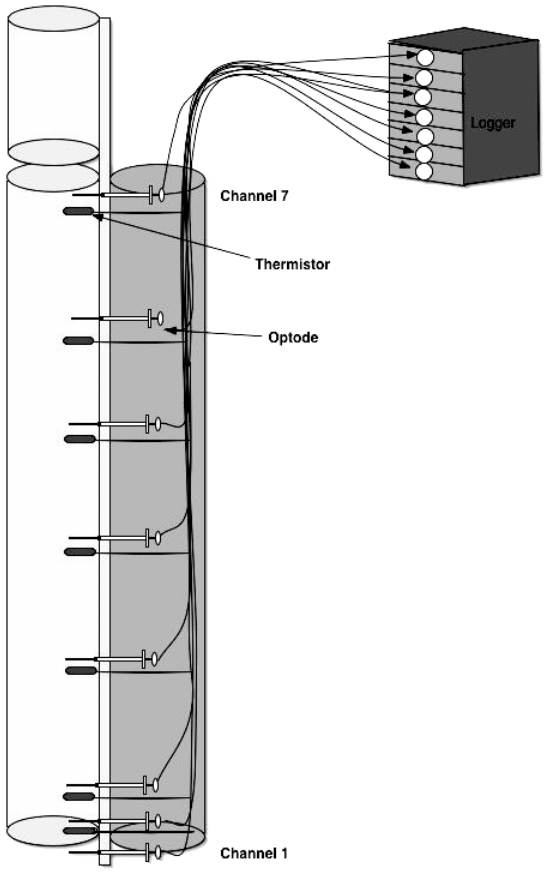

Fig. 4.44: Drawing of the optode array installed in the ice

An array of seven micro optodes was installed in the lower 1 meter of an ice core which was placed back in its original position (Fig. 4.44). Continuous measuring commenced on the 3 December and lasted until the first of January 2005. During this period four reference cores were taken in the vicinity of the optode core to follow changes of temperature, salinity, nutrients and chlorophyll a. Oxygen concentrations of brine were measured in different depths at four events. Oxygen in sea water was measured continuously starting the day we left the floe until 16 January.

Results

Two examples of the measured oxygen concentration are given from below the sea ice (Fig. 4.45) and from the topmost sensor in the ice (Fig. 4.46). Oxygen values in the water underneath the ice showed an increasing tendency over the sampling period. During many days of the sampling time diurnal cycles of concentration changes were observed, but not always.

One possible explanation for this is the current velocity underneath the ice. Thus only on days of slack currents diurnal cycles become evident, otherwise turbulent mixing causes a smoothing of the signal. Concentrations calculated were in the range of values obtained by Winkler titration.

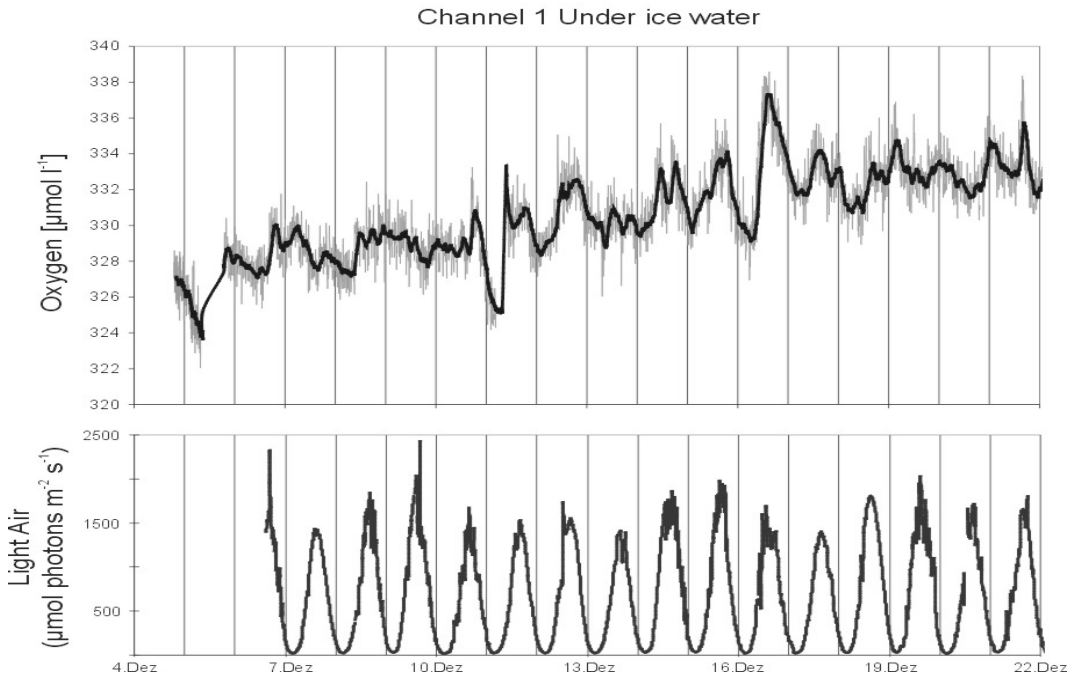

Fig. 4.45: Oxygen concentrations in the water underneath the ice sheet and incoming irradiance at the snow surface from the 4 to 22 December

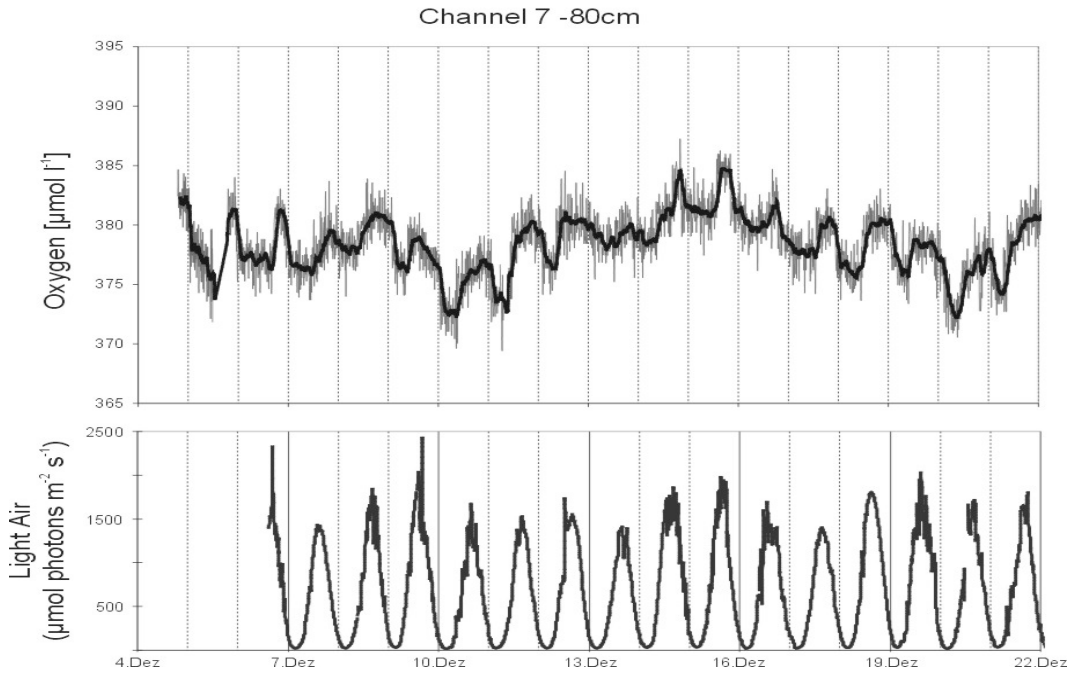

Fig. 4.46: Oxygen concentrations at the topmost ice sensor and incoming irradiance at the snow surface from the 4 to 22 December

Oxygen concentrations in the ice (Fig. 4.46) were elevated compared to water values, which could also be confirmed by Winkler titration and optode measurements in sackholes.

The diurnal cycle in the oxygen concentration was even more pronounced than in the water. However the overall concentration did not change. Back home these data sets will be carefully reanalysed, also in collaboration with the manufacturer of the optodes. Furthermore oxygen fluxes and hence production rates will be calculated and eventually come up with estimates of primary production.

Oxygen concentrations measured at 110 m depth on the way back showed elevated concentrations in the marginal ice zone and in up welling regions west of the South Orkney Islands and South Georgia. This trends could exactly be followed by reversed changes in CO_2 concentrations measured by the Belgian group.

4.9. Zooplankton ecology in the water column

Jan Michels, Sigrid Schiel
Alfred Wegener Institute, Bremerhaven

4.9.1 Objectives

The aim of the water column studies was analyses of zooplankton communities in the Weddell Sea during the transition from the winter to the spring state. Our research focussed on abundance, biomass, species composition, population structure, vertical distribution, maturity of gonads, gut content and molecular genetic studies.

4.9.2 Work at sea

A multiple opening-closing net („midi type“) with an opening of 0.25 m^2 equipped with 5 nets of 100 µm mesh size and with a digital flowmeter was used as a standard device for the quantitative sampling of mesozooplankton. The multinet was towed vertically, sampling the standard layers of 0 - 50 m, 50 - 100 m, 100 - 200 m, 200 – 300 m and 300 to the bottom layer. Sampling was carried out every third day depending on ice conditions. The net samples were preserved in borax-buffered 4 % formaldehyde/sea water solution. For molecular genetic purposes, a „maxi type“ multiple opening-closing net with an opening of 0.5 m^2 equipped with nine nets of 100 µm mesh size and with a digital flowmeter was deployed four times. Nine successive depth layers were sampled between near the sea floor and the surface. These net samples were preserved in 90 %-ethanol. Both nets were towed vertically at 0.5 m sec^{-1}

4.9.3 First results

In general, we found low zooplankton abundances. Plankton communities were dominated at most stations by the large calanoid copepods *Calanoides acutus* and *Metridia gerlachei* and by numerous small cyclopoid and calanoid copepod species. A thorough investigation of the samples will elucidate the seasonal development of

the zooplankton community. This data will be discussed with respect to the life strategies of the species and relationships to hydrography and phytoplankton.

4.10 Algae and protozoa

Harri Kuosa
Finnish Institute of Marine Research

4.10.1 Methodology

During the ISPOL-cruise microscopy was almost totally done using epifluorescence techniques. These were done to find out two parameters:

1) The abundance of autotrophic and heterotrophic protists, including the differentiation of dinoflagellates and ciliates with and without chloroplasts.
2) The rough estimation of physiological status of diatom cells.

For the first goal a number of samples from gap-layers, brine water (sackholes) and ice samples melted in a volume of filtered seawater (FSW) as well as water samples were examined. All samples were fixed with glutaraldehyde (1 % final conc.), stained with proflavine and filtered onto black 0.2 μm pore-sized Nuclepore polycarbonate filters. The samples were examined with blue fluorescence light, which gives the opportunity to observe chlorophyll fluorescence inside the cells. To ascertain the presence of chloroplasts inside the small dinoflagellates with quite strong masking green autofluorescence, some samples were examined without staining and some directly from water sample alive. This proved to be an useful method to verify the presence of chloroplasts in some very small dinoflagellates. Very little is gained on the taxonomy of the cells encountered with the method used, but as proflavine stains also cilia and flagella, some remarks about the systematic groups may be given.

For the second goal the same samples as for the first topic were studied, but in addition a number of directly melted samples were also examined. This gave the possibility to link diatom counts to salinity, chlorophyll and nutrient data from the same samples. Though soft celled protists do not survive direct melting, diatoms will, to some extend, stand it. The procedure for sample preparation was the same as given above. After proflavine staining, the nucleus of diatoms is generally clearly visible as are the chloroplasts. Thus several groups of diatoms were encountered: i) fragments of frustules or broken cells, ii) empty frustules, iii) frustules with nucleus and some cell content (+ chloroplasts) present, iiii) frustules with clear chloroplasts and iiiii) dividing diatom cells. It is quite difficult to link the findings in the epifluorescence data to real activity, but it is certain that the different groups, though only possible to roughly categorise, in fact represent a continuum from cell death to actively growing cells. The presence of chloroplasts inside the smallest cells was again confirmed with the examination of unstained samples or living cells.

All microscopy was done with a Leitz Dialux microscope fitted with a 50 W mercury lamp and a Leitz M_2 filter pack. The total magnifications used were 125x, 500x and 1250x (oil immersion). The magnification used dependent on the size of the organism counted, but only ciliates and the largest diatoms were enumerated with 125x from

the whole filter. Other magnifications were used for dinoflagellates and smaller diatoms (500x) and flagellates and the smallest diatoms (1250x). The sample volume filtered was about 5 ml, which was influenced by the time required for filtering and the high amount of diatoms collected onto the filter at some samples, masking smaller cells. Thus the results do not represent well the number of large diatoms and ciliates except when they were numerous. Species identification of diatoms is also difficult or impossible with the technique. Some samples will be later examined by cleaning diatom frustules with acid and making diatom slides.

4.10.2 Preliminary results

The 6 samples from the Transect study revealed highly different biomass profiles of diatoms. This was partly due to the highly variable ice tickness (from 40 to 250 cm). The thinnest core had very low biomass throughout, but the two intermediate (75-128 cm) cores showed two biomass peaks, one near the top and near the bottom. The 3 thickest cores (214-250 cm) had a diatom biomass maximum only near the bottom only. This maximum consisted either of large centric diatoms or an *Amphiprora* sp. Many of the cells were obviously dead, and together with the location of the bloom about 20 to 30 cm above the bottom of the ice, pointed at an old diatom bloom. Fig. 4.47 shows as an example, the diatom biomass of the thickest ice core, with the dominance of large centric diatoms near the bottom of the core.

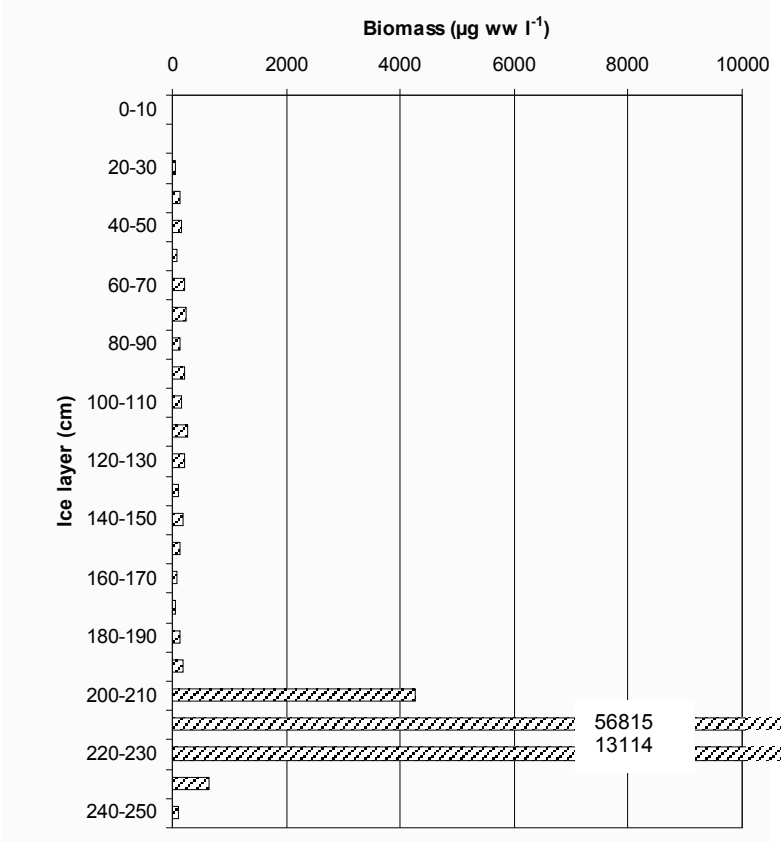

Fig. 4.47: The diatom biomass of the core taken at station TR5. The numbers denote the total biomasses at the layers 210-220 and 220-230 cm.

The ice cores in our floe varied also according to the ice thickness. A clear succession was also apparent. In the beginning, the time series cores (about 100 cm) had only one biomass maximum at the very bottom. However, during our campaign, surface ice layer showed some increase in biomass, and respectively, bottom biomass decreased. Bottom biomass was mainly composed by the diatoms *Amphiprora* sp. and *Cylindrotheca closterium*. The surface community was more variable with the major share by the diatoms *Cylindrotheca closterium* and *Fragilariopsis* spp. and autotrophic dinoflagellates. The bottom community of *Amphiprora* sp. was obviously very active with a considerable share of dividing cells. In all other layers, also at the surface, a considerable share of dead diatom cells was encountered. Thicker ice cores had maxima either at the bottom of the ice or somewhat above it as in the transect, and sometimes additional maxima in the middle of the core.

The amount of bacteriovorous flagellates was low, though a number of bacteria was seen in the samples. Proflavine staining is not suitable for bacterial enumeration, but the bacteria in the ice were generally very large. The only layer with a considerable amount of heterotrophic nanoflagellates, mainly choanoflagellates, was in the time series cores just above the bottom, at a layer of possibly dying diatoms. Heterotrophic ciliates and dinoflagellates were scarce though some brine samples contained a fair amount of ciliates. However, others did not, and it is not clear yet if there are any trends in the other properties of the brine and ciliate abundance. At the end of the time series a large ciliate, *Dysteria* sp., was found in large numbers at the bottommost layer. Mixotrophic or autotrophic ciliates from the genera *Strobilidium* and *Strombidium* were present in the gap layer.

4.11 Flux of particulate organic carbon below sea ice in the Western Weddell Sea during early summer

Gerhard Dieckmann[1)], Andreas Krell[1)], David Neville Thomas[2)], Jan Michels[1)], Sigrid Schiel[1)]

[1)] Alfred Wegener Institute
[2)] School of Ocean Sciences, Anglesey, UK

4.11.1 Introduction

The sea ice interface with the underlying or adjacent sea water probably represents one of the most dynamic biological zones of the sea ice. It is the most productive region and comprises a refuge for metazoans and protozoans which graze on the high algal biomass within the ice or at the ice/water interface.

Because of its relative inaccessibility to conventional methods of investigation it has to date not been possible to obtain representatives estimates of primary production nor of the fate of algae growing at the interface. Coring from above does not provide a truly representative sample of this interface.

Estimates of algal growth rates and production at this interface are scarce. The fate of this production is also very difficult to estimate. Grazing and loss of algae from the interface have rarely been quantified. However, since the ice underside is extremely

dynamic and subjected to continuous changes because of temperature, current and topographical variability the growth and fate of the bottom few centimetres of ice are likely to vary considerably. By deploying sediment traps immediately below the sea ice we intended to obtain information on the flux of particulate matter from the sea ice at the onset of ice melt.

The objective of the present study was to measure the export and the nature of particulate organic matter sedimenting from the pack ice the western Weddell Sea, and asses the flux in the top layers of the water column. One objective was to determine if and when flux from the sea ice commences as well as the temporal progression in early summer. Another objective of the study was to determine the composition and chemistry of the particle flux. Two arrays of 2 sediment traps were deployed below the ISPOL floe and a suite of biogeochemical parameters determined.

4.11.2 Materials and methods

The traps were deployed from 30 November to 30 December. The trap #6 array had to be removed on 7 December due to floe break up and was re-deployed on the same day.

Two arrays each with two sediment traps and an FSI current meter (Fig. 4.48) were deployed (by hand) on 30 November at sites #6 and #9 on the floe. The array was anchored to the overlying sea ice and deployed through holes in the ice. Two types of HYDROBIOS cylindrical sediment traps were deployed, both with opening areas of 0.015 m^2. The trap openings were covered by a plastic grid 40 mm thick, with 40 mm 2 holes. The trap collecting cylinders were 560 mm long.

The 'multiple' traps had six collecting bottles, each programmed to collect samples over 6 days. The 'single' traps were equipped with only one collecting bottle. Prior to deployment all collecting cups were filled with hyper-saline water and poisoned with H_gCl_2.

4.11.3 Preliminary Results

The sediment traps were deployed for approximately 30 days from 30 November to 30 December 2004. The traps all functioned correctly although trap 2 produced results which were difficult to interpret.

After recovery of the traps samples from the trap cups were split on RV *Polarstern* and sub samples taken for POC/PON, Chl*a* and $\delta^{13}C_{POC}$, biogenic silicate determinations and for microscopic examination.

Chlororphyll *a* and Phaeophytin were measured on RV *Polarstern* and the remaining samples were stored for later analyses in home laboratories.

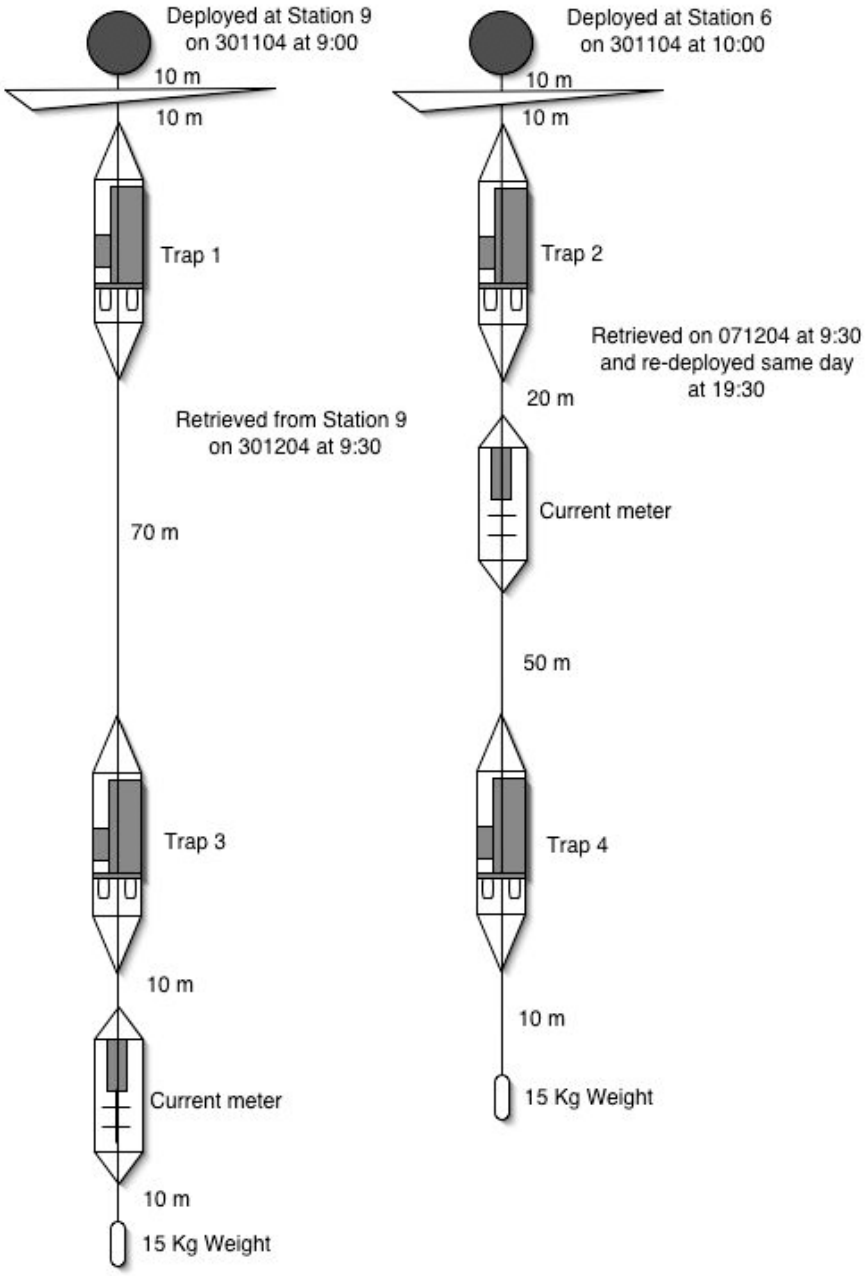

Fig. 4.48: Sediment trap array

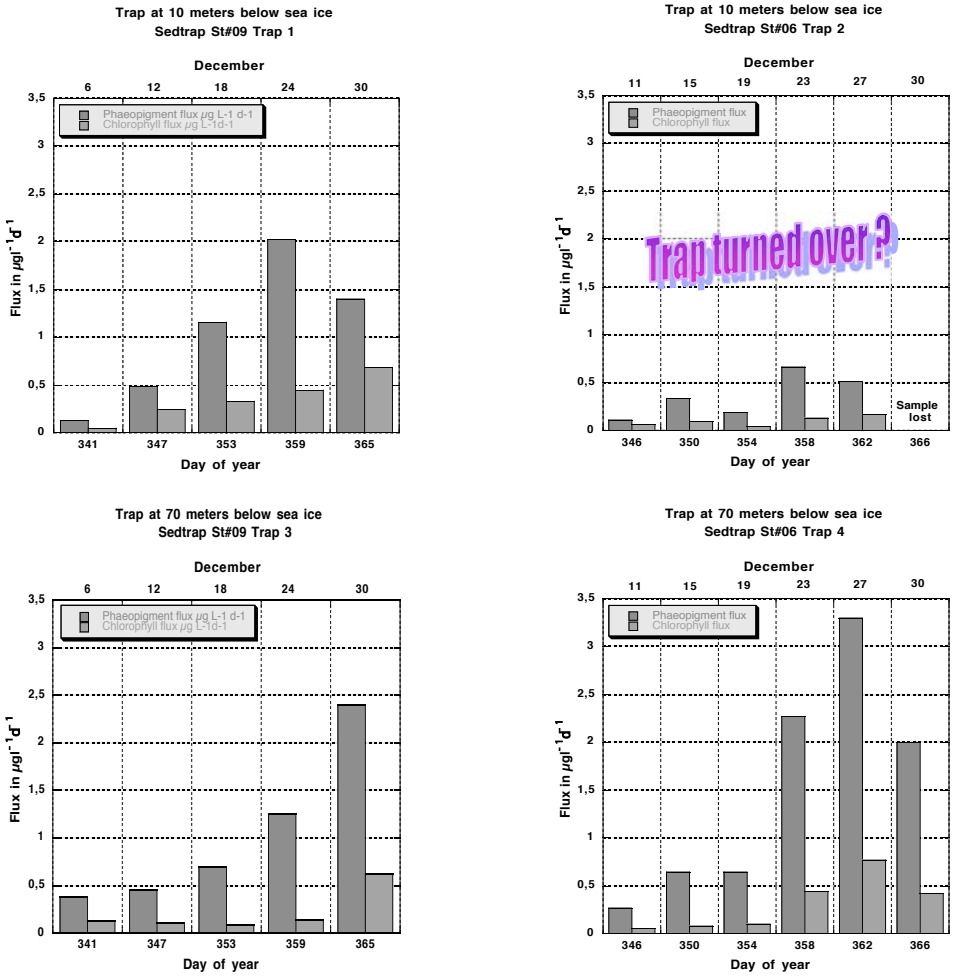

Fig. 4.49: Chlorophyll a and Phaeophytin in sediment trap samples

Figure 4.49 shows the chlorophyll a and Phaeophytin content of the 4 traps. Trap two had generally lower levels which may be attributable to the fact that the trap may have become located between brash ice at the edge of the floe. The other traps revealed a steady increase in both properties during the course of the experiment. Phaeophytin concentrations where high relative to chlorophyll, indicating a larger proportion of dead material in the samples. Further analysis should provide information as to the source of both chlorophyll a and phaeophytin. It appears however, that the sediment traps where deployed at the onset of ice melt which then progressed streadily during December. This means that considerable particle flux occurs below the ice long before the pack ice breaks up. The sediment trap data will have to be related to auxiliary data such as current speed and direction as well as physical processes at the sea ice/water interface before final conclusions as to causes and rates of sedimentation can be interpreted.

4.12 An inventory of DMSP in zooplankton

Jacqueline Stefels
University of Groningen, Haren, The Netherlands

4.12.1 Introduction

The role zooplankton play in the marine sulphur cycle has traditionally be seen as an intermediate in the release of dimethylsulphoniopropionate (DMSP) from algal cells due to grazing. This release can be either directly to the environment due to sloppy feeding or indirectly after the algae have been ingested. During the latter process conversion can take place in the guts or faeces of the animals. This may result in the release of DMS, however the loss of DMSP from algae upon grazing is usually not compensated for by the production of DMS. In several cases it has been suggested that increased demethylation of DMSP had taken place and there are a few indications that copepods are able to store DMSP in their tissues. Experiments with Antarctic krill that grazed on *Phaeocystis* resulted in a sharp increase in DMS production.

In open ocean waters the production of DMSP is restricted to a limited number of algal taxons, amongst which the diatoms are the least producers. In ice, however, diatoms also produce large quantities of DMSP and since they are the main food source for zooplankton, DMSP will pass through the guts of these animals. Little is known about the built-up of DMSP in zooplankton from the Antarctic region, let alone whether DMSP might play a role in the physiology of zooplankton for instance when they have to combat extreme salinity conditions inside the ice.

In this project, a first inventory of DMSP in zooplankton from the sea ice has been made.

4.12.2 Methods

This project is a collaborative action with the following colleagues during the ISPOL expedition:

Rainer Kiko[1)],Rupert Krapp[1)], Jan Michels[2)], Sigrid Schiel[2)], Henrike Schünemann[1)]	[1)] Institute for Polar Ecology (IPÖ), Kiel [2)] Alfred Wegener Institute

A variety of zooplankton specimens were provided by the above mentioned persons and analysed for their DMSP content using a proton transfer reaction mass spectrometer (PTR-MS): depending on size, 1 to 10 specimens of one species was added to 10 mL of milli-Q water and basified with NaOH. The samples were left to react for 24 to 48 hours. Under these conditions DMSP is quantitatively converted into DMS. Subsequently, they were sparged with high purity air and analysed directly by the mass spectrometer. Sweeping of the DMS from the water sample took typically 10 min and could be followed on real-time basis. The resulting peak was integrated and the concentration was calculated using a calibration curve made from DMS-standards that were treated the same way as the sample.

In addition to the inventory of a variety of species, starvation experiments were carried-out, in order to check whether the observed DMSP comes from the gut content or is stored inside the animal's body tissues. The following starvation experiments were carried out:

Collaborator	species
Jan Michels	Copepods: Drescheriella glacialis and Stephos longipes
Henrike Schüneman	Turbularians
Jan Michels, Rainer Kiko	Ctenophores

4.12.3 Preliminary results

In the following table a preliminary overview is presented of the DMSP contents of the species investigated:

species	DMSP (pmol • indiv^{-1})
Amphipods	1.1×10^5
Calanus propinquus	80
Calanoides acutus	40
Metridia gerlachei	150
Polychaeta	4000
Ctenophora	1×10^5
Turbularia	200

For a proper evaluation of these data, normalisation to body volume and biomass is needed, but these numbers already indicate that DMSP is an important compound in Antarctic zooplankton.

Calculated data from the starvation experiments are not yet available, but the raw data indicate that copepods react variable. Turbularians show no change and the DMSP-contents of Ctenophores are reduced by one order of magnitude.

4.13 Antarctic top predators and their prey

Hauke Flores
ALTERRA Texel, Den Burg, The Netherlands

4.13.1 Introduction

In the Antarctic Ocean, the seasonal pack ice zone represents an important habitat for penguins, flying birds, seals and whales. At the ice edge, primary production is enhanced in the water column which in turn supports high stocks of macrozooplankton and micronekton (e.g. salps, krill, larval / juvenile fish, squid) - the prey of these top predators. However, the ice-covered areas can also support considerable stocks of birds, seals and whales. In fact, their food demand based on abundance and species composition can persist towards the inner pack ice. It has

been argued that the primary production in the sea ice itself can explain the apparent paradoxon of low water column production and high top predator occurrence in the inner pack ice.

During ISPOL, an intense study of the under-ice fauna was envisaged, both with the help of a stationary under-ice net, and by sample collection through diving. In a parallel attempt, top predator counts from ship and helicopter were carried out.

4.13.2 Materials and methods

Net catches
For the capture of ice-associated makrozooplankton and nekton, a 2 m x 2 m x 2 m net chamber with four throats was deployed through an icehole. Four 25 m-guidenets were supposed to lead animals towards the central chamber, positioned directly under the ice with the help of floaters. However, standing times of up to 72 hours yielded only a very limited number of organisms, indicating the catchability of the net system to be too low for the intended purpose. The net was entirely destroyed during the forming of a major pressure ridge on 24 December.

Dive sampling
Diving operations, too, were very limited. The diving activities of this expedition were cancelled after only a few dives due to the risks caused by the almost constant presence of Leopard Seals (*Hydrurga leptonyx*) in the area of investigation.

Top predator counts
Flying birds, penguins and sea mammals were counted, both from the ship's crow's nest, and during helicopter flights.

Counts from the crow's nest were performed according to a simple point count procedure. All animals sighted in a 360° viewfield were noted. The viewfield was divided into 4 sectors in order to sort out the effect of ship- and floe activities. The distance of sighted animals was noted in five distance classes: <100 m, <200 m, <500 m, <1000 m, >1000 m. Counts were performed every four hours during the day, if possible. 24 hour day cyle counts were done on three occasions.

Band transect counts were perfomed from the air taking the opportunity of helicopter flights by the EM Bird team (C. Haas and colleagues). Transect patterns and flight details are provided in chapter 3.2. In a total of 13 flights with systematic counting conditions, three were performed in the northern and central Weddell Sea on the way towards the final ISPOL destination, and two could be accomplished on the way out of the ice, the northernmost one reaching the marginal ice zone. The rest was done around the ISPOL floe, up to a distance of 40 nm.

The band transect width was 70 m from a flying height of 100 ft (ca. 32 m). The observer was sitting next to the pilot. The borders of the transect band were estimated through triangular extrapolation with the help of objects present in the viewfield of the observer, such as instruments or the window edge. Counts were performed constantly, as long as the helicopter was flying at the desired height of

100 ft. All animals seen were noted with regard to their presence inside or outside the transect band.

Assuming that all animals inside the narrow band were detected, the density of animals was calculated as individuals per km^2. A mean density for all observed species was calculated for each flight, using the two to three transects of each flight as replicates.

4.13.3 Results and discussion

Point counts
A total of 75 point counts was carried out, revealing a high temporal variability in the abundance of the species observed. Crabeater seals (*Lobodon carcinophaga*) and emperor penguins (*Aptenodytes fosteri*) were the dominant species, with an average number of sightings in a distance <1000 m of 8.6 individuals and 3.1, respectively (Fig. 4.50).

Among the flying birds, snow petrel (*Pagodroma antarctica*), southern giant petrel (*Macronectes giganteus*) and wilson's storm-petrel (*Oceanites oceanicus*) occurred regularly, but in small numbers. The rare occurrence of Antarctic petrel (*Thalassoica antarctica*) was surprising. Adelie penguins (*Pygoscelis adeliae*) were seen more often, but in unexpected low numbers.

Apart from crabeater seals, leopard seals were seen regularly. Weddell seals (*Leptonychotes wedellii*) occurred occasionally. Antarctic minke whales (*Balaenoptera bonarensis*) were seen on several occasions during the first 2 weeks of the ISPOL experiment, but only once during a point count event. Outside the counts, also Arctic tern (*Sterna paradisaea*) and an unidentified gull were reported. The abundance of crabeater seals exhibited a pronounced fluctuation over the course of the investigation. An almost regular pattern could be observed, with peak abundances occuring every 2-4 days (Fig. 4.51). It might be that loose aggregations of these seals strolled through a larger region around the ISPOL floe. Between these patches, low numbers were recorded at the ship. This explanation is supported by observations from the helicopter, where long periods of almost no sightings were in-between patches of sometimes dense aggregations.

Crabeater seals are known to haul out on the ice mainly during midday hours (van Franeker, pers. comm.). This was apparent also from the repeated counts over 24 hour periods. However, there was no clear relationship between time of day and the number of crabeater seals sighted (Fig. 4.52).

Apparently, emperor penguins where attracted by the ship. However, there seemed to be a habituation effect, the number of emperors seen per count dropping from a maximum of 32 in the first week at the ISPOL floe to between 2 and 13 over the rest of the period of investigation.

Band transect counts
Mean abundances of all species at each flight are shown in table 4.1. Crabeater seals and emperor penguins were the dominant species, as already seen from the point counts, their abundance ranging from 0.3 to 1.4 and 0.0 to 0.8 individuals per km^2, respectively. Flying birds could hardly be detected from the helicopter and are therefore probably under-estimated.

On the way towards the ISPOL floe, mean abundances of crabeater seals were lower, the lowest value (0.3 ind. per km^2) recorded at the most northeastern position. Their abundance ranged close to 1.0 animals per km^2 in the ISPOL region. The slight increase to 1.4 individuals km^2 towards the boundary region of the closed pack-ice in the north should be considered with caution because it is based on only one flight, its abundance ranging well within the variability of the more southerly surveys (Fig. 4.53).

No emperor penguins were sighted during the surveys in the northern and central Weddell Sea. The overall mean abundance was close to 0.1 individuals per km^2 in the floe region, but significantly higher on the two more northerly flights (0.7 ind. per km^2 and 0.8 ind. per km^2; Fig. 4.54).

The spatial distribution of seals and emperor penguins in the ISPOL region is shown in figure 4.55. While no clear pattern can be seen for crabeater-, leopard seals and emperor penguins, Weddell seals were found only in the south-western part of the area of investigation. Weddell seals are known to occur mostly on fast ice and in shelf regions. The ISPOL floe being situated over the shelf break, their more westerly occurrence might reflect the transition to the shelf habitat, and their abundance probably increases further to the west. Unfortunately, no surveys could be performed towards the shelf areas in order to verify this hypothesis.

The distribution of air breathing top predators in Antarctic waters is strongly connected to ice conditions, food supply and the physical topography of the ocean region in question. The low abundances of crabeater seals and the absence of emperor penguins in the easterly survey areas are probably connected to the much deeper water there. On the shelf slope, food availabilty is increased and can support more top predators.

The properties of the ice as a site of primary production and thus attractor for prey surely play an important role, too. As soon as more precise data from the ice measurements performed on the flights become available, ice data will be compared with the above presented results in order to address this question in more detail.

Other observations
The lack of adequate sampling of the potential prey for top predators was a major drawback for the aims of this expedition. However, a few looks under the ice revealed a rich amount of macrozooic life. During diving and occasional ROV operations, dense aggregations of krill, presumably *Euphausia superba*, were found. *E. superba* also occured in the few successful net catches. Under the ice, divers saw dense patches of amphipods. In baited traps, lysianassid and eusirid amphipods were caught (see chapter 4.7.7). Larger sized Ctenophores also ocurred under the

ice in greater numbers. One of them was observed feeding on krill. The few observations made could not reveal if fish or squid play a role in this ice-associated species community as well.

These observations stress the importance of the pack-ice habitat as a major source for food for top level predators and the need for further investigations.

Table 4.1: Mean numbers of individuals per km^2 on each flight. Standard deviation in brackets

	FLIGHT NO											
SPECIES	4	5	6	7	9	12	13	14	15	17	18	19
EMPEROR PENGUIN	-	-	-	0.2 (0.27)	0.1 (0.1)	0.1 (0.11)	0.1 (0.11)	0.2 (0.21)	0.2 (0.16)	0.0 (0.09)	0.7 (0.25)	0.8 (0.81)
GIANT PETREL	-	-	-	-	-	-	-	-	-	0.2 (0.35)	0.1 (0.11)	0.1 (0.13)
SNOW PETREL	-	-	0.2 (0.04)	-	0.0 (0.08)	-	-	-	-	-	-	-
CRABEATER SEAL	0.3 (0.48)	0.5 (0.41)	0.8 (0.07)	1.2 (0.94)	1.6 (0.19)	0.8 (0.6)	1.4 (0.44)	1.2 (0.29)	0.8 (0.54)	0.7 (0.77)	1 (0.42)	1.3 (0.2)
LEOPARD SEAL	-	-	0.1 (0.2)	-	-	-	-	-	-	-	0.0 (0.05)	0.1 (0.13)
WEDDELL SEAL	-	-	-	-	-	-	-	-	0.1 (0.12)	0.4 (0.62)	0.1 (0.05)	-
Unidentified SEAL	-	-	0.2 (0.04)	-	-	-	-	-	-	-	-	-

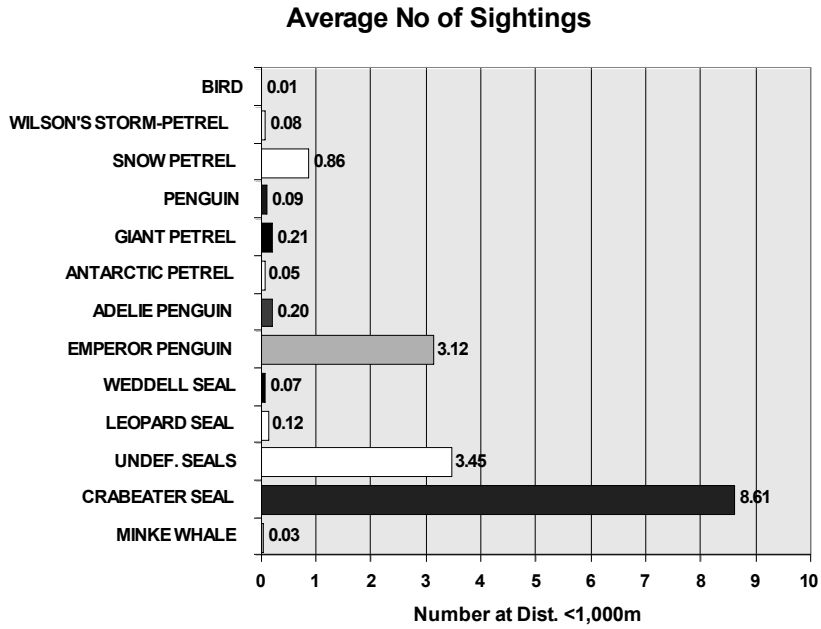

Fig. 4.50: Average number of sightings during point counts

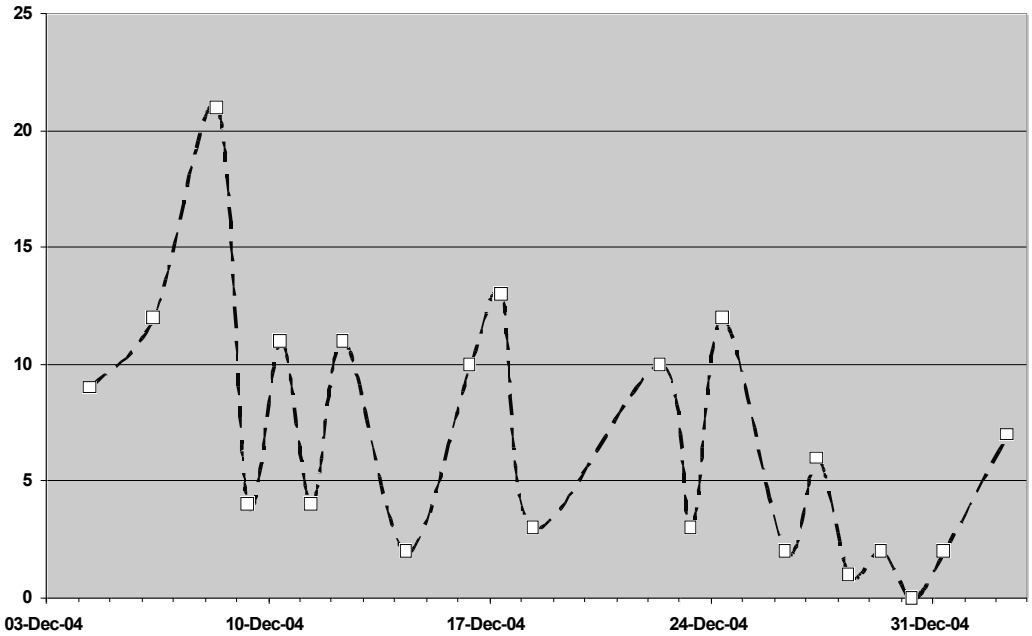

Fig. 4.51: Morning count numbers of crabeater seals sighted in 1000 m radius over the course of the investigation

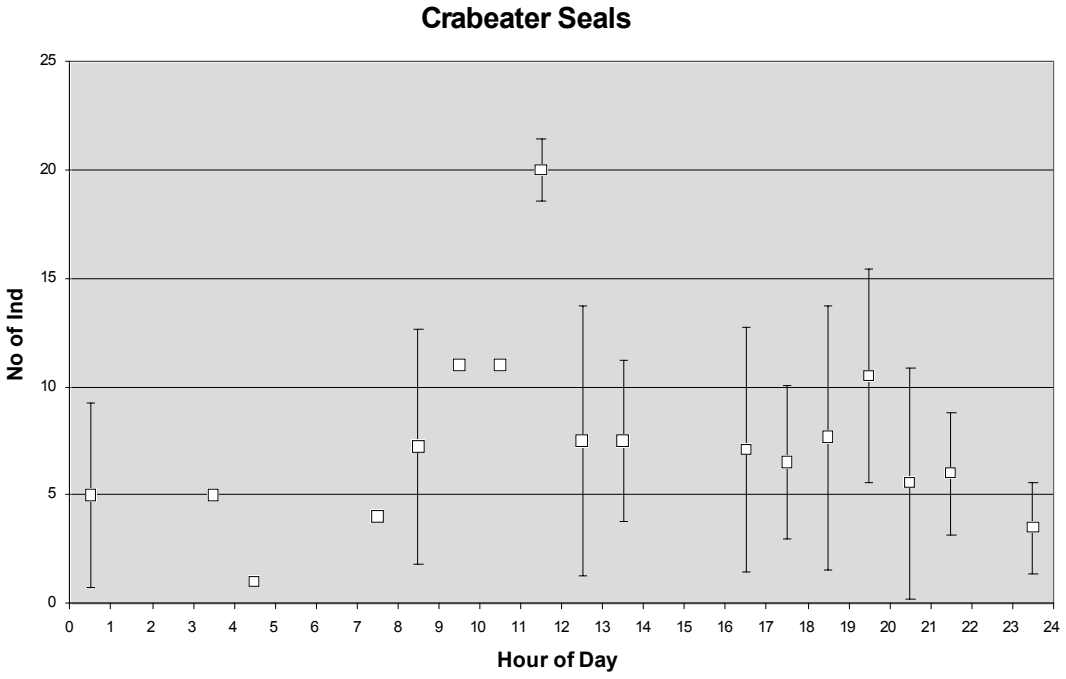

Fig. 4.52: Average numbers of crabeater seals at different hours of the day. Error bars denote standard deviation.

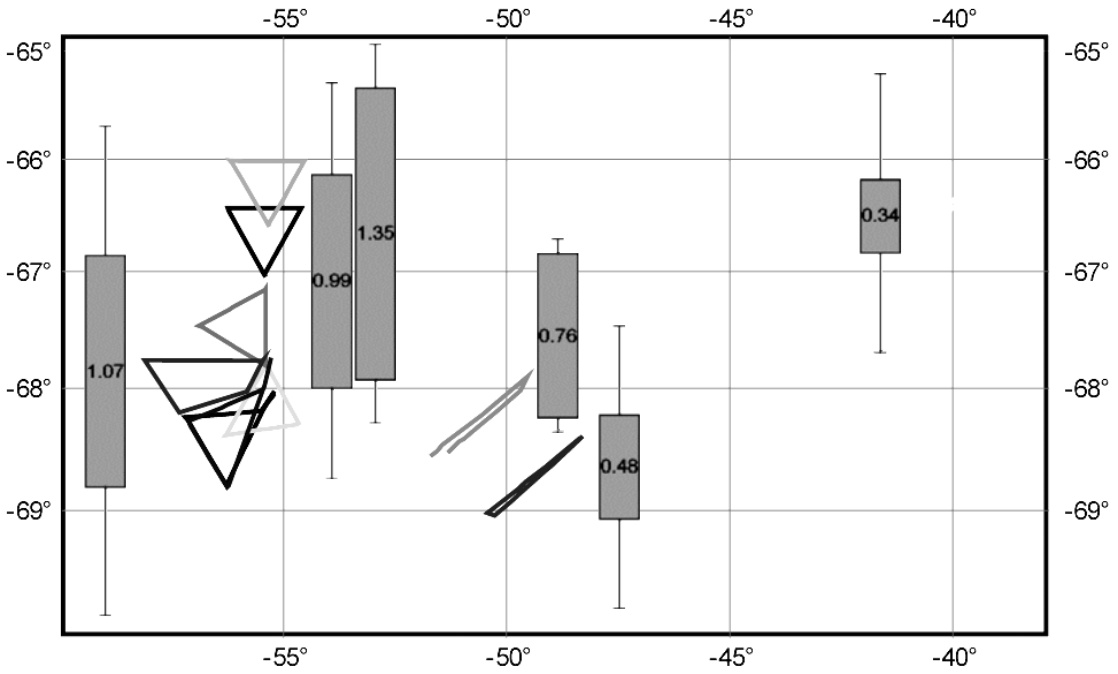

Fig. 4.53: Mean abundance of crabeater seals per km^2 in the area of investigation. Error bars denote standard deviation. Data of surveys in the ISPOL region (flight 7-17) are pooled.

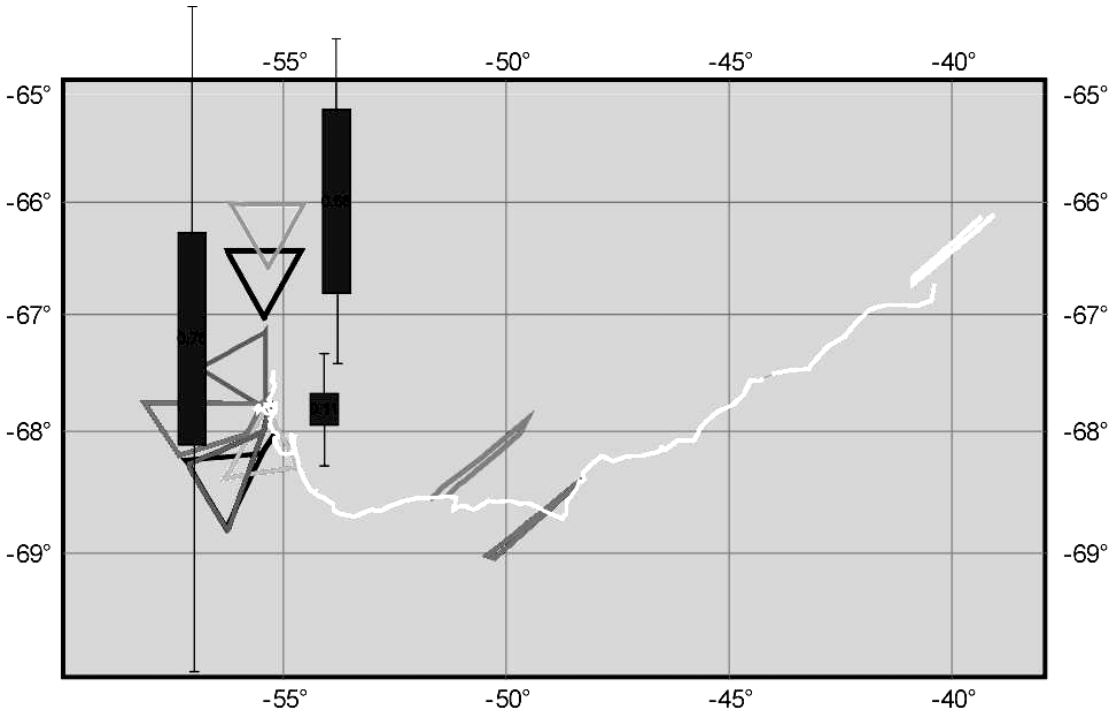

Fig. 4.54: Mean abundance of emperor penguins per km^2 in the area of investigation. Error bars denote standard deviation. Data of surveys in the ISPOL region (flight 7-17) are pooled.

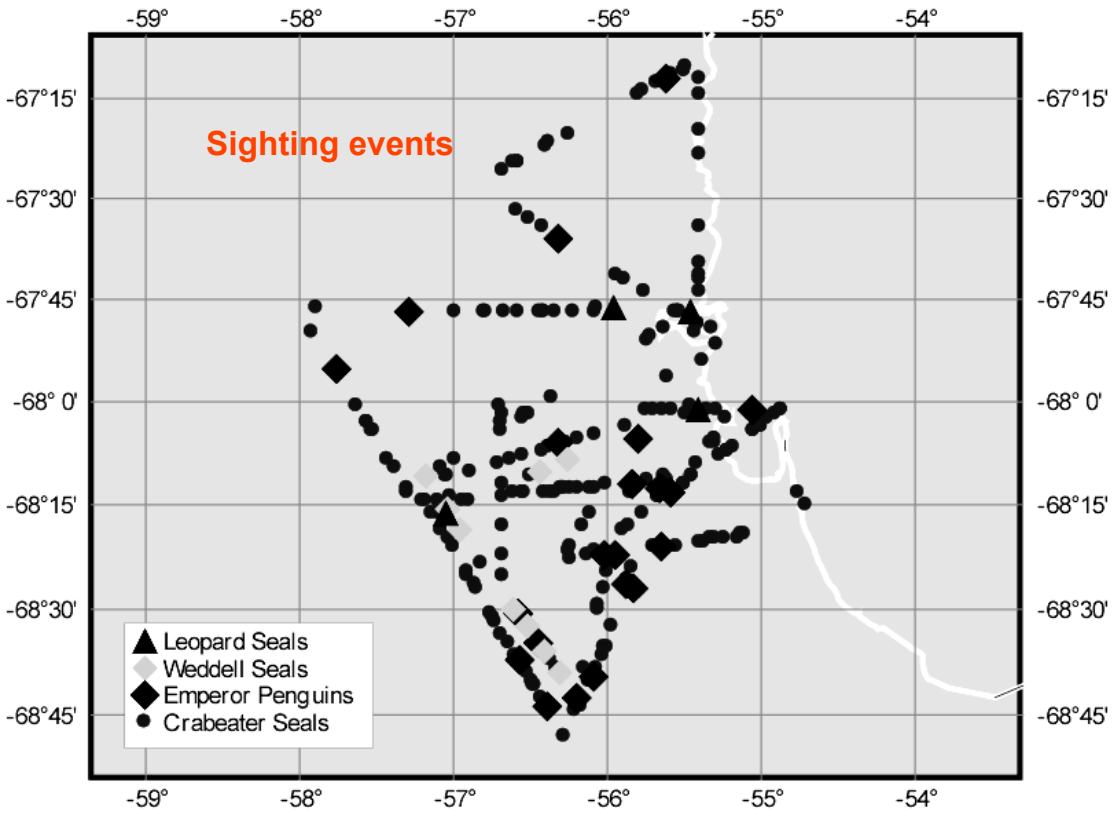

Fig. 4.55: Spatial distribution of sightings of seals and emperor penguins in the ISPOL region. Each mark represents a sighting, irrespective of the number of individuals at that place.

4.14 Underway measurements of DMS in the pack ice and in the marginal ice zone of the Weddell Sea

John W.H. Dacey
Woods Hole Oceanographic Institution, USA

This project involved the use of a prototype automated gas chromatographic (GC) system constructed around an OI Corp Pulsed Flame Photometric Detector with all sample handling and data acquisition controlled by a laptop computer running Agilent Vee.

Water samples were collected by syringe pump and injected into a sparger where DMS was removed by bubbling air through the sample. DMS was trapped on a 1/8” OD Carbopack trap at ambient temperature. (Standard GC systems typically rely on cooling for DMS focusing, using a relatively large dead-volume trap of glass beads in liquid nitrogen or cooled Tenax.) After an appropriate sparging time (dependent on water volume), the trap was rapidly heated to 320°C and the adsorbed compounds were injected onto a capillary column for analysis. During the experiment the volume of samples and standards collected by syringe ranged from 10 mL at low concentrations to 0.2 mL at high concentrations.

The sampling system incorporates a flexible array of samples, standards and blanks. The system was set up to draw samples from the ship’s seawater system (inlet at

11 m depth) once we had arrived at our first station in the pack ice, and ran almost continuously until we approached Cape Town. More than 3000 samples and standards were run over a 6-week period.

At the beginning of the deployment, DMS was <0.2 nM (Fig. 4.56). This is an extremely low concentration, lower than any DMS concentration measured during any season in the top 100 m at Bermuda. As time progressed there was a gradual increase in DMS under the floe to approximately 1 nM when the ship left the floe on 2 January. As the ship moved towards the ice edge, DMS continued to rise slowly, then rose very rapidly as we entered the marginal ice zone. Data from Bruno Delille indicate a significant depletion of CO_2 at the same time, indicative of a substantial phytoplankton bloom. Samples were taken at intervals to determine concentrations of key pigments. Similarly high levels of DMS were encountered as few hours later, and each time lasted for only an hour or so. The GC detector was saturated, indicating that DMS exceeded 180 nM. A point measurement made at the same time on the PTR mass spectrometer of Jacqueline Stefels indicated that DMS exceeded 300 nM. Concentrations remained significantly above 10 nM for several days. We believe the quantities of DMS measured during short intervals near the ice are the highest concentrations of DMS ever measured in oceanic surface water or in any body of natural water.

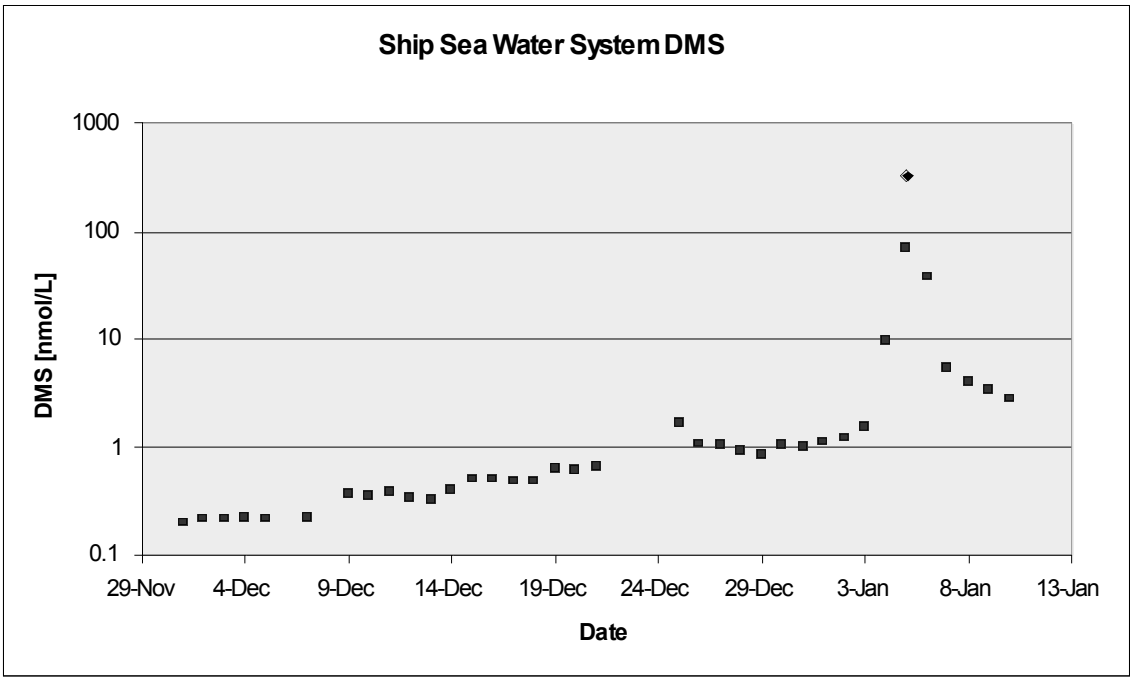

Fig. 4.56: Time-course of DMS concentrations at 11 m depth. DMS concentrations increased more or less monotonically until the ship left the pack ice with the exception of higher values on 25 December when the ship moved to a new location on the floe (after the major floe breakup). Outside the ice margin DMS concentrations reached extremely high levels beyond the measurement of the GC system in its current configuration. Independent measurement by PTR mass spectrometer indicated that DMS concentrations exceeded 300 nM (blue point) on 5 January. Note that the data are plotted on a logarithmic scale. Concentrations measured during this 6 week interval varied by more than 3 orders of magnitude.

5. PHYSICAL OCEANOGRAPHY

5.1 Hydrography and physical properties

Michael Schröder[1)], Michael Schodlok[1)], Andreas Wisotzki[1)], Joao Marcelo Absy[1)], Timo Witte[2)]

[1)]Alfred Wegener Institute, Bremerhaven
[2)]Optimare, Bremerhaven

Identification of source water masses involved in deep and bottom water formation along the western Weddell Sea continental shelf

Objectives

The formation of dense bottom water by mixing of highly ventilated, salty shelf waters with the warm and salty waters of circumpolar origin, and the interaction of both with very cold Ice Shelf Water in the Weddell Sea is of major importance for the renewal of bottom water in the world ocean. In 1992, measurements during the US-Russian drift station ISW-1 over the continental slope along the eastern coast of the Antarctic Peninsula gave a first enroute view of the stratification and pathways of deep and bottom water masses in the western Weddell Sea.

More recent expeditions onboard RV *Polarstern* together with data from two Brazilian/German expeditions show large spatial and temporal variations in the T/S-characteristics of the dense water masses in the northwestern Weddell Sea. These variations are a result of mixing processes which act over different time scales (seasonal, interannual to decadal) and involve waters with different histories from various sources along Weddell Sea's western rim. Therefore, the measured and calculated volumes of the newly formed Weddell Sea Bottom Water are still affected with big uncertainties ranging from 1.5 to 6 Sv. Even less is known about the quantities ventilating Weddell Sea's deep water which has direct access to the world ocean through the deep passages in the South Scotia Ridge.

Model studies using virtual drifter show the sensitivity of the deep and bottom water formation and spreading on sea ice concentration and position of dense water injections along the western Weddell Sea continental shelf break. For the understanding of the formation processes of different bottom water types and for an accurate estimate of the ventilation rate of the deep Weddell Sea it is necessary to measure the source water mass characteristics as close as possible to their origin. Changes in configuration of ice shelves like Filchner-Ronne, and Larsen A, B, and C are of special interest with regard to the modification of shelf waters on the continental shelf and in the sub-ice cavity due to their significant freshwater input. Probably an equal amount of freshwater is added to the surface waters by melting of stranded and drifting icebergs with an impact on composition and amount of sinking dense water masses leading to a high variability in both T/S-characteristics and volume of newly formed bottom water.

Work at Sea

The programme consisted of measurements from the ship using two Sea-Bird 911+ CTDs (SN 561 and SN 485) each one connected to a caroussel (SBE 32, SN 273) with 24-(12-l) resp. (SBE 32, SN 202) with 21-(12-l) water bottles.

The main instrument system(SN 561) contains two sensor pairs of conductivity (SBE 4, SN 2618, SN 2446) and temperature (SBE 3, SN 2678), a high precision pressure sensor Digiquartz 410 K-105 (SN 75659), a high precision thermometer (SBE 35 RT, SN 27), a Wetlabs C-star transmissiometer (SN 267), a BackScat I-fluorometer (Dr. Haardt, SN 8060) and a Benthos altimeter Model 2110-2 (SN 189).

The back-up system from the ship (SN 485) was run with one sensor pair of conductivity (SBE 4, SN 2078) and temperature (SBE 3, SN 2423), a high precision pressure sensor Digiquartz 410 K (SN 68997) and a mechanical bottom alarm. Three water bottles had to be removed to connect the CMiPS instrument of R. Muench to the caroussel.

Both systems were run one after the other every 6 hours. Only when ice was pressed to the starboard side of the ship no cast was possible.

For both CTDs the conductivity and temperature sensor calibration were performed before and after the cruise at Sea-Bird Electronics. The accuracy of the temperature sensors can be given to 2 mK. The readings for the pressure sensors are better than 2 dbar.

The conductivity was corrected using salinity measurements from water samples. IAPSO Standard Seawater from the P-series P144 (K15= 0.99987) was used. A total of 463 water samples were measured using a Guildline Autosal 8400 B. On the basis of the water sample correction, salinity is measured to an accuracy of 0.002.

Underway measurements with the vessel-mounted narrow band ADCP (Acoustic Doppler Current Profiler) from RDI Instruments type Ocean Surveyor with 153.6 kHz transducer were done to provide current data of the top 150 - 300 m. The data will be processed at AWI by means of the CODAS software.

To supply the ship with surface temperature and salinity values the two ships SBE 45 thermo-salinographs were used, one in 6 m depth in the bow thruster tunnel and one in 11 m depth in the keel. Both instruments were controlled by taking water samples which are measured on board.

During the drift at the floe a Helicopter CTD system was in use which consists of a modified SBE 19 (SN 2715) for continuous data aquisition with a 3.14 mm single wired cable. The whole system will be calibrated using the pre and post calibration values from Sea-Bird. The accuracy for temperature is better than 3 mK whereas the salinity is better than 0.005. The pressure sensor measured with an accuracy better than 3 dbar.

Preliminary Results

Already on the way to our drift position one deep CTD station in the inner Weddell Sea basin was done to enlarge a time series of the bottom water temperature of the WSBW (Weddell Sea Bottom Water) which started in 1990 with use of moored instruments in a water depth of 4740 m. Near to position 65°37,6‘S, 36°29,4‘W, the former AWI 208 mooring location, an increase in bottom water temperature of Θ= 0.06 °C was measured between 1990 and 1996. One other CTD measurement in 1998 show a slightly decrease of temperature. Now six years later the WSBW temperature increase is still going on (see Fig. 5.1.1) but with a slightly lower trend in time.

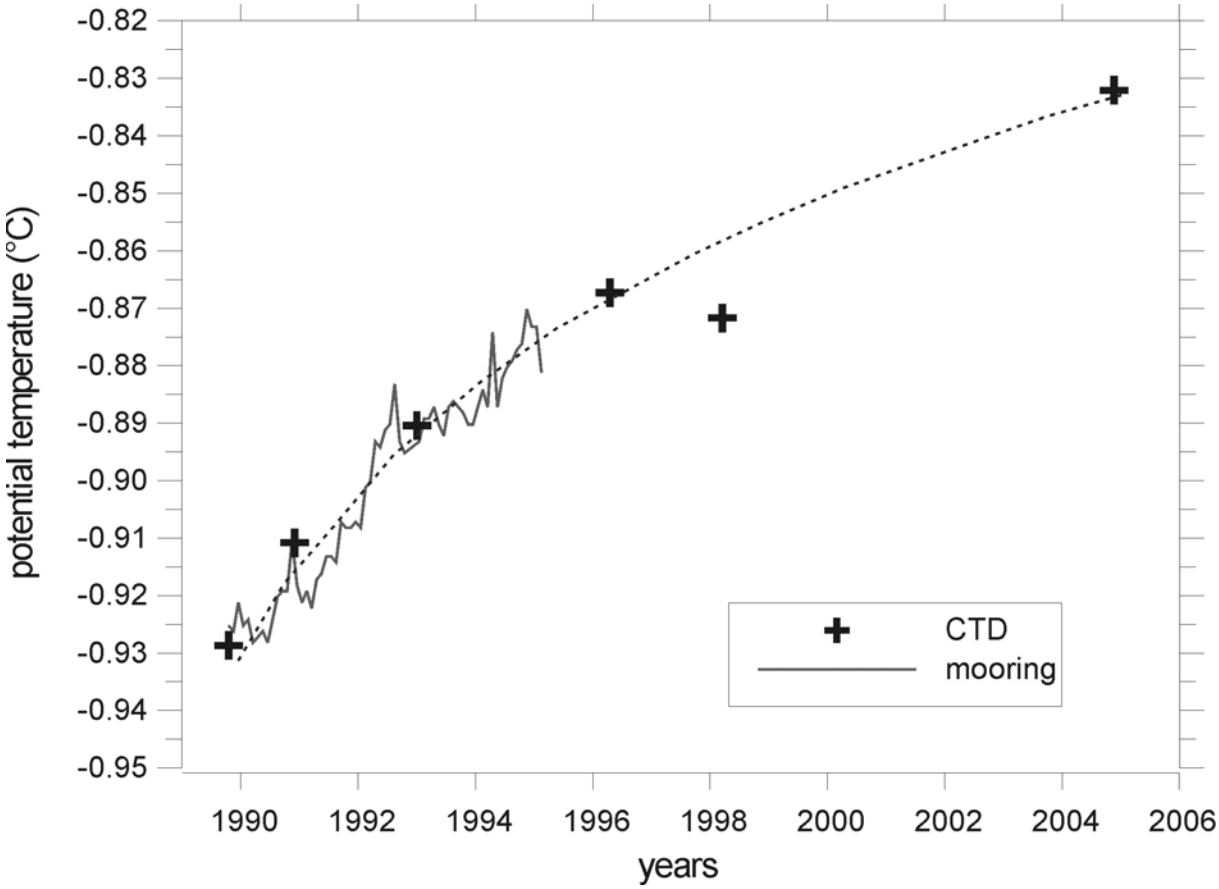

Fig. 5.1: timeseries of bottom temperature AWI 208, 4740 m depth

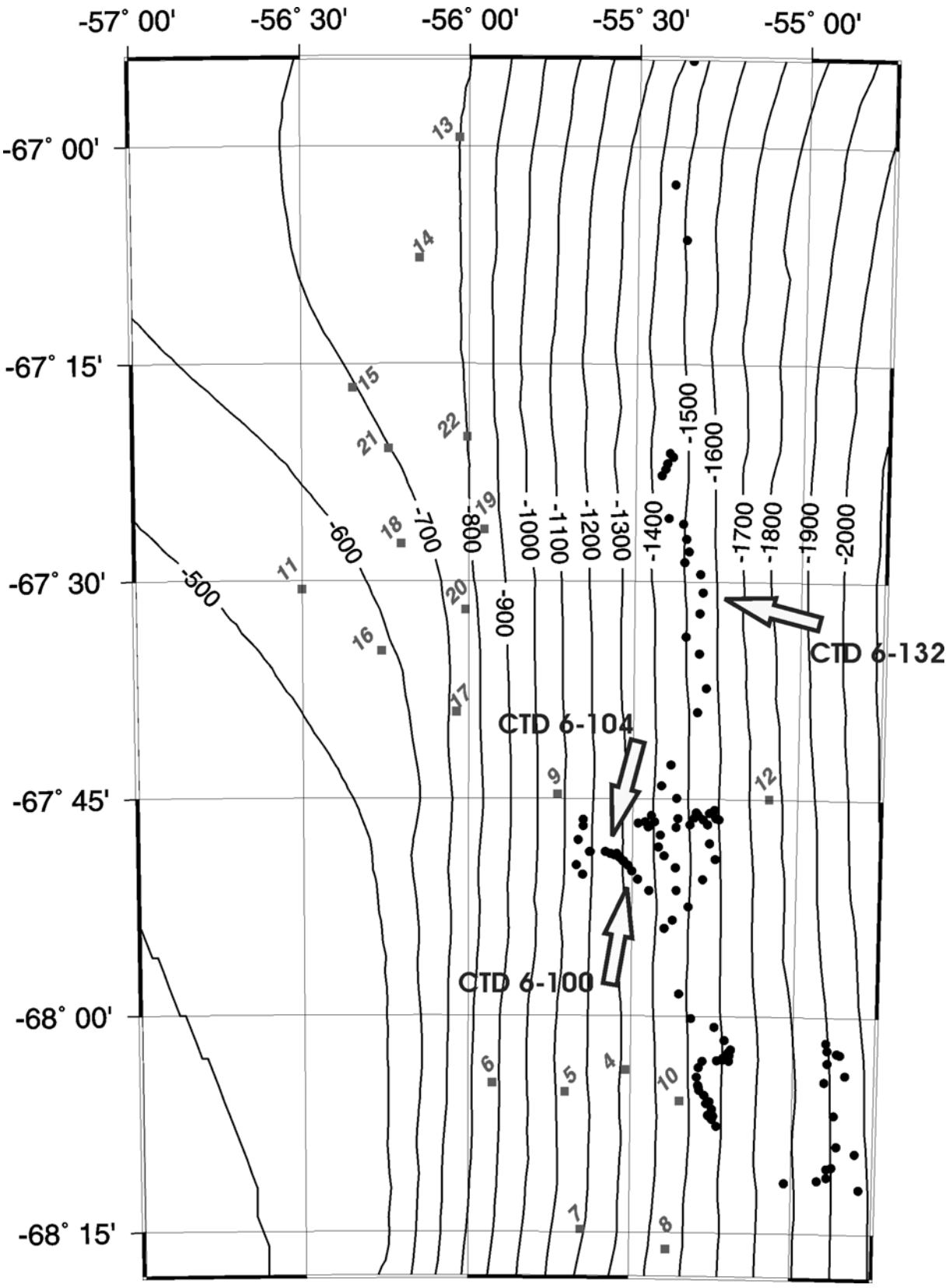

Fig. 5.2: Map of CTD stations during the floe drift. Black dots denote ships CTDs and black squares denote position of helicopter CTDs.

At the drift floe 141 deep CTD casts were done in an 6-hours-interval schedule. Of these 31 casts were run by the ships system and 88 casts by the main system. A map of the casts is shown in figure 5.2. This picture also shows the position of the Helicopter CTDs and ship station 6-104 of which the temperature and salinity profiles are shown in figure 5.3a. Both parameter show the typical form with the cold and fresh Winter Water (WW) in the top 200 m of the water column followed by the main thermocline and the Warm Deep Water (WDW) with the temperature maximum of 0.25°C at 680 m depth. The salinity maximum of 34.655 is more than 100 m deeper at 790 m depth. In the water mass of the WSDW (Weddell Sea Deep Water) and especially in the Weddell Sea Bottom Water (WSBW) both parameter show pronounced intrusions on density lines which can also be seen in the Θ/S-diagram in figure 5.3b. These intrusions reflect the interaction of downflowing dense shelf waters along the shelf break with the ambient water masses over the deep basin.

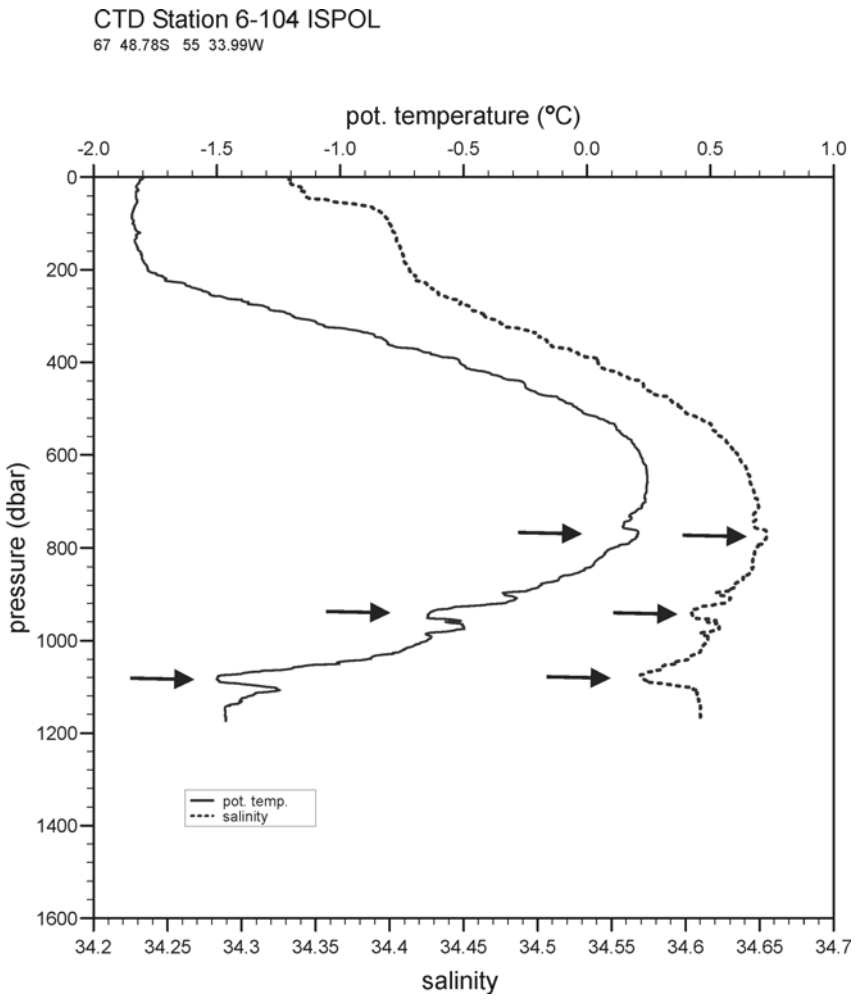

Fig. 5.3a: Temperature and salinity profile from ship station 6-104. Arrows show the posibility of intrusions.

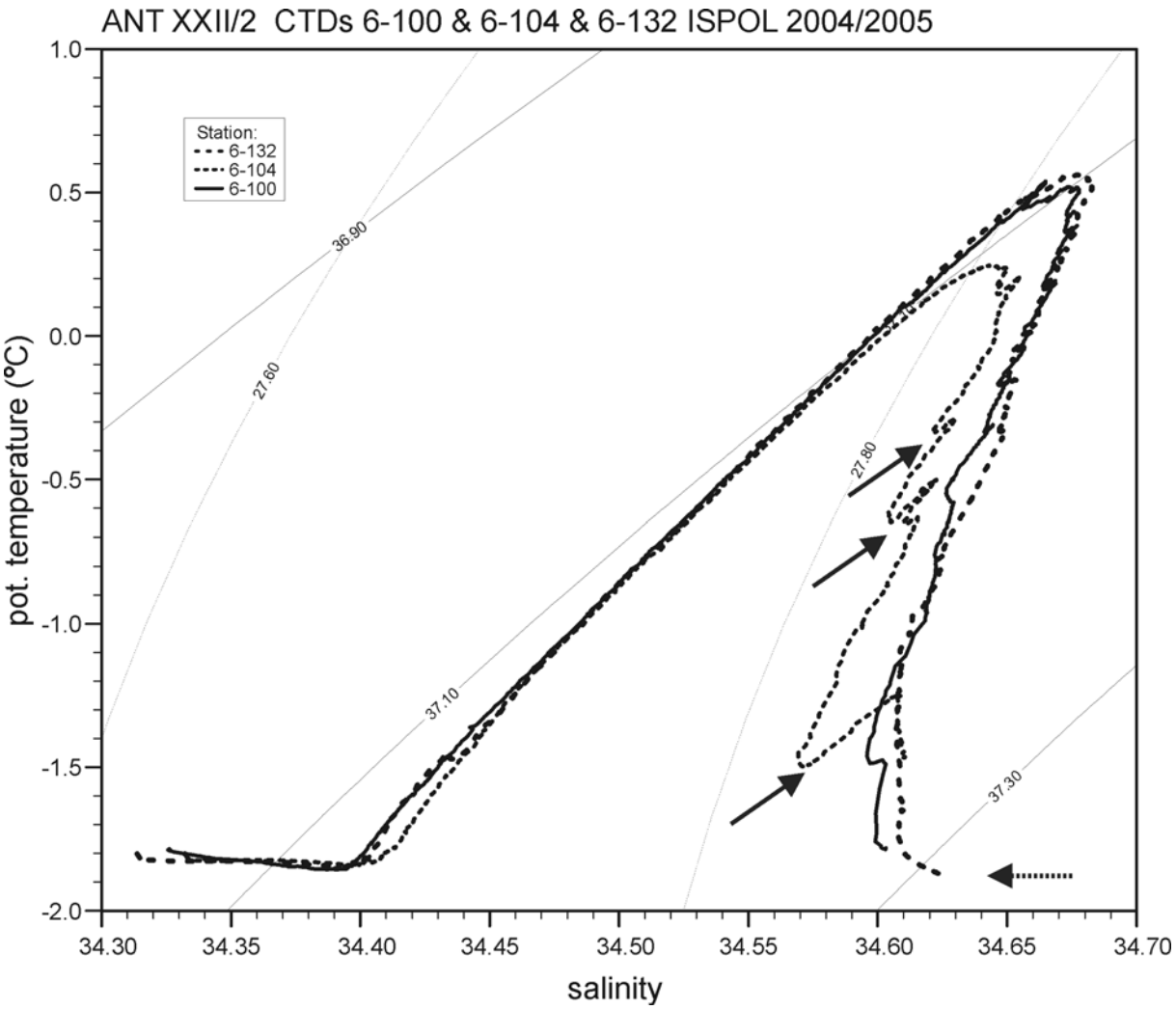

Fig. 5.3b: Θ/S-diagram of three stations, 6-100, 6-104, and 6-132

In the Θ/S-diagram of figure 5.3b also the density lines σ_0 and σ_2 are shown. The hatched arrow indicates the increase in bottom salinity of the coldest station 6-132 which increased to values of

s > 34.62

The distribution of the temperature maximum of the WDW at the continental shelf break is shown in figure 5.4. West of appr. 55°30'W no temperature maximum was detected which corresponds roughly with the 1000 m isobath. Maximum values for t_{max} were measured in the south west with temperatures of Θ > 0.65°C. Minimum values of t_{max} are located in the central part with temperatures of Θ < 0.4°C.

Overall the distribution of the temperature maximum is almost parallel to the bathymetry with some patchy spots included. Connected to this is the depth of the temperature maximum (Fig. 5.5) which has a nearly equal distribution with some

areas of special interest. For example the very close neighborhood of minimum and maximum near 67°45'S and 55°30'W. Here the depth difference between both extrema exceeds 200 m in the vertical within a distance of less than 5 nm.

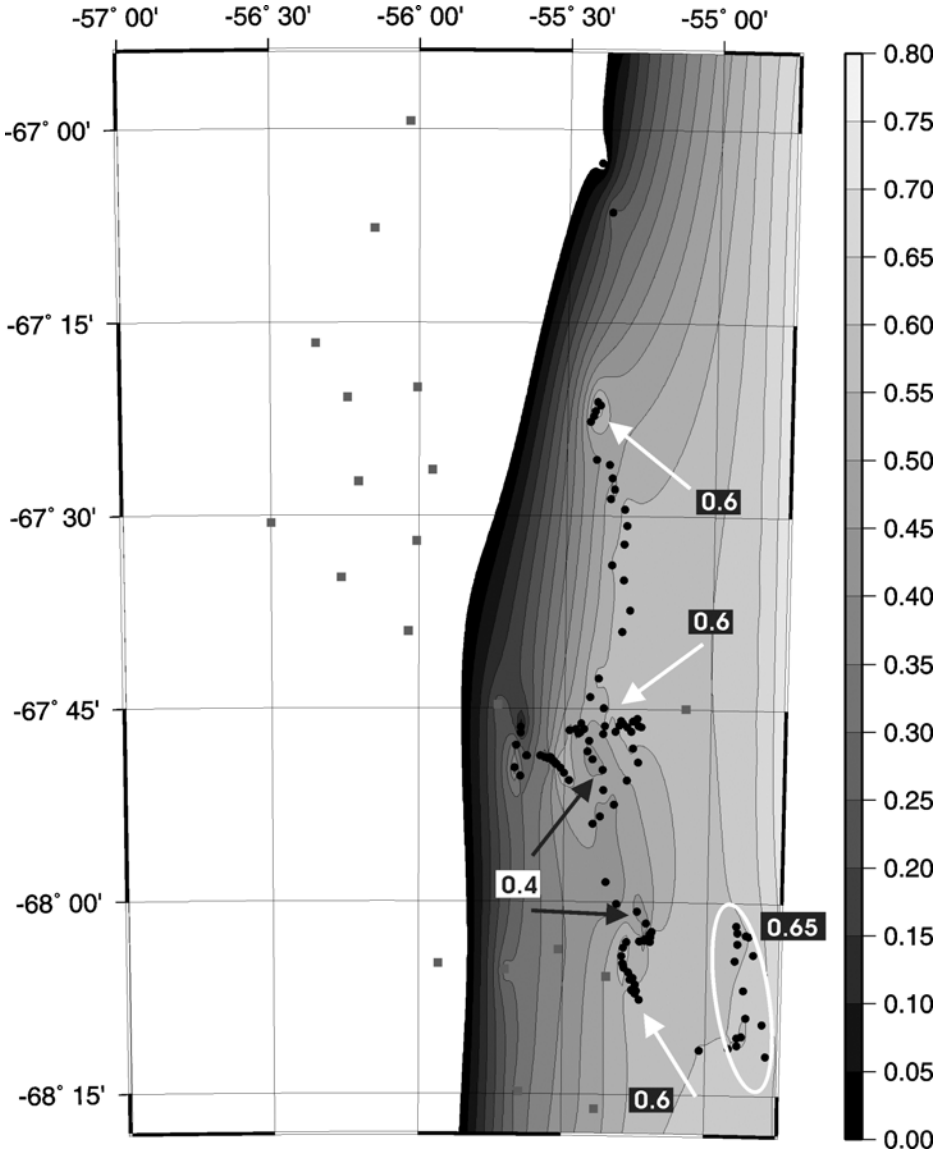

Fig. 5.4: Distribution of the temperature maximum in the WDW water mass, dots are ship CTDs and squares are helicopter CTDs.

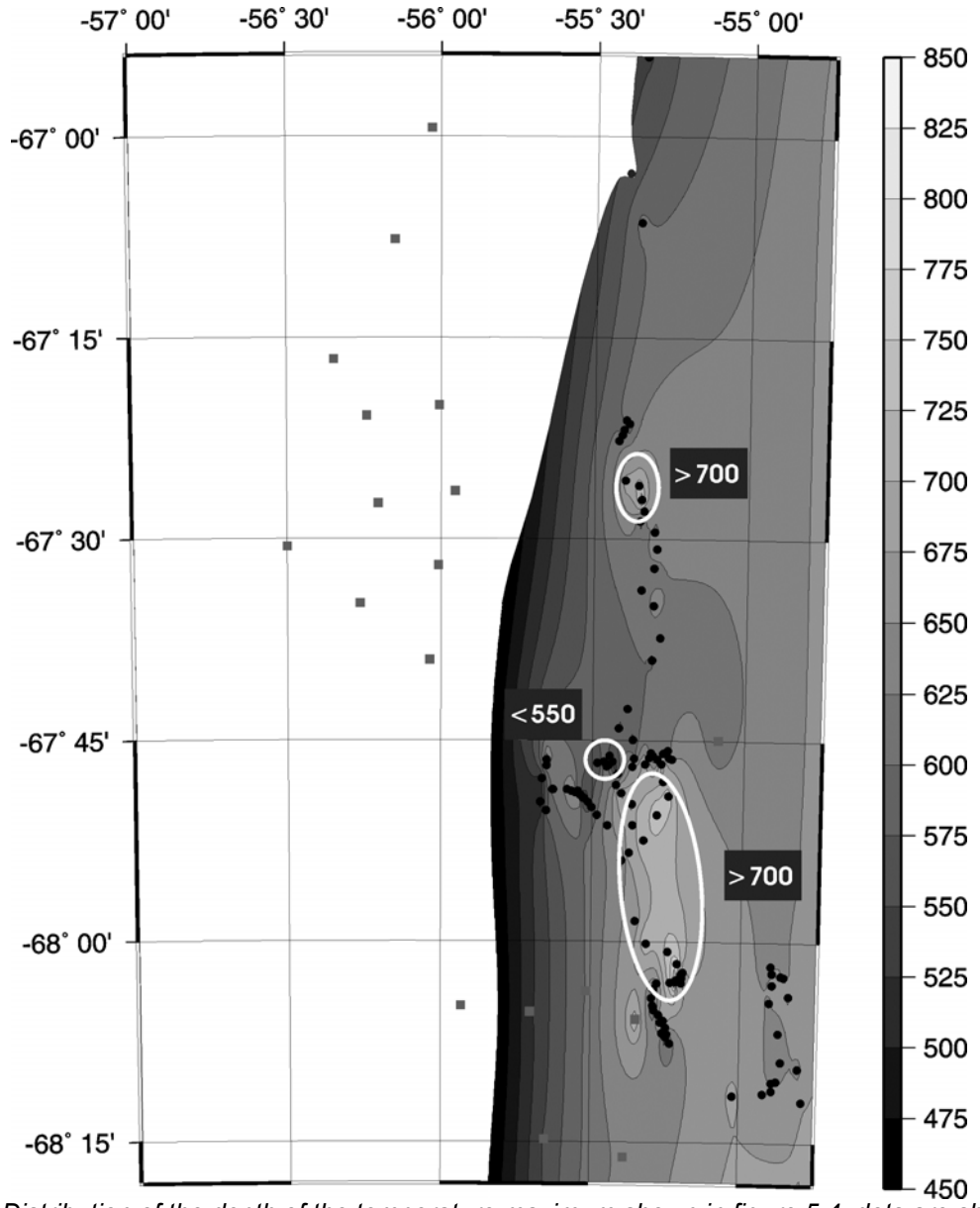

Fig. 5.5: Distribution of the depth of the temperature maximum shown in figure 5.4, dots are ship CTDs and squares are helicopter CTDs.

One of the most important parameter to look at while on cruise is the distribution of the bottom temperature. Together with the salinity of the bottom layer these two parameters are the key to the existance and spreading of dense shelf water masses along the shelf break which are able to dilute and freshen the deep and bottom water masses of the Weddell Sea. From these measurements the position for the next helicopter station was planned to get a nearly equal spaced measurement array over interesting features in the bathymetry as valleys, canyons or troughs. Because the salinity values are not calibrated yet only the temperature distribution in the bottom layer is shown in figure 5.6. As already shown for the T -max layer the bottom temperature is even more heterogenous. Both absolute extrema in bottom temperature are found by use of the heli-CTD with values of $\Theta = -1.91°C$ and

$\Theta = -1.17°C$ in a distance of only 7 nm. The water depth was pretty much the same for both locations with z = 429 m and z = 476 m and did not contribute to the temperature values. Further downslope of both positions the ships CTD measured colder temperatures which did not have a direct connection to the cold shelf waters (z < 500 m). So a direct downflow of dense water into the Weddell Sea interior could not detected.

Even along one isobath at the slope for example the 1200 m line, there is no evidence of a permanent flow of cold and saline bottom water to the north. There are more indications for non permanent pulses of dense waters which form isolated blubs along the bathymetry.

On the shelf with depths less than 500 m different forms of high density water masses are found which are different in the salinity. No indication of Ice Shelf Water (ISW) could be detected but some places of High Salinity Shelf Water (HSSW) were found. Together with the analysis of tracer measurements (see chapter 5.4) a precise calibration of salinity values and water mass analysis has to be done at home.

One reason for the big uncertainties in the area southeast of the Antarctic Peninsula where the floe drift had happened is the unknown and wrong bathymetry as expressed for example in the GEBCO charts. From all our measurements we calculated the depth with correcting the different sound velocities used (GEBCO = 1500 m/s) to the measured value (mean 1465 m/s). The differences of both are shown in figure 5.7. It is obvious that the more or less north-south direction of the isobaths presented in GEBCO no longer holds for this area because dramatic differences in water depth occur. On the shelf the water depths measured are more than 200 m shallower than predicted where on the steep slope the depths are shallower in the range between 50 m and 200 m. Near the ship and this is comparable to the Hydrosweep values the differences are less than 50 m to either side but with a tendency to shallower values. Only at two spots the measured depth is greater than shown in the charts.

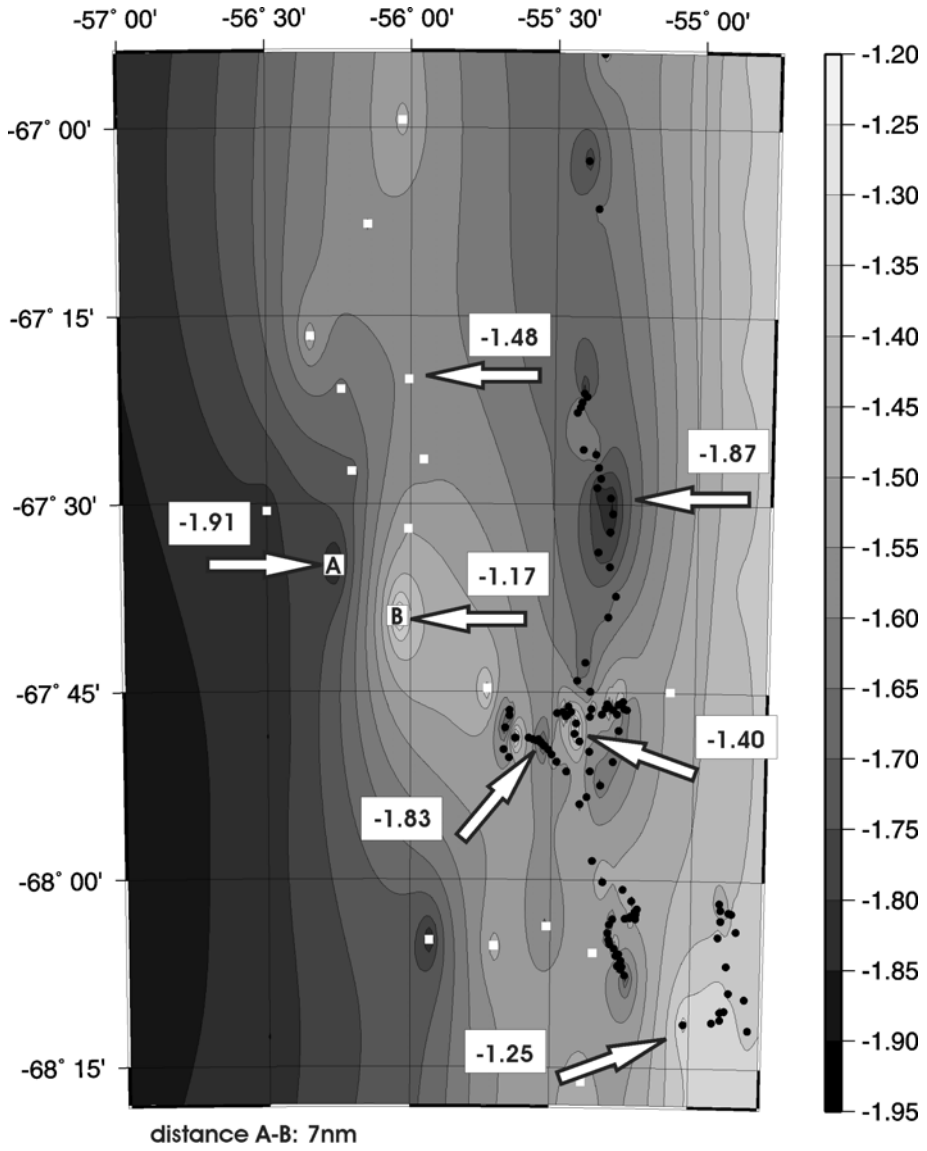

Fig. 5.6: Distribution of bottom temperature derived from ship CTD (black dots) and helicopter CTD (white squares). A,B denote heli-station 16 and 17 which represent the absolute minimum and maximum temperatures in the bottom layer. The distance between both extrema is 7 nm.

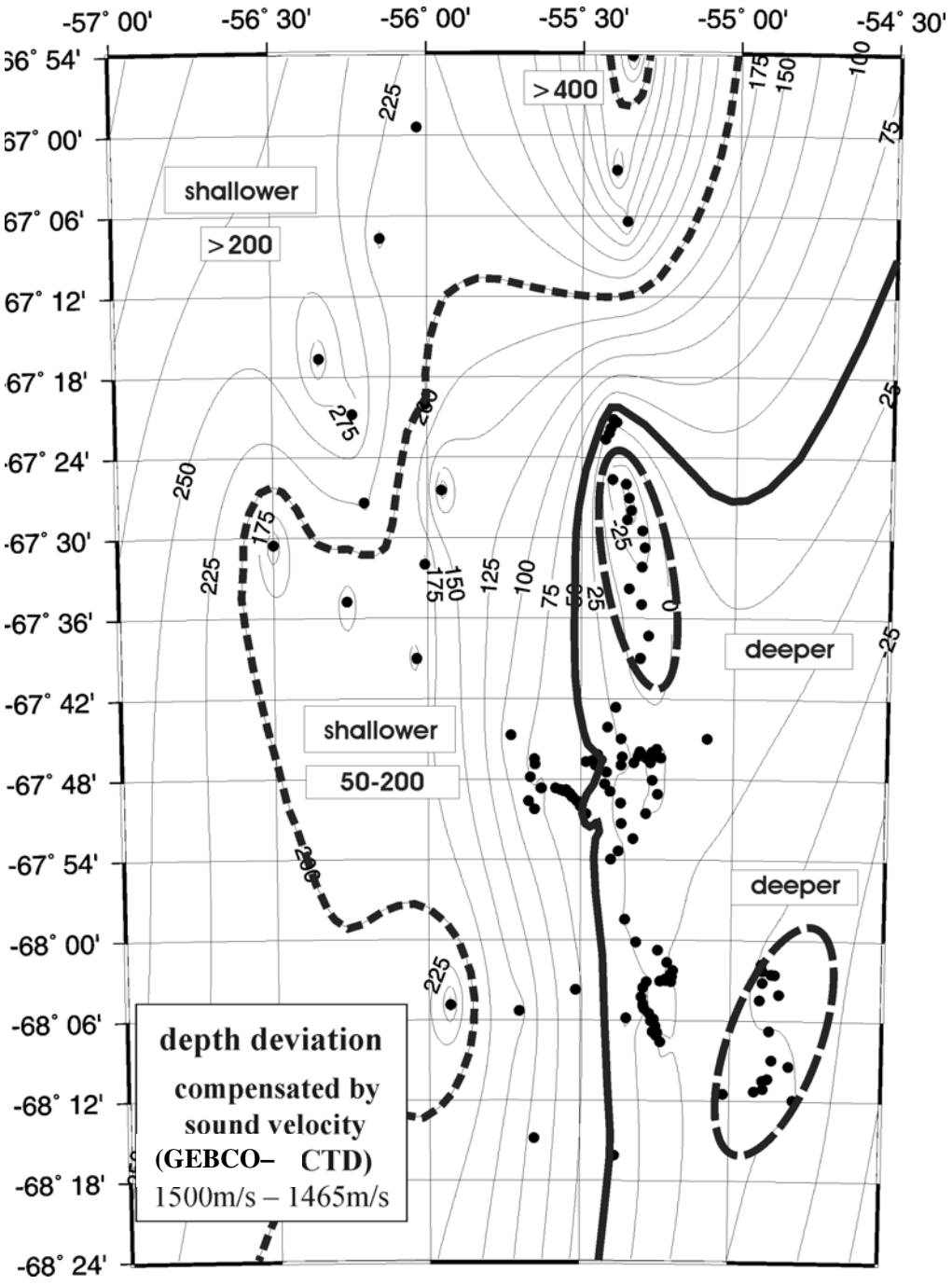

Fig. 5.7: Distribution of depth deviation measured with the use of the CTD profiles.The difference in sound velocity between GEBCO charts (1500 m/s) und measured profiles (1465 m/s) is encountered.

In figure 5.8 the position of two vertical temperature sections are shown which represent the west-east (Fig. 5.9) and north-south (Fig. 5.10) distribution of water masses.

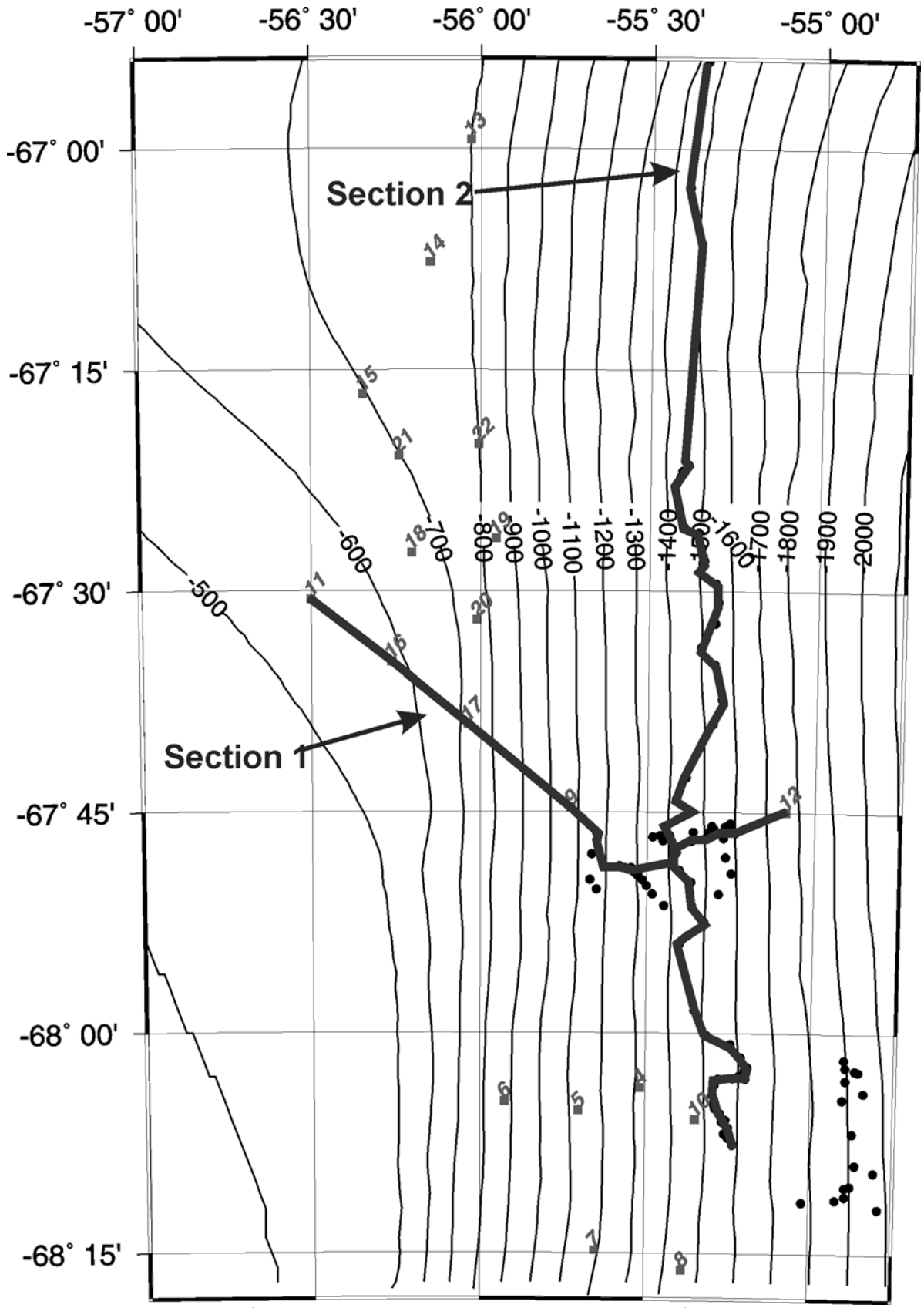

Fig. 5.8: Map of the temperature sections 1 and 2 shown in the following pictures figure 5.9 and figure 5.10

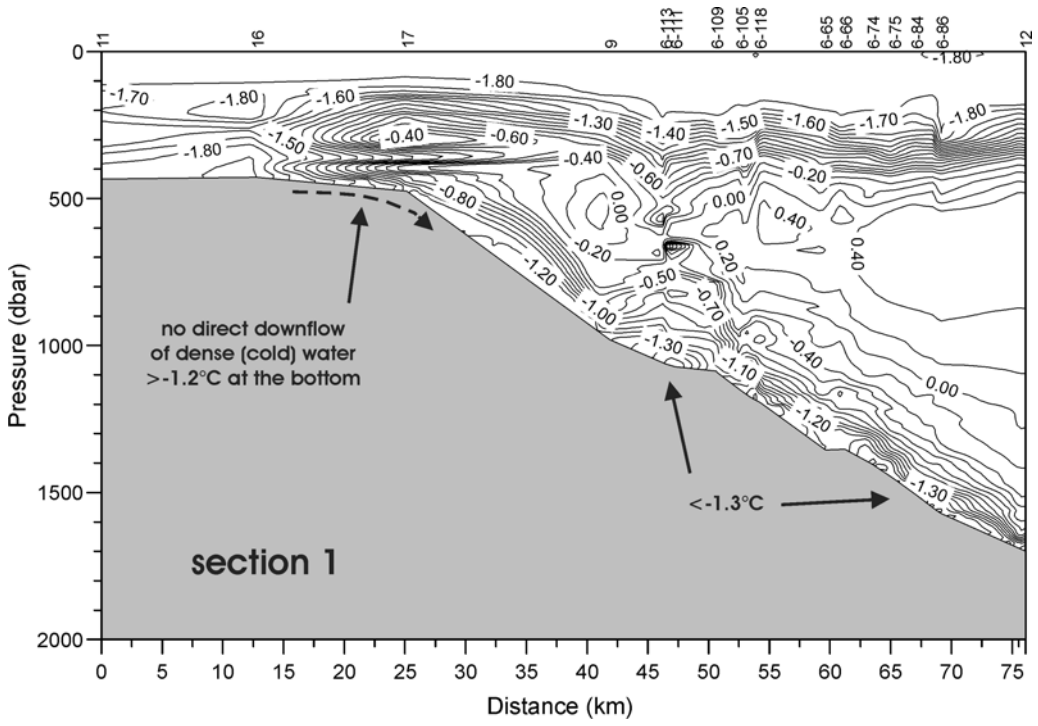

Fig. 5.9: Temperature section 1 in west-east direction down the continental shelf break

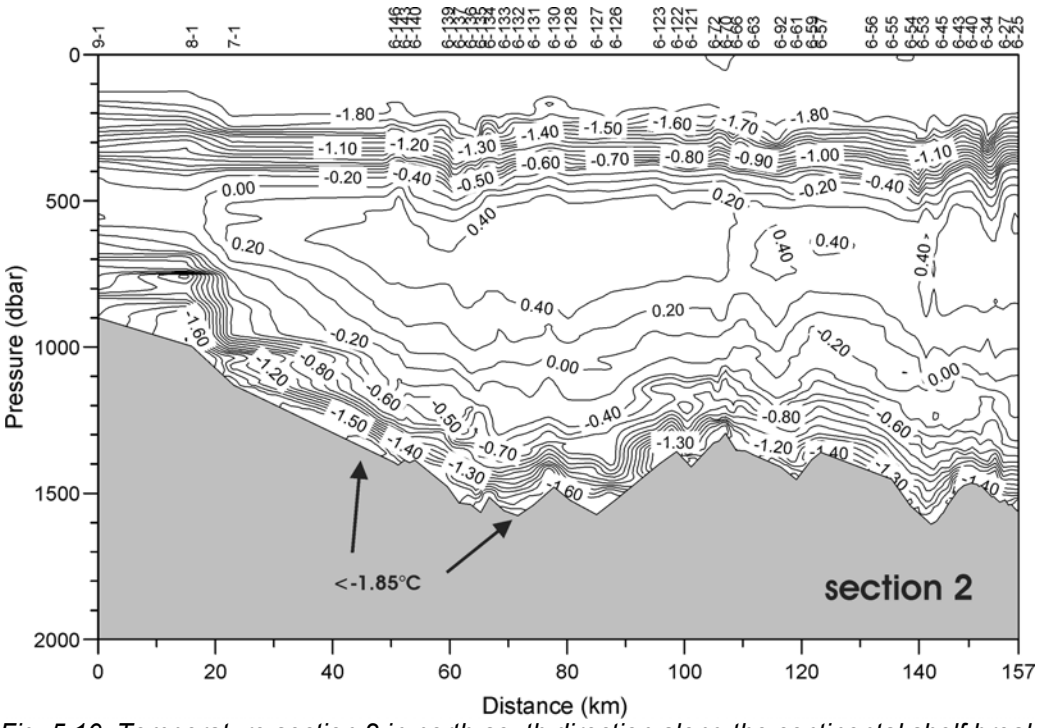

Fig. 5.10: Temperature section 2 in north-south direction along the continental shelf break

5.2 Scalar microstructure observations

Robin D. Muench
Earth & Space Research, Seattle, USA

Introduction

Vertical profiles of thermal microstructure were measured throughout the water column at 26 sites during ISPOL. An additional four measurement attempts were unsuccessful due to thermistor probe failures. Measurements were made nominally twice daily, starting on 29 November and with the final successful attempt made on 16 December. The observations spanned the central western Weddell Sea continental slope, near 68ºS, between bottom depths of about 1300 and 2000 m.

The microstructure observations were made using a CTD-mounted Microstructure Profiling System (CMiPS) manufactured by RGL Consulting, Ltd. of Victoria, Canada. This system uses FP-07 thermistors that are capable of measuring vertical temperature fluctuations to a resolution of about 3 cm at the nominal 0.8 ms^{-1} descent rates that were used. The FP-07 thermistors have become one of the standards for rapid response temperature observations, and their response and spectral characteristics are well documented. The CMiPS was mounted on the water sampling rosette belonging to the vessel's instrument suite and was powered from a Sea-Bird 911+ power supply fed through a Sea-Bird 911 CTD (serial number 485) equipped with single T and C sensors. The CTD data obtained concurrently with the CMiPS data are an integral part of the microstructure dataset, as these provide cast by cast calibrations for the CMiPS data. Data were downloaded from the CMiPS at least once daily, and when possible following individual casts, onto a desktop computer. Diagnostics were then run to monitor instrument performance and data quality. The data are archived as raw binary files that are large (~50 mB each) and require specialized routines, in conjunction with the commercially available Matlab® analysis software suite, for processing.

The FP-07 thermistors used to measure temperature failed at an unanticipated high rate, necessitating frequent changes and rapidly depleting the store of replacements. The programme was terminated following failure of the final available replacement set of thermistors. Despite the somewhat premature cessation of data collection, the observations adequately covered the geographical area of interest. Some of the methods used to derive vertical mixing information from the microstructure data can also be applied, though with lower accuracy, to the raw CTD data, and will be used to expand the coverage over a larger area than would be possible using the data from CMiPS. Confidence in use of the CTD data is greatly increased in this case because we have sufficient microstructure data to effectively calibrate the raw CTD data for computation of vertical turbulence parameters. The measurements that have been acquired will allow a characterization of vertical mixing processes over the western Weddell Sea continental slope, a region of active bottom water transit about which we have few quantitative data, and the effort has been a success despite the disappointing failure rate of the temperature probes.

A Sample Result

An example shown in figure 5.11 illustrates the information that is obtained from scalar microstructure data, where “scalar microstructure” refers here to temperature. The results shown are from ISPOL station 635 and were obtained at about the 1500 m isobath at 68.086ºS by 55.287ºW, on the upper continental slope of the western Weddell Sea. These results typify those at many of the sampled sites and are assumed to represent conditions over the central western Weddell slope. The continental slope in this region is characterized by northward-flowing, bottom-trapped density currents of Weddell Sea Deep Water that has originated through surface densification farther south and that will contribute to Antarctic Bottom Water farther to the north. In the deep water above the density currents, vertical microstructure reflects lateral intrusion of shelf-derived waters from the upper continental slope seaward toward the central Weddell Sea. The upper ocean is separated from the deeper waters by a permanent thermocline. The density flows, intrusions and thermocline are accompanied by vertical shear in the horizontal currents, and this shear contributes to vertical mixing.

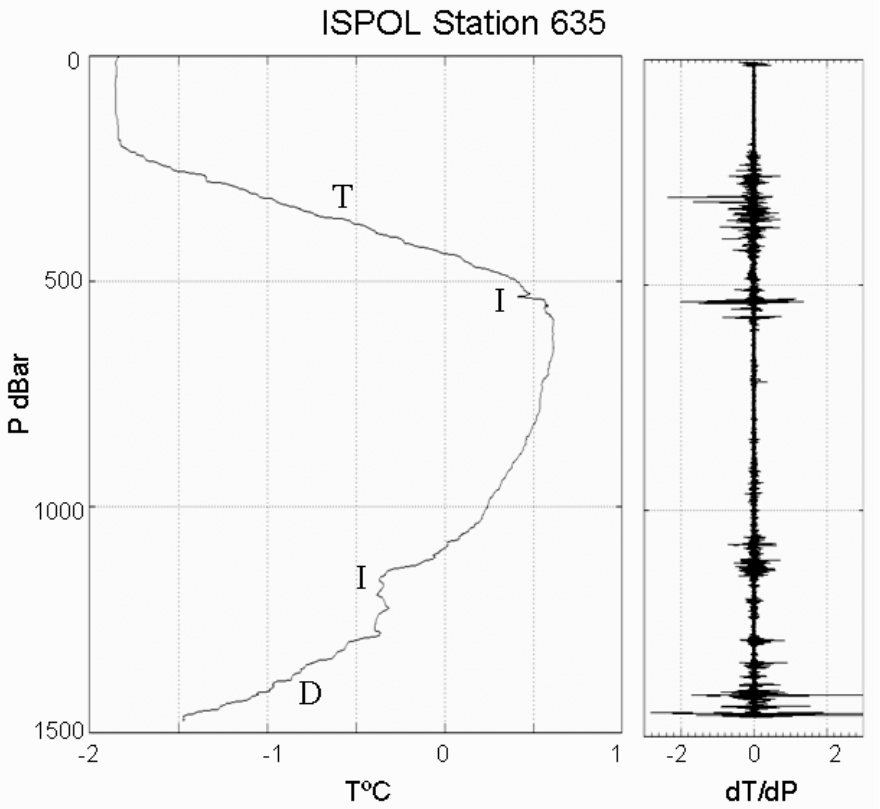

Fig. 5.11: The plot to the left shows the vertical distribution of temperature T derived from CTD data at ISPOL Station 635, while the right-hand plot shows the corresponding scaled vertical distribution of thermal microstructure dT/dP measured using CMiPS. The upper 500 m is dominated by an upper mixed layer about 200 m deep followed with increasing depth by the permanent thermocline, marked “T”. Two intrusions of colder water were present, one just beneath the thermocline near 500 m and a larger one near 1200 m, both marked “I”. The near-bottom density current is indicated by “D”. Each of these features has associated lateral currents and shear that lead to vertical mixing, as reflected in the distribution of thermal microstructure.

Future Plans
A number of parameters that are associated with vertical turbulent mixing can be computed from these data, subject to various physical assumptions. These parameters include the vertical eddy diffusivity K_z, from which other quantities such as the vertical turbulent heat transport can be derived. Various methods can be applied to the data to obtain K_z, with the choice of method depending upon the physical situation to which it is applied. Vertical microstructure temperature gradients can be used to estimate K_z directly using the so-called Osborne-Cox method. In cases where the vertical temperature profile suggests the presence of overturning such as might occur in a strong vertical current shear, the method of Thorpe displacements can be used. Both methods can be applied as well to vertical temperature or density profiles obtained using a CTD. Accuracy of results computed using CTD data is lower than that derived from the CMiPS data and, for computations using the Osborne-Cox method, corrections must be made to the CTD data to allow for the sensor responses which are slow when compared to the CMiPS. Because we obtained concurrent CTD and CMiPS data under ideal conditions of no surface wave-induced ship motion, quantitative intercomparisons between the two separate but complimentary datasets will contribute to techniques for derivation of vertical turbulence information from widely available CTD data.

Impacts
The results of these observations will contribute to our methodology for field assessment of vertical turbulence and will allow a quantitative characterization of the turbulent field associated with the central western boundary of the Weddell Sea. This characterization will in turn enhance the ability to parameterize crucial turbulent processes in ocean General Circulation Models, in particular, turbulence associated with deep density flows and intrusions. These goals have been established as having a high priority by SCOR (Scientific Council on Ocean Research) Working Group 121 on Ocean Mixing, and are of particular interest to the U.S. Office of Naval Research who provided funding for use of CMiPS during the ISPOL1 expedition. Support from the Alfred Wegener Institute for Polar and Marine Research, through provision of a science berth during ISPOL, is most gratefully acknowledged.

5.3 Boundary turbulence

Miles G. McPhee
McPhee Research, Naches, USA

1. Project Description
The ocean turbulence project in ISPOL was to measure mean and turbulent properties of the turbulent flow in the upper ocean below the ISPOL floe, in order to quantify the exchange of heat and salt between the ice underside and the underlying the ocean. Instrumentation deployed comprised:

A primary mast with two turbulence instrument clusters (TICs) separated by 4 m, each measuring three components of velocity along with temperature and conductivity twice per second interfaced to a Sea-Bird 911+ CTD system. One TIC was additionally equipped with a microstructure conductivity meter. Suspended

approximately 2.0 m below the lower cluster were two acoustic Doppler profilers: an upward looking 1.2 MHz RDI instrument and a downward looking 0.6 MHz RDI 5–beam Broadband instrument. The mast was first deployed on 30 November 2004 at a site approximately 300 m from the ship bow, about 70 m from the floe edge. The primary mast operated with brief interruptions until the site was abandoned on 25 December 2004 because of floe breakup. Initially the clusters were positioned at 4 m and 8 m depth, below 2 m thick ice, and lowered to 6 m and 10 m (4 and 8 m below the ice) on 2 December.

A second mast with one TIC mounted 2 m above a downward looking Sontek 500 kHz acoustic Doppler profiler was deployed on 8 December with the TIC at 3 m depth (1 m below the ice). This cluster included a microstructure conductivity sensor, but no standard conductivity instrument. On 18 December the two masts with their separate Sea-Bird 9+ CTDs were combined on a continuous mast, with clusters at 4, 8, and 12 m depth (2, 6, and 10 m from the ice undersurface). The Sontek ADP was deployed separately with its tranducer head 0.5 below the ice undersurface.

After the Christmas Day breakup, a single mast was deployed with TICs at 2 and 4 m depth beneath 1-m thick ice, with the Sontek ADP mounted 2 m below the lower cluster. In this case the upper cluster included a mC sensor. This mast operated from 26 December until 1 January.

2. TIC Measurements

Examples of TIC measurements are shown for approximately 4 days before the Christmas Day breakup in figures 5.12 - 14. The character of events near the start and end of the period is quite different with large stress and substantial downward heat flux in the first event, and comparatively low stress (despite higher current velocities) and modest heat flux near the end of the sample. This is probably due to the prevailing flow direction, which was directly from the nearby lead in the first instance, and across almost the entire floe width in the second. There appears to be a diurnal variation in both stress and heat flux, which may be related to the dominant diurnal tide, or to variation in insolation, or both.

For the flux estimates, the data were divided into 15-minute flow “realizations” with the covariances of the vertical velocity with both components of horizontal velocity and temperature, after removal of linear trends. The 15-min covariance flux estimates were then averaged in three- hour bins. The data will also provide estimates of turbulent salinity flux, but those results await consideration of noise and spike removal from the microstructure conductivity records.

Figure 5.15 shows the evolution of mixed layer temperature and salinity over the period of the drift, with a cross check between the two shipboard profiling CTD systems (SHIP and OCE, both sampled at 10 m depth), and the turbulence mast measurements (predominantly at 8 m depth). The persistent downward trend in mixed layer salinity is probably due to surface meltwater, rather than northward advection, since the floe’s zonal displacement was small during much of the time when there is an approximately linear decrease (see also Fig. 5.16).

3. Drift Analysis
Global positioning system data during the time when the ship was moored to the ISPOL floe were analyzed using a technique called complex demodulation, which fits (by leasts squares minimization) the position record to basis functions derived from the complex inertial and diurnal tidal exponentials. Velocity is obtained by differentiating the position function with respect to time. Fitted drift trajectories, expressed as eastward and northward great circle displacements from a central latitude and longitude, are shown for the two drift phases (before and after the Christmas Day breakup) in figure 5.16. Corresponding velocity (Fig. 5.17) illustrates the central role of tidal fluctuations in the total velocity field. The dashed curves represent an estimate of “mean” velocity with the inertial/semidiurnal and diurnal tidal components removed. They show that the mean drift was relatively sluggish throughout most of the ISPOL deployment.

Drift velocity is required to correct current velocities measured from the floe to actual currents in a fixed-to-earth reference frame. An example (Fig. 5.18) for the same period described in the previous section illustrates this and further shows a comparison between 3-h average currents measured by the lowest turbulence cluster, with currents measured at the same level by the 500 kHz ADP mounted just below the ice interface. For stronger currents the agreement is relatively good, but there are appreciable differences at other times. The Sontek ADP provided acceptable current profiles with 2 m resolution to about 20 m from its deployment depth.

One of the simplest diagnostics of ice motion is the ratio of ice drift (without inertial and/ or tidal components - the dashed curves in Fig. 5.17) to wind speed. This is typically 2 % and 3 % of the 10 m wind speed for Arctic pack ice and first year pack ice (central Weddell), respectively. Comparison of ship wind speed and drift velocity (Fig. 5.19) illustrates that “free drift” conditions were seldom encountered during the ISPOL drift. The mean ratio of ice drift speed to ship wind speed was only about 1.36 %, perhaps surprising for summer conditions.

4. Floe Mapping
It became clear as the underice measurement programme progressed that the influence of ocean heating in nearby leads was an important aspect of the ice/ocean exchange; hence it was important to understand the relationship between current direction and fetch, either from open water or across long stretches of unbroken flow. The floe was mapped by skiing the perimeter, taking GPS position fixes. Drift was removed by subtracting the ship position at the time of the perimeter fixes. Initial mapping was done on 14 December after several large pieces of the floe had already broken away from the original large piece, initially surveyed on 27 November. With the exception of periods of appreciable rotation, the floe remained in its 14 December configuration until 22 December, as shown with most of the scientific sites in figure 5.20. By 24 December, a large piece at the NE corner had broken off, separated by a ~50 m wide lead. Then early on Christmas morning a crack first noticed late in the afternoon of 24 December widened, disrupting most of the science programmes (see chapter 2.2). The ship was moved to the most intact remainder of the floe, which is shown in figure 5.21 as it was surveyed on 29 December. A

comparison of the final floe with its 22 December perimeter (rotated by 75 degrees) is shown in figure 5.22.

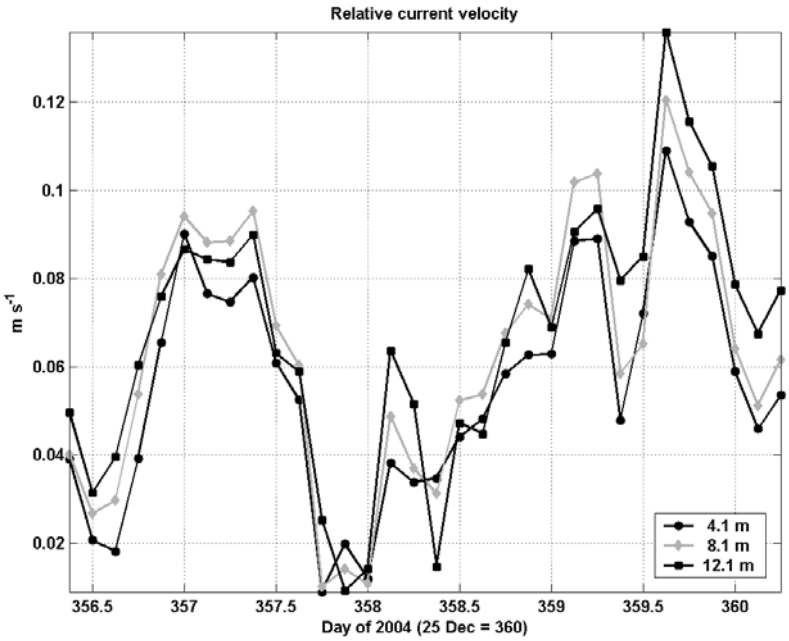

Fig. 5.12: Current speed at three levels on the main turbulence mast for approximately four days before the Christmas Day breakup. Currents are measured in a reference frame drifting with the ice.

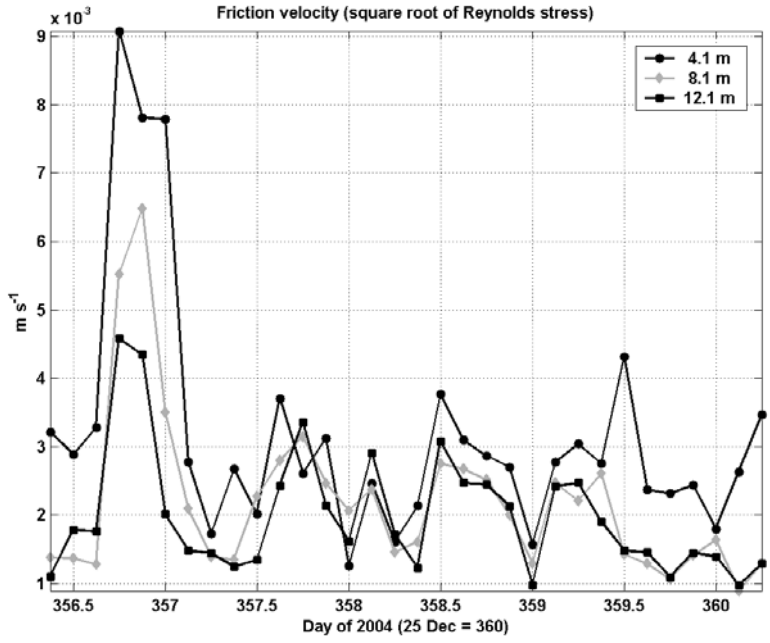

Fig. 5.13: Friction velocity (equal to square root of the turbulent Reynolds stress) at three levels in the upper ocean

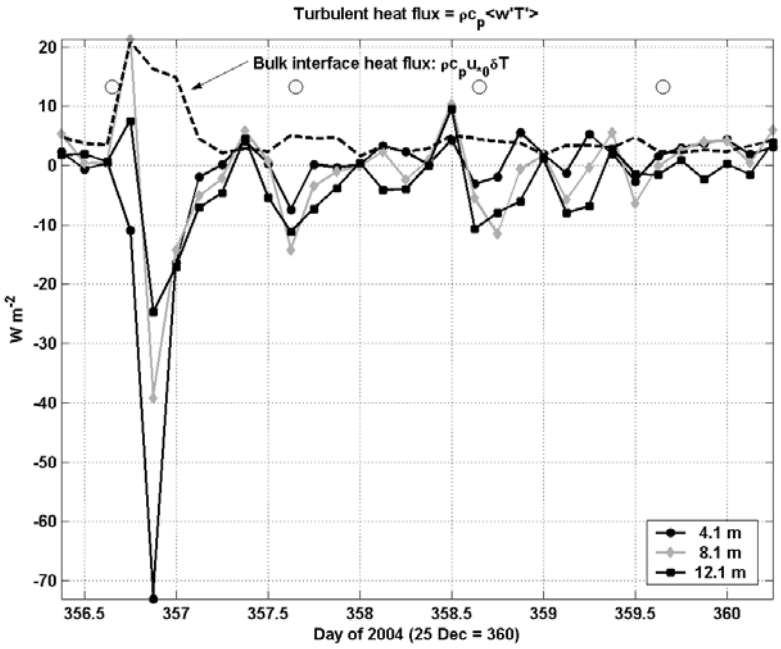

Fig. 5.14: Turbulent heat flux at three levels. Circles indicate local noon, i.e., time of maximum incoming solar radiation. The dashed curve is the bulk interface heat flux estimated from $H_{bulk}=\rho c_p c_h u_{*0}\delta T$ where δT is the elevation of mixed layer temperature above freezing.

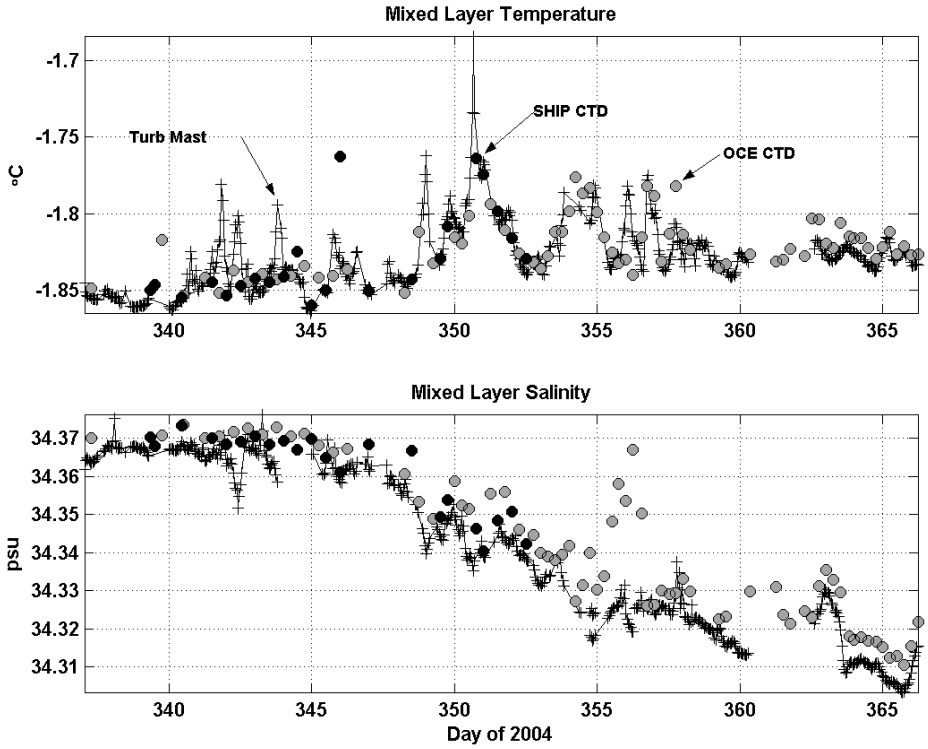

Fig. 5.15: Mixed layer temperature and salinity as determined by shipboard CTD profiling systems sampled at 10 m depth (SHIP and OCE CTD) and by the turbulence mast T/C measurements, made mostly at 8 m depth.

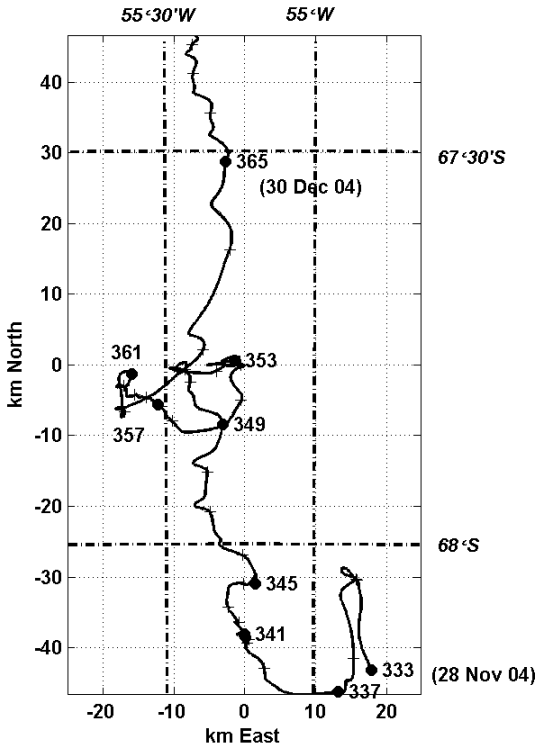

Fig. 5.16: Total trajectory of the ISPOL ice station plotted as eastward and northward great circle displacements from central coordinates (-67.772, -55.234)

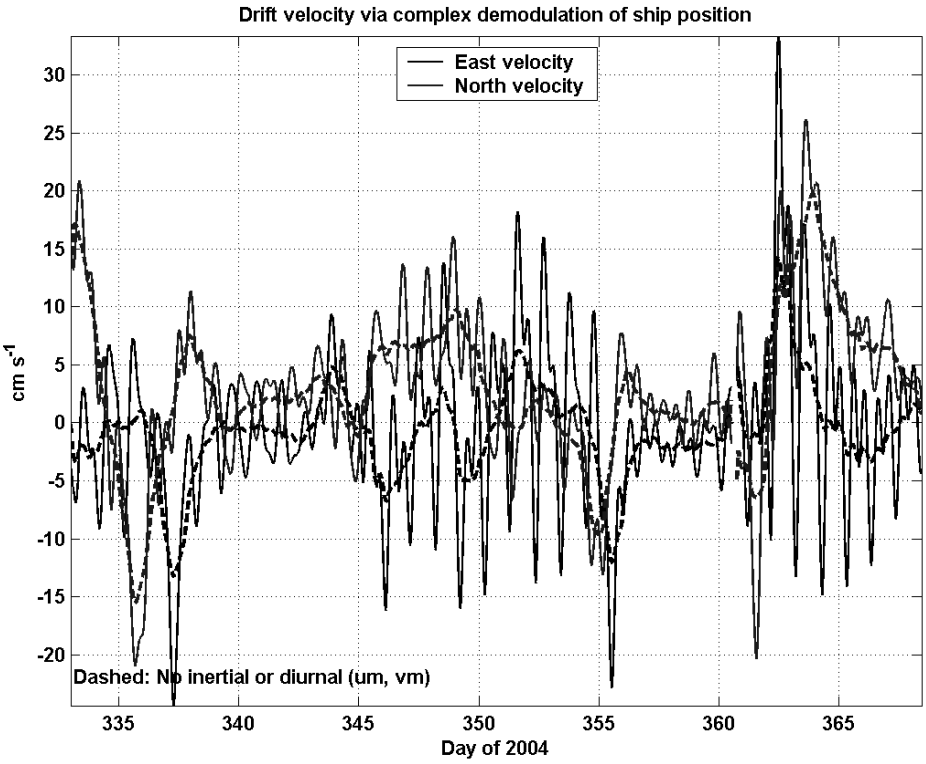

Fig. 5.17: Total ice drift velocity derived from complex demodulation of ship position, from 30 November 04 to 2 January 05. Dashed curves indicate "mean" velocity after removal of inertial/semidiurnal and diurnal tidal components.

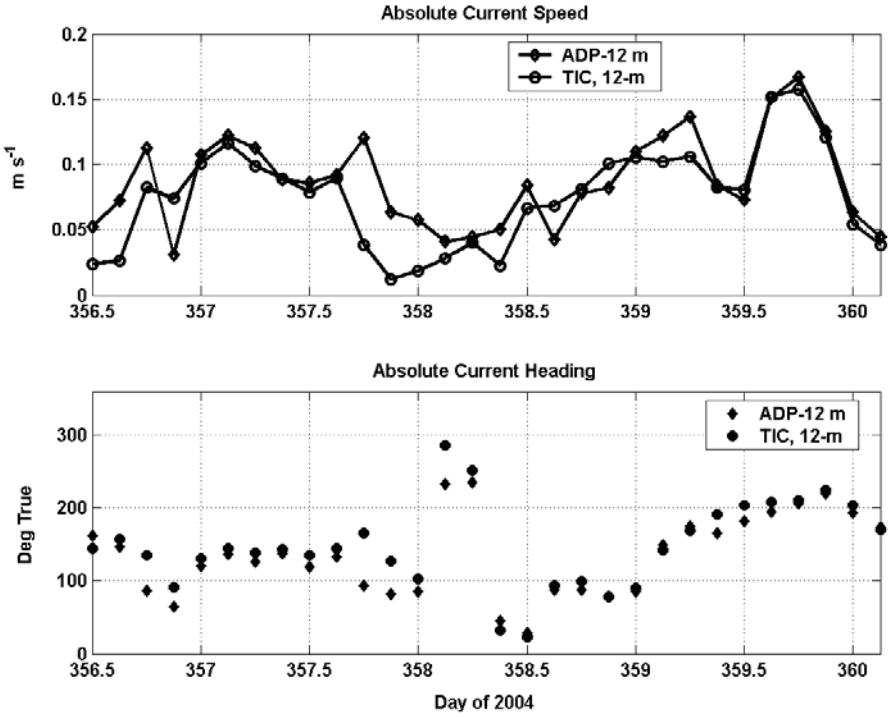

Fig. 5.18: Comparison of currents measured by different instruments at the same depth during the 5-day period before Christmas, after correcting for ice motion. Note that on day 359 (24 Dec) the absolute current exceeded the current measured relative to the ice (Fig. 5.12).

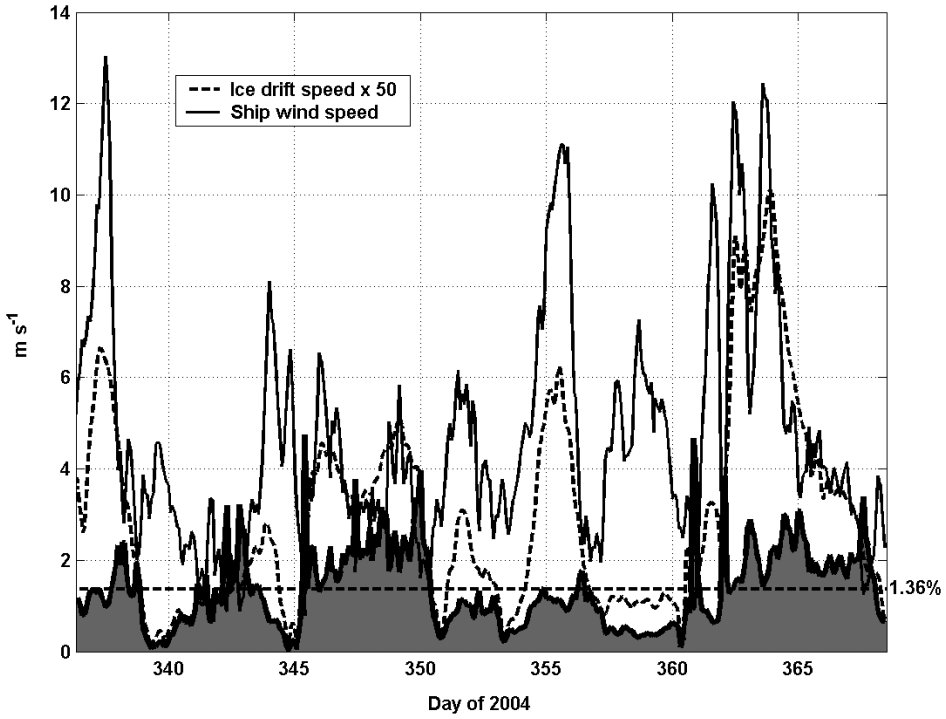

Fig. 5.19: Ship wind speed and "mean" ice speed multiplied by 50. The shaded curve represents their ratio expressed as percentage. Summer multiyear Arctic pack ice usually comforms closely to a 2 % ratio (for 10-m wind), for which the curves would overlie.

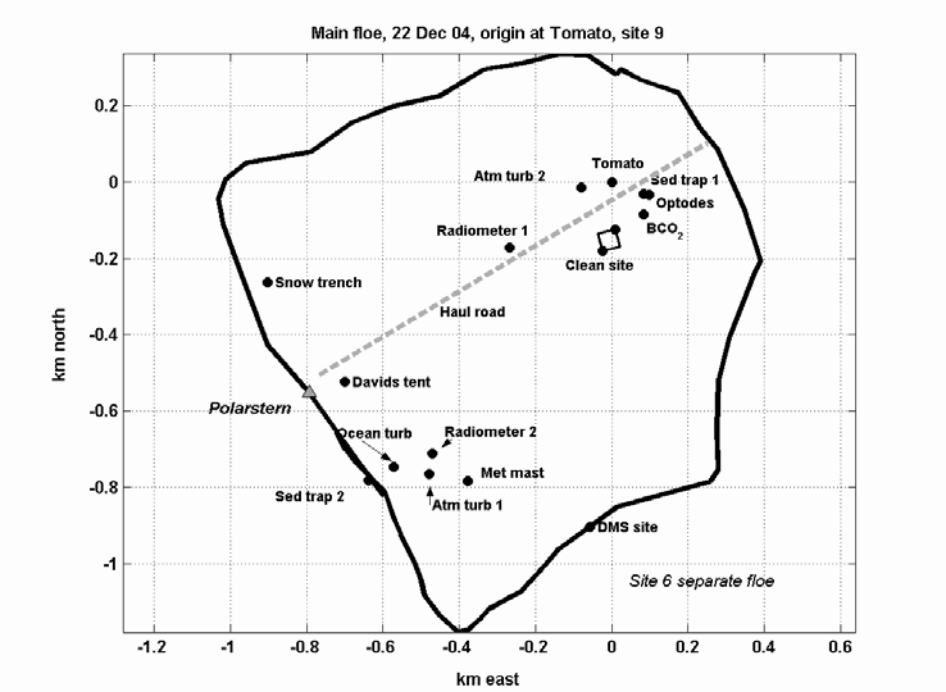

Fig. 5.20: Floe map as of 22 December 2004, showing most of the science programmes that were still situated on the main floe (several were on the separate Site 6 floe).

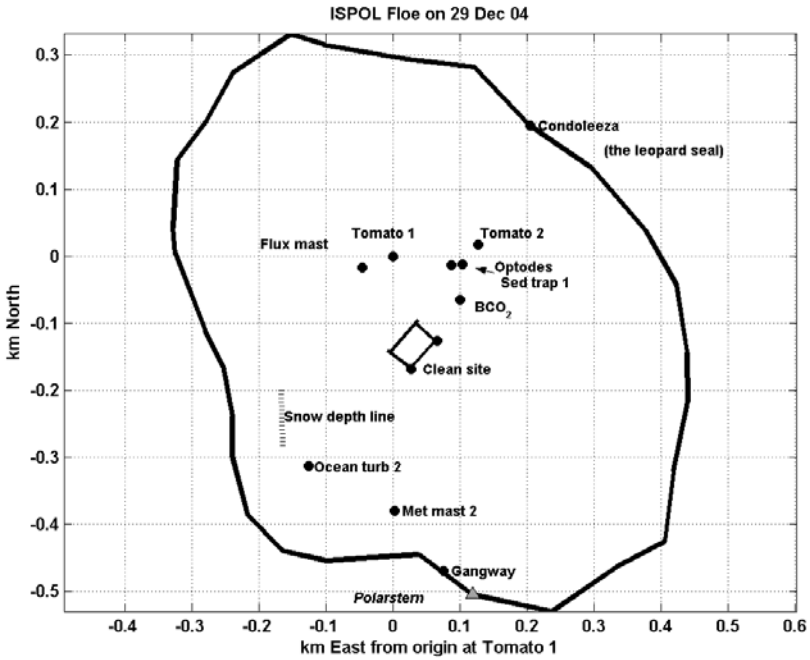

Fig. 5.21: Floe configuration after the Christmas Day break-up and repositioning of the ship

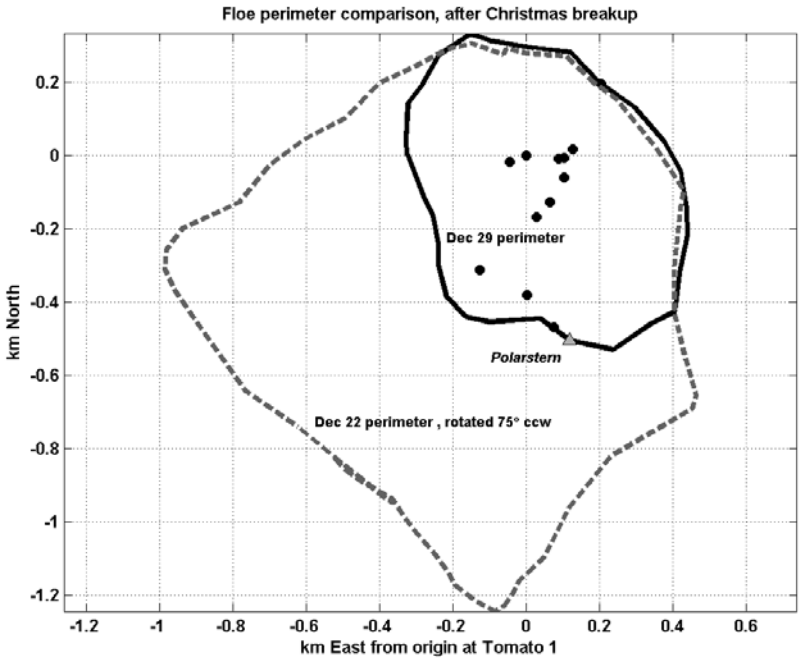

Fig. 5.22: Comparison of floe perimeters on 22 December and 29 December. Note that the 22 December perimeter has been rotated 75° counterclockwise.

5.4 Tracer measurements

Oliver Huhn
Institut für Umweltphysik, Bremen

During ISPOL a total amount of 500 CFC samples where taken as profiles from the sea surface to the bottom from 33 ship bound CTD casts. Further 480 samples for helium where taken as profiles from 32 ship bound CTD casts and as bottom samples from 21 helicopter-CTD stations. Additionally 48 samples for oxygen isotopes where taken as bottom samples from 27 ship bound CTD casts and from 21 helicopter-CTD stations. Most station locations are between 68.5°S and 66.5°S and 57°W and 54°W on the continental slope of the Antarctic Peninsular in water depth between 2000 and 900 m. The major aim was to find evidence of the presence of newly formed Antarctic Deep and Bottom Water (high CFC concentrations) and the contribution of Ice Shelf Water (excess helium concentrations). At least 25 snow samples where taken for tritium measurements from various locations, i.e. from the ISPOL floe, from icebergs and the vicinity if the helicopter-CTD stations.

Tapping the samples for CFCs and helium from the niskin bottles was carefully performed without any contact to the atmosphere to prevent contamination with air. The CFC samples are stored in flame sealed glass ampoules with a pure nitrogen head space. The helium samples are stored in gas tight copper tubes, which are squeezed at both ends. The samples for oxygen isotopes and for tritium are stored in wax sealed glass bottles. All samples are shipped back immediately for analysis in the CFC and noble gas lab at the IUP in Bremen. The CFCs (CFC-11 and CFC-12)

are to be measured by gas chromatography. Helium (He, $^3He/^4He$, Ne), tritium and oxygen isotope samples are to be measured by mass spectrometry. First results from these measurements will be available in summer 2005.

5.5 Iceberg drift

Michael Schodlok
Alfred Wegener Institute, Bremerhaven

The calving of icebergs from Antartic ice shelves and their subsequent drift causes a significant transport and input of freshwater from the ice sheet into the upper ocean. Calving events of gigantic icebergs are known to occur infrequently, but drift and life times of these giants can be easily monitored by satellite. However, a large amount of freshwater is transported away from the Antarctic ice sheet through medium- and small-size icebergs with lengths of the order of a couple of kilometers and less. Since 1999, 59 of medium- and small-sized icebergs have been tagged with GPS buoys in the Weddell Sea to monitor their positions and subsequently their drift tracks.

Iceberg length and width normally varied between 100 m and 1500 m, and freeboard heights between 10 m and 70 m, i.e., the iceberg draft ranged from 80 m to about 550 m. Whereas the origin of icebergs tagged in the southwestern Weddell Sea is well-known the calving sites of icebergs tagged in the eastern Weddell Sea and thus their previous drift and melt history is unknown.

Two types of iceberg buoys are used for deployment and are supplied by Denkmanufaktur (Germany). The first typ of buoys is transmitting daily positions (12:00 h) using the ARGOS satellite system and the second typ via IRIDIUM satellite telephone. The position is recorded in both cases with a GPS device where the position is given with an accuracy of less than 15 m.

The choice of deployment sites depend on the predetermined cruise track of RV *Polarstern* as well as on the availability of icebergs. Previous deployments locations included the south western Weddell Sea continental shelf and along Greenwich Meridian. However, as RV *Polarstern* supplies *Neumayer* Station on a regular basis, the majority of buoys were placed on icebergs in the vicinity of Atka Bay. These buoys and future deployments in the areas mentioned enables to determine seasonal and interannual differences in drift patterns of icebergs in the Antarctic Coastal Current region as well as determine and/or validate possible freshwater export scenarios out of the Weddell Sea. Three freshwater export scenarios out of the Weddell Sea were deduced from the existing buoy data set:

a) export to the west of the South Orkney Islands,
b) export to the east of the South Sandwich Islands,
and
c) no iceberg export at all.

During RV *Polarstern* cruises ANT-XX/II 2 and 3 a total of 19 iceberg buoys were available for deployment. To continue the time series within the Coastal Current a

series of buoys was deployed off *Neumayer* Station at leg 3. At leg 2 buoys are deployed en route to the ice floe, during the ice station and possibly heading back towards Cape Town at the tip of the Antarctic Peninsula.

During ISPOL 5 icebergs were tagged in various locations on route to and from the ice floe and during the ice station. Icebergs tagged with buoys during this cruise were of the size between 250 m and 2100 m in length and width and up to 45 m in freeboard height. Figure 5.23 shows the deployment positions and table 5.1 the iceberg deployment specifications.

The first two buoys (ARGOS IDs #8068 and #9728, provided by Denkmanufaktur, Germany) were deployed to the east of the South Sandwich Islands and thus might be either escape into the Antarctic Circumpolar Current and shed light on export scenario b) or stay in the Weddell Sea to contribute to scenario c).

After reaching the ice station one buoy (ID #14957) was deployed approximately 80 nm to the southwest of the ice station on the western continental shelf.

These last two buoys deployed (#9782 and #14957) ceased transmitting data after sending an initial position. Hence, all remaining buoys available for deployment during ANT-XXII/2+3 were tested, placing them in transmission mode on the floe next to RV *Polarstern*. Only 6 buoys proved to be in working order, with nine of the 2004 set of buoys not transmitting data. The reason for this might have been a combination of an empty buffer-battery and false connections to the ARGOS transmitter. However, repair attempts to two of the buoys were only partially successful.

Despite the failure of the new ARGOS buoys, the IRIDIUM (IR 1) buoy deployed to the west in the vicinity of the floe on the continental shelf proved to work very well. IR 1 and the last buoy (ID #3925) deployed at the sea ice edge on the way towards South Georgia contribute towards studies of export scenario a).

Three buoys are transmitting data. Buoy #8068 (Fig. 5.24c) drifted a northerly course before being trapped in an ACC meander for 17 days and changing to a eastwards progression. It covered about 840 km with a mean drift of 13.4 km/day and a maximum displacement of ~29 km/day. These drift values compare well with previous drift buoys in this area.

Buoys IR 1 and #3925 vary considerably although both being released on the western continental shelf. IR 1 (Fig. 5.24a) transmitting data from a more southerly position was surrounded by a sea ice cover of more than 80 %. Its drift of about 7.7 km/day ± 6.4 km/day, which is about 200 km total distance covered, agrees well with observations in this area.

At the beginning two anticyclonic features determine the drift. The second is related to a deep depression moving across the Weddell Sea and is responsible for the southward progression from the second of January to the fifth when the back of the cyclone changed the drift direction towards the north.

The last of the three buoys was deployed on an iceberg at the current sea ice edge. The iceberg showed no snow cover, was of bluish colour on top, showed little erosion although a number of cracks were visible and lacked crevasses and melt ponds. Ice rafted debris was seen on many surrounding growlers and ice floes and thus together with it rather small freeboard of 20 m it is assumed that it originates from Larsen Ice Shelf. The thick snow cover of the majority of icebergs to the south and west of the ice station suggest that they originated from a more southerly location. As the iceberg was drifting in rather low sea ice concentration to no sea ice at all, the mean speed of 20 km/day ± 10 km/day is rather high. It also showed a high maximum displacement of 40 km/day between 12 and 13 January.

It seemed that the iceberg was entering the Bransfield Strait and thus it is highly likely that it left the Weddell Sea between Elephant Island and the South Orkney Islands as can be expected for the time of the year and its location on the continental shelf.

Only after the cruise it will be known whether the iceberg tagged with the IRIDIUM buoy will follow buoy #3925 on its way out of the Weddell Sea or whether it will follow an easterly course, following the Weddell Gyre. The divergence of these two drift routes might be located to the south of Powell Basin (off Joinville Island) and might also be a seasonal feature. Thus, as buoy IR 1 followed buoy #3925 by about 300 km and was slower in speed it might have reached the tip of the Antarctic Peninsula in autumn, beginning of winter (Ice Station Weddell (1992) suggests relatively little northward progress in this area) and followed then a different path.

Table 5.1: Details of iceberg buoy deployments during ISPOL.

No.	ID	Date	Time	Latitude	Longitude	Length (m)	Width (m)	Freeboard (m)
1	8068	15 11 2004	15:15 h	61° 06.41 'S	22° 37.32 'W	2100	1400	45
2	9728	17 11 2004	10:09 h	62° 32.164'S	27° 14.008'W	300	250	40
3	14975	05 12 2004	20:34 h	68° 24.92 'S	58° 44.14 'W	1150	550	45
4	IR 1	23 12 2004	14:37 h	67° 25.839'S	56° 24.205'W	760	240	60
5	3925	05 01 2005	09:31 h	64° 47.34 'S	54° 30.15 'W	1300	1200	20

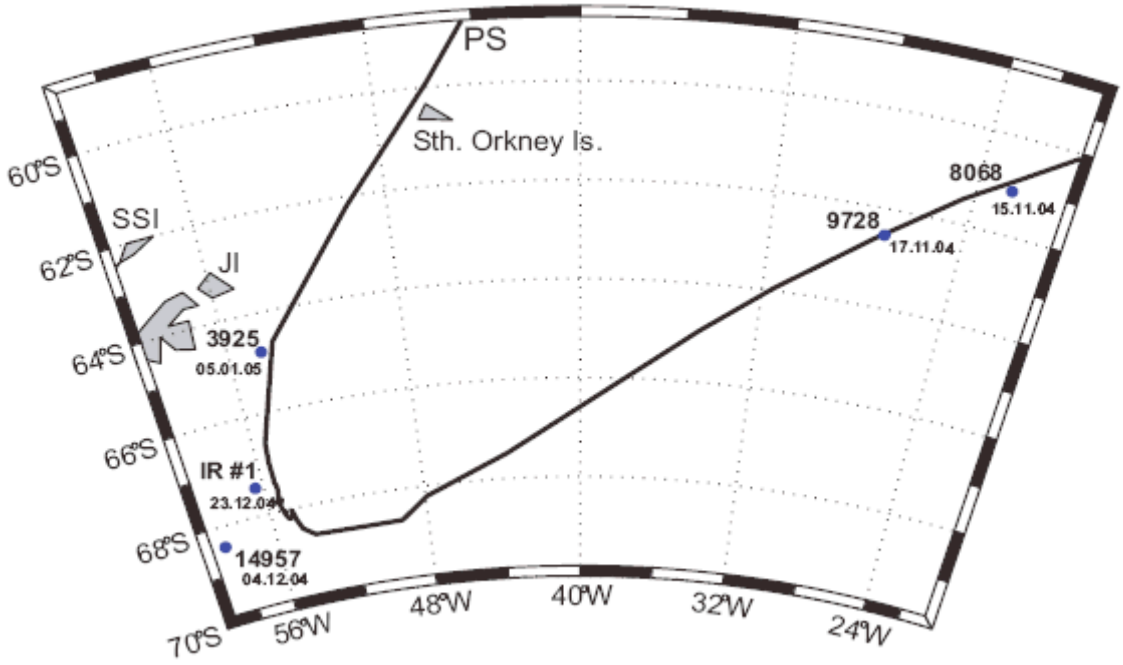

Fig. 5.23: Position and date of iceberg buoy deployments and cruise track of RV Polarstern during ISPOL

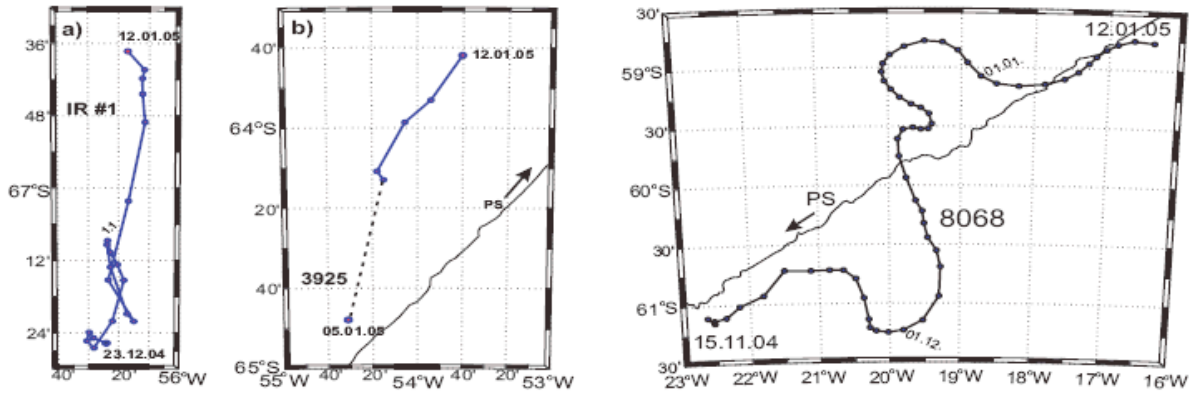

Fig. 5.24: Drift tracks of icebergs tagged with Iridium (a) and ARGOS (b+c) buoys during ISPOL. RV Polarstern cruise track is indicated in b) and c) and the arrow associated to travel direction. The dashed line in b) depicts 3 days without data transmission from buoy 3925.

6. BATHYMETRY

6.1 General sea floor surveying during ISPOL

Andreas Beyer[1)],
Alla Koltsova[2)]

[1)] Alfred Wegener Institute, Bremerhaven
[2)] Vernadsky Institute of Geochemistry and Analytical Chemistry, Moscow, Russia

6.1.1 Introduction

Precise depths measurements are necessary to provide seafloor morphology and structure as basic information for marine sciences. They are used for morphological analyses, modelling of ocean circulations and studies of geological, geophysical and biological processes. Depths data have been recorded during this cruise on the transit of RV *Polarstern* to the final study area. They were processed on board and will be delivered to the International Hydrographic Organization (IHO) later on to improve international nautical and bathymetric charts. In addition to the depths measurements, stratigraphy data has been recorded using a sub-bottom profiling system.

6.1.2 Equipment

6.1.2.1 Multibeam system

The multibeam system Hydrosweep DS-2 installed on board RV *Polarstern* records depths measurements and echo amplitudes of the transmitted acoustic pulse. The amplitudes can be converted into multibeam sidescan and angular backscatter data. The main application of sidescan is to detect small scale features which cannot clearly be recognised in the bathymetry (e. g. shallow channels or iceberg plough marks). Angular backscatter data shows the same resolution as the depths measurements but supplies additional information about physical properties of the seafloor (surface- and volume roughness). Hydrosweep DS-2 operates at 15.5 kHz and transmits sound pulses perpendicular to the ships longitudinal axis. 59 individual beams are determined within the apex angle of 90°. During operation, a width of twice the water depth can be recorded beneath the ship.

The accuracy of the depths measurements is approximately 1 % of the water depth. The refraction of the sonar beams was corrected by automatic cross fan calibration. Regular transmissions of the sonar beams in forward direction are used to determine the current mean sound velocity by comparing nadir depths measurements of the measurement pulse with slant measurements of the calibration pulse. The mean sound velocity is thereafter used to calculate depths from the sound travel times.

6.1.2.2 Sub-bottom profiler

The sub-bottom profiler Parasound transmits two primary frequencies (18 kHz and 22 kHz). They superimpose in the water column and form a narrow beam (4°) of 4 kHz which can penetrate up to 200 m into sediments. The reflection at different sediment layers provides important information about the stratigraphy of the seabed. Potential sediment sampling sites can be determined based on the Parasound data. During this cruise stratigraphy data were recorded by the bathymetry group, since geologists who usually operate the Parasound system did not participate. The main aim was to record data and organize data storage in order to use the opportunity to extend knowledge of an area of rarely available data sets. Data analyses will be carried out at the AWI in conjunction with data recorded during previous cruises.

6.1.3 Bathymetric data

After RV *Polarstern* left the exclusive economic zone of South Africa (200 nm off shore), bathymetry recording and data processing were started on 7 November 2004. The track line and selected areas of significant bathymetric structures are shown in figure 6.1.

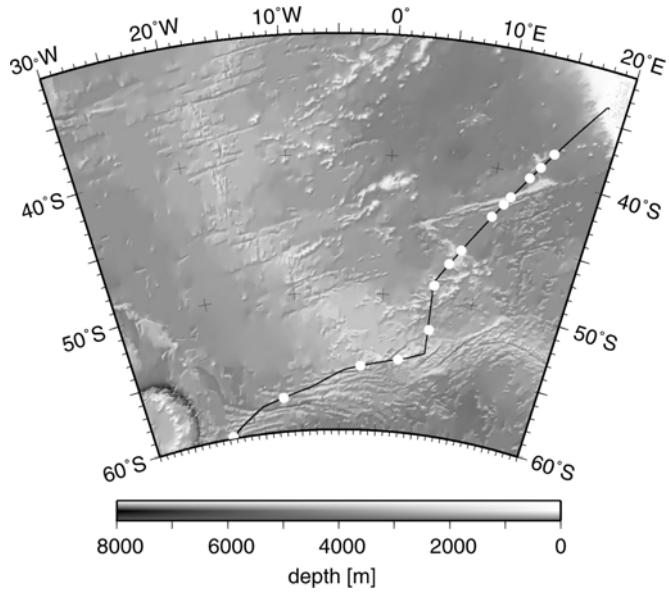

Fig. 6.1: Track line and selected bathymetric structures during the RV Polarstern cruise ANT-XXII/2.

Continuous depths recording was realised within the area shown in figure 6.1. Single track line depths profiles have been recorded that cross various GEBCO sheets (432, 461, 490, 514, 513, 512). This data will be sent to the IHO to improve international nautical charts and correct the terrain models in the area of the covered GEBCO sheets.

At approximately 58°45’ S, 16°45’ W RV *Polarstern* reached the ice edge. Erroneous measurements within ice covered areas were caused by hydroacoustic disturbances and by changing of the ship speed and direction due to ice breaking. Ice conditions required a careful data cleaning to reject incorrect data points from further

processing. The software package CARIS HIPS and SIPS v.5.4 was used for processing.

6.1.4 Results

First on board data processing showed differing seafloor structures in comparison to the existing GEBCO (2003) global data. The individual locations are given in table 6.1 (see also Fig. 6.1). A number of 13 locations have been analysed and bathymetric charts have been generated based on terrain models that combine GEBCO and recent multibeam data. GEBCO contour lines have been adjusted on these maps to obtain a morphological impression of the surveyed areas.

Table 6.1: Locations of significant morphological structures which have been recorded during the recent multibeam survey

Longitude	Latitude	image name	remark
14° 53' E	38° 10' S	dtm_38_10	Seamount
13° 56' E	39° 19' S	dtm_39_19	Seamount
13° 11' E	40° 14' S	dtm_40_14	Seamount
11° 47' E	41° 52' S	dtm_41_52	Agulhas Ridge
10° 20' E	43° 30' S	volcano	Seamount (volcano)
7° 51' E	46° 17' S	dtm_46_17	Ridge
6° 49' E	47° 22' S	dtm_47_22	small ridges
5° 31' E	49° 03' S	dtm_49_03	seamounts
5° 33' E	52° 16' S	dtm_52_16	Ridges
2° 18' E	54° 38' S	dtm_54_38	Ridges
2° 18' W	55° 16' S	dtm_55_16	Mid-Atlantic Ridge
12° 10' W	57° 28' S	dtm_57_28	mounts
19° 30' W	59° 52' S	dtm_59_52	structured ridge

Figure 6.2 shows a seamount that was recorded within the north-west part of the Agulhas Basin at 43°30’ S, 10°20’ E in a water depth of about 4500 m. This mound is differently displayed in the GEBCO data. It has a height of about 1000 m and might be a volcano. The surveyed seamount shows a larger height and a significantly smaller extension (approx. 8 km) than predicted by GEBCO. The colour coded terrain model shows a combination of GEBCO data and recent multibeam surveys. The GEBCO contour lines have been adjusted based on the acquired multibeam data. The southern track line in figure 6.2 was recorded during the cruise ANT-IX/4 (1991) and shows a second seamount that is not displayed in the GEBCO data. The structure of the surrounding seafloor (circular moats) indicates additional seamounts in that area.

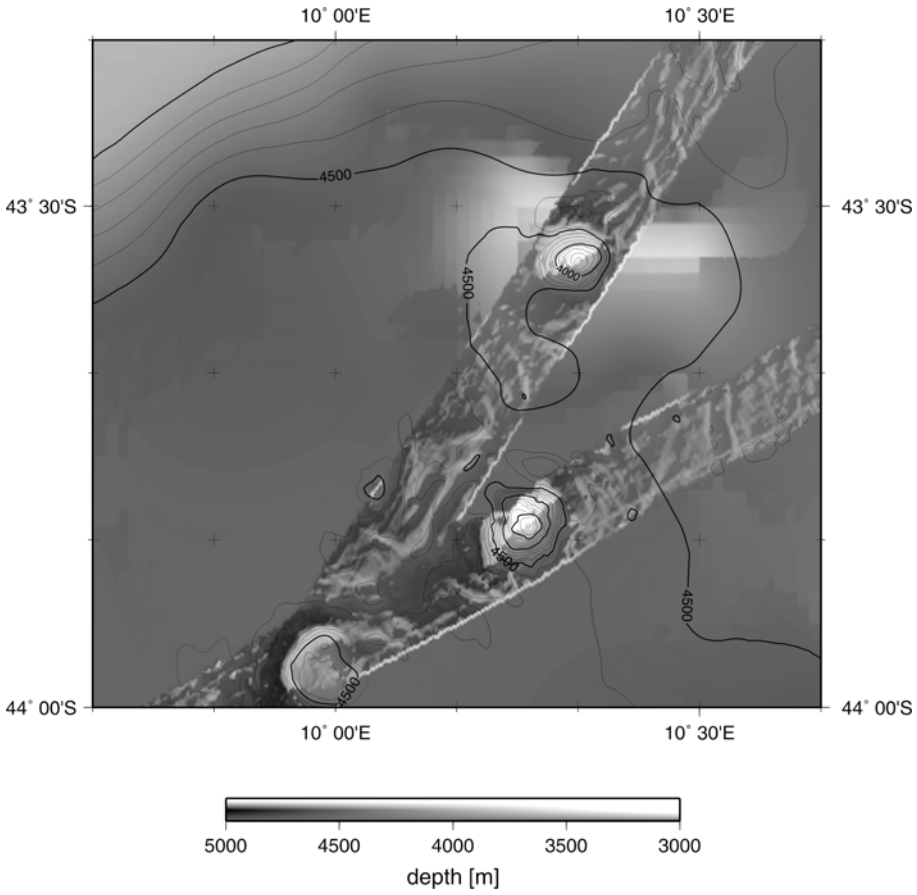

Fig. 6.2: Seamounts in the north-west Agulhas Basin. Size and height are incorrectly displayed in the GEBCO data and have been updated during the recent survey.

Another significant feature was recorded in the area of the America-Antarctic Ridge at about 57°28' S, 12°10' W. It is an elevated plateau structure (about 1000 m above the surroundings) in 3800 m water depth and shows height undulations trending in north-south direction. Wave length and height of the undulations are approximately 1000 m and 100 m, respectively.

Figure 6.3 shows a seamount that is unknown in the GEBCO data. It occurs in a water depth of about 4500 m. This mound has a height of more than 2000 m and a diameter of almost 20 km. Three edges are visible at the slopes of the mound trending in north-east, north-west and southern directions. The displayed terrain model is based on GEBCO and multibeam data. The structure of the mound out side the surveyed area has been modelled based on both, multibeam and GEBCO data.

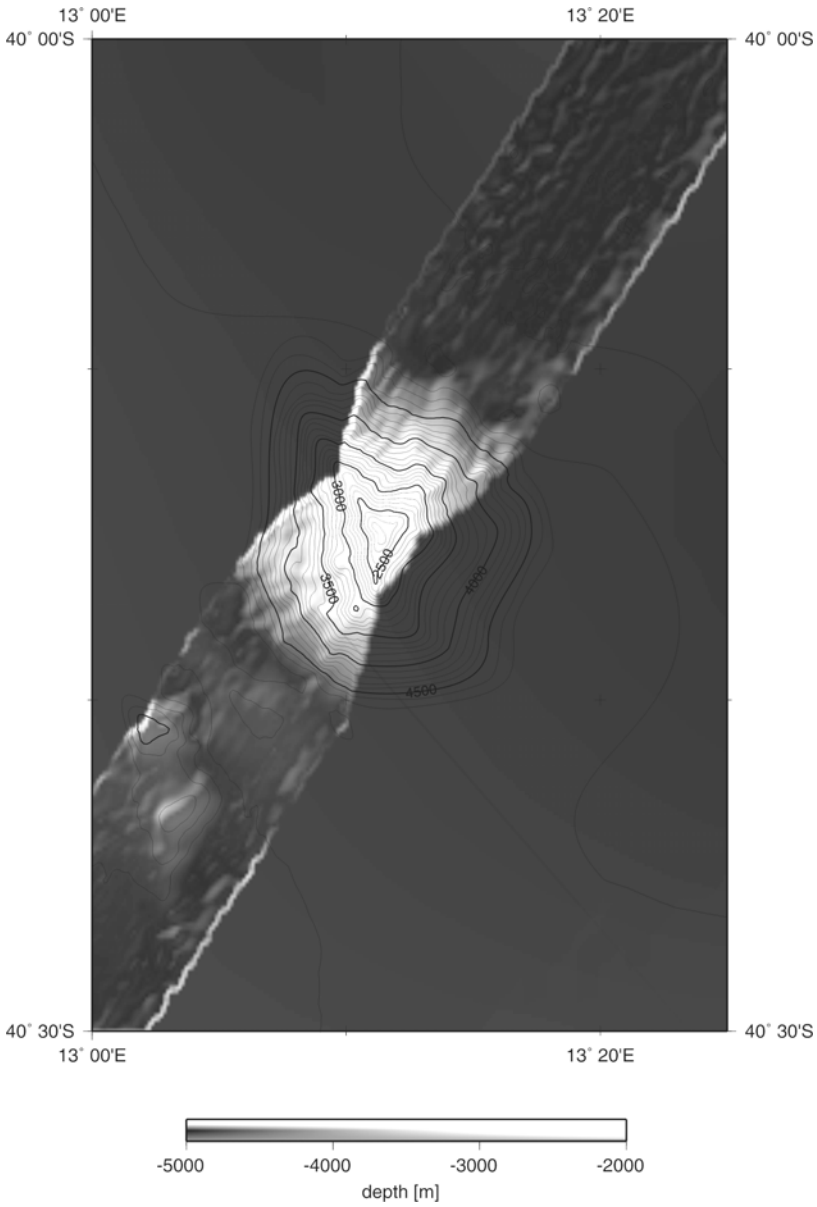

Fig. 6.3: This previously not known seamount shows a height of more than 2000 m .

6.2 Topography and structure of the upper layers of sediments of the ocean floor

Andreas Beyer[1)], Alla Koltsova[2)]

[1)] Alfred Wegener Institute, Bremerhaven
[2)] Vernadsky Institute of Geochemistry and Analytical Chemistry, Moscow, Russia

6.2.1 Approach to the ISPOL drift station

During the approach to the starting point of the ISPOL drift station, RV *Polarstern* reached its most southern position at approximately 68°45' S. This situation reduced the amount of data in the area of the Riser-Larsen ice shelf and Coats Land as previously intended. Due to the ice coverage, multibeam data quality is reduced

because of erroneous measurements during ice breaking. Occasionally complete data loss occurred in heavy ice conditions.

The data are used to study the previously poorly studied area of the probable dissipation of the rifted structure of the eastern part of the Trans-Antarctic Rift. It is possible that the general scheme of a dissipated rifted structure would be similar to the scheme of the rifted structure at the west end of the Trans-Antarctic Rift in the area of the Ross Sea. The recorded data will be combined with existing data at the Vernadsky Institute for further processing and analysing. In order to expand existing bathymetric data sets, depths information was recorded during the approach to the drift station in the area of the Indian-Antarctic mid-oceanic ridge. Morphological studies of the axial zone and its transform faults will also be carried out at the Vernadsky Institute, after the data has been added to the existing data base.

The channel shown in figure 6.4 is situated in the Weddell Sea between the large scale structures San Martin Canyon and the Endurance Canyon. The newly acquired depths data are displayed together with GEBCO data. The recorded part of this channel seems to trend parallel to the slope instead of down slope. Adjacent track lines of previous cruises also show channel structures. Due to the large distance between these track lines, depths data is not sufficient yet to combine these channel pieces to a channel system scheme. In contrast, existing GEBCO data shows no indication of channels in that area. Depths and slope of the seafloor show a significantly larger range of variation compared to the GEBCO data.

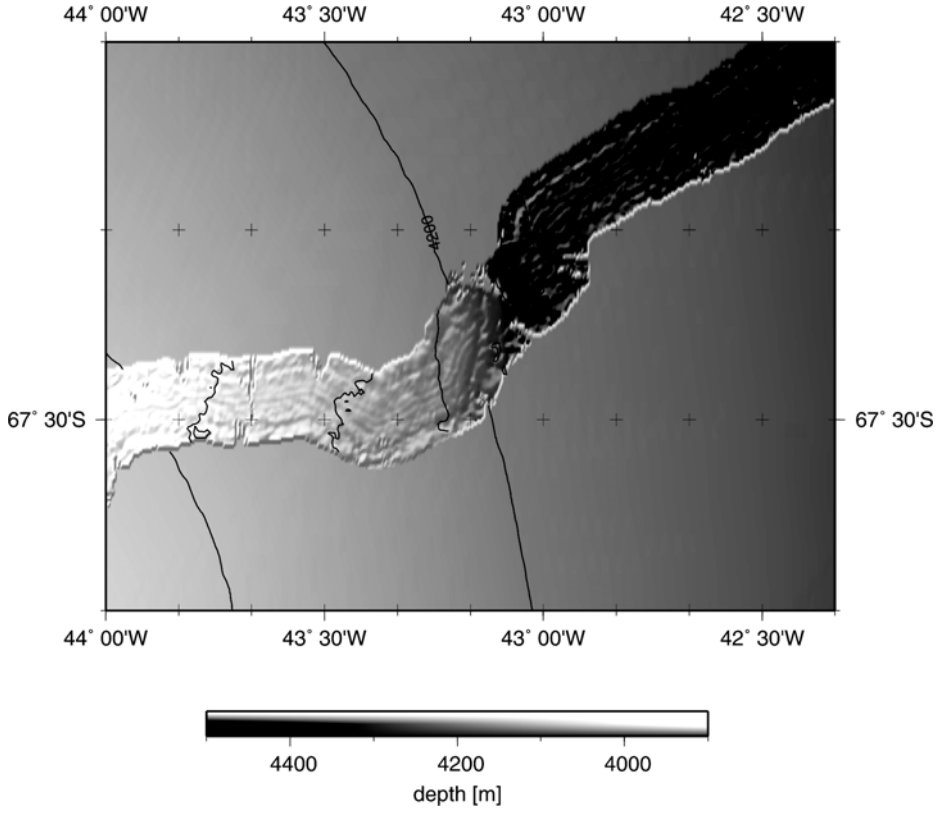

Fig. 6.4: Slope parallel channel structure between the San Martin Canyon and the Endurance Canyon in the Weddell Sea

6.2.2 ISPOL drift station

6.2.2.1 Multibeam data

RV *Polarstern* reached its position at the drifting ISPOL ice floe at 68°13'S, 54°47'W on 27 November 2004. The drift station was left on 2 January 2005 to reach Cape Town safely in time. The drift velocity was in a range between 0 knots and 0.4 knots.

During the drift of RV *Polarstern*, the western part of the Weddell Gyre was examined focusing on the occurrence of submarine channels at the continental slope and their morphology. The chart of the ISPOL drift is shown in figure 6.5. It shows multibeam data of the cruises ANT-XIX/2 (2002) and ANT-XXII/2 (this cruise) together with GEBCO (2003) global data. The existing GEBCO contour lines have been adjusted to the newly acquired data. During the drift, RV *Polarstern* moved mainly towards northern directions, covering a distance of approximately 80 nm and 40 nm in north-south and east-west direction, respectively. Due to variable drift directions, track crossings occurred resulting in a denser covered seafloor area at these locations. Due to the slow drifting in oblique direction with respect to the ships forward direction (the drift direction rarely coincided with the ships forward direction), maximum seafloor coverage was reduced. Drifting and rotation of the floe changed the amount of coverage within hours. Therefore, an optimal adjustment of the position of the ship at the floe could not be realised (drifting in forward direction). However, existing east-west survey lines of the ANT-XIX/2 cruise were successfully connected by the northward drift indicating small scale morphological structures at the continental margin. In the area around 67°30'S, east-west trending small scale ridges have been recorded. Due to the comparatively flat seafloor, the terrain model is affected by track parallel multibeam artefacts which should not be considered as morphological structures. An east-west trending channel like structure around 68°10' S is affected by the multibeam artefacts. However, it is assumed to be a real structure, since it is also visible in depth data of adjacent track lines. Over all, the bathymetry shown in figure 6.5 shows good agreement with GEBCO data in the north-west and south-east part. However, differences up to 100 m have been observed in the north-east (deeper depths) and south-west part (shallower depths), indicating a steeper slope. The recorded large scale morphology corresponds to the GEBCO data.

Recorded small scale structures in the area of study show depths variations of less than 20 m. Due to the measurement accuracy of 1 % of water depth in combination with multibeam artefacts, depths data of these structures are close to the accuracy limit of the multibeam system. Parallel survey lines at slow ship speed (ca. 5 kn) are necessary to improve and expand the recorded data set. However, due to existing ice conditions, it is difficult to realise parallel survey lines.

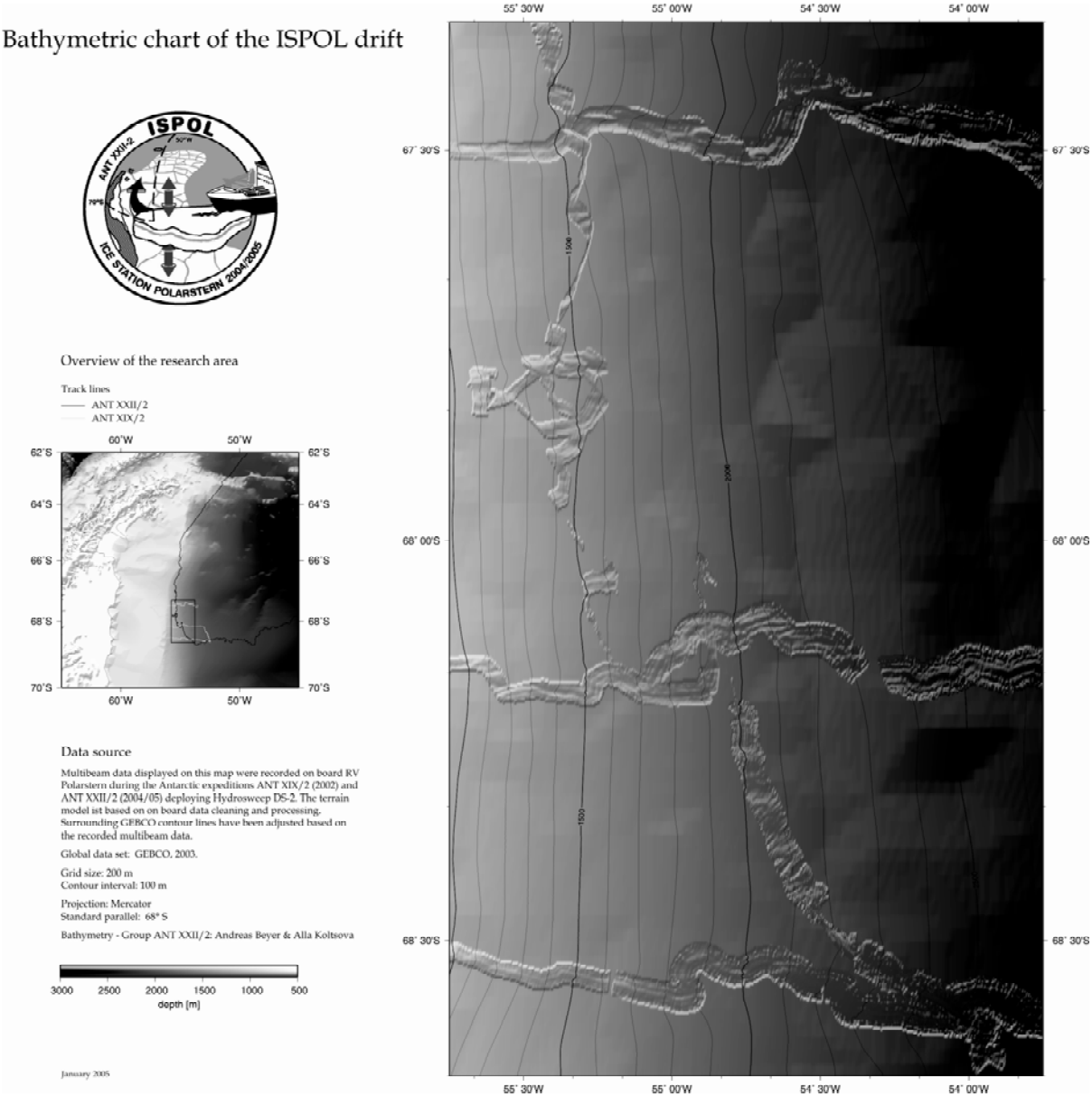

Fig. 6.5: Bathymetric chart of the ISPOL drift

6.2.2.2 Sub-bottom profiler data

The sub-bottom profiling system Parasound was deployed to record stratigraphy information of the seafloor along the ship track. Figure 6.6 shows an overview of the locations, where interesting sub-bottom structures have been recorded. The individual positions are given in table 6.2. These locations include areas of up to 100 m penetration into the seafloor, evenly layered sediments, refilled channel structures and ridges. These locations contribute to the study of processes in the Weddell Sea and adjacent parts of the ocean. They provide position information about locations that are suitable for sampling using gravity cores.

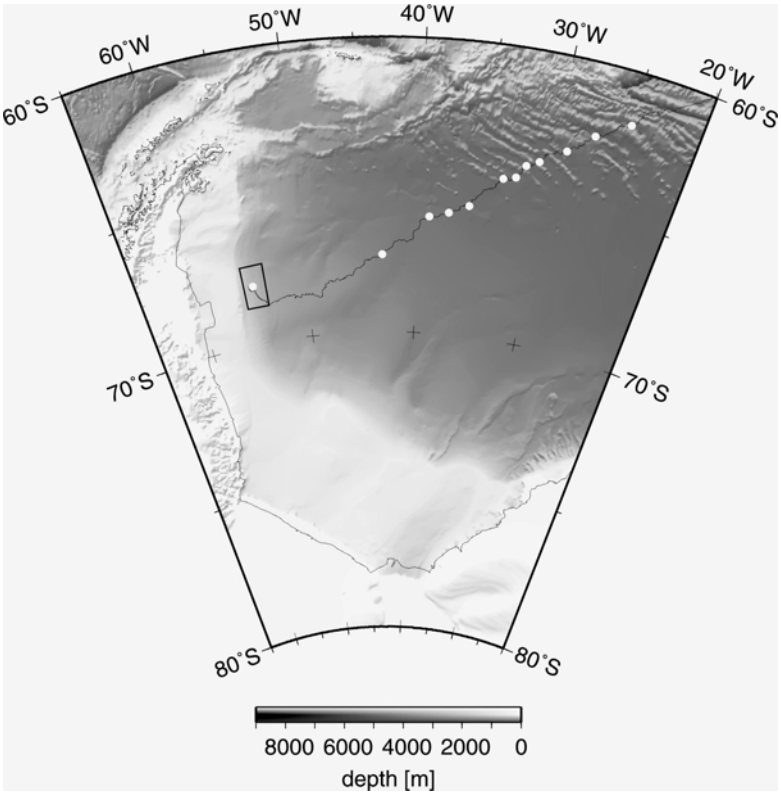

Fig. 6.6: Overview of locations of distinct stratigraphy of the seafloor

Table 6.2: Locations of depicted Parasound profiles indicating layered sediments, refilled channel structures and ridges.

Longitude	Latitude	image name	remark
-24.97502	-61.82610	041116.bmp	refilled channel
-27.27277	-62.50437	041117_1.bmp	ridge
-29.06362	-63.22040	041117_2.bmp	layered sediments
-30.92013	-63.76815	041118_1.bmp	refilled channel
-31.88167	-63.97903	041118_2.bmp	layered sediments
-32.52000	-64.42705	041118_3.bmp	refilled channel
-33.48615	-64.54185	041119_1.bmp	refilled channel
-35.88377	-65.59462	041119_2.bmp	layered sediments
-37.52760	-65.89610	041120_1.bmp	refilled channel
-39.11025	-66.06622	041120_2.bmp	layered sediments
-43.07365	-67.39412	041121.bmp	channel
-54.89711	-68.03773	041129_1.bmp	--
-54.85596	-68.04350	041129_2.bmp	layered sediments
-55.17710	-68.14930	041203.bmp	layered sediments
-55.37494	-67.74083	041228_1.bmp	layered sediments
-55.39944	-67.71695	041228_2.bmp	--
-55.28498	-67.62607	041228_3.bmp	layered sediments
-55.39856	-67.39304	050101.bmp	artefacts
-50.33793	-62.60872	050106_1.bmp	refilled channel
-49.94223	-62.35168	050106_2.bmp	layered sediments

Figure 6.7 shows the Parasound profile of the channel whose bathymetry is given in figure 6.4. Evenly layered sediment extends downslope and upslope of the channel. However, very little penetration is seen at the channel bottom indicating recent activity.

Large areas of the studied continental slope of the Weddell Sea show a hard reflector at the seabed surface with hardly penetration. This indicates that sedimentation is affected by the slope and by currents that transport away loose material.

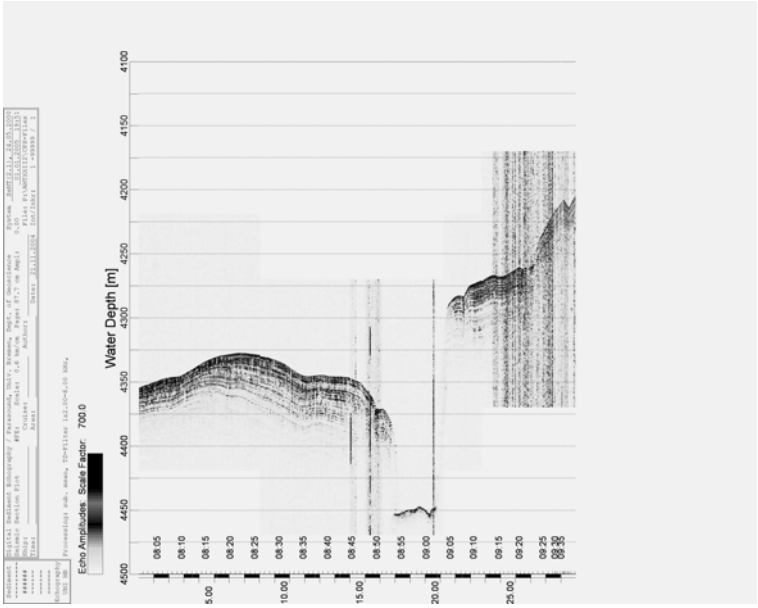

Fig. 6.7: Sediment profile of the channel shown in figure 6.4

APPENDIX

A.1 PARTICIPATING INSTITUTIONS

A.2 PARTICIPANTS

A.3 SHIP's CREW

A.4 ISPOL STATION LIST

A.5 POLARSTERN STATION LIST

A.1 PARTICIPATING INSTITUTIONS

AAD	Australian Antarctic Division Channel Highway Kingston, 7050 Tasmania Australia
ALTERRA	ALTERRA Texel University of Groningen Postbus 167 1790 AD Den Burg (Texel) The Netherlands
AWI	Alfred-Wegener-Institut für Polar- und Meeresforschung in der Helmholtz-Gemeinschaft Postfach 120161 27515 Bremerhaven
DWD	Deutscher Wetterdienst Bernhard-Nocht-Str. 76 20359 Hamburg
ESR	Earth & Space Research 1910 Fairview Ave. E Seattle, WA 9802 USA
Ferra Dynamics	Ferra Dynamics Inc. 4070 Powderhorn Cres Mississauga, ONT Canada
FIMR	Finnish Institute of Marine Research Lyypekinkuja 3 A P.O. Box 33, FIN-00931 Helsinki Finland
FSU	Florida State University Department of Oceanography Tallahassee- FL 32306-4320 USA

HeliTransair	HeliTransair GmbH Am Flugplatz 63329 Egelsbach
IARC	International Arctic Research Center University of Alaska Fairbanks PO Box 757320 Fairbanks, Alaska 99775-7320 USA
IPÖ	Institut für Polarökologie Wischhofstr. 1-3, Geb. 12 24148 Kiel
IUP	Institut für Umweltphysik Universität Bremen Otto-Hahn-Allee 1 28359 Bremen
MPR	McPhee Research Naches, WA98937 USA
Optimare	Optimare Sensorsysteme AG Am Luneort 15a 27572 Bremerhaven
RAS	Vernadsky Institute of Geochemistry and Analytical Chemistry Russian Academy of Sciences 19, Kosygin Street Moscow Russia 119991
SOS	School of Ocean Sciences, University of Wales-Bangor, Menai Bridge, Anglesey LL59 5AB UK
UEA	University of East Anglia Norwich NRW 7TJ U. K.
UG	University of Groningen Dept. of Marine Biology PO Box 14, 9750 AA Haren The Netherlands

ULB	Université Libre de Bruxelles Bvd. Du Triomphe, 1050 – Bruxelles Belgium
UOC	Unite d'Oceanographie Chimique Université de Liège Allee du 6 Aout, 17-BAT B5 4000 Liège Belgium
UTR	Universität Trier FB VI, Fach Klimatologie 54286 Trier
WHOI	Woods Hole Oceanographic Institution, MS 32 Woods Hole, Massachusetts 02543 USA

A.2 CRUISE PARTICIPANTS

Name	Institute
Absy, Joao Marcelo	AWI
Arndt, Ingo	Photographer
Batzke, Anja	AWI
Beyer, Andreas	AWI
Bock, Karl-Heinz	DWD
Brandt, Saskia	AWI
Brauer, Jens	HeliTransair
Büchner, Jürgen	HeliTransair
Buldt, Klaus	DWD
Dacey, John	WHOI
De Jong, Johannes	University Brussels
Delille, Bruno	University Liege
Dieckmann, Gerhard	AWI
Dittmar, Thorsten	University Florida
Eßer, Markus	University Köln
Federovitz, Marcus	HeliTransair
Flores, Hauke	Alterra
Gerdes, Birte	AWI
Haas, Christian	AWI
Hoffman, Carl	AAD
Houghton, Leah	WHOI
Huhn, Oliver	University Bremen
Johansson, Milla	FIMR Helsinki
Kiko, Rainer	IPÖ Kiel
Koch, Boris	AWI
Kolzova, Alla	RAS
Kosloff, Pekka	FIMR Helsinki
Krapp, Rupert	IPÖ Kiel
Krell, Andreas	AWI
Kuosa, Harri	University Helsinki
Lannuzel, Delphine	University Brussels
Launiainen, Jouko	FIMR Helsinki
Lieckfeld, Claus-Peter	Journalist
Lobach, John	Ferra Dynam.
McPhee, Miles	McPhee Res.
Michels, Jan	AWI
Muench, Robin	Earth Space Res.
Nicolaus, Marcel	AWI

Name	Institute
Papadimitrou, Stathys	University Wales
Scheltz, Annette	IPÖ Kiel
Schiel, Sigrid	AWI
Schodlok, Michael	AWI
Schröder, Michael	AWI
Schünemann, Henrike	IPÖ Kiel
Spindler, Michael	IPÖ Kiel
Stefels, Jacqueline	University Groningen
Steffens, Matthias	IPÖ Kiel
Thomas, David Neville	University Wales
Tison, Jean-Louis	University Brussels
Tivy, Adrienne	IARC
Wanke, Carsten	AWI
Will, Jan Martin	HeliTransair
Willmes, Sascha	University Trier
Wisotzki, Andreas	AWI
Witte, Timo	Optimare
Worby, Anthony	Austr. Ant. Div.
Zemmelink, Hendrik	University East Anglia

A.3 SHIP'S CREW

No.	Name	Rank	Nationality
01.	Pahl, Uwe	Master	German
02.	Spielke, Steffen	1.Offc.	German
03.	Schulz, Volker	Ch. Eng.	German
04.	Grimm, Sebastian	2.Offc.	German
05.	Hartung, Rene	3.Offc.	German
06.	Wunderlich, Thomas	Doctor	German
07.	Kapieske, Uwe	R. Offc.	German
08.	Koch, Georg	1. Eng.	German
09.	Erreth Monostori, Gyula	2.Eng.	German
10.	Kotnik, Herbert	2.Eng.	Austrian
11.	Simon, Wolfgang	ELO	German
12.	Holtz, Hartmut	ELO	German
13.	Bohlmann, Harald	ELO	German
14.	Feiertag, Thomas	Elec.	German
15.	Froeb, Martin	ELO	German
16.	Hoffmann, Mathias	Boatsw.	German
17.	Clasen, Burkhard	Carpenter	German
18.	Neisner,Winfried	A.B.	German
19.	Kreis, Reinhard	A.B.	German
20.	Schultz, Ottomar	A.B.	German
21.	Burzan, G.-Ekkehard	A.B.	German
22.	Schröder, Norbert	A.B.	German
23.	Moser, Siegfried	A.B.	German
24.	Pousada Martinez, S.	A.B.	Spanish
25.	Hartwig-Labahn, A.	A.B.	German
26.	Niehusen, Arne	Storek	German
27.	Beth, Detlef	Mot-man	German
28.	Toeltl, Siegfried	Mot-man	German
29.	Fritz, Günter	Mot-man	Austrian
30.	Krösche, Eckard	Mot-man	German
31.	Dinse, Horst	Mot-man	German
32.	Scholl, Christoph	Cook	German
33.	Mueller-Hornburg, R.-D.	Cooksmate	German
34.	Tupy,Mario	Cooksmate	German
35.	Martens, Michael	1.Stwdess	German
36.	Dinse, Petra	2.Stwdess	German
37.	Schöndorfer,Ottilie	2.Steward	German
38.	Streit, Christina	2.Steward	German
39.	Schmidt,Maria	2.Steward	German
40 .	Schmutzler, Gudrun	Laundrym.	German
41.	Tu, Jian Min		Chinese
42.	Wu, Chi Lung		German
43.	Yu, Chung Leung		China

A.4 ISPOL STATION LIST

For ISPOL, a meta data base has been developed allowing all PIs to enter information about their measurements and observations on a daily basis. This was particularly useful for the measurements performed on the ice, which are not included in the normal RV Polarstern station book (Appendix A5). The meta data base is accessible through the ISPOL web site at http://www.ispol.de. The following table is an extract from the data base listing the most important parameters. Data have also been forwarded to the international Global Change Master Directory GCMD

A.4 ISPOL station list

Startdate	Latitude	Longitude	Instruments	Parameters	Site	Station_id	Comment
14.11.2004 12:00	-59,00	-17,63	SHIP-BASED ICE OBSERVATIONS	Floe size//Ice concentration//Ice & snow type and thicknes//Topography	Underway transect	Ship based ice obs	Noon position given.
14.11.2004 15:00	-59,21	-17,99	ICE CORES	Chlorophyll//Meiofauna//Nutrients //Phytoplankton composition//POC/POM//Salinity/ /Stable C/N	Floes on Transect	041114TR11 - 13	conducted in co-operation with Sigi Schiel et al. (AWI), David Thomas et al. (Univ. Wales) and Harri Kuosa (Univ. Helsinki)
14.11.2004 15:00	-59,21	-17,99	SNOW PITS	Temperature//Density//Wetness// Stratigraphy//Thickness profile	Floes on Transect	041114TR	
14.11.2004 15:00	-59,21	-17,99	ICE CORES	Salinity//Texture	Floes on Transect	041114TR01	First station on big level floe, together with IPOE
15.11.2004 12:00	-60,77	-22,27	SHIP-BASED ICE OBSERVATIONS	Floe size//Ice concentration//Ice & snow type and thicknes//Topography	Underway transect	Ship based ice obs	Noon position given.
15.11.2004 12:00	-61,10	-22,62	SNOW PITS	Tritium	Underway transect	xxx	snow sample
15.11.2004 13:00	-60,93	-22,59	ICE CORES	Salinity//Texture	Floes on Transect	041115TR	
15.11.2004 13:00	-60,93	-22,59	SNOW PITS	Temperature//Density//Wetness// Stratigraphy//Thickness profile	Floes on Transect	041115TR	
15.11.2004 15:15	-61,11	-22,62	DRIFTING BUOYS	GPS	Ice properties	--	iceberg buoy, ARGOS ID 8068, size: 2100 m x 1400 m x 45 m;no Ice properties
16.11.2004 8:30	-61,47	-24,38	SNOW PITS	Albedo//Temperature//Density//W etness//Stratigraphy//Thickness profile	Floes on Transect	041116TR	
16.11.2004 8:30	-61,47	-24,38	ICE CORES	Chlorophyll//Meiofauna//Nutrients //Phytoplankton composition//POC/POM//Salinity/ /Stable C/N	Floes on Transect	041116TR11 - 13	conducted in co-operation with Sigi Schiel et al. (AWI), David Thomas et al. (Univ. Wales) and Harri Kuosa (Univ. Helsinki)
16.11.2004 8:30	-61,47	-24,38	ICE CORES	Salinity//Texture	Floes on Transect	041116TR	
16.11.2004 12:00	-61,47	-24,40	SHIP-BASED ICE OBSERVATIONS	Floe size//Ice concentration//Ice & snow type and thicknes//Topography	Underway transect	Ship based ice obs	Noon position given.
17.11.2004 0:00	-62,76	-27,86	SNOW PITS	Albedo//Temperature//Density//W etness//Stratigraphy//Thickness profile	Floes on Transect	041117TR	
17.11.2004 10:10	-62,54	-27,23	DRIFTING BUOYS		--	9728	iceberg buoy, ARGOS ID 9728, size: 300 m x 250 m x 40 m;no ice properties, transmitted only one position
17.11.2004 12:00	-62,65	-27,60	SHIP-BASED ICE OBSERVATIONS	Floe size//Ice concentration//Ice & snow type and thicknes//Topography	Underway transect	Ship based ice obs	Noon position given.
17.11.2004 13:00	-62,76	-27,86	ICE CORES	Salinity//Texture	Floes on Transect	041117TR	
18.11.2004 12:00	-63,95	-31,48	SHIP-BASED ICE OBSERVATIONS	Floe size//Ice concentration//Ice & snow type and thicknes//Topography	Underway transect	Ship based ice obs	Noon position given.

Startdate	Latitude	Longitude	Instruments	Parameters	Site	Station_id	Comment
18.11.2004 13:30	-64,03	-32,05	ICE CORES	Chlorophyll//Meiofauna//Nutrients //Phytoplankton composition//POC/POM//Salinity/ /Stable C/N	Floes on Transect	041118TR11 - 13	conducted in co-operation with Sigi Schiel et al. (AWI), David Thomas et al. (Univ. Wales) and Harri Kuosa (Univ. Helsinki)
18.11.2004 13:30	-64,03	-32,05	ICE CORES	Salinity//Texture	Floes on Transect	041118TR	
18.11.2004 13:30	-64,03	-32,05	SNOW PITS	Albedo//Temperature//Density//Wetness//Stratigraphy//Thickness profile	Floes on Transect	041118TR	
19.11.2004 12:00	-64,93	-34,37	SHIP-BASED ICE OBSERVATIONS	Floe size//Ice concentration//Ice & snow type and thicknes//Topography	Underway transect	Ship based ice obs	Noon position given.
19.11.2004 13:00	-65,06	-35,01	ICE CORES	Salinity//Texture	Floes on Transect	041119TR	
19.11.2004 13:00	-65,06	-35,01	SNOW PITS	Albedo//Temperature//Density//Wetness//Stratigraphy//Thickness profile	Floes on Transect	041119TR	
19.11.2004 22:45	-65,62	-36,34	CTD			PS67 00501	Teststation ;AWI208
19.11.2004 22:50	-65,00	-36,00	WATER BOTTLES	DOC/DON//Nutrients	--	005 01	Only from 1000 m botle
20.11.2004 12:00	-65,62	-36,30	WATER BOTTLES	CFCs	Polarstern	501	test station (all in 1000 m depth)
20.11.2004 12:00	-65,93	-37,67	SHIP-BASED ICE OBSERVATIONS	Floe size//Ice concentration//Ice & snow type and thicknes//Topography	Underway transect	Ship based ice obs	Noon position given.
20.11.2004 12:00	-67,00	-55,00	WATER BOTTLES	d18O//DOC/DON//Nutrients	--	006 92	from 50, 100 & 1391m
20.11.2004 13:00	-66,05	-38,17	SNOW PITS	Albedo//Temperature//Density//Wetness//Stratigraphy//Thickness profile	Floes on Transect	041120TR	
20.11.2004 13:00	-66,05	-38,17	ICE CORES	Salinity//Texture	Floes on Transect	041120TR	
20.11.2004 13:00	-64,05	-38,17	ICE CORES	Chlorophyll//Meiofauna//Nutrients //Phytoplankton composition//POC/POM//Salinity/ /Stable C/N	Floes on Transect	041120TR11 - 13	conducted in co-operation with Sigi Schiel et al. (AWI), David Thomas et al. (Univ. Wales) and Harri Kuosa (Univ. Helsinki)
20.11.2004 16:00	-66,40	-40,00	AEM	Ice thickness//Photography//Ridging	Floes on Transect	041120HEM	60 miles bird flight from ship to 230 deg
20.11.2004 23:00	-65,62	-36,33	WATER BOTTLES	Amino acids//DOC/DON//DOM	Polarstern	PS67/005-1	One depth: 1000 m (He-minimum)
21.11.2004 10:30	-67,47	-43,64	ICE CORES	Salinity//Texture	Floes on Transect	041121TR	
21.11.2004 10:30	-67,47	-43,64	SNOW PITS	Albedo//Temperature//Density//Wetness//Stratigraphy//Thickness profile	Floes on Transect	041121TR	
21.11.2004 12:00	-67,48	-43,60	SHIP-BASED ICE OBSERVATIONS	Floe size//Ice concentration//Ice & snow type and thicknes//Topography	Underway transect	Ship based ice obs	Noon position given.
22.11.2004 12:00	-68,22	-47,83	SHIP-BASED ICE OBSERVATIONS	Floe size//Ice concentration//Ice & snow type and thicknes//Topography	Underway transect	Ship based ice obs	Noon position given.
22.11.2004 12:45	-68,34	-48,52	SNOW PITS	Albedo//Temperature//Density//Wetness//Stratigraphy//Thickness profile	Floes on Transect	041122TR	
22.11.2004 12:45	-68,34	-48,52	ICE CORES	Salinity//Texture	Floes on Transect	041122TR	

Startdate	Latitude	Longitude	Instruments	Parameters	Site	Station_id	Comment
22.11.2004 12:45	-68,34	-48,52	ICE CORES	Chlorophyll//Meiofauna//Nutrients //Phytoplankton composition//POC/POM//Salinity/ /Stable C/N	Floes on Transect	041122TR11 - 13	conducted in co-operation with Sigi Schiel et al. (AWI), David Thomas et al. (Univ. Wales) and Harri Kuosa (Univ. Helsinki)
22.11.2004 16:00	-68,80	-49,50	AEM	Ice thickness//Photography//Ridging	Floes on Transect	041122HEM	60 miles bird flight from ship to 230 deg
23.11.2004 12:00	-68,63	-49,37	SHIP-BASED ICE OBSERVATIONS	Floe size//Ice concentration//Ice & snow type and thicknes//Topography	Underway transect	Ship based ice obs	Noon position given.
23.11.2004 15:50	-68,63	-50,31	SNOW PITS	Albedo//Temperature//Density//Wetness//Stratigraphy//Thickness profile	Floes on Transect	041123TR	
24.11.2004 12:00	-68,63	-51,22	SHIP-BASED ICE OBSERVATIONS	Floe size//Ice concentration//Ice & snow type and thicknes//Topography	Underway transect	Ship based ice obs	Noon position given.
24.11.2004 13:40	-68,20	-50,50	AEM	Ice thickness//Photography//Ridging	Floes on Transect	041124HEM	60 miles bird flight from ship to 50 deg
24.11.2004 16:00	-68,59	-51,67	SNOW PITS	Temperature//Density//Wetness//Stratigraphy//Thickness profile	Floes on Transect	041124TR	
24.11.2004 16:00	-68,59	-51,67	ICE CORES	Texture	Floes on Transect	041124TR	
25.11.2004 12:00	-68,60	-53,97	SHIP-BASED ICE OBSERVATIONS	Floe size//Ice concentration//Ice & snow type and thicknes//Topography	Underway transect	Ship based ice obs	Noon position given.
26.11.2004 12:00	-68,43	-54,55	SHIP-BASED ICE OBSERVATIONS	Floe size//Ice concentration//Ice & snow type and thicknes//Topography	Underway transect	Ship based ice obs	Noon position given.
27.11.2004 9:00	-68,26	-54,76	SNOW PITS	Albedo//Density//Temperature//Stratigraphy//Wetness	Floes on Transect	041127TR	
27.11.2004 18:00	-68,20	-54,80	WATER BOTTLES	CFCs//Helium	Polarstern	602	profile
27.11.2004 18:05	-68,20	-54,79	CTD			602	1. CTD an der Eisscholle
27.11.2004 20:00	-68,00	-55,00	AEM	Ice thickness//Photography//Ridging	--	041127HEMFloeGrid	Bird grid survey of ISPOL floe
28.11.2004 0:00	-68,00	-54,00	WATER BOTTLES	d18O//DOC/DON//Nutrients	--	006 05	from 50, 100 & 1960 m
28.11.2004 0:10	-68,16	-54,80	CTD			603	
28.11.2004 9:15	-68,21	-56,90	DRIFTING BUOYS	GPS	Ice properties	Drifting buoy	FIMR BUOY, ARGOS PTT 1154.
28.11.2004 9:15	-68,00	-55,00	DRIFTING BUOYS		Drifting buoy	1154	52292
28.11.2004 10:30	-68,21	-56,55	DRIFTING BUOYS	GPS	Ice properties	Drifting buoy	IARC BUOY - ARGOS PTT 53539
28.11.2004 10:30	-68,77	-56,04	DRIFTING BUOYS	GPS	Ice properties	Drifting buoy	AAD BUOY, ARGOS PTT 20139
28.11.2004 11:00	-68,21	-56,20	DRIFTING BUOYS	GPS	Ice properties	Drifting buoy	AWI BUOY, ARGOS PTT 8064
28.11.2004 11:00	-68,64	-55,86	DRIFTING BUOYS	GPS	Ice properties	Drifting buoy	AAD BUOY, ARGOS PTT 19021
28.11.2004 11:15	-68,31	-56,75	DRIFTING BUOYS	GPS	Ice properties	Drifting buoy	IARC BUOY, ARGOS PTT 53538
28.11.2004 11:25	-68,31	-56,40	DRIFTING BUOYS	GPS	Ice properties	Drifting buoy	AWI BUOY, ARGOS PTT 9803
28.11.2004 11:30	-68,66	-56,21	DRIFTING BUOYS	GPS	Ice properties	Drifting buoy	AAD BUOY, ARGOS PTT 19020
28.11.2004 12:00	-68,54	-56,42	DRIFTING BUOYS	GPS	Ice properties	Drifting buoy	AAD BUOY, ARGOS PTT 18848
28.11.2004 12:10	-68,43	-56,55	DRIFTING BUOYS	GPS	Ice properties	Drifting buoy	IARC BUOY, ARGOS PTT 53541
28.11.2004 12:30	-68,54	-56,04	DRIFTING BUOYS	GPS	Ice properties	Drifting buoy	AAD BUOY, ARGOS PTT 19228
28.11.2004 13:00	-68,55	-55,67	DRIFTING BUOYS	GPS	Ice properties	Drifting buoy	AAD BUOY, ARGOS PTT 19035

Startdate	Latitude	Longitude	Instruments	Parameters	Site	Station_id	Comment
28.11.2004 14:00	-68,00	-55,00	THICKNESS PROFILES	EM	5&6		EM31 profile from ship across Field 6 and
28.11.2004 15:00	-68,21	-55,16	DRIFTING BUOYS	GPS	Ice properties	Drifting buoy	AAD BUOY, ARGOS PTT 20141
28.11.2004 15:30	-68,42	-56,20	DRIFTING BUOYS	GPS	Ice properties	Drifting buoy	IARC BUOY, NO ARGOS
28.11.2004 15:45	-68,43	-55,47	DRIFTING BUOYS	GPS	Ice properties	Drifting buoy	IARC BUOY, ARGOS PTT 53536
28.11.2004 16:00	-68,43	-55,85	DRIFTING BUOYS	GPS	Ice properties	Drifting buoy	IARC BUOY, NO ARGOS
28.11.2004 16:15	-68,21	-55,87	DRIFTING BUOYS	GPS	Ice properties	Drifting buoy	AWI BUOY, ARGOS PTT 14955
28.11.2004 16:30	-68,37	-55,96	DRIFTING BUOYS	GPS	Ice properties	Drifting buoy	IARC BUOY, NO ARGOS
28.11.2004 17:00	-68,22	-55,47	DRIFTING BUOYS	GPS	Ice properties	Drifting buoy	IARC BUOY, ARGOS PTT 53537
28.11.2004 17:00	-68,00	-54,00	SNOW PITS	Density//Temperature//Thickness profile//Stratigraphy//Wetness	--	041128Snow_P6	
28.11.2004 17:00	-68,37	-56,11	DRIFTING BUOYS		Drifting buoy	Buoy Array Site L	IARC BUOY, NO ARGOS
28.11.2004 17:45	-68,31	-56,05	DRIFTING BUOYS	GPS	Ice properties	Drifting buoy	IARC BUOY, NO ARGOS
28.11.2004 18:00	-68,07	-54,84	CTD			604	
28.11.2004 18:00	-68,07	-54,83	WATER BOTTLES	CFCs//Helium	Polarstern	604	profile
28.11.2004 21:00	-68,00	-55,00	THERMISTOR STICK	Ice temperature	6 Bio coring	041128-LO	setup of continuous logging station with 12 temperature sensors within the ice. Distance between sensors is 7 cm.
28.11.2004 21:00	-68,00	-55,00	RADIOMETER	PAR	6 Bio coring	041128-LO	setup of continuous logging station with irradiance (PAR) sensors above (2pi) and below (4pi) the ice
29.11.2004 0:10	-68,04	-54,85	CTD			605	
29.11.2004 5:40	-68,04	-54,85	CMiPS	-	--	605	Vertical scalar microstructure
29.11.2004 6:05	-68,04	-54,89	CTD			606	
29.11.2004 10:00	-68,00	-55,00	UNDERWATER PUMP	Chlorophyll	6 Bio coring	041129-TS	
29.11.2004 10:00	-68,00	-55,00	SALINOMETER		6 Bio coring	041129-TS	
29.11.2004 10:30	-68,00	-55,00	SNOW PITS	Bacterial stock//Chlorophyll//Nutrients	Phytoplankton composition//Iron	041129BB	
29.11.2004 10:30	-68,00	-55,00	LICOR SOIL GAS CHAMBER	CO2 flux	9 Clean site	041129BB	
29.11.2004 10:30	-68,00	-55,00	UNDERWATER PUMP	Alkalinity/PH//Bacterial stock	9 Clean site	041129BB	
29.11.2004 10:30	-68,00	-55,00	ICE CORES	Bacterial stock	9 Clean site	041129BB	
29.11.2004 10:30	-68,00	-5,00	SACK HOLES	Alkalinity/PH//Bacterial stock	9 Clean site	041129BB	
29.11.2004 11:00	-68,00	-55,00	UNDERWATER PUMP	Zooplankton	6 Bio coring	041129-TS	
29.11.2004 12:00	-68,03	-54,90	WATER BOTTLES	Amino acids//DOC/DON//DOM	Polarstern	PS67/006-7	One depth: 35 m
29.11.2004 12:00	-68,00	-55,00	WATER BOTTLES	d18O//DOC/DON//Nutrients	--	006 07	For 35m only
29.11.2004 12:10	-68,03	-54,90	CMiPS	-	--	607	Vertical scalar microstructure observations
29.11.2004 12:10	-68,03	-54,90	CTD			607	
29.11.2004 12:20	-68,30	-56,50	AEM	Ice thickness//Photography//Ridging	--	041129HHEM	Bird flight 30 miles west and south of ship
29.11.2004 14:00	-68,13	-55,23	HELICOPTER CTD			Helic 001	first test station to 630 m depth
29.11.2004 14:00	-68,00	-55,00	UNDERWATER VIDEO CAMERA & PHOTO		6 Bio coring	041129-TS	

Startdate	Latitude	Longitude	Instruments	Parameters	Site	Station_id	Comment
29.11.2004 14:00	-68,00	-55,00	SLUSH/GAP LAYER SAMPLING	Alkalinity/PH//Chlorophyll//d18O//DOC/DON//Nutrients//Oxygen//Phytoplankton composition//POC/POM//Salinity//Stable C/N	5&6	41129	
29.11.2004 14:30	-68,00	-54,00	SNOW PITS	Density//Temperature//Thickness profile//Stratigraphy//Wetness	--	041129Snow_P5	
29.11.2004 18:05	-68,04	-54,87	CTD			609	
29.11.2004 18:15	-68,04	-54,87	CMiPS	-	--	609	Vertical scalar microstructure observations
29.11.2004 21:00	-68,18	-55,18	AERIAL DIGITAL CAMERA	Ice type	floe size	Flight 3	First flight around edge of buoy array.;Waypoints: Buoy Array site F - A - W - F.;Surface Temp measurements with IR Radiometer.
30.11.2004 0:00	-68,04	-54,86	UNDERWATER TURBULENCE MAST		9 Ocean turbulence	ISPOL	2 clusters u, v, w, T, C, 1 w/microC
30.11.2004 0:00	-68,05	-54,88	CMiPS	-	--	610	Scalar vertical microstructure observations. Accompanying CTD cast was interrupted by computer malfunction.
30.11.2004 0:05	-68,04	-54,86	CTD			610	
30.11.2004 6:00	-68,05	-54,89	CTD			611	
30.11.2004 9:00	-68,00	-54,00	SEDIMENT TRAP		9 Sediment trap	041130 ST	Sediment trap deployed at 9:00 am set to begin at 10:00 am and rotating every 6 days
30.11.2004 10:00	-68,00	-54,00	SEDIMENT TRAP		6 Sediment trap	041130 ST	Sediment trap lowered 10:00 and set to rotate at 11:00. rotation every 6 days
30.11.2004 12:00	-68,00	-55,00	WATER BOTTLES	d18O//DOC/DON//Nutrients	--	006 12	from 20 depths
30.11.2004 12:00	-68,07	-54,90	WATER BOTTLES	Amino acids//DOC/DON//DOM	Polarstern	PS67/006-12	Profile: 20 depths
30.11.2004 12:15	-68,07	-54,90	CMiPS	-	--	612	Vertical scalar microstructure observations
30.11.2004 12:15	-68,07	-54,90	CTD			612	
30.11.2004 14:00	-68,00	-55,00	ICE CORES	Species experiments	6 Bio coring	041130-ZO	sampling of 30 ice cores (bottom 5 cm segments) for experimental studies
30.11.2004 14:45	-68,31	-55,78	DRIFTING BUOYS	GPS	Ice properties	Drifting buoy	IARC BUOY, NO ARGOS
30.11.2004 15:30	-67,32	-56,01	DRIFTING BUOYS	GPS	Ice properties	Drifting buoy	FIMR BUOY, ARGOS PTT 5892
30.11.2004 18:00	-68,12	-54,87	WATER BOTTLES	CFCs//d18O//Helium	Polarstern	613	profile
30.11.2004 18:05	-68,11	-54,87	CTD			613	
30.11.2004 20:30	-68,00	-55,00	SONIC ANEMOMETERS	Momentum	sensible heat flux	latent heat flux	Sonic anemometer (Metek)
30.11.2004 23:55	-68,15	-54,86	CMiPS	-	--	614	Vertical scalar microstructure observations
01.12.2004 0:00	-68,15	-54,86	CTD			614	
01.12.2004 6:05	-68,17	-54,87	CTD			615	
01.12.2004 8:40	-68,17	-54,88	MULTINET		Polarstern	PS67/006-16	mesh size 100 µm;;net 1: 1000 - 500 m;net 2: 500 - 200 m;net 3: 200 - 100 m;net 4: 100 - 50 m;net 5: 50 - 0 m;;for formalin fixed zooplankton samples
01.12.2004 10:00	-68,00	-55,00	ICE CORES	Species experiments	6 Bio coring	041201-Zo	10 cores taken, bottom 5 cm melted to isolate species for experimental studies

Startdate	Latitude	Longitude	Instruments	Parameters	Site	Station_id	Comment
01.12.2004 11:40	-68,17	-54,89	MULTINET		Polarstern	PS67/006-17	mesh size 100 µm;;net 1: 1800 - 1700 m;net 2: 1700 - 1500 m;net 3: 1500 - 1000 m;net 4: 1000 - 700 m;net 5: 700 - 500 m;net 6: 500 - 200 m;net 7: 200 - 100 m;net 8: 100 - 50 m;net 9: 50 - 0 m;;for ethanol fixed zooplankton samples
01.12.2004 13:00	-68,17	-54,88	WATER BOTTLES	Amino acids//DOC/DON//DOM	Polarstern	PS67/006-18	Profile: 3 depths
01.12.2004 13:05	-68,17	-54,89	CTD			618	
01.12.2004 13:05	-68,17	-54,89	CMiPS	-	--	618	Vertical scalar microstructure profile
01.12.2004 14:00	-68,00	-55,00	THICKNESS PROFILES	EM		9	EM31 profile from ship across fields 9 and 10
01.12.2004 15:00	-68,00	-55,00	UNDERICE NET	Krill//Icefauna	6 Diving site	Divehole-hand-net01	sampled under-ice amphipods with diver hand-net around the ice hole for MAA analysis, general pigment composition and taxonomy
01.12.2004 15:00	-68,00	-55,00	THICKNESS PROFILES	DRILLING		--	Deployment of thickness gauges on several places over the floe
01.12.2004 15:00	-68,00	-55,00	SACK HOLES	Alkalinity/PH//Chlorophyll//d18O//DOC/DON//Nutrients//Oxygen//POC/POM//Salinity//Stable C/N isotopes//Temperature	9 Sediment trap	41201	
01.12.2004 17:00	-68,03	-55,20	UNDERWATER TURBULENCE MAST	-	Ocean heat flux array	ISPOL	Dec 1: main ocean turbulence mast deployed at site 300 m west of ship in 2 m ice, 70 cm snow. The mast measures:;6 m depth (4 m from ice): T, C, microC, u, v w;10 m: T, C, u, v, w;9.5 m downward looking 600 kHz acoustic doppler current profiler; upward looking 1.2 Mhz ADCP;;;Dec 6 install 500 kHz ADCP 2 m below ice;Install ADV no 3 at 1 m below ice;;Dec 8;replaced upper (4m) ADV on the main mast to test suspect readings. The problem appears to be in the SBE A/D circuits. Workaround installed tomorrow
01.12.2004 18:00	-68,00	-55,00	ICE CORES	Species experiments	6 Bio coring	041201-ZO	sampling of 30 ice cores (bottom 5 cm segments) for experimental studies
01.12.2004 18:10	-68,18	-54,89	CTD			619	
01.12.2004 20:00	-68,00	-55,00	SNOW PITS		7 Eppley radiation station	snow density&snow elevation	
01.12.2004 20:00	-68,18	-54,90	SNOW PITS	Tritium	6 Floe edge	xxx	snow sample
01.12.2004 23:55	-68,19	-54,92	CMiPS	-	--	620	Vertical scalar microstructure profile
02.12.2004 0:00	-68,19	-54,91	CTD			620	

Startdate	Latitude	Longitude	Instruments	Parameters	Site	Station_id	Comment
02.12.2004 0:00	-68,19	-54,19	UNDERWATER TURBULENCE MAST		Ocean heat flux array	ispol	2 clusters u, v, w, T, C, microC
02.12.2004 0:00	-67,00	-55,00	SLUSH/GAP LAYER SAMPLING	DOC/DON//Amino acids//DOM	9	Brine Pool1	
02.12.2004 0:00	-67,00	-55,00	UNDERWATER PUMP	Amino acids//DOC/DON//DOM	9	UIW1	Under ice water, pumped through a core hole
02.12.2004 6:25	-68,19	-55,01	CTD			621	
02.12.2004 10:00	-68,00	-55,00	SACK HOLES	Alkalinity/PH//Chlorophyll//d18O//DOC/DON//Nutrients//Oxygen//Phytoplankton composition//POC/POM//Salinity//Stable C/N	9 Sediment trap	41202	
02.12.2004 10:30	-68,00	-55,00	LICOR SOIL GAS CHAMBER	CO2 flux	9 pCO2 site	041202BCO2	
02.12.2004 10:30	-68,00	-55,00	ICE CORES	Gas composition (O2	9 pCO2 site	041202BCO2	
02.12.2004 13:50	-68,00	-54,00	SNOW PITS	Density//Temperature//Thickness profile//Wetness	--	41202	
03.12.2004 0:00	-68,08	-55,29	UNDERWATER TURBULENCE MAST	-	9 Ocean turbulence	ispol	2 clusters u, v, w, T, C, microC, 1.2 Mhz, 0.6 Mhz ADCP
03.12.2004 8:00	-68,00	-55,00	SNOW PITS	Density//Temperature//Wetness	--	041203Snow	Diurnal study at patches 6 and 8
03.12.2004 13:00	-68,13	-55,23	HELICOPTER CTD			Helic 002	
03.12.2004 14:00	-68,00	-55,00	ICE CORES	Species experiments	6 Bio coring	041203-ZO	sampling of 60 ice cores (bottom 5 cm segments) for experimental studies
03.12.2004 16:00	-68,00	-55,00	OPTODES		9 Sediment trap	041203 OP	
04.12.2004 8:00	-68,00	-55,00	SNOW PITS	Temperature//Wetness	--	041204Snow	Diurnal study at patches 6 and 8
04.12.2004 8:05	-68,11	-55,24	CTD			622	
04.12.2004 8:05	-68,12	-55,24	CMiPS	-	--	622	Vertical scalar microstructure profile
04.12.2004 9:00	-68,00	-55,00	ICE CORES	d18O//Salinity//Texture	6 Bio coring	041204TS11	
04.12.2004 9:00	-68,00	-55,00	ICE CORES	Chlorophyll//DMS/DMSP//H2O2//HPLC pigments//Meiofauna//Nutrients//Phytoplankton composition//POC/POM//Salinity//Stable C/N isotopes//Temperature//Texture	6 Bio coring	041204-TS	
04.12.2004 10:00	-68,00	-55,00	ICE CORES	Chlorophyll//Nutrients//Salinity//Temperature	9 Optodes	041204 OP	
04.12.2004 10:00	-68,00	-55,00	UNDERWATER PUMP	Chlorophyll	6 Bio coring	41204	
04.12.2004 10:00	-68,00	-55,00	SALINOMETER		6 Bio coring	041204-TS	
04.12.2004 10:15	-68,00	-55,00	LICOR SOIL GAS CHAMBER	CO2 flux	9 Clean site	041204BB	
04.12.2004 10:15	-68,00	-55,00	SACK HOLES	Alkalinity/PH//Bacterial stock	9 Clean site	041204BB	
04.12.2004 10:15	-68,00	-55,00	ICE CORES	Bacterial stock	9 Clean site	041204BB	
04.12.2004 10:15	-68,00	-55,00	UNDERWATER PUMP	Alkalinity/PH//Bacterial stock	9 Clean site	041204BB	
04.12.2004 10:15	-68,00	-55,00	SNOW PITS	Chlorophyll//Nutrients	Phytoplankton composition//Iron	041204BB	

Startdate	Latitude	Longitude	Instruments	Parameters	Site	Station_id	Comment
04.12.2004 11:00	-68,00	-55,00	UNDERWATER VIDEO CAMERA & PHOTO		6 Bio coring	41204	
04.12.2004 12:00	-68,12	-55,25	CMiPS	-	--	623	Vertical scalar microstructure profile
04.12.2004 12:00	-68,00	-55,00	WATER BOTTLES	d18O//DOC/DON//Nutrients	--	006 23	from 50, 100 & 1516m
04.12.2004 12:05	-68,12	-55,25	CTD			623	
04.12.2004 13:00	-68,13	-55,23	DC IN-SITU ICE CONDUCTIVITY METER	Sea ice conductivity structure		9 Worby DC 1	
04.12.2004 13:45	-68,12	-55,25	MULTINET		Polarstern	PS67/006-24	mesh size 55 µm;;net 1: 100 - 50 m;net 2: 50 - 0 m;;for stable isotope samples
04.12.2004 14:00	-68,00	-55,00	UNDERWATER PUMP	Zooplankton	6 Bio coring	041204-TS	
04.12.2004 15:00	-68,13	-55,23	DC IN-SITU ICE CONDUCTIVITY METER	Sea ice conductivity structure		8 Worby DC 2	DC measurements made near Haas 50 m snow line aft of ship.
04.12.2004 18:00	-68,13	-55,23	WATER BOTTLES	CFCs//d18O//Helium	Polarstern	625	profile
04.12.2004 18:05	-68,13	-55,24	CTD			625	
05.12.2004 8:00	-68,00	-55,00	SNOW PITS	Temperature//Wetness	--	41205	Diurnal study at patches 6 and 8
05.12.2004 10:00	-68,00	-55,00	SACK HOLES	Alkalinity/PH//Chlorophyll//d18O//DOC/DON//Nutrients//Oxygen//Phytoplankton composition//POC/POM//Salinity//Stable C/N	9 Sediment trap	51204	
05.12.2004 10:35	-68,11	-55,26	CMiPS	-	--	626	Vertical scalar microstructure profile
05.12.2004 10:40	-68,11	-55,26	CTD			626	
05.12.2004 11:55	-68,11	-55,26	CTD			627	
05.12.2004 15:00	-68,00	-55,00	THERMISTOR STICK	Ice temperature	6 Bio coring	041205-LO	new setup of continuous logging station with 12 temperature sensors within the ice (dataloggers & sensors had to be recovered from the previous location since the floe cracked at that site). Upon installation, ice thickness was at approx. 90 cm and snow thickness at approx. 27 cm. Distance between sensors is 7 cm.
05.12.2004 15:00	-68,00	-55,00	RADIOMETER	PAR	6 Bio coring	041205-LO	new setup of continuous logging station with irradiance (PAR) sensors above (2pi) and below (4pi) the ice (dataloggers & sensors had to be recovered from the previous location since the floe cracked at that site). Upon installation, ice thickness was at approx. 90 cm and snow thickness at approx. 27 cm.
05.12.2004 20:35	-68,42	-58,74	DRIFTING BUOYS	GPS	Ice properties	--	iceberg buoy, ARGOS ID 14957, size: 1150 m x 550 m x 45 m, ;transmitted only one position
06.12.2004 6:05	-68,11	-55,25	CTD			629	

Startdate	Latitude	Longitude	Instruments	Parameters	Site	Station_id	Comment
06.12.2004 8:00	-68,00	-55,00	SNOW PITS	Temperature//Wetness	--	041206Snow	Dirunal study at patches 6 and 8
06.12.2004 11:20	-68,09	-57,47	HELICOPTER CTD			Helic 003	
06.12.2004 12:00	-68,10	-55,26	CTD			630	
06.12.2004 12:00	-68,00	-55,00	SNOW PITS	Iron	Iron isotopes	9 Clean site	AWI-ANTXXII-2-ISPOL-P000015
06.12.2004 12:00	-68,10	-55,26	CMiPS	-	--	630	Vertical scalar microstructure profile
06.12.2004 12:00	-68,00	-55,00	WATER BOTTLES	d18O//DOC/DON//Nutrients	--	006 030	from 50, 100 & 1490m
06.12.2004 12:25	-69,09	-57,00	WATER BOTTLES	d18O//Helium	--	xxx	Heli-CTD (bottom sample)
06.12.2004 12:25	-68,09	-57,47	SNOW PITS	Tritium	--	xxx	Heli-CTD (snow sample)
06.12.2004 13:55	-68,10	-55,27	MULTINET		Polarstern	PS67/006-31	mesh size 100 µm;;net 1: 1000 - 500 m;net 2: 500 - 200 m;net 3: 200 - 100 m;net 4: 100 - 50 m;net 5: 50 - 0 m;;for formalin fixed zooplankton samples
06.12.2004 14:00	-68,00	-55,00	ICE CORES	Chlorophyll//d18O//Salinity//Temperature//Texture	8	041206TEX11	Ice core at snow sampling site
06.12.2004 14:00	-67,00	-55,00	EXPERIMENTS	Amino acids//DOC/DON//Amino acids//DOM	9 Besides Polarstern	Photodegradation Experiment 1	Photodegradation experiment #1 (unfiltered brine from station 9, incubated on snow surface);Collaborative experiment;additional paramenters:;David Thomas / Stathis Papadimitriou: nutrients, CDOM, oxygen, alkalinity;Harri Kuosa: species composition;Birte Gerdes: bacterial activity;Andreas Krell: H2O2;Jaqueline Stefels: DMS;Rupert
06.12.2004 15:00	-68,00	-55,00	RADIOMETER	PAR//Spectral radiation//UV radiation	8 Scott tent	Photodegradation-run01	RAMSES spectroradiometer together with 2pi- and 4pi- LICOR quantum sensors operated continuously out of Scott tent, monitoring spectral irradiance and quantum flow at photodegradation experiment site in 5min. intervals
06.12.2004 18:00	-68,10	-55,26	CTD			632	
06.12.2004 18:00	-68,10	-55,27	WATER BOTTLES	CFCs//d18O//Helium	Polarstern	632	profile
06.12.2004 23:55	-68,10	-55,26	CMiPS	-	--	633	Vertical scalar microstructure profile
06.12.2004 23:55	-68,10	-55,25	CTD			633	
07.12.2004 5:55	-68,09	-55,27	CTD			634	
07.12.2004 8:00	-68,00	-55,00	SNOW PITS	Temperature//Wetness	--	041207Snow	Diurnal study at patches 6 and 8
07.12.2004 10:00	-68,00	-55,00	ICE CORES	Species experiments	6 Bio coring	41207	30 cores taken, bottom 5 cm melted to isolate species for experimental studies
07.12.2004 12:00	-68,09	-55,29	CMiPS	-	--	635	Vertical scalar microstructure profile
07.12.2004 12:00	-68,09	-55,29	CTD			635	
07.12.2004 16:00	-68,23	-55,57	SAR RADAR REFLECTOR		Drifting buoy	Site F	Deployed radar reflector.
07.12.2004 18:00	-68,08	-55,29	CTD			638	
07.12.2004 18:00	-68,08	-55,28	WATER BOTTLES	CFCs//d18O//Helium	Polarstern	638	profile
08.12.2004 0:00	-68,08	-55,29	CMiPS	-	--	639	Vertical scalar microstructure profile.

Startdate	Latitude	Longitude	Instruments	Parameters	Site	Station_id	Comment
08.12.2004 0:00	-67,80	-55,64	UNDERWATER TURBULENCE MAST		9 Ocean turbulence	ispol	3 clusters u, v, w, T, C;3 ADCPS 0.5, 0.6, 1.2 MHz
08.12.2004 0:05	-68,08	-55,29	CTD			639	
08.12.2004 6:00	-68,07	-55,30	CTD			640	
08.12.2004 9:00	-68,00	-55,00	SACK HOLES	CO2	9 pCO2 site	041208BCO2	
08.12.2004 9:00	-68,00	-55,00	ICE CORES	Temperature	9 pCO2 site	041208BCO2	
08.12.2004 9:00	-68,00	-55,00	LICOR SOIL GAS CHAMBER	CO2 flux	9 pCO2 site	041208BCO2	
08.12.2004 10:00	-68,00	-55,00	SACK HOLES	Alkalinity/PH//Chlorophyll//d18O//DOC/DON//Nutrients//Oxygen//Phytoplankton composition//POC/POM//Salinity//Stable C/N		9 41208	In conjunction with Belgian Team measurements
08.12.2004 12:00	-68,06	-55,29	CTD			641	
08.12.2004 12:00	-68,00	-55,00	WATER BOTTLES	d18O//DOC/DON//Nutrients	--	006 41	from 50, 100 & 1473m
08.12.2004 12:05	-68,06	-55,29	CMiPS	-	--	641	Vertical scalar microstructure profile.
08.12.2004 13:20	-68,06	-55,29	MULTINET		Polarstern	PS67/006-42	mesh size 55 µm;;net 1: 100 - 50 m;net 2: 50 - 0 m;;for stable isotope samples
08.12.2004 14:20	-68,06	-55,52	HELICOPTER CTD			Helic 004	
08.12.2004 14:25	-68,06	-55,51	SNOW PITS	Tritium	--	xxx	Heli-CTD (snow sample)
08.12.2004 14:25	-68,06	-55,51	WATER BOTTLES	Helium	--	xxx	Heli-CTD (bottom sample)
08.12.2004 17:00	-68,00	-55,00	SNOW PITS	Temperature//Tritium	--	041208Snow	1 snow pit at sites 6 and 8
08.12.2004 18:00	-68,05	-55,28	WATER BOTTLES	CFCs//d18O//Helium	Polarstern	643	profile
08.12.2004 18:00	-68,05	-55,28	CTD			643	
08.12.2004 19:00	-68,20	-55,55	AERIAL DIGITAL CAMERA	Ice type	floe size	Flight 4	Low cloud caused problems on this flight.
09.12.2004 0:00	-67,30	-56,30	SNOW PITS	Albedo//Density//Stratigraphy//Temperature//Thickness profile//Wetness	--	041209HeloSnow	Station at FIMR buoy 5892
09.12.2004 0:05	-68,05	-55,24	CMiPS	-	--	644	Vertical scalar microstructure profile.
09.12.2004 0:05	-68,05	-55,24	CTD			644	
09.12.2004 6:00	-68,05	-55,22	CTD			645	
09.12.2004 7:45	-68,05	-55,21	MULTINET		Polarstern	PS67/006-46	mesh size 100 µm;;net 1: 1000 - 500 m;net 2: 500 - 200 m;net 3: 200 - 93 m;net 4: 93 - 50 m;net 5: 50 - 0 m;;for formalin fixed zooplankton samples
09.12.2004 9:00	-68,60	-56,50	AEM	DGPS//Ice thickness//Photography//Ridging	--	041209BuoyTriangle	Flight along margin of buoy triangle. Had to be abandoned due to low fuel.
09.12.2004 9:30	-68,00	-55,00	ICE CORES	Chlorophyll//DMS/DMSP//H2O2//HPLC pigments//Meiofauna//Nutrients//Phytoplankton composition//POC/POM//Salinity//Stable C/N isotopes//Temperature//Texture	6 Bio coring	041209-TS	conducted in co-operation with the groups of Gerhard Dieckmann et al. (AWI), Christian Haas et al. (AWI), Harri Kuosa (Univ. Helsinki), Sigi Schiel et al. (AWI), Jacqueline Stefels (Univ. Groningen) and David Thomas et al. (Univ. Wales)

Startdate	Latitude	Longitude	Instruments	Parameters	Site	Station_id	Comment
09.12.2004 9:45	-68,00	-55,00	INCUBATOR	Bacterial activity//Bacterial stock	9 Clean site	041209BB	Iron isotopes//Microbial community /Nutrients//Phytoplankton//Phytoplankton composition /Phytoplankton viability//POC/POM
09.12.2004 10:00	-68,00	-55,00	LICOR SOIL GAS CHAMBER	CO2 flux	9 Clean site	041209BB	
09.12.2004 10:00	-68,00	-55,00	SACK HOLES	Alkalinity/PH//Bacterial stock	9 Clean site	041209BB	
09.12.2004 10:00	-68,00	-55,00	ICE CORES	Bacterial stock	9 Clean site	041209BB	
09.12.2004 10:00	-68,00	-55,00	SNOW PITS	Bacterial stock//Chlorophyll//Nutrients	Phytoplankton composition//Iron	Iron isotopes//Salinity// Temperature	041209BB
09.12.2004 10:00	-68,00	-55,00	UNDERWATER PUMP	Alkalinity/PH//Bacterial stock	9 Clean site	041209BB	
09.12.2004 10:00	-68,00	-55,00	SALINOMETER	Water salinity / temperature	6 Bio coring	041209-TS	
09.12.2004 10:00	-68,00	-55,00	UNDERWATER PUMP	Chlorophyll	6 Bio coring	41209	
09.12.2004 12:00	-68,03	-55,20	WATER BOTTLES	Amino acids//DOC/DON//DOM	Polarstern	PS67/006-47	One depth: 1590 m
09.12.2004 12:00	-68,00	-45,00	WATER BOTTLES	d18O//DOC/DON//Nutrients	--	006 47	only from 1590m
09.12.2004 12:00	-68,04	-55,19	CMiPS	-	--	647	Vertical scalar microstructure profile.
09.12.2004 12:00	-68,04	-55,19	CTD			647	
09.12.2004 13:00	-68,00	-55,00	UNDERWATER VIDEO CAMERA & PHOTO		6 Bio coring	041209-TS	
09.12.2004 13:00	-68,19	-55,49	AERIAL DIGITAL CAMERA	Ice type	floe size	Flight 5	
09.12.2004 13:10	-68,09	-55,72	HELICOPTER CTD			Helic 005	
09.12.2004 13:15	-68,09	-55,70	WATER BOTTLES	d18O//Helium	--	xxx	Heli-CTD (bottom sample)
09.12.2004 13:15	-68,09	-55,70	SNOW PITS	Tritium	--	xxx	Heli-CTD (snow sample)
09.12.2004 14:00	-68,00	-55,00	UNDERWATER PUMP	Zooplankton	6 Bio coring	41209	
09.12.2004 14:00	-68,00	-55,00	SLUSH/GAP LAYER SAMPLING	Alkalinity/PH//Chlorophyll//d18O//DOC/DON//Nutrients//Oxygen//Phytoplankton composition//POC/POM//Salinity//Stable C/N	6	41209	
09.12.2004 17:00	-68,00	-55,00	SNOW PITS	Temperature//Wetness	--	041209Snow	Snow pits at sites 6 and 8
09.12.2004 18:00	-68,05	-55,20	WATER BOTTLES	CFCs//d18O//Helium	Polarstern	649	profile
09.12.2004 18:00	-68,04	-55,20	CTD			648	
09.12.2004 19:00	-67,60	-54,00	AEM	DGPS//Ice thickness//Photography//Ridging	--	041209NE	Flight to NE of ship, across prominent vast floes
09.12.2004 23:55	-68,05	-55,20	CMiPS	-	--	649	Vertical scalar microstructure profile.
10.12.2004 0:00	-68,05	-55,20	CTD			649	
10.12.2004 6:00	0,00	0,00	CTD			650	
10.12.2004 10:00	-68,00	-55,00	ADONIS	Under ice water properties	9 Sediment trap	41210	Adonis deployed for underice sea water properties: Oxygen, chla, DMS, H2O2, Microbiology, pH/Alkalinity, Phytoplankton, nutrients, DOC/DON
10.12.2004 12:00	-68,05	-55,20	CMiPS	-	--	651	Vertical scalar microstructure profile.
10.12.2004 12:00	-68,05	-55,20	CTD			651	

Startdate	Latitude	Longitude	Instruments	Parameters	Site	Station_id	Comment
10.12.2004 14:20	-68,08	-55,93	HELICOPTER CTD			Helic 006	
10.12.2004 14:25	-68,08	-55,93	WATER BOTTLES	d18O//Helium	--	xxx	Heli-CTD (bottom sample)
10.12.2004 14:25	-68,07	-55,93	SNOW PITS	Tritium	--	xxx	Heli-CTD (snow sample)
10.12.2004 14:35	-68,04	-55,19	MULTINET		Polarstern	PS67/006-52	mesh size 100 µm;;net 1: 1500 - 1300 m;net 2: 1300 - 1200 m;net 3: 1200 - 1000 m;net 4: 1000 - 700 m;net 5: 700 - 500 m;net 6: 500 - 200 m;net 7: 200 - 100 m;net 8: 100 - 50 m;net 9: 50 - 0 m;;for ethanol fixed zooplankton samples
10.12.2004 17:00	-68,00	-55,00	SNOW PITS	Temperature//Wetness	--	041210Snow	2 pits at sites 6 and 8
10.12.2004 18:00	-68,03	-55,22	WATER BOTTLES	CFCs//d18O//Helium	Polarstern	653	profile
10.12.2004 18:05	-68,03	-55,21	CTD			653	
10.12.2004 23:55	-68,01	-55,24	CMiPS	-	--	654	Vertical scalar microstructure profile
11.12.2004 0:00	-68,01	-55,24	CTD			654	
11.12.2004 6:00	-68,00	-55,31	CTD			655	
11.12.2004 12:50	-68,25	-55,65	HELICOPTER CTD				Helic 007
11.12.2004 12:55	-68,25	-55,65	WATER BOTTLES	d18O//Helium	--	xxx	Heli-CTD (bottom sample)
11.12.2004 12:55	-68,25	-55,65	SNOW PITS	Tritium	--	xxx	Heli-CTD (snow sample)
11.12.2004 14:50	-68,00	-55,00	ICE CORES	Chlorophyll//HPLC pigments//Meiofauna//Nutrients//Phytoplankton composition	7 Floe edge diving site	IE 01	first under-ice core drilled successfully by diver-operated hand drill
11.12.2004 15:15	-68,00	-55,00	ICE CORES	Chlorophyll//Nutrients//Salinity//Temperature	9 Optodes	041211 OP	
11.12.2004 17:00	-68,00	-55,00	SNOW PITS	Temperature//Wetness	--	041211Snow	Several snow pits over the day, and sampling of first occurrences of superimposed ice.
12.12.2004 0:00	-67,96	-55,35	CTD			656	
12.12.2004 9:00	-68,00	-55,00	ICE CORES	Chlorophyll//d18O//DOC/DON//Nutrients//Phytoplankton composition//POC/POM//Salinity//Stable C/N	9 Sediment trap	41212	Core centrifuged for brine samples
12.12.2004 10:00	-68,00	-55,00	SNOW PITS	Density//Stratigraphy//Temperature//Wetness	--	041212Snow	Several snow pits over the day at different sites, and sampling of first occurrences of superimposed ice.
12.12.2004 13:00	-68,53	-56,07	SAR RADAR REFLECTOR		Drifting buoy	Site T	Deployed radar reflector

Startdate	Latitude	Longitude	Instruments	Parameters	Site	Station_id	Comment
12.12.2004 14:00	-67,00	-55,00	EXPERIMENTS	Amino acids//DOC/DON//Amino acids//DOM	9 Besides Polarstern	Photodegradation experiment 2	Photodegradation experiment #2 (0.2um filtered brine from station 9, incubated on snow surface); Collaborative experiment; additional paramenters:;David Thomas / Stathis Papadimitriou: nutrients, CDOM, oxygen, alkalinity;Harri Kuosa: species composition;Birte Gerdes: bacterial activity;Andreas Krell: H2O2;Jaqueline Stefels: DMS;Rupert Krapp: light profiles
13.12.2004 0:00	-68,00	-55,00	SNOW PITS	Stratigraphy//Temperature//Thickness profile//Wetness	--	041213Snow	Several snow pits over the day, and sampling of first occurrences of superimposed ice.
13.12.2004 6:05	-67,90	-55,40	CTD			657	
13.12.2004 7:50	-67,90	-55,41	MULTINET		Polarstern	PS67/006-58	mesh size 100 µm;;net 1: 1000 - 500 m;net 2: 500 - 200 m;net 3: 200 - 100 m;net 4: 100 - 50 m;net 5: 50 - 0 m;;for formalin fixed zooplankton samples
13.12.2004 12:00	-68,00	-55,00	WATER BOTTLES	d18O//DOC/DON//Nutrients	--	006 59	from 700m
13.12.2004 12:00	-67,88	-55,37	WATER BOTTLES	Amino acids//DOC/DON//DOM	Polarstern	PS67/006-59	One depth: 700 m
13.12.2004 12:00	-67,89	-55,38	CTD			659	
13.12.2004 14:55	-68,27	-55,39	HELICOPTER CTD			Helic 008	
13.12.2004 15:00	-68,27	-55,39	SNOW PITS	Tritium	--	xxx	Heli-CTD (snow sample)
13.12.2004 15:00	-68,27	-55,39	WATER BOTTLES	d18O//Helium	--	xxx	Heli-CTD (bottom sample)
13.12.2004 18:00	-67,88	-55,33	CTD			661	
13.12.2004 18:00	-67,87	-55,33	WATER BOTTLES	CFCs//d18O//Helium	Polarstern	661	profile
14.12.2004 0:00	-68,00	-55,00	UNDERWATER PUMP	Chlorophyll		7 041214-TS	
14.12.2004 6:00	-67,83	-55,36	CTD			662	
14.12.2004 9:30	-68,00	-55,00	ICE CORES	Chlorophyll//DMS/DMSP//H2O2//HPLC pigments//Meiofauna//Nutrients//Phytoplankton composition//POC/POM//Salinity//Stable C/N isotopes//Temperature//Texture	6 Bio coring	041214-TS	conducted in co-operation with the groups of Gerhard Dieckmann et al. (AWI), Christian Haas et al. (AWI), Harri Kuosa (Univ. Helsinki), Sigi Schiel et al. (AWI), Jacqueline Stefels (Univ. Groningen) and David Thomas et al. (Univ. Wales)
14.12.2004 9:50	-68,00	-55,00	LICOR SOIL GAS CHAMBER	CO2 flux	9 Clean site	041214BB	
14.12.2004 9:50	-68,00	-55,00	SACK HOLES	Alkalinity/PH//Bacterial stock	9 Clean site	041214BB	Iron isotopes//DMS/ DOC/DON/ Nutrients/ Oxygen//Phytoplankton composition//Pigments//POC/POM//Salinity//Temperature
14.12.2004 9:50	-68,00	-55,00	ICE CORES	Bacterial stock	9 Clean site	041214BB	Virus//Chlorophyll//d18O//DMS/DMSP//DOC/DON//Gas composition (O2

Startdate	Latitude	Longitude	Instruments	Parameters	Site	Station_id	Comment
14.12.2004 9:50	-68,00	-55,00	SNOW PITS	Bacterial stock//Chlorophyll//Nutrients		041214BB	Iron isotopes//DMS//Salinity//Temperature Phytoplankton composition//Iron
14.12.2004 9:50	-68,00	-55,00	UNDERWATER PUMP	Alkalinity/PH//Bacterial stock	9 Clean site	041214BB	Virus//Chlorophyll//CO2
14.12.2004 10:00	-68,30	-55,50	AEM	DGPS//Ice thickness//Photography//Ridging	--	041214SHEM	First flight of the day, to the South
14.12.2004 10:30	-68,00	-55,00	ICE CORES	Salinity//Texture	6 Bio coring	041214TS11	Entered site 6 by boat, across lead covered with 2 cm of dark nilas. Cold air <-5°C
14.12.2004 10:30	-68,00	-55,00	SNOW PITS	Temperature//Wetness	--	041214Snow	Several snow pits over the day, at 6, 8, and 9. Note temperature gradient reversals in thin snow.
14.12.2004 12:00	-68,00	-55,00	WATER BOTTLES	d18O//DOC/DON//Nutrients	--	006 63	ph/Alkalinity, oxygen also taken;from 50m, 100m & 1360m
14.12.2004 12:00	-67,82	-55,40	CMiPS	-	--	663	Vertical scalar microstructure profile.
14.12.2004 12:00	-67,82	-55,40	CTD			663	
14.12.2004 13:00	-67,20	-55,50	AEM	DGPS//Ice thickness//Photography//Ridging	--	041214NHEM	Second flight of the day, to the North. Rubble fields in the NW
14.12.2004 14:00	-67,81	-55,41	MULTINET		Polarstern	PS67/006-64	mesh size 55 µm;;net 1: 1000 - 500 m;net 2: 500 - 200 m;net 3: 200 - 100 m;net 4: 100 - 50 m;net 5: 50 - 0 m;;for stable isotope samples
14.12.2004 15:00	-68,00	-55,00	SALINOMETER	Water salinity / temperature		7 041214-TS	Pobes not taken at same site, as the rest of the temporal study due to a crack, which we were not able to pass with the heavy equipment
14.12.2004 15:30	-68,00	-55,00	SACK HOLES	Alkalinity/PH//Chlorophyll//d18O//DOC/DON//Nutrients//Oxygen//Phytoplankton composition//POC/POM//Salinity//Stable C/N	9 Sediment trap	41214	
14.12.2004 16:00	-68,00	-55,00	UNDERWATER VIDEO CAMERA & PHOTO			7 041214-TS	
14.12.2004 18:00	-67,81	-55,42	CMiPS	-	--	665	Vertical scalar microstructure profile.
14.12.2004 18:00	-67,80	-55,42	WATER BOTTLES	CFCs//d18O//Helium	Polarstern	006_65	profile
14.12.2004 18:00	-67,81	-55,42	CTD			665	
14.12.2004 19:00	-68,00	-55,00	UNDERWATER PUMP			7 041214-TS	
15.12.2004 0:00	-67,79	-55,42	CTD			666	together with SBE 19
15.12.2004 0:00	-67,79	-55,42	WATER BOTTLES	CFCs//d18O//Helium	Polarstern	006-66	bottom sample
15.12.2004 0:00	-67,00	-55,00	SLUSH/GAP LAYER SAMPLING	DOC/DON//Amino acids//DOM		9 Brine Pool2	
15.12.2004 0:00	-67,00	-55,00	ICE CORES	DOC/DON//Amino acids//DOM		9 9	
15.12.2004 6:00	-67,78	-55,46	CTD			667	

Startdate	Latitude	Longitude	Instruments	Parameters	Site	Station_id	Comment
15.12.2004 10:30	-68,00	-55,00	THICKNESS PROFILES	EM		--	EM31 profile along skidoo tracks towards patches 6 and 10, and along snow thickness profiles on 8 and 9
15.12.2004 10:40	-67,75	-55,73	HELICOPTER CTD			Helic 009	
15.12.2004 10:45	-67,75	-55,73	WATER BOTTLES	d18O//Helium	--	xxx	Heli-CTD (bottom sample)
15.12.2004 10:45	-67,75	-55,73	SNOW PITS	Tritium	--	xxx	Heli-CTD (snow sample)
15.12.2004 12:05	-67,78	-55,49	CTD			668	
15.12.2004 14:00	-68,00	-55,00	RADIOMETER	PAR//Spectral radiation//UV radiation	7 Floe edge diving site	RAMSES-insitu01	spectral and quantum irradiance profile of PAR/UV intensities at floe edge, in open water and under ice
15.12.2004 14:30	-67,70	-58,00	AEM	DGPS//Ice thickness//Photography//Ridging	--	041215HEM	Bird flight along northern branch of buoy triangle (F-A) an further to the W, into high SAR backscatter region
15.12.2004 14:30	-68,00	-55,00	UNDERICE SYRINGE		7 Floe edge diving site	Floe edge syringe02	
15.12.2004 14:50	-68,00	-55,00	ICE CORES	Chlorophyll//Meiofauna//Phytoplankton composition	7 Floe edge diving site	under ice corer 03-04	one core drilled through under-ice slush/platelet layer, another at clean ice undersurface
15.12.2004 16:30	-67,00	-55,00	EXPERIMENTS	Amino acids//DOC/DON//Amino acids//DOM	9 Besides Polarstern	Photodegradation experiment 3	Photodegradation experiment #3 (filtered brine from station 9, incubated under snow: surface, 50cm, 90cm);Collaborative experiment;additional paramenters:;David Thomas / Stathis Papadimitriou: nutrients, CDOM, oxygen, alkalinity;Harri Kuosa: species composition;Birte Gerdes: bacterial activity;Andreas Krell: H2O2;Jaqueline Stefels: DMS;Rupert Krapp: light profiles
15.12.2004 18:00	-67,78	-55,45	WATER BOTTLES	CFCs//d18O//Helium	Polarstern	006-70	profile
15.12.2004 18:10	-67,78	-55,45	CTD			670	
15.12.2004 19:00	-68,00	-55,00	SNOW PITS	Albedo//Temperature//Thickness profile//Wetness	--	041215Snow	Several snow pits on 6, 8, and elsewhere
16.12.2004 0:00	-67,78	-55,44	CTD			671	
16.12.2004 6:00	-67,77	-55,44	CTD			672	
16.12.2004 10:30	-68,10	-55,34	HELICOPTER CTD			Helic 010	
16.12.2004 10:35	-68,10	-55,35	WATER BOTTLES	d18O//Helium	--	xxx	Heli-CTD (bottom sample)
16.12.2004 10:35	-68,10	-55,35	SNOW PITS	Tritium	--	xxx	Heli-CTD (snow sample)
16.12.2004 12:00	-67,78	-55,45	CTD			673	
16.12.2004 12:00	-67,78	-55,45	CMiPS	-	--	673	Vertical scalar microstructure profile. This is the last such profile obtained during ISPOL 1, as CMiPS operations were terminated due to failure of all thermistor probes.
16.12.2004 15:00	-68,50	-56,40	ICE CORES	d18O//Salinity//Texture	Drifting buoy	041216TEX11	Ice core taken at buoy site A, southernmost point of buoy triangle

Startdate	Latitude	Longitude	Instruments	Parameters	Site	Station_id	Comment
16.12.2004 17:00	-68,00	-55,00	SNOW PITS	Temperature//Wetness	--	041216Snow	Several snow measurements on ISPOL floe and buoy sites
16.12.2004 18:00	-67,78	-55,37	WATER BOTTLES	CFCs//d18O//Helium	Polarstern	006-74	profile
16.12.2004 18:05	-67,78	-55,37	CTD			674	
17.12.2004 0:00	-67,78	-55,33	CTD			675	
17.12.2004 6:05	-67,77	-55,31	CTD			676	
17.12.2004 8:00	-67,77	-55,33	MULTINET		Polarstern	PS67/006-77	mesh size 100 µm;;net 1: 1000 - 500 m;net 2: 500 - 200 m;net 3: 200 - 100 m;net 4: 100 - 50 m;net 5: 50 - 0 m;;for formalin fixed zooplankton samples
17.12.2004 9:30	-68,00	-55,00	SACK HOLES	CO2	9 Optodes	041217BO2	Iron isotopes
17.12.2004 9:30	-68,00	-55,00	ICE CORES	Gas composition (O2	9 Optodes	041217BO2	In collaboration with A. Krell/ AWI
17.12.2004 10:00	-68,00	-55,00	SNOW PITS	Temperature//Thickness profile//Wetness		9 041217Snow	Snow thickness profile from ship to floe edge at 9, and several snow pits over the day at 6, 8, and 9.
17.12.2004 10:00	-68,00	-55,00	SACK HOLES	Alkalinity/PH//Chlorophyll//d18O//DOC/DON//Nutrients//Oxygen//Phytoplankton composition//POC/POM//Salinity//Stable C/N		9 41217	Done together with Belgium Team
17.12.2004 12:00	-67,77	-55,36	CTD			678	
17.12.2004 12:00	-67,77	-55,37	WATER BOTTLES	Amino acids//DOC/DON//DOM	Polarstern	PS67/006-78	Profile, 3 depths: 200 m, 400 m, 1000 m
17.12.2004 14:00	-67,51	-56,50	HELICOPTER CTD			Helic 011	
17.12.2004 14:00	-68,00	-55,00	INCUBATOR	Phytoplankton	6 Bio coring	041217-IN	measurement of algal primary production (ice & water) by use of in-situ incubations on patch 6
17.12.2004 14:00	-68,00	-55,00	ICE CORES	Chlorophyll//Gas composition (O2	9 pCO2 site	041217BCO2	N2)//Salinity//Temperature//Total gas content
17.12.2004 14:00	-68,00	-55,00	SACK HOLES	CO2	9 pCO2 site	041217BCO2	Iron isotopes//Temperature
17.12.2004 14:00	-68,00	-55,00	LICOR SOIL GAS CHAMBER	CO2 flux	9 pCO2 site	041217BCO2	
17.12.2004 14:05	-67,51	-56,50	SNOW PITS	Tritium	--	xxx	Heli-CTD (snow sample)
17.12.2004 14:05	-67,51	-56,50	WATER BOTTLES	d18O//Helium	--	xxx	Heli-CTD (bottom sample)
17.12.2004 18:00	-67,77	-55,30	WATER BOTTLES	Amino acids//DOC/DON//DOM	Polarstern	PS67/006-79	Profile with 19 depths
17.12.2004 18:00	-67,77	-55,30	WATER BOTTLES	CFCs//d18O//Helium	Polarstern	006-79	profile
17.12.2004 18:00	-68,00	-55,00	WATER BOTTLES	d18O//DOC/DON//Nutrients	--	006 79	from 19 depths
17.12.2004 18:05	-67,77	-55,31	CTD			679	
17.12.2004 19:20	-68,00	-55,00	SONIC ANEMOMETERS		9 Turbulence mast 2	Sonic anemometer	
17.12.2004 23:55	-67,77	-55,27	CTD			680	
18.12.2004 0:00	-68,00	-55,00	SNOW PITS	Temperature//Wetness	--	041218Snow	Several snow pits on 6, 8, and 9 + surface ice sampling
18.12.2004 6:00	-67,76	-55,25	CTD			681	
18.12.2004 10:00	-68,50	-56,25	AEM	DGPS//Ice thickness//Photography//Ridging	--	041218HEM	Bird flight along edges of buoy triangle + three overflights of ISPOL floe
18.12.2004 12:05	-67,76	-55,30	CTD			682	
18.12.2004 14:00	-67,75	-55,09	HELICOPTER CTD			Helic 012	

Startdate	Latitude	Longitude	Instruments	Parameters	Site	Station_id	Comment
18.12.2004 14:00	-67,77	-55,31	DC IN-SITU ICE CONDUCTIVITY METER	Sea ice conductivity structure		9 DC-1	Repeat measurements at Site 9
18.12.2004 14:00	-68,00	-55,00	ICE CORES	Chlorophyll//Nutrients//Salinity//Temperature	9 Optodes	041218 OP	
18.12.2004 14:05	-67,77	-55,31	MULTINET		Polarstern	PS67/006-83	mesh size 100 µm;;net 1: 1450 - 1400 m;net 2: 1400 - 1000 m;net 3: 1000 - 700 m;net 4: 700 - 500 m;net 5: 500 - 200 m;net 6: 200 - 150 m;net 7: 150 - 100 m;net 8: 100 - 50 m;net 9: 50 - 0 m;;for ethanol fixed zooplankton samples
18.12.2004 14:05	-67,75	-55,09	WATER BOTTLES	d18O//Helium	--	xxx	Heli-CTD (bottom sample)
18.12.2004 14:05	-67,75	-55,09	SNOW PITS	Tritium	--	xxx	Heli-CTD (snow sample)
18.12.2004 14:50	-68,00	-55,00	UNDERICE NET	Icefauna	6 Floe edge	floe edge dive site 02	dive interrupted by visiting leopard seal
18.12.2004 15:00	-68,00	-55,00	SLUSH/GAP LAYER SAMPLING	Alkalinity/PH//Bacterial activity//Chlorophyll//d18O//DOC/DON//Nutrients//Oxygen//Phytoplankton composition//POC/POM//Salinity//Stable C/N		8 41218	
18.12.2004 18:00	-67,77	-55,25	WATER BOTTLES	CFCs//d18O//Helium	Polarstern	006-84	profile
18.12.2004 18:05	-67,77	-55,29	CTD			684	
19.12.2004 0:05	-67,77	-55,25	CTD			685	
19.12.2004 6:00	-67,77	-55,24	CTD			686	
19.12.2004 8:00	-68,00	-55,00	SLUSH/GAP LAYER SAMPLING	Alkalinity/PH//Bacterial activity//Chlorophyll//DMS/DMSP//d18O//DOC/DON//Nutrients//Oxygen//Phytoplankton composition//POC/POM//Salinity//Stable C/N		8 41219	
19.12.2004 9:30	-68,00	-55,00	ICE CORES	Chlorophyll//DMS/DMSP//H2O2//HPLC pigments//Meiofauna//Nutrients//Phytoplankton composition//POC/POM//Salinity//Stable C/N isotopes//Temperature//Texture	6 Bio coring	041219-TS	conducted in co-operation with the groups of Gerhard Dieckmann et al. (AWI), Christian Haas et al. (AWI), Harri Kuosa (Univ. Helsinki), Sigi Schiel et al. (AWI), Jacqueline Stefels (Univ. Groningen) and David Thomas et al. (Univ. Wales)
19.12.2004 9:45	-68,00	-55,00	LICOR SOIL GAS CHAMBER	CO2 flux	9 Clean site	041219BB	
19.12.2004 9:45	-68,00	-55,00	UNDERWATER PUMP	Alkalinity/PH//Bacterial stock	9 Clean site	041219BB	Iron isotopes//DMS//DOC/DON//Oxygen//Pigments//POC/POM

Startdate	Latitude	Longitude	Instruments	Parameters	Site	Station_id	Comment
19.12.2004 9:45	-68,00	-55,00	ICE CORES	Bacterial stock	9 Clean site	041219BB	Iron isotopes//Nutrients//Phytoplankton composition//Phytoplankton viability//Pigments//POC/POM//Salinity//Temperature//Texture//Total gas content
19.12.2004 9:45	-68,00	-55,00	SNOW PITS	Bacterial stock//Chlorophyll//Nutrients		041219BB	Phytoplankton composition//Iron Iron isotopes//Salinity//Temperature
19.12.2004 9:45	-68,00	-55,00	SACK HOLES	Alkalinity/PH//Bacterial stock	9 Clean site	041219BB	Iron isotopes//DMS/ DOC/DON/ Nutrients//Oxygen/ Phytoplankton composition/ Pigments/ POC/POM/ Salinity//Temperature
19.12.2004 10:00	-68,00	-55,00	UNDERWATER PUMP	Chlorophyll	6 Bio coring	041219-TS	
19.12.2004 10:00	-68,00	-55,00	SALINOMETER	Water salinity / temperature	6 Bio coring	041219-TS	
19.12.2004 11:00	-68,00	-55,00	UNDERWATER VIDEO CAMERA & PHOTO		6 Bio coring	041219-TS	
19.12.2004 11:15	-66,99	-56,03	HELICOPTER CTD			Helic 013	
19.12.2004 11:20	-66,99	-56,03	WATER BOTTLES	d18O//Helium	--	xxx	Heli-CTD (bottom sample)
19.12.2004 11:20	-66,99	-56,03	SNOW PITS	Tritium	--	xxx	snow sample
19.12.2004 12:00	-68,00	-55,00	UNDERWATER PUMP	Zooplankton	6 Bio coring	041219-TS	
19.12.2004 12:00	-67,78	-55,27	CTD			687	
19.12.2004 16:00	-68,00	-55,00	AERIAL DIGITAL CAMERA	Ice type		Flight 6	Unsuccessful flight. only usable images are from first 2/3 of leg 1 (F--> A).;;Waypoints:;;F: 68º01.1'S, 55º29.7'W;A: 68º19.9'S, 57º08.1'W;W: 68º52.5'S, 56º13.1'W;;Planned Route: F --> A --> W;;AiT: -5c;wind: 8 m/s from NE;Heavy cloud on the western side of the array.
19.12.2004 16:00	-68,00	-55,00	SLUSH/GAP LAYER SAMPLING	Alkalinity/PH//Bacterial activity//Chlorophyll//DMS/DMSP/ /d18O//DOC/DON//Nutrients//Oxygen//Phytoplankton composition//POC/POM//Salinity/ /Stable C/N		8 41219	
19.12.2004 17:00	-68,00	-55,00	SNOW PITS	Temperature//Wetness	--	041219Snow	Seevral snow pits on several patches (6, 8, 9) over the day
19.12.2004 18:00	-67,80	-55,27	CTD			689	
19.12.2004 18:00	-67,80	-55,27	WATER BOTTLES	CFCs//d18O//Helium	Polarstern	006-89	profiles
19.12.2004 18:00	-68,00	-55,00	SLUSH/GAP LAYER SAMPLING	Meiofauna	--	041219-Sl	Temperature, Salinity and Chlorophyll a were also measured. Probes were taken at different sites on Floes 6 and 9. 8 Probes in total.
20.12.2004 0:00	-67,00	-55,00	SLUSH/GAP LAYER SAMPLING	DOC/DON//Amino acids//DOM		9 Brine Pool3	
20.12.2004 0:00	-67,82	-55,24	CTD			690	
20.12.2004 6:00	-67,84	-55,28	CTD			691	

Startdate	Latitude	Longitude	Instruments	Parameters	Site	Station_id	Comment
20.12.2004 8:00	-68,00	-55,00	SLUSH/GAP LAYER SAMPLING	Alkalinity/PH//Bacterial activity//Chlorophyll//DMS/DMSP/ /d18O//DOC/DON//Nutrients//Oxygen//Phytoplankton composition//POC/POM//Salinity/ /Stable C/N		8 41220	
20.12.2004 12:00	-68,27	-56,20	DRIFTING BUOYS	GPS	Ice properties	Drifting buoy	Premature recovery of AWI Buoy ID 14955 because it stopped transmitting on 06/12/04. Recorded position based upon last transmitted position rather than actual position during pickup due to loss of data.;;We replaced it with IARC buoy 53540, only to have that buoy fail as well, 2 days later. Site D therefore has very little data.
20.12.2004 12:00	-68,00	-55,00	WATER BOTTLES	DOC/DON//Nutrients	--	006 92	pH/ DIC also taken;from 50, 100 & 1391
20.12.2004 12:10	-67,85	-55,36	CTD			692	
20.12.2004 13:25	-67,86	-55,38	MULTINET		--	PS67/006-93	mesh size 55 µm;;net 1: 100 - 48 m;net 2: 48 - 0 m;;for stable isotope samples
20.12.2004 14:00	-68,00	-55,00	SNOW PITS	Density//Stratigraphy//Temperature//Thickness profile//Wetness		5 041220Snow	Extensive snow measurements on 5 and several others at 6, 8, 9 over the day
20.12.2004 16:00	-68,00	-55,00	SLUSH/GAP LAYER SAMPLING	Alkalinity/PH//Bacterial activity//Chlorophyll//DMS/DMSP/ /d18O//DOC/DON//Nutrients//Oxygen//Phytoplankton composition//POC/POM//Salinity/ /Stable C/N		8 41220	Taken in conjunction with core by Christian Haas at same site
20.12.2004 16:00	-68,00	-55,00	ICE CORES	d18O//Salinity//Texture	--	041220TEX11	Core taken at SOS surface feature on old refrozen lead
20.12.2004 18:00	-67,86	-55,45	WATER BOTTLES	CFCs//d18O//Helium	Polarstern	006-94	profiles
20.12.2004 18:05	-67,86	-55,45	CTD			64	
21.12.2004 0:00	-67,84	-55,48	CTD			695	
21.12.2004 6:00	-67,83	-55,50	CTD			696	
21.12.2004 7:40	-67,83	-55,50	MULTINET		Polarstern	PS67/006-97	mesh size 100 µm;;net 1: 1000 - 500 m;net 2: 500 - 200 m;net 3: 200 - 100 m;net 4: 100 - 50 m;net 5: 50 - 0 m;;for formalin fixed zooplankton samples
21.12.2004 8:00	-68,00	-55,00	SLUSH/GAP LAYER SAMPLING	Alkalinity/PH//Bacterial activity//Chlorophyll//DMS/DMSP/ /d18O//DOC/DON//Nutrients//Oxygen//Phytoplankton composition//POC/POM//Salinity/ /Stable C/N		8 41221	
21.12.2004 9:00	-68,00	-55,00	ADONIS		9 Sediment trap	041221 AD	
21.12.2004 10:00	-68,00	-55,00	CTD			041221 CTD	

Startdate	Latitude	Longitude	Instruments	Parameters	Site	Station_id	Comment
21.12.2004 13:30	-67,83	-55,51	CTD			698	
21.12.2004 13:45	-67,13	-56,15	HELICOPTER CTD			Helic 014	
21.12.2004 13:50	-67,13	-56,15	SNOW PITS	Tritium	--	xxx	snow sample
21.12.2004 13:50	-67,13	-56,15	WATER BOTTLES	d18O//Helium	--	xxx	Heli-CTD (bottom sample)
21.12.2004 14:00	-68,00	-55,00	SLUSH/GAP LAYER SAMPLING	Alkalinity/PH//Bacterial activity//Chlorophyll//d18O//DOC/ DON//Nutrients//Oxygen//Phytopl ankton composition//POC/POM//Salinity/ /Stable C/N		5 41221	In conjunction with core taken by Christian haas at the same site
21.12.2004 17:00	-68,00	-55,00	SNOW PITS	Temperature//Wetness	--	041221Snow	Several snow pits over the day
21.12.2004 17:00	-68,00	-55,00	AERIAL DIGITAL CAMERA	Ice type	floe size	Flight 7	Flight aborted enroute to first waypoint due to cloud. No images produced. Returned to ship at low level and took images of Polarstern floe at 300-1000 ft.
21.12.2004 18:00	-67,82	-55,53	WATER BOTTLES	CFCs//d18O//Helium	Polarstern	006-99	profiles
21.12.2004 18:00	-67,82	-55,53	CTD			699	
22.12.2004 0:00	-68,00	-55,00	WATER BOTTLES	d18O//DOC/DON//Nutrients	--	006 100	taken from 575 m
22.12.2004 0:00	-68,00	-55,00	SACK HOLES	Oxygen	9 Optodes	041222 SH	Together with Belgian team
22.12.2004 0:00	-67,82	-55,53	WATER BOTTLES	Amino acids//DOC/DON//DOM	Polarstern	PS67/006-100	One depth: 575 m (WDW)
22.12.2004 0:00	-67,82	-55,53	CTD			6100	
22.12.2004 6:10	-67,82	-55,54	CTD			6101	
22.12.2004 8:00	-68,00	-55,00	SLUSH/GAP LAYER SAMPLING	Alkalinity/PH//Bacterial activity//Chlorophyll//DMS/DMSP/ /d18O//DOC/DON//Nutrients//Ox ygen//Phytoplankton composition//POC/POM//Salinity/ /Stable C/N		8 41222	
22.12.2004 10:55	-67,28	-56,35	HELICOPTER CTD			Helic 015	
22.12.2004 11:00	-67,28	-56,35	WATER BOTTLES	d18O//Helium	--	xxx	Heli-CTD (bottom sample)
22.12.2004 11:00	-67,28	-56,35	SNOW PITS	Tritium	--	xxx	Heli-CTD (snow sample)
22.12.2004 11:00	-68,00	-55,00	SACK HOLES	CO2	9 pCO2 site	041222BCO2	
22.12.2004 11:00	-68,00	-55,00	LICOR SOIL GAS CHAMBER	CO2 flux	9 pCO2 site	041222BCO2	
22.12.2004 12:20	-67,82	-55,54	CTD			6102	
22.12.2004 14:00	-68,00	-55,00	ICE CORES	Gas composition (O2	9 pCO2 site	041222BCO2	
22.12.2004 15:00	-68,00	-55,00	ICE CORES	Gas composition (O2	9 Optodes	041222BO2	In collaboration with A. Krell / AWI
22.12.2004 15:00	-68,00	-55,00	SACK HOLES	CO2	9 Optodes	041222BO2	
22.12.2004 15:00	-68,00	-55,00	SLUSH/GAP LAYER SAMPLING	Alkalinity/PH//Bacterial activity//Chlorophyll//d18O//DOC/ DON//Nutrients//Oxygen//Phytopl ankton composition//POC/POM//Salinity/ /Stable C/N		5 41222	

Startdate	Latitude	Longitude	Instruments	Parameters	Site	Station_id	Comment
22.12.2004 15:00	-68,00	-55,00	ICE CORES	Chlorophyll//d18O//DOC/DON//Nutrients//Phytoplankton composition//POC/POM//Salinity//Stable C/N		5 41222	Done at same time as slush/gap layer sampling
22.12.2004 17:00	-68,00	-55,00	THICKNESS PROFILES	EM		--	EM31 profile along skidoo tracks to 6, 8, and 9
22.12.2004 17:00	-68,00	-55,00	SNOW PITS	Temperature//Wetness	--	042212Snow	Several snow pits over the day, on 6, 8, and 9
22.12.2004 18:00	-67,82	-55,56	WATER BOTTLES	CFCs//d18O//Helium	Polarstern	006-103	profile
22.12.2004 18:05	-67,81	-55,56	CTD			6103	
23.12.2004 0:00	-67,81	-55,57	CTD			6104	
23.12.2004 0:00	-68,00	-55,00	AEM	Ridging	Drifting buoy	041223FIMRBuoy	Bird II laser flight to FIMR buoy 52292 close by, profiling of surface roughness in vicinity of former sonic anemometer
23.12.2004 6:00	-67,81	-55,58	CTD			6105	
23.12.2004 9:00	-68,00	-55,00	INCUBATOR	Phytoplankton//Microbial community	6 Bio coring	041223-IN	measurement of bacterial & algal primary production (ice & water) by use of in-situ incubations on patch 6. Bacterial production was measured by Birte Gerdes (AWI).
23.12.2004 10:55	-67,58	-56,26	HELICOPTER CTD			Helic 016	
23.12.2004 11:00	-67,58	-56,26	WATER BOTTLES	d18O//Helium	--	xxx	Heli-CTD (bottom sample)
23.12.2004 11:00	-67,58	-56,26	SNOW PITS	Tritium	--	xxx	Heli-CTD (snow sample)
23.12.2004 14:35	-67,43	-56,40	DRIFTING BUOYS	GPS	Ice properties	--	iceberg buoy, IRIDIUM #1, size: 760 m x 240 m x 60 m
23.12.2004 15:00	-68,00	-55,00	SACK HOLES	Alkalinity/PH//Chlorophyll//d18O//DOC/DON//Nutrients//Oxygen//Phytoplankton composition//POC/POM//Salinity//Stable C/N		8 41223	Near Christian et al. snow site
23.12.2004 17:00	-68,00	-55,00	SNOW PITS	Temperature//Wetness	--	041223Snow	Several snow pits over the day, at 6, 8, and 9
23.12.2004 18:10	-67,81	-55,60	CTD			6107	cancelled at 75 m due to ice press
24.12.2004 6:00	-67,81	-55,63	CTD			6108	
24.12.2004 8:00	-68,00	-55,00	SLUSH/GAP LAYER SAMPLING	Alkalinity/PH//Bacterial activity//Chlorophyll//DMS/DMSP//d18O//DOC/DON//Nutrients//Oxygen//Phytoplankton composition//POC/POM//Salinity//Stable C/N		8 41224	
24.12.2004 10:10	-67,65	-56,04	HELICOPTER CTD			Helic 017	
24.12.2004 10:15	-67,65	-56,04	SNOW PITS		--	xxx	Heli-CTD (snow sample)
24.12.2004 10:15	-67,65	-56,04	WATER BOTTLES	d18O//Helium	--	xxx	Heli-CTD (bottom samples)
24.12.2004 11:00	-68,00	-55,00	SNOW PITS	Temperature//Wetness		8 041224Snow	
24.12.2004 12:00	-67,81	-55,63	CTD			6109	
24.12.2004 12:00	-68,00	-55,00	WATER BOTTLES	d18O//DOC/DON//Nutrients	--	006 109	from 850 m
24.12.2004 12:00	-67,82	-55,63	WATER BOTTLES	Amino acids//DOC/DON//DOM	Polarstern	PS67/006-109	One depth: 850 m (upper bottom water)

Startdate	Latitude	Longitude	Instruments	Parameters	Site	Station_id	Comment
24.12.2004 12:00	-67,81	-55,63	WATER BOTTLES	CFCs//d18O//Helium	Polarstern	006-108	profile
24.12.2004 14:00	-68,00	-55,00	INCUBATOR	Phytoplankton	6 Bio coring	041224-IN	measurement of algal primary production (ice & water) by use of in-situ incubations on patch 6
25.12.2004 8:00	-68,00	-55,00	SLUSH/GAP LAYER SAMPLING	Alkalinity/PH//Bacterial activity//Chlorophyll//DMS/DMSP/ /d18O//DOC/DON//Nutrients//Oxygen//Phytoplankton composition//POC/POM//Salinity/ /Stable C/N		8 41225	
25.12.2004 8:20	-67,80	-55,67	CTD			6110	
25.12.2004 9:00	-68,00	-55,00	SLUSH/GAP LAYER SAMPLING	Meiofauna	--	041225-Sl	Temperature, Salinity and Chlorophyll a were also measured.;Probes were taken at different sites on Floe 9. 5 Probes in total.
25.12.2004 11:00	-68,00	-55,00	SNOW PITS	Temperature//Wetness	--	041225Snow	Several snow pits on 8 and 6
25.12.2004 14:00	-68,00	-55,00	ICE CORES	Chlorophyll//DMS/DMSP//H2O2// HPLC pigments//Meiofauna//Nutrients// Phytoplankton composition//POC/POM//Salinity/ /Stable C/N isotopes//Temperature//Texture	6 Bio coring	041225-TS	conducted in co-operation with the groups of Gerhard Dieckmann et al. (AWI), Christian Haas et al. (AWI), Harri Kuosa (Univ. Helsinki), Sigi Schiel et al. (AWI), Jacqueline Stefels (Univ. Groningen) and David Thomas et al. (Univ. Wales)
25.12.2004 16:00	-68,00	-55,00	ICE CORES	d18O//Salinity//Texture	6 Bio coring	041225TS11	
25.12.2004 21:00	-68,00	-55,00	ICE CORES	Chlorophyll//Nutrients//Phytoplankton composition//Salinity//Temperature	9 Optodes	041225 OP	
25.12.2004 21:15	-68,00	-55,00	LICOR SOIL GAS CHAMBER	CO2 flux	9 Clean site	041225BB	
25.12.2004 21:15	-68,00	-55,00	ICE CORES	Bacterial stock	9 Clean site	41225	
25.12.2004 21:15	-68,00	-55,00	SNOW PITS	Bacterial stock//Chlorophyll//Nutrients		041225BB	
25.12.2004 21:15	-68,00	-55,00	UNDERWATER PUMP	Alkalinity/PH//Bacterial stock	9 Clean site	041225BB	Iron isotopes//DMS//DOC/DON//Oxygen//Pigments//POC/POM
25.12.2004 21:15	-68,00	-55,00	SACK HOLES	Alkalinity/PH//Bacterial stock	9 Clean site	041225BB	Iron isotopes//DMS//DOC/DON//Nutrients//Oxygen//Phytoplankton composition//Pigments//POC/POM//Salinity//Temperature
25.12.2004 21:15	-68,00	-55,00	INCUBATOR	Bacterial activity//Bacterial stock	9 Clean site	041225BB	Iron isotopes//Microbial community//Nutrients//Phytoplankton//Phytoplankton composition//Phytoplankton viability//POC/POM

Startdate	Latitude	Longitude	Instruments	Parameters	Site	Station_id	Comment
26.12.2004 0:00	-67,50	-55,50	SNOW PITS	Temperature//Thickness profile//Wetness	9 Snow depth line	041226Snow	Several snow pit measuremens on 9 and 6
26.12.2004 6:00	-67,78	-55,65	CTD			6111	
26.12.2004 7:40	-67,78	-55,66	MULTINET		Polarstern	PS67/006-112	mesh size 100 µm;;net 1: 1000 - 500 m;net 2: 500 - 200 m;net 3: 200 - 100 m;net 4: 100 - 50 m;net 5: 50 - 0 m;;for formalin fixed zooplankton samples
26.12.2004 10:00	-67,00	-55,00	WATER BOTTLES	d18O//DOC/DON//Nutrients//Oxygen	--	006 113	ph taken, ;DIC;from 17 depths
26.12.2004 10:00	-68,00	-55,00	SLUSH/GAP LAYER SAMPLING	Alkalinity/PH//Bacterial activity//Chlorophyll//d18O//DOC/DON//Nutrients//Oxygen//Phytoplankton composition//POC/POM//Salinity//Stable C/N		5 41226	
26.12.2004 10:55	-67,45	-56,20	HELICOPTER CTD			Helic 018	
26.12.2004 11:00	-67,46	-56,20	WATER BOTTLES	d18O//Helium	--	xxx	Heli-CTD (bottom samples)
26.12.2004 11:00	-67,46	-56,20	SNOW PITS	Tritium	--	xxx	Heli-CTD (snow sample)
26.12.2004 12:00	-68,00	-55,00	SLUSH/GAP LAYER SAMPLING	Meiofauna		6 041226-Sl	Temperature, Salinity and Chlorophyll a were also measured.;Probes were taken at different sites on Floe 6. 3 Probes in total.
26.12.2004 12:15	-67,81	-55,65	CTD			613	
26.12.2004 13:00	-68,00	-55,00	UNDERWATER PUMP	Chlorophyll	6 Bio coring	041225-TS	
26.12.2004 13:40	-67,81	-55,65	MULTINET		Polarstern	PS67/006-114	mesh size 55 µm;;net 1: 300 - 250 m;net 2: 250 - 200 m;net 3: 200 - 100 m;net 4: 100 - 50 m;net 5: 50 - 0 m;;for stable isotope samples
26.12.2004 15:00	-68,00	-55,00	UNDERWATER PUMP	Zooplankton	6 Bio coring	041225-TS	Under-ice video didn`t work.
26.12.2004 15:00	-68,57	-56,58	DRIFTING BUOYS	GPS	Ice properties	Drifting buoy	Recovered IARC-NA buoy (Logger B(f)).;;Measurements:;;zIce: 247 cm;zSnow: 40 cm;Freeboard: -13 cm
26.12.2004 15:45	-68,63	-56,61	DRIFTING BUOYS	GPS	Ice properties	Drifting buoy	Recovered IARC-NA Buoy (Logger G).;;Measurements:;;zIce: 71 cm;zSnow: 25 cm;Freeboard: -5 cm
26.12.2004 16:30	-68,50	-56,48	DRIFTING BUOYS	GPS	Ice properties	Drifting buoy	Recovered IARC-NA buoy (Logger D).;;Measurements:;;zIce: 188 cm;zSnow: 42 cm;Freeboard: 8 cm
26.12.2004 16:45	-68,56	-56,44	DRIFTING BUOYS	GPS	Ice properties	Drifting buoy	Recovered IARC-NA Buoy (Logger A).;;Measurements:;;zIce: 242 cm;zSnow: 32 cm;Freeboard: -15 cm

Startdate	Latitude	Longitude	Instruments	Parameters	Site	Station_id	Comment
26.12.2004 17:00	-67,00	-55,00	EXPERIMENTS	Amino acids//DOC/DON//Amino acids//DOM	9 Besides Polarstern	Photodegradation experiment 4	Photodegradation experiment #4 (unfiltered gap water, incubated 15cm under snow);Collaborative experiment;additional paramenters:;David Thomas / Stathis Papadimitriou: nutrients, CDOM, oxygen, alkalinity;Harri Kuosa: species composition;Birte Gerdes: bacterial activity;Andreas Krell: H2O2;Jaqueline Stefels: DMS;Rupert Krapp: light profiles
26.12.2004 18:00	-67,84	-55,65	WATER BOTTLES	CFCs//d18O//Helium	Polarstern	006-115	profiles
26.12.2004 18:05	-67,84	-55,65	CTD			6115	
27.12.2004 0:00	-67,40	-55,41	UNDERWATER TURBULENCE MAST		9 Ocean turbulence	ispol	2 clusters u, v, w, T, C, microC;1 ADCP 500kHz
27.12.2004 6:30	-67,83	-55,67	CTD			6116	
27.12.2004 9:00	-68,00	-55,00	INCUBATOR	Phytoplankton//Microbial community	9 German tomato	041227-IN	measurement of bacterial & algal primary production (ice & water) by use of in-situ incubations on patch 9. Bacterial production was measured by Birte Gerdes (AWI).
27.12.2004 11:35	-67,44	-55,96	HELICOPTER CTD			Helic 019	
27.12.2004 11:40	-67,44	-55,95	WATER BOTTLES	d18O//Helium	--	xxx	Heli-CTD (bottom samples)
27.12.2004 11:40	-67,44	-55,95	SNOW PITS	Tritium	--	xxx	Heli-CTD (snow sample)
27.12.2004 12:00	-67,81	-55,56	CTD			6118	
27.12.2004 12:00	-67,82	-55,55	WATER BOTTLES	Amino acids//DOC/DON//DOM	Polarstern	PS67/006-118	One depth: 100 m
27.12.2004 14:00	-67,50	-55,50	ICE CORES	Salinity//Temperature//Texture	9 Sediment trap	041227OP	Ice core from optode site
27.12.2004 14:00	-68,00	-55,00	CTD			041227 CTD	
27.12.2004 15:00	-68,00	-55,00	ICE CORES	Salinity//Temperature//Texture	9 Optodes	041227 OP	
27.12.2004 17:00	-67,50	-55,50	SNOW PITS	Temperature//Thickness profile//Wetness	9 Snow depth line	041227Snow	Several snow pits on 6 and 9
27.12.2004 17:00	-68,56	-56,20	DRIFTING BUOYS	GPS	Ice properties	Drifting buoy	Recovered IARC-NA buoy (Logger E).;;Measurements:;;zIce: 108 cm;zSnow: 50 cm;Freeboard: 0
27.12.2004 18:00	-67,78	-55,45	WATER BOTTLES	CFCs//d18O//Helium	Polarstern	006-120	profiles
27.12.2004 18:05	-67,78	-55,45	CTD			6120	
28.12.2004 0:00	-67,75	-55,37	CTD			6121	
28.12.2004 6:00	-67,71	-55,39	CTD			6122	
28.12.2004 10:40	-67,53	-56,02	HELICOPTER CTD	T	S	p	Helic 020
28.12.2004 11:00	-67,53	-56,02	SNOW PITS	Tritium	--	xxx	Heli-CTD (snow sample)
28.12.2004 11:00	-67,53	-56,02	WATER BOTTLES	d18O//Helium	--	xxx	Heli-CTD (bottom samples)
28.12.2004 12:05	-67,71	-55,39	CTD			6123	

Startdate	Latitude	Longitude	Instruments	Parameters	Site	Station_id	Comment
28.12.2004 14:10	-67,70	-55,36	MULTINET		Polarstern	PS67/006-124	mesh size 100 µm;;net 1: 1350 - 1150 m;net 2: 1150 - 1050 m;net 3: 1050 - 1000 m;net 4: 1000 - 700 m;net 5: 700 - 500 m;net 6: 500 - 200 m;net 7: 200 - 100 m;net 8: 100 - 50 m;net 9: 50 - 0 m;;for ethanol fixed zooplankton samples
28.12.2004 14:15	-68,43	-55,84	DRIFTING BUOYS	GPS	Ice properties	Drifting buoy	Recovered AAD Buoy ptt: 19035 - to be redeployed at Site F. Recovered Radar Reflector (still in perfect condition, no snow accumulation and still upright).
28.12.2004 14:55	-68,60	-56,00	DRIFTING BUOYS	GPS	Ice properties	Drifting buoy	Recovered AAD Buoy 19021 and 2 flags. Buoy was completely horizontal and covered in a thin layer of snow. Had to cut T(ice) cable which was deep under solid ice due to melt/refreeze. Cause of melt/refreeze probably due to buoy\'s casing.
28.12.2004 15:00	-67,50	-55,50	ICE CORES	d18O//Salinity//Temperature//Texture		8 041228SC1-3	Final sampling on broken off, former site 8, looking for surface ice layers
28.12.2004 15:00	-68,23	-55,78	DRIFTING BUOYS	GPS	Ice properties	Drifting buoy	Recovered IARC-NA, Logger K(c);;Thickness measurements:;;zIce: 173;zSnow: 30;Freeboard: -1
28.12.2004 15:00	-67,50	-55,50	SNOW PITS	Density//Stratigraphy//Temperature//Thickness profile//Wetness		8 041228Snow	Final sampling on broken off, former site 8
28.12.2004 15:20	-68,55	-56,22	DRIFTING BUOYS	GPS	Ice properties	Drifting buoy	Recovered AAD Buoy 19228. Buoy was still upright. Had to chip T(ice) probe out of ice, but it was undamaged.
28.12.2004 15:30	-68,26	-55,58	DRIFTING BUOYS	GPS	Ice properties	Drifting buoy	Recovered IARC buoy 53536.;;Measurements:;;zIce: 62;zSnow: 10;Freeboard: -13
28.12.2004 16:00	-68,15	-55,74	DRIFTING BUOYS	GPS	Ice properties	Drifting buoy	Recovered IARC Buoy 53537.;;Measurements:;;zIce: > 2m;zSnow: 20;Freeboard: -5
28.12.2004 17:40	-68,24	-55,96	DRIFTING BUOYS	GPS	Ice properties	Drifting buoy	Recovered IARC-NA Buoy (data logger only). Buoy found at 2.3 nm from calculated position.
28.12.2004 18:00	-67,65	-55,31	WATER BOTTLES	CFCs//d18O//Helium	Polarstern	006-126	profiles
28.12.2004 18:15	-67,66	-55,32	CTD			6125	cancelled due to ice press

Startdate	Latitude	Longitude	Instruments	Parameters	Site	Station_id	Comment
28.12.2004 18:30	-67,93	-55,62	DRIFTING BUOYS	GPS	Ice properties	Drifting buoy	Recovered AAD-Met ptt: 20141;Re-Deployed ARISE ptt: 19035;Recovered radar reflector.;;Site was severely flooded. Ping pong ball was re-attached. Buoy deployed in small ridge at a 30 degree angle.
28.12.2004 19:45	-67,65	-55,31	CTD			6126	
28.12.2004 23:55	-67,63	-55,28	CTD			6127	
29.12.2004 6:00	-67,59	-55,30	CTD			6128	
29.12.2004 7:55	-67,58	-55,32	MULTINET		Polarstern	PS67/006-129	mesh size 100 µm;;net 1: 1000 - 500 m;net 2: 500 - 200 m;net 3: 200 - 100 m;net 4: 100 - 50 m;net 5: 50 - 0 m;;for formalin fixed zooplankton samples
29.12.2004 10:50	-68,00	-55,00	SACK HOLES	CO2	9 Dutch tomato	041229BDMS	
29.12.2004 10:50	-68,00	-55,00	ICE CORES	DMS/DMSP//Salinity//Temperature	9 Dutch tomato	041229BDMS	
29.12.2004 11:00	-67,34	-56,24	HELICOPTER CTD			Helic 021	
29.12.2004 11:05	-67,35	-56,24	WATER BOTTLES	d18O//Helium	--	xxx	Heli-CTD (bottom samples)
29.12.2004 11:05	-67,35	-56,24	SNOW PITS	Tritium	--	xxx	Heli-CTD (snow sample)
29.12.2004 12:00	-68,00	-55,00	WATER BOTTLES	d18O//DOC/DON//Nutrients	--	006 130	from 30, 950 & 1356m
29.12.2004 12:00	-67,56	-55,35	CTD			6130	
29.12.2004 14:00	-68,00	-55,00	SACK HOLES	Alkalinity/PH//Bacterial activity//Chlorophyll//d18O//DOC/DON//Nutrients//Oxygen//Phytoplankton composition//POC/POM//Salinity//Stable C/N		9 41229	In conjunction with the Belgium team
29.12.2004 14:00	-68,00	-55,00	SACK HOLES	CO2	9 Optodes	041229BO2	
29.12.2004 14:00	-68,00	-55,00	ICE CORES	Gas composition (O2	9 Optodes	041229BO2	
29.12.2004 15:00	-68,60	-56,30	AEM	DGPS//Ice thickness//Photography//Ridging	Drifting buoy	041229BuoyTriangle	Flight along edges of buoy triangle
29.12.2004 16:00	-68,00	-55,00	RADIOMETER	PAR//Spectral radiation//UV radiation	9 Besides Polarstern	snowdepth01	RAMSES-spectroradiometer and LI-COR 4pi quantum sensor inserted in 50cm of undisturbed snow cover for in situ-radiation measurements, 15min. sampling interval
29.12.2004 17:00	-67,50	-55,50	SNOW PITS	Temperature//Wetness	9 Snow depth line	041229Snow	Several snow pit measurements over the day

Startdate	Latitude	Longitude	Instruments	Parameters	Site	Station_id	Comment
29.12.2004 17:00	-67,78	-55,62	AERIAL DIGITAL CAMERA	Ice type	float size	Flight 9	Unsuccessful flight - aborted due to heavy cloud south of A, on leg 2. Eastern leg had some patchy cloud and images are usable.;;From Ship;To F 67°49.4'S, 55°38.5'W;To A 68°11.4'S, 57°10.6'W;;usable images: F --> A: Image #s 2080 - 2147;;Upon decision to abort, we went looking to recover buoys. Recovered site G, but were unable to find Site N.;;Enroute back to ship, some low-altitude images were taken detailing melt ponds, brash, etc. These are Image #\'s 2148-2400. Image 2182 contains the flag and buoy at site G.
29.12.2004 18:00	-67,54	-55,30	WATER BOTTLES	CFCs//d18O//Helium	Polarstern	006-131	profiles
29.12.2004 18:00	-67,00	-55,00	WATER BOTTLES	d18O//DOC/DON//Nutrients//Oxygen	--	006 131	19 depths sampled;pH, DIC also taken
29.12.2004 18:00	-67,53	-55,30	WATER BOTTLES	Amino acids//DOC/DON//DOM	Polarstern	PS67/006-131	Profile: 19 depths
29.12.2004 18:10	-67,54	-55,30	CTD			6131	
29.12.2004 18:10	-68,29	-57,02	DRIFTING BUOYS	GPS	Ice properties	Drifting buoy	Recovered IARC Buoy 53538.
29.12.2004 18:20	-68,00	-55,00	SACK HOLES	CO2	9 pCO2 site	041229BCO2	
29.12.2004 18:20	-68,00	-55,00	LICOR SOIL GAS CHAMBER	CO2 flux	9 pCO2 site	041229BCO2	
29.12.2004 18:20	-68,00	-55,00	ICE CORES	Chlorophyll//Gas composition	9 pCO2 site	041229BCO2	
30.12.2004 0:05	-67,51	-55,30	CTD			6132	
30.12.2004 6:00	-67,49	-55,30	CTD			6133	
30.12.2004 9:30	-68,00	-55,00	SEDIMENT TRAP		--	41230	Sediment traps retrieved and 5 bottles used at 6 days each
30.12.2004 10:00	-68,00	-55,00	UNDERWATER PUMP	Chlorophyll	6 Bio coring	041230-TS	
30.12.2004 10:00	-68,00	-55,00	SALINOMETER	Water salinity / temperature	6 Bio coring	041230-TS	
30.12.2004 10:00	-68,00	-55,00	UNDERWATER PUMP	Alkalinity/PH//Bacterial stock	9 Clean site	041230BB	Virus//Chlorophyll//CO2
30.12.2004 10:00	-68,00	-55,00	SACK HOLES	Alkalinity/PH//Bacterial stock	9 Clean site	041230BB	Virus//Chlorophyll//CO2
30.12.2004 10:00	-68,00	-55,00	SNOW PITS	Bacterial stock//Chlorophyll//Nutrients	Phytoplankton composition//Iron	Iron isotopes//Salinity// Temperature	041230BB
30.12.2004 10:00	-68,00	-55,00	ICE CORES	Bacterial stock	9 Clean site	041230BB	Virus//Chlorophyll//d18O//DMS/DMSP//DOC/DON//Gas composition (O2
30.12.2004 10:30	-68,00	-58,00	LICOR SOIL GAS CHAMBER	CO2 flux	9 Clean site	041230BB	
30.12.2004 10:45	-67,33	-56,01	HELICOPTER CTD			Helic 022	
30.12.2004 11:00	-68,00	-55,00	UNDERWATER VIDEO CAMERA & PHOTO		6 Bio coring	041230-TS	

Startdate	Latitude	Longitude	Instruments	Parameters	Site	Station_id	Comment
30.12.2004 11:00	-68,00	-55,00	SLUSH/GAP LAYER SAMPLING	Meiofauna	--	041230-Sl	Salinity, Temperature and Chlorophyll a also measured.;Probes taken at different sites on Floes 6 and 9.;8 Probes in total.
30.12.2004 11:00	-67,00	-56,00	SNOW PITS	Tritium	--	xxx	Heli-CTD (snow sample)
30.12.2004 11:00	-67,00	-56,00	WATER BOTTLES	d18O//Helium	--	xxx	Heli-CTD (bottom samples)
30.12.2004 11:00	-67,50	-55,50	THICKNESS PROFILES	EM		9	Skidoo profile along common tracks on floe 9
30.12.2004 11:00	-68,00	-55,00	ICE CORES	Chlorophyll//DMS/DMSP//H2O2//HPLC pigments//Meiofauna//Nutrients//Phytoplankton composition//POC/POM//Salinity//Stable C/N isotopes//Temperature//Texture	6 Bio coring	041230-TS	conducted in co-operation with the groups of Gerhard Dieckmann et al. (AWI), Christian Haas et al. (AWI), Harri Kuosa (Univ. Helsinki), Sigi Schiel et al. (AWI), Jacqueline Stefels (Univ. Groningen) and David Thomas et al. (Univ. Wales)
30.12.2004 12:00	-67,48	-55,35	CTD			6134	
30.12.2004 12:00	-68,00	-55,00	UNDERWATER PUMP	Zooplankton	6 Bio coring	041230-TS	
30.12.2004 14:00	-67,50	-55,50	ICE CORES	d18O//Salinity//Temperature//Texture	6 Bio coring	041230TS11 SC1-8	& Time series core and severa surface cores to finally quantify occurence and development of superimposed ice and gaps on floe 6
30.12.2004 14:00	-67,48	-55,35	DC IN-SITU ICE CONDUCTIVITY METER	Sea ice conductivity structure		9 DC-1	Repeat measurements at Site 9
30.12.2004 14:00	-67,00	-55,00	UNDERWATER PUMP	Amino acids//DOC/DON//DOM		9 UIW2	Under ice water, pumped through a core hole.
30.12.2004 14:30	-68,15	-56,49	DRIFTING BUOYS	GPS	Ice properties	Drifting buoy	Recovered AWI Buoy Id: 8064. Position recorded here is last transmitted position, not actual position recorded at pickup time due to the loss of that data.;;Measurements:;;zIce: 174 cm;zSnow: 55 cm;Freeboard: 0
30.12.2004 15:00	-68,19	-56,86	DRIFTING BUOYS	GPS	Ice properties	Drifting buoy	Recovered IARC Buoy 53539. Position data recorded here is from last reported position and not actual found position due to the loss of that data.;;Measurements:;;zIce: > 2m;zSnow: 25 cm;Freeboard: 0

Startdate	Latitude	Longitude	Instruments	Parameters	Site	Station_id	Comment
30.12.2004 15:30	-68,38	-56,81	DRIFTING BUOYS	GPS	Ice properties	Drifting buoy	Recovered IARC Buoy 53541.;;Measurements:;;zIce: Approx 220 cm (didn\'t hit bottom measuring ice thickness, but hit soft, brown ice.);;zSnow: 30cm;Freeboard: 0
30.12.2004 16:00	-68,26	-56,68	DRIFTING BUOYS	GPS	Ice properties	Drifting buoy	Recovered AWI Buoy 9803.;;Measurements:;;zIce: > 2m;zSnow: 85cm;Freeboard: 0
30.12.2004 17:00	-67,50	-55,50	SNOW PITS	Temperature//Thickness profile//Wetness	--	041230Snow	Several snow pits over the day, on sites 6 and 9
30.12.2004 18:10	-67,47	-55,34	CTD			6135	
30.12.2004 18:15	-67,47	-55,34	WATER BOTTLES	CFCs//d18O//Helium	Polarstern	006-135	profiles
31.12.2004 0:00	-67,45	-55,35	CTD			6136	
31.12.2004 0:00	-67,50	-55,50	SNOW PITS	Temperature//Wetness		9 041231Snow	Several snow pits over the day
31.12.2004 0:00	-67,50	-55,50	ICE CORES	d18O//Salinity//Temperature//Texture		5 041231SC1-3 David	& Final sampling of superimposed ice and gap layers on floe 5, 4 km away from ship
31.12.2004 6:00	-67,43	-55,35	CTD			6137	
31.12.2004 10:00	-68,00	-55,00	ICE CORES	Chlorophyll//d18O//DOC/DON//Nutrients//Phytoplankton composition//POC/POM//Salinity//Stable C/N		5 41231	
31.12.2004 10:00	-68,00	-55,00	SLUSH/GAP LAYER SAMPLING	Alkalinity/PH//Bacterial activity//Chlorophyll//d18O//DOC/DON//Nutrients//Oxygen//Phytoplankton composition//POC/POM//Salinity//Stable C/N		5 41231	
31.12.2004 10:50	-67,43	-55,40	CTD			6139	calibration with SBE 19
31.12.2004 10:50	-67,43	-55,40	WATER BOTTLES	CFCs//d18O//Helium	Polarstern	006-139	profiles
31.12.2004 13:00	-68,00	-55,00	SALINOMETER	Water salinity / temperature	6 Bio coring	041225-TS	
01.01.2005 0:00	-67,78	-55,62	AERIAL DIGITAL CAMERA	Ice type	floe size	Flight 9	Weather was overcast, with high cloud above 5000\'. Ground contrast was poor. Overall, the images show poor detail of floe surfaces. 2-3 images along leg 3 has small amounts of low cloud.;;AiT (at 5000\'): -16c;;Waypoints not kept, but can be gotten from pictures.;;From ship to F: No photos;;Leg 1: F to A: Images 2412 – 2488.;Leg 2: A to W: Images 2489 – 2548.;Leg 3: W to F: Images 2549 – 2646.;;8 photos taken after F: Images 2647 – 2653.

Startdate	Latitude	Longitude	Instruments	Parameters	Site	Station_id	Comment
01.01.2005 0:00	-67,50	-55,50	ICE CORES	d18O//Salinity//Temperature//Texture	6 Sediment trap	050101SC5&6	Surface cores from sediment trap and belgian site, looking for superimposed ice
01.01.2005 9:00	-67,50	-55,50	AEM	Ice thickness//Ridging		9 040101HEM	Two profiles of station floe
01.01.2005 10:00	-68,00	-55,00	INCUBATOR	Phytoplankton	6 Bio coring	050101-IN	measurement of algal primary production (ice & water) by use of in-situ incubations on patch 6
01.01.2005 10:00	-67,50	-55,50	THICKNESS PROFILES	EM		9 Sediment trap	Drill-hole vs EM31 calibration, and ladder measurements for inversion and comparison with Australian DE electrics soundings
01.01.2005 10:00	-67,38	-55,42	CTD			6140	calibration with Heli-CTD
01.01.2005 10:00	-67,00	-55,00	WATER BOTTLES	d18O//DOC/DON//Nutrients	--	006 140	from 50, 100 & 1368m
01.01.2005 10:30	-68,00	-55,00	ICE CORES	Chlorophyll//Nutrients//Salinity//Temperature//Texture	9 Optodes	050101 OP	
01.01.2005 10:50	-68,42	-56,72	DRIFTING BUOYS	GPS	Ice properties	Drifting buoy	Recovered AAD Buoy 18848. Buoy was still upright. Position on floe was only about 20 meters from lead (200-300 meters long and 50 meters wide). Extgensive leads in region. Floes mostly 20-500 m.
01.01.2005 11:00	-68,51	-56,51	DRIFTING BUOYS	GPS	Ice properties	Drifting buoy	Recovered AAD Buoy 19020. Extensive open water and small floes in area.
01.01.2005 11:15	-68,60	-56,31	DRIFTING BUOYS	GPS	Ice properties	Drifting buoy	Recovered AAD-Met buoy 20139. Still in middle of large floe approx. 1 km but alot of open water and small floes in area.;;Redeployed AAD Buoy 19020 (recovered from Site U).
01.01.2005 11:20	-67,38	-55,43	MULTINET		Polarstern	PS67/006-141	mesh size 55 µm;;net 1: 500 - 300 m;net 2: 300 - 200 m;net 3: 200 - 100 m;net 4: 100 - 50 m;net 5: 50 - 0 m;;for stable isotope samples
01.01.2005 14:00	-67,09	-56,52	ICE CORES	Salinity//Temperature//Texture	--	050101SC1-4	Surface cores at northernmost FIMR buoy
01.01.2005 16:00	-67,50	-55,50	ICE CORES	Salinity//Temperature	9 Sediment trap	050101Tex11	Ice core taken as background information for DC and EM31 inversion measurements
01.01.2005 17:00	-67,50	-55,50	SNOW PITS	Temperature//Thickness profile//Wetness		9 050101Snow	Several snow pits over the day
01.01.2005 18:05	-67,37	-55,41	CTD			6142	calibration with SBE 19
01.01.2005 18:10	-67,37	-55,41	WATER BOTTLES	CFCs//d18O//Helium	Polarstern	006-142	profiles
01.01.2005 22:00	-68,00	-55,00	SLUSH/GAP LAYER SAMPLING	Meiofauna	9 Floe edge	050101-Sl	Probes were taken at different distances away from the ice-edge. 10 Probes in total.
02.01.2005 0:00	-67,36	-55,41	CTD			6143	calibration with SBE 19

Startdate	Latitude	Longitude	Instruments	Parameters	Site	Station_id	Comment
02.01.2005 0:00	-66,60	-59,33	SNOW PITS	Stratigraphy//Temperature	--	050102LarsenIcebergs	Visiting of two prominent vast icebergs off the Larsen Ice Shelf, with characteristically different SAR backscatter properties
02.01.2005 6:00	-67,36	-55,39	CTD			6144	calibration with SBE 19
02.01.2005 7:40	-67,36	-55,39	MULTINET		Polarstern	PS67/006-145	mesh size 100 µm;;net 1: 1000 - 500 m;net 2: 500 - 200 m;net 3: 200 - 100 m;net 4: 100 - 50 m;net 5: 50 - 0 m;;for formalin fixed zooplankton samples
02.01.2005 10:00	-67,35	-55,40	CTD			6146	calibration with SBE 19;end of ice flow
02.01.2005 12:00	-67,35	-55,42	SHIP-BASED ICE OBSERVATIONS	Floe size//Ice concentration//Ice & snow type and thicknes//Topography	Underway transect	Ship based ice obs	Noon position given
03.01.2005 7:05	-67,11	-55,36	CTD			701	calibration with SBE 19
03.01.2005 7:10	-67,11	-55,36	WATER BOTTLES	CFCs//d18O//Helium	Polarstern	007-01	profiles
03.01.2005 12:00	-67,13	-55,43	SHIP-BASED ICE OBSERVATIONS	Floe size//Ice concentration//Ice & snow type and thicknes//Topography	Underway transect	Ship based ice obs	Noon position given.
04.01.2005 0:00	-66,10	-55,50	AEM	Ice thickness//Photography//Ridging	--	050104HEM	Bird flight towards ice edge and into former Larsen polynya ice
04.01.2005 1:40	-67,04	-55,40	CTD			801	calibration with SBE 19
04.01.2005 1:45	-67,04	-55,39	WATER BOTTLES	CFCs//Helium	Polarstern	008-01	profiles
04.01.2005 5:00	-66,00	-55,00	WATER BOTTLES	d18O//DOC/DON//Nutrients	--	009 1	
04.01.2005 5:00	-66,90	-55,35	WATER BOTTLES	Amino acids//DOC/DON//DOM	Polarstern	PS67/009-1	One depth: 900 m (bottom water)
04.01.2005 5:05	-66,90	-55,35	WATER BOTTLES	CFCs//Helium	Polarstern	009-01	profiles
04.01.2005 12:00	-66,60	-55,37	SHIP-BASED ICE OBSERVATIONS	Floe size//Ice concentration//Ice & snow type and thicknes//Topography	Underway transect	Ship based ice obs	Noon position given.
04.01.2005 15:00	-66,18	-55,26	ICE CORES	Salinity//Temperature//Texture	Floes on Transect	050104SC1&2	Surface cores from two floes in the same area with progressed snow metamorphosis and superimposed ice and gap layer formation
05.01.2005 5:05	-66,90	-55,35	CTD			901	calibration with SBE 19;last station within the ice
05.01.2005 9:30	-64,79	-54,50	DRIFTING BUOYS	GPS	Ice properties	--	iceberg buoy, ARGOS ID 3925, size: 1300 m x 1200 m x 20 m, ;blueish surface but no melt ponds, no snow cover
05.01.2005 12:00	-64,58	-53,80	SHIP-BASED ICE OBSERVATIONS	Floe size//Ice concentration//Ice & snow type and thicknes//Topography	Underway transect	Ship based ice obs	Noon position given. Last observation at 1230 Z.
07.01.2005 6:00	-65,00	-56,00	WATER BOTTLES	d18O//DOC/DON//Nutrients	--	011 1	from 4240 m
07.01.2005 6:10	-59,86	-45,99	CTD			1101	
07.01.2005 8:55	-59,89	-45,97	CTD			1102	

Startdate	Latitude	Longitude	Instruments	Parameters	Site	Station_id	Comment
07.01.2005 9:20	-66,00	-55,00	WATER BOTTLES	d18O//DOC/DON//Nutrients	--	011 2	from 1500m
07.01.2005 10:35	-59,90	-45,93	CTD			1103	
07.01.2005 10:35	-59,91	-45,91	WATER BOTTLES	CFCs	Polarstern	011-03	profile

A.5 Polarstern station list

Station	Date	Time	Position Lat	Position Lon	Depth [m]	Gear Abbreviation	Action
PS67/001-1	26.10.04	14:00	5° 0,25' S	7° 2,86' W	4418,7	GWS	Information
PS67/001-1	26.10.04	14:30	5° 0,28' S	7° 2,82' W	0,0	GWS	on deck
PS67/001-2	26.10.04	16:17	5° 0,35' S	7° 2,76' W	0,0	GWS	surface
PS67/001-2	26.10.04	16:42	5° 0,37' S	7° 2,69' W	4419,9	GWS	Information
PS67/001-2	26.10.04	17:02	5° 0,38' S	7° 2,70' W	4418,2	GWS	Information
PS67/001-2	26.10.04	17:32	5° 0,43' S	7° 2,55' W	4422,8	GWS	on deck
PS67/002-1	29.10.04	08:07	14° 60,00' S	1° 15,96' E	5551,5	GWS	surface
PS67/002-1	29.10.04	08:58	14° 59,81' S	1° 16,21' E	5551,5	GWS	Information
PS67/002-1	29.10.04	09:18	14° 59,73' S	1° 16,33' E	5550,6	GWS	Information
PS67/002-1	29.10.04	10:10	14° 59,63' S	1° 16,58' E	0,0	GWS	on deck
PS67/002-2	29.10.04	11:55	14° 59,53' S	1° 17,07' E	5550,0	GWS	surface
PS67/002-2	29.10.04	12:44	14° 59,46' S	1° 17,34' E	5534,5	GWS	Information
PS67/002-2	29.10.04	13:06	14° 59,41' S	1° 17,46' E	5516,9	GWS	Information
PS67/002-2	29.10.04	13:54	14° 59,18' S	1° 17,62' E	5504,1	GWS	on deck
PS67/003-1	30.10.04	12:02	18° 12,98' S	4° 0,54' E	5428,8	GWS	surface
PS67/003-1	30.10.04	12:42	18° 13,21' S	4° 0,68' E	5429,9	GWS	Information
PS67/003-1	30.10.04	13:01	18° 13,22' S	4° 0,78' E	2983,4	GWS	Information
PS67/003-1	30.10.04	13:42	18° 13,20' S	4° 1,13' E	5475,7	GWS	on deck
PS67/003-2	30.10.04	15:08	18° 21,25' S	4° 7,61' E	5411,4	GWS	surface
PS67/003-2	30.10.04	15:48	18° 21,36' S	4° 7,70' E	5000,5	GWS	Information
PS67/003-2	30.10.04	16:06	18° 21,44' S	4° 7,76' E	5751,3	GWS	Information
PS67/003-2	30.10.04	16:46	18° 21,58' S	4° 7,82' E	5422,2	GWS	on deck
PS67/004-1	10.11.04	14:00	50° 4,74' S	5° 26,15' E	3061,2	TD	surface
PS67/005-1	19.11.04	22:40	65° 37,57' S	36° 20,58' \	4768,0	CTD	surface
PS67/005-1	20.11.04	00:10	65° 37,03' S	36° 18,14' \	4771,0	CTD	at depth
PS67/005-1	20.11.04	01:41	65° 36,20' S	36° 14,57' \	4777,0	CTD	on deck
PS67/006-1	27.11.04	15:22	68° 13,05' S	54° 46,84' \	2009,0	ICE	Alongside floe
PS67/006-1	27.11.04	15:53	68° 12,84' S	54° 46,90' \	2007,0	ICE	ice gangway on ice
PS67/006-2	27.11.04	18:01	68° 11,95' S	54° 47,32' \	1978,4	CTD/RO	surface
PS67/006-2	27.11.04	18:39	68° 11,67' S	54° 47,46' \	1974,8	CTD/RO	at depth
PS67/006-2	27.11.04	19:26	68° 11,33' S	54° 47,62' \	1970,0	CTD/RO	on deck
PS67/006-3	28.11.04	00:08	68° 9,58' S	54° 48,15' \	1967,2	CTD	surface
PS67/006-3	28.11.04	00:42	68° 9,42' S	54° 48,26' \	1966,4	CTD	at depth
PS67/006-3	28.11.04	01:08	68° 9,30' S	54° 48,36' \	1959,6	CTD	on deck
PS67/006-4	28.11.04	17:58	68° 4,05' S	54° 50,34' \	1966,0	CTD/RO	surface
PS67/006-4	28.11.04	18:32	68° 3,90' S	54° 50,43' \	1964,8	CTD/RO	at depth
PS67/006-4	28.11.04	19:10	68° 3,74' S	54° 50,51' \	1963,6	CTD/RO	on deck
PS67/006-5	29.11.04	00:08	68° 2,67' S	54° 51,15' \	1955,6	CTD/RO	surface
PS67/006-5	29.11.04	00:48	68° 2,58' S	54° 51,27' \	1952,0	CTD/RO	at depth
PS67/006-5	29.11.04	01:19	68° 2,52' S	54° 51,38' \	1948,0	CTD/RO	on deck
PS67/006-6	29.11.04	06:01	68° 2,31' S	54° 53,43' \	1918,8	CTD/RO	surface
PS67/006-6	29.11.04	06:35	68° 2,28' S	54° 53,67' \	1915,6	CTD/RO	at depth
PS67/006-6	29.11.04	07:07	68° 2,25' S	54° 53,87' \	1913,2	CTD/RO	on deck
PS67/006-7	29.11.04	12:12	68° 1,79' S	54° 54,04' \	1914,8	CTD/RO	surface
PS67/006-7	29.11.04	12:45	68° 1,79' S	54° 53,89' \	1915,6	CTD/RO	at depth
PS67/006-7	29.11.04	13:23	68° 1,81' S	54° 53,67' \	1918,4	CTD/RO	on deck
PS67/006-8	29.11.04	13:32	68° 1,82' S	54° 53,62' \	1918,8	BONGO	surface
PS67/006-8	29.11.04	14:11	68° 1,87' S	54° 53,40' \	1920,8	BONGO	at depth
PS67/006-8	29.11.04	14:41	68° 1,92' S	54° 53,20' \	1922,8	BONGO	on deck
PS67/006-9	29.11.04	18:17	68° 2,40' S	54° 52,14' \	1936,0	CTD/RO	surface
PS67/006-9	29.11.04	18:54	68° 2,48' S	54° 51,94' \	1938,4	CTD/RO	at depth
PS67/006-9	29.11.04	19:35	68° 2,48' S	54° 51,85' \	1941,6	CTD/RO	on deck

Station	Date	Time	Position Lat	Position Lon	Depth [m]	Gear Abbreviation	Action
PS67/006-10	30.11.04	00:03	68° 2,56' S	54° 51,28' W	1952,8	CTD/RO	surface
PS67/006-10	30.11.04	00:46	68° 2,65' S	54° 51,36' W	1952,4	CTD/RO	at depth
PS67/006-10	30.11.04	01:21	68° 2,64' S	54° 51,40' W	1952,0	CTD/RO	on deck
PS67/006-11	30.11.04	06:00	68° 3,11' S	54° 53,32' W	1918,8	CTD/RO	surface
PS67/006-11	30.11.04	06:36	68° 3,24' S	54° 53,58' W	1912,4	CTD/RO	at depth
PS67/006-11	30.11.04	07:10	68° 3,24' S	54° 53,86' W	1907,6	CTD/RO	on deck
PS67/006-12	30.11.04	12:03	68° 4,23' S	54° 54,32' W	1904,4	CTD/RO	surface
PS67/006-12	30.11.04	12:06	68° 4,25' S	54° 54,31' W	1904,8	CTD/RO	Information
PS67/006-12	30.11.04	12:09	68° 4,26' S	54° 54,30' W	1904,8	CTD/RO	surface
PS67/006-12	30.11.04	12:53	68° 4,49' S	54° 54,14' W	1907,2	CTD/RO	at depth
PS67/006-12	30.11.04	13:27	68° 4,69' S	54° 53,99' W	1909,2	CTD/RO	on deck
PS67/006-13	30.11.04	18:02	68° 6,53' S	54° 52,31' W	1916,8	CTD/RO	surface
PS67/006-13	30.11.04	18:40	68° 6,77' S	54° 52,21' W	1916,8	CTD/RO	at depth
PS67/006-13	30.11.04	19:27	68° 7,05' S	54° 52,15' W	1911,2	CTD/RO	on deck
PS67/006-14	30.11.04	23:57	68° 8,71' S	54° 51,70' W	1907,6	CTD/RO	surface
PS67/006-14	01.12.04	00:36	68° 8,93' S	54° 51,64' W	1907,2	CTD/RO	at depth
PS67/006-14	01.12.04	01:12	68° 9,12' S	54° 51,61' W	1908,8	CTD/RO	on deck
PS67/006-15	01.12.04	06:02	68° 10,32' S	54° 52,33' W	1902,4	CTD/RO	surface
PS67/006-15	01.12.04	06:35	68° 10,37' S	54° 52,44' W	1875,2	CTD/RO	at depth
PS67/006-15	01.12.04	07:17	68° 10,40' S	54° 52,58' W	1899,6	CTD/RO	on deck
PS67/006-16	01.12.04	08:02	68° 10,41' S	54° 52,71' W	1897,2	MN	surface
PS67/006-16	01.12.04	08:41	68° 10,40' S	54° 52,84' W	1896,0	MN	at depth
PS67/006-16	01.12.04	08:41	68° 10,40' S	54° 52,84' W	1896,0	MN	Hoisting
PS67/006-16	01.12.04	09:24	68° 10,37' S	54° 52,98' W	1894,8	MN	on deck
PS67/006-17	01.12.04	10:34	68° 10,35' S	54° 53,22' W	1892,4	MN	surface
PS67/006-17	01.12.04	11:39	68° 10,35' S	54° 53,38' W	1889,6	MN	at depth
PS67/006-17	01.12.04	11:39	68° 10,35' S	54° 53,38' W	1889,6	MN	Hoisting
PS67/006-17	01.12.04	12:50	68° 10,41' S	54° 53,47' W	1888,0	MN	on deck
PS67/006-18	01.12.04	13:02	68° 10,42' S	54° 53,48' W	1888,0	CTD/RO	surface
PS67/006-18	01.12.04	13:43	68° 10,49' S	54° 53,47' W	1886,4	CTD/RO	at depth
PS67/006-18	01.12.04	14:24	68° 10,57' S	54° 53,43' W	1885,6	CTD/RO	on deck
PS67/006-19	01.12.04	18:12	68° 11,04' S	54° 53,23' W	1888,0	CTD/RO	surface
PS67/006-19	01.12.04	18:46	68° 11,09' S	54° 53,34' W	1887,6	CTD/RO	at depth
PS67/006-19	01.12.04	19:20	68° 11,13' S	54° 53,45' W	1887,2	CTD/RO	on deck
PS67/006-20	01.12.04	23:59	68° 11,31' S	54° 54,79' W	1872,8	CTD/RO	surface
PS67/006-20	02.12.04	00:40	68° 11,30' S	54° 55,11' W	1867,2	CTD/RO	at depth
PS67/006-20	02.12.04	01:15	68° 11,29' S	54° 55,42' W	1862,8	CTD/RO	on deck
PS67/006-21	02.12.04	06:21	68° 11,47' S	55° 0,59' W	1782,4	CTD/RO	surface
PS67/006-21	02.12.04	06:53	68° 11,49' S	55° 1,25' W	1771,6	CTD/RO	at depth
PS67/006-21	02.12.04	07:24	68° 11,51' S	55° 1,87' W	1761,6	CTD/RO	on deck
PS67/006-22	04.12.04	08:01	68° 6,89' S	55° 14,49' W	1560,8	CTD/RO	surface
PS67/006-22	04.12.04	08:35	68° 6,91' S	55° 14,62' W	1557,6	CTD/RO	at depth
PS67/006-22	04.12.04	09:01	68° 6,93' S	55° 14,70' W	1556,0	CTD/RO	on deck
PS67/006-23	04.12.04	12:04	68° 7,08' S	55° 14,88' W	1554,8	CTD/RO	surface
PS67/006-23	04.12.04	12:40	68° 7,12' S	55° 14,87' W	1555,6	CTD/RO	at depth
PS67/006-23	04.12.04	13:16	68° 7,17' S	55° 14,83' W	1556,4	CTD/RO	on deck
PS67/006-24	04.12.04	13:39	68° 7,20' S	55° 14,79' W	1557,6	MN	surface
PS67/006-24	04.12.04	13:43	68° 7,21' S	55° 14,79' W	1557,6	MN	at depth
PS67/006-24	04.12.04	13:44	68° 7,21' S	55° 14,79' W	1557,6	MN	Hoisting
PS67/006-24	04.12.04	13:55	68° 7,23' S	55° 14,77' W	1558,4	MN	on deck
PS67/006-25	04.12.04	18:03	68° 7,56' S	55° 14,10' W	1571,2	CTD/RO	surface
PS67/006-25	04.12.04	18:35	68° 7,59' S	55° 14,02' W	1572,4	CTD/RO	at depth
PS67/006-25	04.12.04	19:17	68° 7,64' S	55° 13,91' W	1573,6	CTD/RO	on deck
PS67/006-26	05.12.04	10:36	68° 6,88' S	55° 15,44' W	1538,0	CTD/RO	surface
PS67/006-26	05.12.04	11:09	68° 6,86' S	55° 15,50' W	1540,4	CTD/RO	at depth

Station	Date	Time	Position Lat	Position Lon	Depth [m]	Gear Abbreviat-ion	Action
PS67/006-26	05.12.04	11:32	68° 6,85' S	55° 15,52' \	1540,0	CTD/RO	on deck
PS67/006-27	05.12.04	11:49	68° 6,84' S	55° 15,53' \	1539,6	CTD/RO	surface
PS67/006-27	05.12.04	12:20	68° 6,83' S	55° 15,54' \	1539,6	CTD/RO	at depth
PS67/006-27	05.12.04	12:51	68° 6,82' S	55° 15,54' \	1539,2	CTD/RO	on deck
PS67/006-28	05.12.04	13:10	68° 6,82' S	55° 15,52' \	1539,2	BONGO	surface
PS67/006-28	05.12.04	13:31	68° 6,82' S	55° 15,51' \	1539,6	BONGO	at depth
PS67/006-28	05.12.04	13:44	68° 6,82' S	55° 15,50' \	1540,0	BONGO	on deck
PS67/006-29	06.12.04	06:00	68° 6,46' S	55° 14,83' \	1549,2	CTD/RO	surface
PS67/006-29	06.12.04	06:27	68° 6,43' S	55° 14,90' \	1547,6	CTD/RO	at depth
PS67/006-29	06.12.04	06:51	68° 6,40' S	55° 14,96' \	1546,8	CTD/RO	on deck
PS67/006-30	06.12.04	11:59	68° 6,07' S	55° 15,80' \	1530,0	CTD/RO	surface
PS67/006-30	06.12.04	12:34	68° 6,03' S	55° 15,90' \	1527,2	CTD/RO	at depth
PS67/006-30	06.12.04	13:05	68° 6,00' S	55° 15,97' \	1525,2	CTD/RO	on deck
PS67/006-31	06.12.04	13:20	68° 5,98' S	55° 16,01' \	1524,0	MN	surface
PS67/006-31	06.12.04	13:54	68° 5,95' S	55° 16,07' \	1522,8	MN	at depth
PS67/006-31	06.12.04	13:55	68° 5,95' S	55° 16,07' \	1522,8	MN	Hoisting
PS67/006-31	06.12.04	14:36	68° 5,91' S	55° 16,09' \	1521,6	MN	on deck
PS67/006-32	06.12.04	17:57	68° 5,89' S	55° 15,79' \	1526,8	CTD/RO	surface
PS67/006-32	06.12.04	18:28	68° 5,91' S	55° 15,70' \	1528,4	CTD/RO	at depth
PS67/006-32	06.12.04	19:13	68° 5,94' S	55° 15,55' \	1531,6	CTD/RO	on deck
PS67/006-33	06.12.04	23:57	68° 5,93' S	55° 15,24' \	1537,2	CTD/RO	surface
PS67/006-33	07.12.04	00:29	68° 5,91' S	55° 15,31' \	1535,6	CTD/RO	at depth
PS67/006-33	07.12.04	00:58	68° 5,89' S	55° 15,37' \	1534,0	CTD/RO	on deck
PS67/006-34	07.12.04	05:55	68° 5,50' S	55° 16,20' \	1512,0	CTD/RO	surface
PS67/006-34	07.12.04	06:25	68° 5,45' S	55° 16,28' \	1510,8	CTD/RO	at depth
PS67/006-34	07.12.04	06:50	68° 5,42' S	55° 16,35' \	1509,2	CTD/RO	on deck
PS67/006-35	07.12.04	11:57	68° 5,16' S	55° 17,12' \	1492,8	CTD/RO	surface
PS67/006-35	07.12.04	12:31	68° 5,15' S	55° 17,18' \	1492,4	CTD/RO	at depth
PS67/006-35	07.12.04	13:00	68° 5,14' S	55° 17,23' \	1492,4	CTD/RO	on deck
PS67/006-36	07.12.04	13:08	68° 5,13' S	55° 17,24' \	1492,4	BONGO	surface
PS67/006-36	07.12.04	13:39	68° 5,11' S	55° 17,29' \	1491,6	BONGO	at depth
PS67/006-36	07.12.04	14:02	68° 5,10' S	55° 17,32' \	1491,6	BONGO	on deck
PS67/006-37	07.12.04	14:03	68° 5,10' S	55° 17,32' \	1491,6	BONGO	surface
PS67/006-37	07.12.04	15:27	68° 5,04' S	55° 17,39' \	1490,8	BONGO	at depth
PS67/006-37	07.12.04	16:41	68° 4,99' S	55° 17,41' \	1491,2	BONGO	on deck
PS67/006-38	07.12.04	17:56	68° 4,93' S	55° 17,41' \	1491,6	CTD/RO	surface
PS67/006-38	07.12.04	18:25	68° 4,91' S	55° 17,38' \	1491,6	CTD/RO	at depth
PS67/006-38	07.12.04	19:07	68° 4,89' S	55° 17,34' \	1491,6	CTD/RO	on deck
PS67/006-39	08.12.04	00:00	68° 4,81' S	55° 17,42' \	1488,8	CTD/RO	surface
PS67/006-39	08.12.04	00:33	68° 4,79' S	55° 17,48' \	1487,6	CTD/RO	at depth
PS67/006-39	08.12.04	01:01	68° 4,77' S	55° 17,53' \	1486,0	CTD/RO	on deck
PS67/006-40	08.12.04	05:58	68° 4,30' S	55° 17,81' \	1476,0	CTD/RO	surface
PS67/006-40	08.12.04	06:29	68° 4,23' S	55° 17,79' \	1478,0	CTD/RO	at depth
PS67/006-40	08.12.04	06:55	68° 4,18' S	55° 17,77' \	1479,2	CTD/RO	on deck
PS67/006-41	08.12.04	12:00	68° 3,61' S	55° 17,44' \	1484,8	CTD/RO	surface
PS67/006-41	08.12.04	12:34	68° 3,55' S	55° 17,44' \	1485,2	CTD/RO	at depth
PS67/006-41	08.12.04	13:02	68° 3,51' S	55° 17,43' \	1484,8	CTD/RO	on deck
PS67/006-42	08.12.04	13:14	68° 3,49' S	55° 17,43' \	1485,2	MN	surface
PS67/006-42	08.12.04	13:19	68° 3,48' S	55° 17,43' \	1485,6	MN	at depth
PS67/006-42	08.12.04	13:19	68° 3,48' S	55° 17,43' \	1485,6	MN	Hoisting
PS67/006-42	08.12.04	13:27	68° 3,47' S	55° 17,42' \	1486,4	MN	on deck
PS67/006-43	08.12.04	18:00	68° 3,15' S	55° 16,88' \	1502,0	CTD/RO	surface
PS67/006-43	08.12.04	18:27	68° 3,12' S	55° 16,74' \	1503,2	CTD/RO	at depth
PS67/006-43	08.12.04	19:05	68° 3,08' S	55° 16,51' \	1508,0	CTD/RO	on deck
PS67/006-44	09.12.04	00:00	68° 3,04' S	55° 14,23' \	1556,4	CTD/RO	surface

Station	Date	Time	Position Lat	Position Lon	Depth [m]	Gear Abbreviat-ion	Action
PS67/006-44	09.12.04	00:37	68° 3,07' S	55° 14,07' \	1560,8	CTD/RO	at depth
PS67/006-44	09.12.04	01:06	68° 3,09' S	55° 13,98' \	1563,2	CTD/RO	on deck
PS67/006-45	09.12.04	05:58	68° 2,94' S	55° 13,02' \	1581,6	CTD/RO	surface
PS67/006-45	09.12.04	06:30	68° 2,89' S	55° 12,88' \	1586,0	CTD/RO	at depth
PS67/006-45	09.12.04	07:04	68° 2,81' S	55° 12,72' \	1590,4	CTD/RO	on deck
PS67/006-46	09.12.04	07:13	68° 2,79' S	55° 12,67' \	1592,0	MN	surface
PS67/006-46	09.12.04	07:47	68° 2,72' S	55° 12,50' \	1596,8	MN	at depth
PS67/006-46	09.12.04	08:25	68° 2,63' S	55° 12,31' \	1603,2	MN	on deck
PS67/006-47	09.12.04	11:56	68° 2,29' S	55° 11,60' \	1622,8	CTD/RO	surface
PS67/006-47	09.12.04	12:34	68° 2,28' S	55° 11,57' \	1623,6	CTD/RO	at depth
PS67/006-47	09.12.04	13:14	68° 2,28' S	55° 11,58' \	1623,6	CTD/RO	on deck
PS67/006-48	09.12.04	17:58	68° 2,50' S	55° 11,97' \	1614,4	CTD/RO	surface
PS67/006-48	09.12.04	18:29	68° 2,53' S	55° 12,03' \	1612,8	CTD/RO	at depth
PS67/006-48	09.12.04	19:12	68° 2,57' S	55° 12,09' \	1610,4	CTD/RO	on deck
PS67/006-49	09.12.04	23:57	68° 3,08' S	55° 11,91' \	1606,8	CTD/RO	surface
PS67/006-49	10.12.04	00:33	68° 3,09' S	55° 11,85' \	1608,4	CTD/RO	at depth
PS67/006-49	10.12.04	01:03	68° 3,10' S	55° 11,84' \	1608,4	CTD/RO	on deck
PS67/006-50	10.12.04	05:59	68° 3,01' S	55° 12,87' \	1586,8	CTD/RO	surface
PS67/006-50	10.12.04	06:30	68° 3,00' S	55° 12,95' \	1584,8	CTD/RO	at depth
PS67/006-50	10.12.04	06:56	68° 2,98' S	55° 12,99' \	1583,2	CTD/RO	on deck
PS67/006-51	10.12.04	11:59	68° 2,75' S	55° 11,91' \	1608,0	CTD/RO	surface
PS67/006-51	10.12.04	12:38	68° 2,69' S	55° 11,73' \	1612,8	CTD/RO	at depth
PS67/006-51	10.12.04	13:27	68° 2,59' S	55° 11,63' \	1616,8	CTD/RO	on deck
PS67/006-52	10.12.04	13:40	68° 2,56' S	55° 11,60' \	1618,0	MN	surface
PS67/006-52	10.12.04	14:36	68° 2,41' S	55° 11,59' \	1621,6	MN	at depth
PS67/006-52	10.12.04	14:36	68° 2,41' S	55° 11,59' \	1621,6	MN	Hoisting
PS67/006-52	10.12.04	15:40	68° 2,21' S	55° 11,78' \	1623,2	MN	on deck
PS67/006-53	10.12.04	18:00	68° 1,76' S	55° 12,56' \	1602,4	CTD/RO	surface
PS67/006-53	10.12.04	18:34	68° 1,67' S	55° 12,74' \	1596,8	CTD/RO	at depth
PS67/006-53	10.12.04	19:19	68° 1,57' S	55° 12,93' \	1592,4	CTD/RO	on deck
PS67/006-54	10.12.04	23:57	68° 0,82' S	55° 14,33' \	1566,8	CTD/RO	surface
PS67/006-54	11.12.04	00:28	68° 0,76' S	55° 14,64' \	1562,0	CTD/RO	at depth
PS67/006-54	11.12.04	00:57	68° 0,71' S	55° 14,98' \	1555,2	CTD/RO	on deck
PS67/006-55	11.12.04	05:59	68° 0,21' S	55° 18,81' \	1470,0	CTD/RO	surface
PS67/006-55	11.12.04	06:28	68° 0,16' S	55° 18,97' \	1466,4	CTD/RO	at depth
PS67/006-55	11.12.04	06:50	68° 0,12' S	55° 19,06' \	1465,2	CTD/RO	on deck
PS67/006-56	11.12.04	23:57	67° 57,55' S	55° 21,03' \	1447,2	CTD/RO	surface
PS67/006-56	12.12.04	00:30	67° 57,48' S	55° 21,21' \	1442,4	CTD/RO	at depth
PS67/006-56	12.12.04	00:56	67° 57,43' S	55° 21,38' \	1438,0	CTD/RO	on deck
PS67/006-57	13.12.04	06:00	67° 53,99' S	55° 23,85' \	1379,6	CTD/RO	surface
PS67/006-57	13.12.04	06:28	67° 53,96' S	55° 24,07' \	1374,4	CTD/RO	at depth
PS67/006-57	13.12.04	06:59	67° 53,92' S	55° 24,27' \	1370,4	CTD/RO	on deck
PS67/006-58	13.12.04	07:15	67° 53,89' S	55° 24,35' \	1368,4	MN	surface
PS67/006-58	13.12.04	07:52	67° 53,83' S	55° 24,49' \	1365,2	MN	at depth
PS67/006-58	13.12.04	08:32	67° 53,75' S	55° 24,54' \	1364,8	MN	on deck
PS67/006-59	13.12.04	11:58	67° 53,48' S	55° 23,00' \	1395,2	CTD/RO	surface
PS67/006-59	13.12.04	12:29	67° 53,39' S	55° 22,57' \	1402,8	CTD/RO	at depth
PS67/006-59	13.12.04	12:57	67° 53,32' S	55° 22,23' \	1411,6	CTD/RO	on deck
PS67/006-60	13.12.04	13:10	67° 53,29' S	55° 22,07' \	1415,2	BONGO	surface
PS67/006-60	13.12.04	13:28	67° 53,25' S	55° 21,87' \	1419,6	BONGO	at depth
PS67/006-60	13.12.04	13:47	67° 53,20' S	55° 21,68' \	1424,8	BONGO	on deck
PS67/006-61	13.12.04	17:57	67° 52,54' S	55° 19,80' \	1469,2	CTD/RO	surface
PS67/006-61	13.12.04	18:28	67° 52,44' S	55° 19,66' \	1470,0	CTD/RO	at depth
PS67/006-61	13.12.04	19:11	67° 52,28' S	55° 19,47' \	1470,8	CTD/RO	on deck
PS67/006-62	14.12.04	05:58	67° 49,80' S	55° 21,72' \	1440,4	CTD/RO	surface

Station	Date	Time	Position Lat	Position Lon	Depth [m]	Gear Abbreviat-ion	Action
PS67/006-62	14.12.04	06:27	67° 49,76' S	55° 22,13' \	1432,8	CTD/RO	at depth
PS67/006-62	14.12.04	06:49	67° 49,73' S	55° 22,43' \	1427,2	CTD/RO	on deck
PS67/006-63	14.12.04	11:59	67° 49,03' S	55° 24,20' \	1384,8	CTD/RO	surface
PS67/006-63	14.12.04	12:36	67° 48,91' S	55° 24,25' \	1385,6	CTD/RO	at depth
PS67/006-63	14.12.04	13:06	67° 48,82' S	55° 24,31' \	1384,4	CTD/RO	on deck
PS67/006-64	14.12.04	13:22	67° 48,77' S	55° 24,33' \	1383,2	MN	surface
PS67/006-64	14.12.04	14:01	67° 48,66' S	55° 24,44' \	1380,8	MN	at depth
PS67/006-64	14.12.04	14:41	67° 48,56' S	55° 24,57' \	1378,8	MN	on deck
PS67/006-65	14.12.04	18:02	67° 48,34' S	55° 25,15' \	1367,6	CTD/RO	surface
PS67/006-65	14.12.04	18:32	67° 48,32' S	55° 25,23' \	1347,2	CTD/RO	at depth
PS67/006-65	14.12.04	19:16	67° 48,29' S	55° 25,34' \	1365,2	CTD/RO	on deck
PS67/006-66	15.12.04	00:00	67° 47,56' S	55° 25,04' \	1365,6	CTD/RO	surface
PS67/006-66	15.12.04	00:28	67° 47,46' S	55° 25,00' \	1366,4	CTD/RO	at depth
PS67/006-66	15.12.04	00:51	67° 47,39' S	55° 24,98' \	1370,4	CTD/RO	on deck
PS67/006-67	15.12.04	05:58	67° 46,62' S	55° 27,36' \	1309,2	CTD/RO	surface
PS67/006-67	15.12.04	06:24	67° 46,60' S	55° 27,69' \	1302,8	CTD/RO	at depth
PS67/006-67	15.12.04	06:48	67° 46,57' S	55° 27,98' \	1297,2	CTD/RO	on deck
PS67/006-68	15.12.04	12:02	67° 46,64' S	55° 29,14' \	1276,0	CTD/RO	surface
PS67/006-68	15.12.04	12:28	67° 46,68' S	55° 29,05' \	1278,4	CTD/RO	at depth
PS67/006-68	15.12.04	13:09	67° 46,70' S	55° 28,87' \	1282,0	CTD/RO	on deck
PS67/006-69	15.12.04	13:20	67° 46,70' S	55° 28,80' \	1282,8	BONGO	surface
PS67/006-69	15.12.04	13:50	67° 46,69' S	55° 28,64' \	1284,4	BONGO	at depth
PS67/006-69	15.12.04	14:19	67° 46,70' S	55° 28,43' \	1285,6	BONGO	on deck
PS67/006-70	15.12.04	18:05	67° 46,92' S	55° 27,29' \	1310,0	CTD/RO	surface
PS67/006-70	15.12.04	18:36	67° 46,95' S	55° 27,20' \	1312,8	CTD/RO	at depth
PS67/006-70	15.12.04	19:17	67° 46,97' S	55° 27,09' \	1315,6	CTD/RO	on deck
PS67/006-71	15.12.04	23:59	67° 46,63' S	55° 26,25' \	1333,6	CTD/RO	surface
PS67/006-71	16.12.04	00:29	67° 46,55' S	55° 26,09' \	1338,0	CTD/RO	at depth
PS67/006-71	16.12.04	00:51	67° 46,50' S	55° 25,99' \	1340,4	CTD/RO	on deck
PS67/006-72	16.12.04	05:58	67° 46,14' S	55° 26,44' \	1341,2	CTD/RO	surface
PS67/006-72	16.12.04	06:25	67° 46,15' S	55° 26,66' \	1338,8	CTD/RO	at depth
PS67/006-72	16.12.04	06:47	67° 46,17' S	55° 26,83' \	1335,2	CTD/RO	on deck
PS67/006-73	16.12.04	11:58	67° 46,76' S	55° 27,27' \	1311,6	CTD/RO	surface
PS67/006-73	16.12.04	12:28	67° 46,83' S	55° 26,91' \	1319,6	CTD/RO	at depth
PS67/006-73	16.12.04	12:54	67° 46,86' S	55° 26,55' \	1327,6	CTD/RO	on deck
PS67/006-74	16.12.04	18:01	67° 46,94' S	55° 22,30' \	1416,4	CTD/RO	surface
PS67/006-74	16.12.04	18:29	67° 46,95' S	55° 22,08' \	1420,8	CTD/RO	at depth
PS67/006-74	16.12.04	19:11	67° 46,97' S	55° 21,73' \	1426,0	CTD/RO	on deck
PS67/006-75	16.12.04	23:57	67° 46,80' S	55° 19,81' \	1466,4	CTD/RO	surface
PS67/006-75	17.12.04	00:32	67° 46,75' S	55° 19,57' \	1471,2	CTD/RO	at depth
PS67/006-75	17.12.04	00:54	67° 46,71' S	55° 19,41' \	1474,0	CTD/RO	on deck
PS67/006-76	17.12.04	06:01	67° 46,29' S	55° 18,54' \	1486,8	CTD/RO	surface
PS67/006-76	17.12.04	06:31	67° 46,26' S	55° 18,73' \	1483,2	CTD/RO	at depth
PS67/006-76	17.12.04	07:04	67° 46,24' S	55° 19,00' \	1477,6	CTD/RO	on deck
PS67/006-77	17.12.04	07:22	67° 46,24' S	55° 19,18' \	1473,2	MN	surface
PS67/006-77	17.12.04	08:01	67° 46,22' S	55° 19,60' \	1464,4	MN	at depth
PS67/006-77	17.12.04	08:42	67° 46,22' S	55° 20,10' \	1452,8	MN	on deck
PS67/006-78	17.12.04	11:59	67° 46,29' S	55° 21,84' \	1420,4	CTD/RO	surface
PS67/006-78	17.12.04	12:30	67° 46,32' S	55° 21,82' \	1421,6	CTD/RO	at depth
PS67/006-78	17.12.04	13:03	67° 46,34' S	55° 21,71' \	1424,0	CTD/RO	on deck
PS67/006-79	17.12.04	18:00	67° 46,14' S	55° 18,44' \	1492,0	CTD/RO	surface
PS67/006-79	17.12.04	18:29	67° 46,11' S	55° 18,11' \	1502,0	CTD/RO	at depth
PS67/006-79	17.12.04	19:16	67° 46,08' S	55° 17,64' \	1517,6	CTD/RO	on deck
PS67/006-80	17.12.04	23:56	67° 45,96' S	55° 16,12' \	1540,4	CTD/RO	surface
PS67/006-80	18.12.04	00:24	67° 45,96' S	55° 16,01' \	1542,4	CTD/RO	at depth

Station	Date	Time	Position Lat	Position Lon	Depth [m]	Gear Abbreviat-ion	Action
PS67/006-80	18.12.04	00:48	67° 45,96' S	55° 15,90' \	1543,6	CTD/RO	on deck
PS67/006-81	18.12.04	05:57	67° 45,75' S	55° 15,01' \	1563,6	CTD/RO	surface
PS67/006-81	18.12.04	06:28	67° 45,74' S	55° 15,10' \	1562,8	CTD/RO	at depth
PS67/006-81	18.12.04	06:53	67° 45,73' S	55° 15,22' \	1560,8	CTD/RO	on deck
PS67/006-82	18.12.04	12:00	67° 45,87' S	55° 18,18' \	1504,0	CTD/RO	surface
PS67/006-82	18.12.04	12:28	67° 45,92' S	55° 18,40' \	1501,6	CTD/RO	at depth
PS67/006-82	18.12.04	12:54	67° 45,97' S	55° 18,57' \	1499,6	CTD/RO	on deck
PS67/006-83	18.12.04	13:10	67° 46,00' S	55° 18,64' \	1498,4	MN	surface
PS67/006-83	18.12.04	14:02	67° 46,11' S	55° 18,76' \	1486,4	MN	at depth
PS67/006-83	18.12.04	14:03	67° 46,11' S	55° 18,76' \	1486,4	MN	Hoisting
PS67/006-83	18.12.04	15:01	67° 46,21' S	55° 18,69' \	1487,6	MN	on deck
PS67/006-84	18.12.04	18:00	67° 46,39' S	55° 17,45' \	1512,0	CTD/RO	surface
PS67/006-84	18.12.04	18:28	67° 46,39' S	55° 17,19' \	1518,4	CTD/RO	at depth
PS67/006-84	18.12.04	19:11	67° 46,38' S	55° 16,77' \	1542,0	CTD/RO	on deck
PS67/006-85	19.12.04	00:00	67° 46,31' S	55° 14,95' \	1570,4	CTD/RO	surface
PS67/006-85	19.12.04	00:30	67° 46,30' S	55° 14,83' \	1573,6	CTD/RO	at depth
PS67/006-85	19.12.04	00:56	67° 46,31' S	55° 14,75' \	1575,6	CTD/RO	on deck
PS67/006-86	19.12.04	05:58	67° 46,37' S	55° 14,23' \	1587,2	CTD/RO	surface
PS67/006-86	19.12.04	06:30	67° 46,38' S	55° 14,25' \	1587,6	CTD/RO	at depth
PS67/006-86	19.12.04	06:53	67° 46,39' S	55° 14,28' \	1586,8	CTD/RO	on deck
PS67/006-87	19.12.04	12:00	67° 46,70' S	55° 16,00' \	1565,0	CTD/RO	surface
PS67/006-87	19.12.04	12:32	67° 46,75' S	55° 16,37' \	1566,0	CTD/RO	at depth
PS67/006-87	19.12.04	13:03	67° 46,83' S	55° 16,55' \	1552,8	CTD/RO	on deck
PS67/006-88	19.12.04	13:10	67° 46,85' S	55° 16,59' \	1547,2	BONGO	surface
PS67/006-88	19.12.04	13:39	67° 46,94' S	55° 16,72' \	1534,8	BONGO	at depth
PS67/006-88	19.12.04	14:11	67° 47,04' S	55° 16,80' \	1527,6	BONGO	on deck
PS67/006-89	19.12.04	18:00	67° 47,93' S	55° 16,20' \	1538,4	CTD/RO	surface
PS67/006-89	19.12.04	18:27	67° 48,04' S	55° 16,00' \	1543,6	CTD/RO	at depth
PS67/006-89	19.12.04	19:01	67° 48,17' S	55° 15,73' \	1550,8	CTD/RO	on deck
PS67/006-90	20.12.04	00:00	67° 49,01' S	55° 14,69' \	1580,0	CTD/RO	surface
PS67/006-90	20.12.04	00:30	67° 49,11' S	55° 14,90' \	1579,2	CTD/RO	at depth
PS67/006-90	20.12.04	00:55	67° 49,21' S	55° 15,09' \	1575,2	CTD/RO	on deck
PS67/006-91	20.12.04	06:00	67° 50,46' S	55° 16,98' \	1530,4	CTD/RO	surface
PS67/006-91	20.12.04	06:30	67° 50,55' S	55° 17,14' \	1528,8	CTD/RO	at depth
PS67/006-91	20.12.04	06:55	67° 50,64' S	55° 17,30' \	1527,2	CTD/RO	on deck
PS67/006-92	20.12.04	12:09	67° 51,26' S	55° 21,38' \	1438,4	CTD/RO	surface
PS67/006-92	20.12.04	12:38	67° 51,29' S	55° 21,96' \	1424,4	CTD/RO	at depth
PS67/006-92	20.12.04	13:10	67° 51,33' S	55° 22,61' \	1412,8	CTD/RO	on deck
PS67/006-93	20.12.04	13:19	67° 51,34' S	55° 22,79' \	1409,2	MN	surface
PS67/006-93	20.12.04	13:24	67° 51,34' S	55° 22,89' \	1415,2	MN	at depth
PS67/006-93	20.12.04	13:25	67° 51,35' S	55° 22,91' \	1407,2	MN	Hoisting
PS67/006-93	20.12.04	13:33	67° 51,35' S	55° 23,07' \	1404,4	MN	on deck
PS67/006-94	20.12.04	18:00	67° 51,40' S	55° 26,82' \	1322,8	CTD/RO	surface
PS67/006-94	20.12.04	18:26	67° 51,35' S	55° 26,91' \	1320,8	CTD/RO	at depth
PS67/006-94	20.12.04	19:05	67° 51,28' S	55° 27,02' \	1319,2	CTD/RO	on deck
PS67/006-95	20.12.04	23:58	67° 50,61' S	55° 28,87' \	1286,8	CTD/RO	surface
PS67/006-95	21.12.04	00:20	67° 50,56' S	55° 29,00' \	1284,4	CTD/RO	at depth
PS67/006-95	21.12.04	00:41	67° 50,51' S	55° 29,12' \	1282,0	CTD/RO	on deck
PS67/006-96	21.12.04	05:59	67° 50,02' S	55° 30,08' \	1259,6	CTD/RO	surface
PS67/006-96	21.12.04	06:25	67° 50,00' S	55° 30,09' \	1259,6	CTD/RO	at depth
PS67/006-96	21.12.04	06:53	67° 49,98' S	55° 30,11' \	1259,2	CTD/RO	on deck
PS67/006-97	21.12.04	07:03	67° 49,98' S	55° 30,11' \	1259,2	MN	surface
PS67/006-97	21.12.04	07:40	67° 49,97' S	55° 30,12' \	1258,8	MN	at depth
PS67/006-97	21.12.04	08:22	67° 49,96' S	55° 30,12' \	1259,2	MN	on deck
PS67/006-98	21.12.04	13:25	67° 49,65' S	55° 30,67' \	1244,8	CTD/RO	surface

Station	Date	Time	Position Lat	Position Lon	Depth [m]	Gear Abbreviat-ion	Action
PS67/006-98	21.12.04	13:50	67° 49,61' S	55° 30,78' W	1242,4	CTD/RO	at depth
PS67/006-98	21.12.04	14:11	67° 49,57' S	55° 30,88' W	1240,0	CTD/RO	on deck
PS67/006-99	21.12.04	18:00	67° 49,30' S	55° 31,62' W	1225,2	CTD/RO	surface
PS67/006-99	21.12.04	18:25	67° 49,29' S	55° 31,64' W	1225,2	CTD/RO	at depth
PS67/006-99	21.12.04	19:03	67° 49,29' S	55° 31,64' W	1225,2	CTD/RO	on deck
PS67/006-10	21.12.04	23:56	67° 49,32' S	55° 31,69' W	1222,8	CTD/RO	surface
PS67/006-10	22.12.04	00:21	67° 49,30' S	55° 31,71' W	1223,2	CTD/RO	at depth
PS67/006-10	22.12.04	00:48	67° 49,29' S	55° 31,74' W	1222,8	CTD/RO	on deck
PS67/006-10	22.12.04	06:08	67° 49,07' S	55° 32,22' W	1217,6	CTD/RO	surface
PS67/006-10	22.12.04	06:33	67° 49,06' S	55° 32,24' W	1217,6	CTD/RO	at depth
PS67/006-10	22.12.04	06:53	67° 49,05' S	55° 32,25' W	1217,6	CTD/RO	on deck
PS67/006-10	22.12.04	12:18	67° 49,05' S	55° 32,32' W	1216,0	CTD/RO	surface
PS67/006-10	22.12.04	12:42	67° 49,05' S	55° 32,38' W	1215,6	CTD/RO	at depth
PS67/006-10	22.12.04	13:03	67° 49,04' S	55° 32,44' W	1214,4	CTD/RO	on deck
PS67/006-10	22.12.04	18:01	67° 48,88' S	55° 33,30' W	1201,6	CTD/RO	surface
PS67/006-10	22.12.04	18:26	67° 48,87' S	55° 33,33' W	1201,2	CTD/RO	at depth
PS67/006-10	22.12.04	19:05	67° 48,86' S	55° 33,36' W	1200,8	CTD/RO	on deck
PS67/006-10	23.12.04	00:00	67° 48,78' S	55° 33,93' W	1189,2	CTD/RO	surface
PS67/006-10	23.12.04	00:24	67° 48,78' S	55° 33,99' W	1188,0	CTD/RO	at depth
PS67/006-10	23.12.04	00:43	67° 48,78' S	55° 34,05' W	1186,4	CTD/RO	on deck
PS67/006-10	23.12.04	05:59	67° 48,68' S	55° 34,93' W	1178,0	CTD/RO	surface
PS67/006-10	23.12.04	06:20	67° 48,67' S	55° 34,94' W	1169,6	CTD/RO	at depth
PS67/006-10	23.12.04	06:40	67° 48,66' S	55° 34,94' W	1169,2	CTD/RO	on deck
PS67/006-10	23.12.04	14:58	67° 48,79' S	55° 35,48' W	1153,2	BONGO	surface
PS67/006-10	23.12.04	15:10	67° 48,78' S	55° 35,49' W	1153,2	BONGO	at depth
PS67/006-10	23.12.04	15:25	67° 48,77' S	55° 35,51' W	1153,2	BONGO	on deck
PS67/006-10	23.12.04	17:58	67° 48,62' S	55° 35,69' W	1153,2	CTD/RO	surface
PS67/006-10	23.12.04	18:20	67° 48,60' S	55° 35,77' W	1152,8	CTD/RO	on deck
PS67/006-10	24.12.04	05:59	67° 48,69' S	55° 37,66' W	1108,8	CTD/RO	surface
PS67/006-10	24.12.04	06:20	67° 48,68' S	55° 37,69' W	1107,6	CTD/RO	at depth
PS67/006-10	24.12.04	06:50	67° 48,67' S	55° 37,72' W	1106,8	CTD/RO	on deck
PS67/006-10	24.12.04	11:56	67° 48,66' S	55° 37,86' W	1101,2	CTD/RO	surface
PS67/006-10	24.12.04	12:19	67° 48,66' S	55° 37,86' W	1100,8	CTD/RO	at depth
PS67/006-10	24.12.04	12:46	67° 48,66' S	55° 37,87' W	1100,8	CTD/RO	on deck
PS67/006-11	25.12.04	08:17	67° 47,87' S	55° 39,96' W	1051,2	CTD/RO	surface
PS67/006-11	25.12.04	08:39	67° 47,85' S	55° 39,93' W	1051,2	CTD/RO	at depth
PS67/006-11	25.12.04	09:01	67° 47,84' S	55° 39,92' W	1051,2	CTD/RO	on deck
PS67/006-1	25.12.04	13:08	67° 47,89' S	55° 39,33' W	1063,6	ICE	Ice Gangway on board
PS67/006-1	25.12.04	13:08	67° 47,89' S	55° 39,33' W	1063,6	ICE	Departure from floe
PS67/006-1	25.12.04	13:50	67° 48,16' S	55° 38,59' W	1085,6	ICE	Alongside Floe
PS67/006-1	25.12.04	19:00	67° 47,75' S	55° 37,70' W	1101,2	ICE	Departure from floe
PS67/006-1	25.12.04	19:30	67° 47,74' S	55° 37,51' W	1106,4	ICE	Alongside Floe
PS67/006-11	26.12.04	05:57	67° 46,85' S	55° 38,86' W	1091,2	CTD/RO	surface
PS67/006-11	26.12.04	06:19	67° 46,87' S	55° 39,01' W	1088,0	CTD/RO	at depth
PS67/006-11	26.12.04	06:43	67° 46,90' S	55° 39,15' W	1085,6	CTD/RO	on deck
PS67/006-11	26.12.04	07:01	67° 46,92' S	55° 39,24' W	1084,0	MN	surface
PS67/006-11	26.12.04	07:39	67° 47,00' S	55° 39,40' W	1080,0	MN	at depth
PS67/006-11	26.12.04	08:25	67° 47,14' S	55° 39,48' W	1065,2	MN	on deck
PS67/006-11	26.12.04	12:14	67° 48,32' S	55° 39,14' W	1076,0	CTD/RO	surface
PS67/006-11	26.12.04	12:37	67° 48,46' S	55° 39,10' W	1077,2	CTD/RO	at depth
PS67/006-11	26.12.04	13:11	67° 48,68' S	55° 39,04' W	1075,6	CTD/RO	on deck
PS67/006-11	26.12.04	13:25	67° 48,77' S	55° 39,01' W	1075,2	MN	surface

Station	Date	Time	Position Lat	Position Lon	Depth [m]	Gear Abbreviation	Action
PS67/006-11	26.12.04	13:38	67° 48,86' S	55° 38,98' W	1074,8	MN	at depth
PS67/006-11	26.12.04	13:38	67° 48,86' S	55° 38,98' W	1074,8	MN	Hoisting
PS67/006-11	26.12.04	13:54	67° 48,96' S	55° 38,96' W	1075,2	MN	on deck
PS67/006-11	26.12.04	18:03	67° 50,17' S	55° 39,04' W	1074,0	CTD/RO	surface
PS67/006-11	26.12.04	18:26	67° 50,23' S	55° 39,09' W	1072,0	CTD/RO	at depth
PS67/006-11	26.12.04	19:00	67° 50,30' S	55° 39,08' W	1066,4	CTD/RO	on deck
PS67/006-11	27.12.04	06:26	67° 49,61' S	55° 40,29' W	1048,4	CTD/RO	surface
PS67/006-11	27.12.04	06:47	67° 49,61' S	55° 40,26' W	1049,2	CTD/RO	at depth
PS67/006-11	27.12.04	07:04	67° 49,61' S	55° 40,23' W	1050,4	CTD/RO	on deck
PS67/006-11	27.12.04	08:15	67° 49,62' S	55° 39,69' W	1063,6	BG	surface
PS67/006-11	27.12.04	08:36	67° 49,62' S	55° 39,37' W	1069,6	BG	at sea bottom
PS67/006-11	27.12.04	08:59	67° 49,61' S	55° 38,95' W	1076,8	BG	on deck
PS67/006-11	27.12.04	12:00	67° 48,96' S	55° 33,65' W	1190,8	CTD/RO	surface
PS67/006-11	27.12.04	12:24	67° 48,79' S	55° 32,93' W	1211,2	CTD/RO	at depth
PS67/006-11	27.12.04	12:50	67° 48,56' S	55° 32,24' W	1231,2	CTD/RO	on deck
PS67/006-11	27.12.04	13:14	67° 48,39' S	55° 31,67' W	1241,2	BONGO	surface
PS67/006-11	27.12.04	14:13	67° 47,97' S	55° 30,58' W	1261,2	BONGO	at depth
PS67/006-11	27.12.04	15:11	67° 47,61' S	55° 29,57' W	1280,0	BONGO	on deck
PS67/006-12	27.12.04	18:00	67° 46,94' S	55° 27,29' W	1312,4	CTD/RO	surface
PS67/006-12	27.12.04	18:25	67° 46,85' S	55° 26,94' W	1319,6	CTD/RO	at depth
PS67/006-12	27.12.04	18:53	67° 46,75' S	55° 26,53' W	1328,4	CTD/RO	on deck
PS67/006-12	27.12.04	23:56	67° 45,12' S	55° 22,23' W	1426,8	CTD/RO	surface
PS67/006-12	28.12.04	00:27	67° 44,95' S	55° 22,10' W	1426,8	CTD/RO	at depth
PS67/006-12	28.12.04	00:50	67° 44,84' S	55° 22,07' W	1425,2	CTD/RO	on deck
PS67/006-12	28.12.04	05:58	67° 44,11' S	55° 24,60' W	1378,8	CTD/RO	surface
PS67/006-12	28.12.04	06:23	67° 44,09' S	55° 24,78' W	1375,6	CTD/RO	at depth
PS67/006-12	28.12.04	06:44	67° 44,07' S	55° 24,92' W	1372,8	CTD/RO	on deck
PS67/006-12	28.12.04	12:00	67° 42,82' S	55° 23,57' E	1406,4	CTD	surface
PS67/006-12	28.12.04	12:27	67° 42,63' S	55° 23,17' W	1415,6	CTD	at depth
PS67/006-12	28.12.04	12:58	67° 42,39' S	55° 22,70' W	1419,2	CTD	on deck
PS67/006-12	28.12.04	13:15	67° 42,25' S	55° 22,43' W	1422,8	MN	surface
PS67/006-12	28.12.04	14:09	67° 41,78' S	55° 21,60' W	1440,8	MN	at depth
PS67/006-12	28.12.04	14:10	67° 41,77' S	55° 21,59' W	1441,2	MN	Hoisting
PS67/006-12	28.12.04	15:09	67° 41,26' S	55° 20,79' W	1479,6	MN	on deck
PS67/006-12	28.12.04	18:12	67° 39,85' S	55° 19,20' W	1510,8	CTD/RO	surface
PS67/006-12	28.12.04	18:31	67° 39,71' S	55° 19,09' W	1507,2	CTD/RO	on deck
PS67/006-12	28.12.04	19:45	67° 39,19' S	55° 18,64' W	1518,0	CTD/RO	surface
PS67/006-12	28.12.04	20:11	67° 39,01' S	55° 18,48' W	1538,4	CTD/RO	at depth
PS67/006-12	28.12.04	20:42	67° 38,80' S	55° 18,28' W	1548,0	CTD/RO	on deck
PS67/006-12	28.12.04	23:55	67° 37,52' S	55° 17,07' W	1586,4	CTD/RO	surface
PS67/006-12	29.12.04	00:22	67° 37,34' S	55° 16,92' W	1590,4	CTD/RO	at depth
PS67/006-12	29.12.04	00:47	67° 37,18' S	55° 16,79' W	1588,4	CTD/RO	on deck
PS67/006-12	29.12.04	06:00	67° 35,20' S	55° 17,95' W	1546,0	CTD/RO	surface
PS67/006-12	29.12.04	06:27	67° 35,06' S	55° 18,25' W	1541,2	CTD/RO	at depth
PS67/006-12	29.12.04	06:59	67° 34,92' S	55° 18,63' W	1534,4	CTD/RO	on deck
PS67/006-12	29.12.04	07:18	67° 34,84' S	55° 18,85' W	1534,0	MN	surface
PS67/006-12	29.12.04	07:55	67° 34,70' S	55° 19,26' W	1528,0	MN	at depth
PS67/006-12	29.12.04	08:35	67° 34,56' S	55° 19,68' W	1520,0	MN	on deck
PS67/006-13	29.12.04	11:59	67° 33,88' S	55° 20,80' W	1490,4	CTD/RO	surface
PS67/006-13	29.12.04	12:25	67° 33,80' S	55° 20,69' W	1496,0	CTD/RO	at depth
PS67/006-13	29.12.04	13:00	67° 33,68' S	55° 20,47' W	1498,8	CTD/RO	on deck
PS67/006-13	29.12.04	18:06	67° 32,33' S	55° 18,30' W	1556,4	CTD/RO	surface
PS67/006-13	29.12.04	18:35	67° 32,18' S	55° 18,24' W	1557,2	CTD/RO	at depth
PS67/006-13	29.12.04	19:25	67° 31,92' S	55° 18,21' W	1562,8	CTD/RO	on deck
PS67/006-13	30.12.04	00:00	67° 30,82' S	55° 17,84' W	1590,4	CTD/RO	surface

Station	Date	Time	Position Lat	Position Lon	Depth [m]	Gear Abbreviation	Action
PS67/006-13	30.12.04	00:29	67° 30,73' S	55° 17,71' W	1593,2	CTD/RO	at depth
PS67/006-13	30.12.04	00:55	67° 30,64' S	55° 17,61' W	1586,8	CTD/RO	on deck
PS67/006-13	30.12.04	05:59	67° 29,58' S	55° 17,95' W	1582,4	CTD/RO	surface
PS67/006-13	30.12.04	06:27	67° 29,49' S	55° 18,22' W	1577,2	CTD/RO	at depth
PS67/006-13	30.12.04	06:52	67° 29,41' S	55° 18,49' W	1573,2	CTD/RO	on deck
PS67/006-13	30.12.04	12:03	67° 28,70' S	55° 21,17' W	1529,6	CTD/RO	surface
PS67/006-13	30.12.04	12:31	67° 28,68' S	55° 21,15' W	1530,0	CTD/RO	at depth
PS67/006-13	30.12.04	13:06	67° 28,65' S	55° 21,11' W	1531,2	CTD/RO	on deck
PS67/006-13	30.12.04	18:05	67° 28,04' S	55° 20,29' W	1581,6	CTD/RO	surface
PS67/006-13	30.12.04	18:34	67° 27,95' S	55° 20,35' W	1580,4	CTD/RO	at depth
PS67/006-13	30.12.04	19:13	67° 27,83' S	55° 20,48' W	1575,6	CTD/RO	on deck
PS67/006-13	30.12.04	23:57	67° 27,12' S	55° 20,89' W	1549,2	CTD/RO	surface
PS67/006-13	31.12.04	00:25	67° 27,05' S	55° 20,84' W	1552,8	CTD/RO	at depth
PS67/006-13	31.12.04	00:49	67° 26,98' S	55° 20,79' W	1557,6	CTD/RO	on deck
PS67/006-13	31.12.04	05:58	67° 26,09' S	55° 21,18' W	1555,6	CTD/RO	surface
PS67/006-13	31.12.04	06:26	67° 26,02' S	55° 21,41' W	1552,4	CTD/RO	at depth
PS67/006-13	31.12.04	06:51	67° 25,97' S	55° 21,64' W	1548,0	CTD/RO	on deck
PS67/006-13	31.12.04	07:02	67° 25,95' S	55° 21,75' W	1544,8	BONGO	surface
PS67/006-13	31.12.04	08:03	67° 25,85' S	55° 22,37' W	1530,4	BONGO	at depth
PS67/006-13	31.12.04	09:08	67° 25,77' S	55° 23,04' W	1517,2	BONGO	on deck
PS67/006-13	31.12.04	10:49	67° 25,67' S	55° 23,89' W	1500,4	CTD/RO	surface
PS67/006-13	31.12.04	11:15	67° 25,64' S	55° 24,03' W	1497,2	CTD/RO	at depth
PS67/006-13	31.12.04	11:45	67° 25,61' S	55° 24,16' W	1495,6	CTD/RO	on deck
PS67/006-14	01.01.05	09:59	67° 22,69' S	55° 25,23' W	1408,8	CTD/RO	surface
PS67/006-14	01.01.05	10:25	67° 22,68' S	55° 25,40' W	1405,2	CTD/RO	at depth
PS67/006-14	01.01.05	10:49	67° 22,66' S	55° 25,55' W	1385,6	CTD/RO	on deck
PS67/006-14	01.01.05	11:00	67° 22,65' S	55° 25,61' W	1401,6	MN	surface
PS67/006-14	01.01.05	11:18	67° 22,63' S	55° 25,69' W	1400,0	MN	at depth
PS67/006-14	01.01.05	11:40	67° 22,62' S	55° 25,77' W	1398,4	MN	on deck
PS67/006-14	01.01.05	18:04	67° 22,28' S	55° 24,85' W	1411,2	CTD/RO	surface
PS67/006-14	01.01.05	18:31	67° 22,24' S	55° 24,79' W	1412,0	CTD/RO	at depth
PS67/006-14	01.01.05	19:08	67° 22,20' S	55° 24,73' W	1412,4	CTD/RO	on deck
PS67/006-14	01.01.05	23:58	67° 21,85' S	55° 24,49' W	1405,2	CTD/RO	surface
PS67/006-14	02.01.05	00:23	67° 21,83' S	55° 24,42' W	1405,2	CTD/RO	at depth
PS67/006-14	02.01.05	00:43	67° 21,80' S	55° 24,35' W	1406,0	CTD/RO	on deck
PS67/006-14	02.01.05	05:59	67° 21,45' S	55° 23,36' W	1422,4	CTD/RO	surface
PS67/006-14	02.01.05	06:24	67° 21,41' S	55° 23,36' W	1421,6	CTD/RO	surface
PS67/006-14	02.01.05	06:52	67° 21,38' S	55° 23,39' W	1419,6	CTD/RO	on deck
PS67/006-14	02.01.05	07:02	67° 21,37' S	55° 23,41' W	1419,2	MN	surface
PS67/006-14	02.01.05	07:38	67° 21,32' S	55° 23,47' W	1418,0	MN	at depth
PS67/006-14	02.01.05	08:20	67° 21,27' S	55° 23,58' W	1416,4	MN	on deck
PS67/006-14	02.01.05	10:00	67° 21,18' S	55° 23,93' W	1412,4	CTD/RO	surface
PS67/006-14	02.01.05	10:26	67° 21,16' S	55° 24,02' W	1411,6	CTD/RO	at depth
PS67/006-14	02.01.05	10:50	67° 21,15' S	55° 24,09' W	1410,8	CTD/RO	on deck
PS67/006-1	02.01.05	12:05	67° 21,16' S	55° 24,28' W	1406,0	ICE	Ice Gangway on board
PS67/006-1	02.01.05	12:06	67° 21,16' S	55° 24,28' W	1405,6	ICE	Departure from floe
PS67/007-1	03.01.05	07:02	67° 6,38' S	55° 21,55' W	1142,4	CTD/RO	surface
PS67/007-1	03.01.05	07:24	67° 6,40' S	55° 21,49' W	1144,0	CTD/RO	at depth
PS67/007-1	03.01.05	07:58	67° 6,43' S	55° 21,46' W	1144,8	CTD/RO	on deck
PS67/008-1	04.01.05	01:40	67° 2,59' S	55° 23,88' W	1003,6	CTD/RO	surface
PS67/008-1	04.01.05	02:01	67° 2,60' S	55° 23,56' W	1012,0	CTD/RO	at depth
PS67/008-1	04.01.05	02:26	67° 2,67' S	55° 23,38' W	1016,4	CTD/RO	on deck
PS67/009-1	04.01.05	05:03	66° 53,99' S	55° 20,72' W	1821,6	CTD/RO	surface

Station	Date	Time	Position Lat	Position Lon	Depth [m]	Gear Abbreviat-ion	Action
PS67/009-1	04.01.05	05:22	66° 54,05' S	55° 20,70' \	0,0	CTD/RO	at depth
PS67/009-1	04.01.05	05:49	66° 54,22' S	55° 20,66' \	1856,0	CTD/RO	on deck
PS67/010-1	05.01.05	21:13	63° 44,35' S	52° 19,07' \	899,2	BUCKET	surface
PS67/010-1	05.01.05	21:14	63° 44,23' S	52° 18,92' \	900,0	BUCKET	on deck
PS67/011-1	07.01.05	06:05	59° 51,88' S	45° 59,66' \	4202,7	CTD/RO	surface
PS67/011-1	07.01.05	07:14	59° 52,27' S	45° 59,17' \	4259,6	CTD/RO	at depth
PS67/011-1	07.01.05	08:13	59° 52,75' S	45° 58,74' \	4301,2	CTD/RO	on deck
PS67/011-2	07.01.05	08:55	59° 53,12' S	45° 58,25' \	4279,4	CTD/RO	surface
PS67/011-2	07.01.05	09:21	59° 53,33' S	45° 57,63' \	4210,9	CTD/RO	at depth
PS67/011-2	07.01.05	09:46	59° 53,52' S	45° 56,93' \	4144,7	CTD/RO	on deck
PS67/011-3	07.01.05	10:33	59° 53,91' S	45° 55,86' \	4185,4	CTD/RO	surface
PS67/011-3	07.01.05	11:40	59° 54,61' S	45° 54,60' \	4339,7	CTD/RO	at depth
PS67/011-3	07.01.05	13:00	59° 54,85' S	45° 53,63' \	4358,9	CTD/RO	on deck

„Berichte zur Polarforschung“
Eine Titelübersicht der Hefte 1 bis 376 (1981 - 2000) erschien zuletzt im Heft 413 der nachfolgenden Reihe „Berichte zur Polar- und Meeresforschung“. Ein Verzeichnis aller Hefte beider Reihen sowie eine Zusammenstellung der Abstracts in englischer Sprache finden Sie im Internet unter der Adresse:
http://www.awi-bremerhaven.de/Resources/publications.html

Ab dem Heft-Nr. 377 erscheint die Reihe unter dem Namen:
„Berichte zur Polar- und Meeresforschung“

Heft-Nr. 377/2000 – „Rekrutierungsmuster ausgewählter Wattfauna nach unterschiedlich strengen Wintern“ von Matthias Strasser

Heft-Nr. 378/2001 – „Der Transport von Wärme, Wasser und Salz in den Arktischen Ozean“, von Boris Cisewski

Heft-Nr. 379/2001 – „Analyse hydrographischer Schnitte mit Satellitenaltimetrie“, von Martin Losch

Heft-Nr. 380/2001 – „Die Expeditionen ANTARKTIS XI/1-2 des Forschungsschiffes POLARSTERN 1998/1999“, herausgegeben von Eberhard Fahrbach und Saad El Naggar.

Heft-Nr. 381/2001 – „UV-Schutz- und Reparaturmechanismen bei antarktischen Diatomeen und Phaeocystis antarctica“, von Lieselotte Riegger.

Heft-Nr. 382/2001 – „Age determination in polar Crustacea using the autofluorescent pigment lipofuscin“, by Bodil Bluhm.

Heft-Nr. 383/2001 – „Zeitliche und räumliche Verteilung, Habitatspräferenzen und Populationsdynamik benthischer Copepoda Harpacticoida in der Potter Cove (King George Island, Antarktis)“, von Gritta Veit-Köhler.

Heft-Nr. 384/2001 – „Beiträge aus geophysikalischen Messungen in Dronning Maud Land, Antarktis, zur Auffindung eines optimalen Bohrpunktes für eine Eiskerntiefbohrung“, von Daniel Steinhage.

Heft-Nr. 385/2001 – „Actinium-227 als Tracer für Advektion und Mischung in der Tiefsee“, von Walter Geibert.

Heft-Nr. 386/2001 – „Messung von optischen Eigenschaften troposphärischer Aerosole in der Arktis“ von Rolf Schumacher.

Heft-Nr. 387/2001 – „Bestimmung des Ozonabbaus in der arktischen und subarktischen Stratosphäre“, von Astrid Schulz.

Heft-Nr. 388/2001 – „Russian-German Cooperation SYSTEM LAPTEV SEA 2000: The Expedition LENA 2000“, edited by Volker Rachold and Mikhail N. Grigoriev.

Heft-Nr. 389/2001 – „The Expeditions ARKTIS XVI/1 and ARKTIS XVI/2 of the Research Vessel ‘Polarstern’ in 2000“, edited by Gunther Krause and Ursula Schauer.

Heft-Nr. 390/2001 – „Late Quaternary climate variations recorded in North Atlantic deep-sea ostracodes“, by Claudia Didié.

Heft-Nr. 391/2001 – „The polar and subpolar North Atlantic during the last five glacial-interglacial cycles“, by Jan. P. Helmke.

Heft-Nr. 392/2000 – „Geochemische Untersuchungen an hydrothermal beeinflußten Sedimenten der Bransfield Straße (Antarktis)“, von Anke Dählmann.

Heft-Nr. 393/2001 – „The German-Russian Project on Siberian River Run-off (SIRRO): Scientific Cruise Report of the Kara-Sea Expedition ‘SIRRO 2000’ of RV ‘Boris Petrov’ and first results“, edited by Ruediger Stein and Oleg Stepanets.

Heft-Nr. 394/2001 – „Untersuchung der Photooxidantien Wasserstoffperoxid, Methylhydroperoxid und Formaldehyd in der Troposphäre der Antarktis“, von Katja Riedel.

Heft-Nr. 395/2001 – „Role of benthic cnidarians in the energy transfer processes in the Southern Ocean marine ecosystem (Antarctica)“, by Covadonga Orejas Saco del Valle.

Heft-Nr. 396/2001 – „Biogeochemistry of Dissolved Carbohydrates in the Arctic“, by Ralph Engbrodt.

Heft-Nr. 397/2001 – „Seasonality of marine algae and grazers of an Antarctic rocky intertidal, with emphasis on the role of the limpet Nacilla concinna Strebel (Gastropoda: Patellidae)“, by Dohong Kim.

Heft-Nr. 398/2001 – „Polare Stratosphärenwolken und mesoskalige Dynamik am Polarwirbelrand“, von Marion Müller.

Heft-Nr. 399/2001 – „North Atlantic Deep Water and Antarctic Bottom Water: Their Interaction and Influence on Modes of the Global Ocean Circulation“, by Holger Brix.

Heft-Nr. 400/2001 – „The Expeditions ANTARKTIS XVIII/1-2 of the Research Vessel ‘Polarstern’ in 2000“ edited by Victor Smetacek, Ulrich Bathmann, Saad El Naggar.

Heft-Nr. 401/2001 – „Variabilität von CH_2O (Formaldehyd) - untersucht mit Hilfe der solaren Absorptionsspektroskopie und Modellen“ von Torsten Albrecht.

Heft-Nr. 402/2001 – „The Expedition ANTARKTIS XVII/3 (EASIZ III) of RV ‘Polarstern’ in 2000“, edited by Wolf E. Arntz and Thomas Brey.

Heft-Nr. 403/2001 – „Mikrohabitatansprüche benthischer Foraminiferen in Sedimenten des Südatlantiks“, von Stefanie Schumacher.

Heft-Nr. 404/2002 – „Die Expedition ANTARKTIS XVII/2 des Forschungsschiffes ‘Polarstern’ 2000“, herausgegeben von Jörn Thiede und Hans Oerter.

Heft-Nr. 405/2002 – „Feeding Ecology of the Arctic Ice-Amphipod Gammarus wilkitzkii. Physiological, Morphological and Ecological Studies“, by Carolin E. Arndt.

Heft-Nr. 406/2002 – „Radiolarienfauna im Ochotskischen Meer - eine aktuopaläontologische Charakterisierung der Biozönose und Taphozönose“, von Anja Nimmergut.

Heft-Nr. 407/2002 – „The Expedition ANTARKTIS XVIII/5b of the Research Vessel ‘Polarstern’ in 2001, edited by Ulrich Bathmann.

Heft-Nr. 408/2002 – „Siedlungsmuster und Wechselbeziehungen von Seepocken (Cirripedia) auf Muschelbänken (Mytilus edulis L.) im Wattenmeer“, von Christian Buschbaum.

Heft-Nr. 409/2002 – „Zur Ökologie von Schmelzwassertümpeln auf arktischem Meereis - Charakteristika, saisonale Dynamik und Vergleich mit anderen aquatischen Lebensräumen polarer Regionen“, von Marina Carstens.

Heft-Nr. 410/2002 – „Impuls- und Wärmeaustausch zwischen der Atmosphäre und dem eisbedeckten Ozean“, von Thomas Garbrecht.

Heft-Nr. 411/2002 – „Messung und Charakterisierung laminarer Ozonstrukturen in der polaren Stratosphäre“, von Petra Wahl.

Heft-Nr. 412/2002 – „Open Ocean Aquaculture und Offshore Windparks. Eine Machbarkeitsstudie über die multifunktionale Nutzung von Offshore-Windparks und Offshore-Marikultur im Raum Nordsee“, von Bela Hieronymus Buck.

Heft-Nr. 413/2002 – „Arctic Coastal Dynamics. Report of an International Workshop. Potsdam (Germany) 26-30 November 2001“, edited by Volker Rachold, Jerry Brown and Steve Solomon.

Heft-Nr. 414/2002 – „Entwicklung und Anwendung eines Laserablations-ICP-MS-Verfahrens zur Multielementanalyse von atmosphärischen Einträgen in Eisbohrkernen“, von Heiko Reinhardt.

Heft-Nr. 415/2002 – „Gefrier- und Tauprozesse im sibirischen Permafrost – Untersuchungsmethoden und ökologische Bedeutung“, von Wiebke Müller-Lupp.

Heft-Nr. 416/2002 – „Natürliche Klimavariationen der Arktis in einem regionalen hochauflösenden Atmosphärenmodell“, von Wolfgang Dorn.

Heft-Nr. 417/2002 – „Ecological comparison of two sandy shores with different wave energy and morphodynamics in the North Sea“, by Iris Menn.

Heft-Nr. 418/2002 – „Numerische Modellierung turbulenter Umströmungen von gebäuden“, von Simón Domingo López.

Heft-Nr. 419/2002 – „Scientific Cruise Report of the Kara-Sea Expedition 2001 of RV „Academic Petrov“: The German-Russian Project on Siberian River Run-off (SIRRO) and the Project „ESTABLISH“, edited by Ruediger Stein and Oleg Stepanets.

Heft-Nr. 420/2002 – „Vulkanologie und Geochemie pliozäner bis rezenter Vulkanite beiderseits der Bransfield-Straße / West-Antarktis“, von Andreas Veit.

Heft-Nr. 421/2002 – „POLARSTERN ARKTIS XVII/2 Cruise Report: AMORE 2001 (Arctic Mid-Ocean Ridge Expedition)“, by J. Thiede et al.

Heft-Nr. 422/2002 – „The Expedition „AWI of RV „L’Atalante“ in 2001“, edited by Michael Klages, Benoit Mesnil, Thomas Soltwedel and Alain Christophe with contributions of the participants.

Heft-Nr. 423/2002 – „Über die Tiefenwasserausbreitung im Weddellmeer und in der Scotia-Sea: Numerische Untersuchungen der Transport- und Austauschprozesse in der Weddell-Scotia-Konfluenz-Zone“, von Michael Schodlok.

Heft-Nr. 424/2002 – „Short- and Long-Term Environmental Changes in the Laptev Sea (Siberian Arctic) During the Holocene“, von Thomas Müller-Lupp.

Heft-Nr. 425/2002 – „Characterisation of glacio-chemical and glacio-meteorological parameters of Amundsenisen, Dronning Maud Land, Antarctica“, by Fidan Göktas.

Heft-Nr. 426/2002 – „Russian-German Cooperation SYSTEM LAPTEV SEA 2000: The Expedition LENA 2001“, edited by Eva-Maria Pfeiffer and Mikhail N. Grigoriev.

Heft-Nr. 427/2002 – „From the Inner Shelf to the Deep Sea: Depositional Environments on the West Antarctic Peninsula Margin – A Sedimentological and Seismostratigraphic Study (ODP Leg 178)“, by Tobias Mörz.

Heft-Nr. 428/2002 – „Concentration and Size Distribution of Microparticles in the NGRIP Ice Core (Central Greenland) during the Last Glazial Period“, by Urs Ruth.

Heft-Nr. 429/2002 – „Interpretation von FCKW-Daten im Weddellmeer“, von Olaf Klatt.

Heft-Nr. 430/2002 – „Thermal History of the Middle and Late Miocene Southern Ocean - Diatom Evidence“, by Bernd M. Censarek.

Heft-Nr. 431/2002 – „Radium-226 and Radium-228 in the Atlantic Sector of the Southern Ocean“, by Claudia Hanfland.

Heft-Nr. 432/2002 – „Population dynamics and ecology of the surf clam Donax serra (Bivalvia, Donacidae) inhabiting beaches of the Benguela upwelling system“, by Jürgen Laudien.

Heft-Nr. 433/2002 – „Die Expedition ARKTIS XVII/1 des Forschungsschiffes POLARSTERN 2001“, herausgegeben von Eberhard Fahrbach.

Heft-Nr. 434/2002 – „The Rôle of Sponges in High-Antarctic Carbon and Silicon Cycling – a Modelling Approach“, by Susanne Gatti.

Heft-Nr. 435/2003 – „Sedimente des Changeable-Sees, Oktoberrevolutions-Insel (Severnaja Zemlja), als Archive der Paläoumwelt Mittelsibiriens seit dem Frühweichsel“, von Alexandra Raab.

Heft-Nr. 436/2003 – „The charnockite-anorthosite suite of rocks exposed in central Dronning Maud Land, East Antarctica: a study on fluid-rock interactions, and post-entrapment change of metamorphic fluid inclusions“, by Bärbel Kleinefeld.

Heft-Nr. 437/2003 – „Variable C:N Ratios of Particulate Organic Matter and Their Influence on the Marine Carbon Cycle“, by Birgit Schneider.

Heft-Nr. 438/2003 – „Population ecology and genetics of the polychaete Scoloplos armiger (Orbiniidae)“, by Inken Kruse.

Heft-Nr. 439/2003 – „Architecture and geodynamic evolution of the Svalbard Archipelago, the Yermak Plateau and the Fram Strait oceanic Province from deep seismic experiments“, by Oliver Ritzmann.

Heft-Nr. 440/2003 – „Occurrence, induction and physiological importance of UV-absorbing substances in polar macroalgae“, by Kirsten Hoyer.

Heft-Nr. 441/2003 – „Sea ice conditions in the Transpolar Drift in August/September 2001. Observations during POLARSTERN cruise ARKTIS XVII/2“, compiled by Christian Haas and Jan J. Lieser.

Heft-Nr. 442/2003 – Süßwassereintrag und Festeis in der ostsibirischen Arktis - Ergebnisse aus Boden- und Satelliten-beobachtungen sowie Sensitivitätsstudien mit einem thermodynamischen Festeismodell“, von Jörg Bareiss.

Heft-Nr. 443/2003 – „Arctic Coastal Dynamics. Report of the 3rd International Workshop. University of Oslo (Norway) 2-5 December 2002“, edited by Volker Rachold, Jerry Brown, Steven Solomon and Johan Ludvig Sollid.

Heft-Nr. 444/2003 – „Ventilation der Grönlandsee – Variabilität und ihre Ursachen 1994-2001“, von Stephanie Ronski.

Heft-Nr. 445/2003 – „Die Expedition ANTARKTIS XVIII/3-4 des Forschungsschiffes POLARSTERN 2000/2001 sowie die Aktivitäten an Land und bei der Neumayer-Station“, herausgegeben von Eberhard Fahrbach, Dieter Fütterer, Saad El Naggar und Hans Oerter.

Heft-Nr. 446/2003 – „The Expedition ARKTIS XVIII/1 a, b of the Research Vessel „Polarstern“ in 2002“, edited by Peter Lemke

Heft-Nr. 447/2003 – „Investigation of the Greenland Atmospheric Boundary Layer over Summit 2002 (IGLOS). Field Phase Report“, by Clemens Drüe and Günther Heinemann.

Heft-Nr. 448/2003 – „Die Expedition ANTARKTIS XIX mit FS „Polarstern“ 2001/2002. Bericht von den Fahrtabschnitten 1 und 2“, herausgegeben von Wilfried Jokat und Gunther Krause.

Heft-Nr. 449/2003 – „The Expedition ARKTIS XVIII/2 of RV „Polarstern“ in 2002. Contributions of the Participants“, edited by Wilfried Jokat.

Heft-Nr. 450/2003 – „Scientific Cruise Report of the joint Russian-German Kara Sea Expedition in 2002 with RV „Akademik Boris Petrov“, edited by Frank Schoster and Michael Levitan.

Heft-Nr. 451/2003 – „Die Krustenstruktur der Fjordregion Ostgrönlands zwischen dem präkambrischen Schild und den rezenten mittelozeanischen Rücken: Ergebnisse seismischer und gravimetrischer Modellierungen“, von Mechita Schmidt-Aursch.

Heft-Nr. 452/2003 – „Untersuchungen zur Biodiversität antarktischer benthischer Amphipoda (Malacostraca, Crustacea)“, von Anne-Nina Lörz.

Heft-Nr. 453/2003 – „The Antarctic Circumpolar Current: Dynamics of a circumpolar channel with blocked geostrophic contours“, by Daniel Borowski.

Heft-Nr. 454/2003 – „The effects of climate induced temperature changes on Cod (Gadus morhua L.): Linking ecological and physiological investigations“, by Torsten Fischer.

Heft-Nr. 455/2003 – „Sediment Transport on Arctic Shelves – Seasonal Variations in Suspended Particulate Matter Dynamics on the Laptev Sea Shelf (Siberian Arctic)“, by Carolyn Wegner.

Heft-Nr. 456/2003 – „Dynamics of the Ocean Surface in the Polar and Subpolar North Atlantic over the last 500 000 Years“, by Evguenia S. Kandiano

Heft-Nr. 457/2003 – „Structure and dynamics of a submarine continent: Tectonic-magmatic evolution of the Campbell Plateau (New Zealand). report of the RV „SONNE“ cruise SO-169, Project CAMP, 17 January to 24 February 2003“, edited by Karsten Gohl

Heft-Nr. 458/2003 – „Antioxidative properties of marine macroalgae from the Arctic“ by Angelika Dummermuth.

Heft-Nr. 459/2003 – „Analysing benthic communities in the Weddell Sea (Antarctica): a landscape approach“, by Núria Teixidó Ullod

Heft-Nr. 460/2003 – „The Expeditions Amery Oasis, East Antarctica, in 2001/02 and Taylor Valley, Southern Victoria Land, in 2002“, by Bernd Wagner.

Heft-Nr. 461/2003 – „Late Quaternary climate history of Northern Siberia – evidence from ground ice“, by Hanno Meyer.

Heft-Nr. 462/2003 – „The Expedition ANTARKTIS XIX/5 (LAMPOS) of RV ‘Polarstern’ in 2002“, edited by Wolf E. Arntz and Thomas Brey.

Heft-Nr. 463/2003 – „Distribution, composition, flux and variability of organic carbon in Fram Strait/Yermak Plateau (Arctic Ocean) and (palaeo) environmental significance“, by Daniel Birgel.

Heft-Nr. 464/2003 – „The influence of aerosols on the oceanic sedimentation and environmental conditions in the Arctic“, by Vladimir Shevchenko.

Heft-Nr. 465/2003 – „Chemical ecology and palatability of marine invertebrates in the sub-Arctic Kongsfjord (Spitsbergen), by Heike Lippert.

Heft-Nr. 466/2003 – „Russian-German Cooperation SYSTEM LAPTEV SEA. The Expedition LENA 2002“, edited by Mikhail N. Grigoriev, Volker Rachold, Dmitry Yu. Bolshianov, Eva-Maria Pfeiffer, Lutz Schirrmeister, Dirk Wagner and Hans-Wolfgang Hubberten.

Heft-Nr. 467/2003 – „Effekte von UV-Strahlung auf die antarktische Rotalge Palmaria decipiens“, von Frank Poppe.

Heft-Nr. 468/2003 – „Einfluss arktischer Süßwasserquellen auf die Zirkulation im Nordmeer und im Nordatlantik in einem prognostischen Ozean-Meereis-Modell“, von Matthias Prange.

Heft-Nr. 469/2003 – „Acclimation of the photosynthetic apparatus of the endemic Antarctic red marcroalga Palmaria decipiens to seasonally changing light conditions“, by Ulrike H. Lüder.

Heft-Nr. 470/2003 – „The Expeditions ANTARKTIS-XIX/3-4 of the Research Vessel POLARSTERN in 2002 (ANDEEP I and II: Antarctic benthic deep-sea biodiversity – colonization, history and recent community patterns)“, edited by Dieter K. Fütterer, Angelika Brandt and Gary C. B. Poore.

Heft-Nr. 471/2004 – „Late Quaternary Sedimentation History of the Lena Delta“, by Georg Johannes Schwamborn

Heft-Nr. 472/2004 – „Late Jurassic to Early Cretaceous black shale formation and paleoenvironment in high northern latitudes“, by Uwe Langrock.

Heft-Nr. 473/2004 – „Melatoningehalt in marinen Makroalgen. Entwicklung und Validierung quantitativer Bestimmungen mittels HPLC und Enzym-gekoppeltem Immunoassay“, von Carsten Pape.

Heft-Nr. 474/2004 – „On the nature, interpretation, and application of electromagnetic reflections in cold ice“, by Olaf Eisen.

Heft-Nr. 475/2004 – „The Expedition ARKTIS XIX/4 of the Research Vessel POLARSTERN in 2003. Reports of Legs 4a and 4b“, edited by Wilfried Jokat.

Heft-Nr. 476/2004 – „Variabilität chemischer und physikalischer Parameter des Aerosols in der antarktischen Troposphäre“, von Claudia Piel.

Heft-Nr. 477/2004 – „Die Entwicklung der deutschen Wattforschung: Ein wissenschaftshistorischer Beitrag zur Bedeutung der Pionierarbeiten“, von Hauke Bietz.

Heft-Nr. 478/2004 – „Multidecadal and NAO related variability in a numerical model of the North Atlantic circulation“, by Jennifer P. Brauch

Heft-Nr. 479/2004 – „Scientific Cruise Report of the Kara Sea Expedition with RV „Akademik Boris Petrov“ in 2003 within the frames of the Russian-German project „SIRRO“ and the Russian-Norwegian project „MAREAS“, edited by Frank Schoster and Michael Levitan.

Heft-Nr. 480/2004 – „Environment, adaptation and evolution: Scallop ecology across the latitudinal gradient“, by Olaf Heilmayer.

Heft-Nr. 481/2004 – „The Expedition ARKTIS XIX/1 a, b and XIX/2 of the Research Vessel „POLARSTERN“ in 2003“, edited by Ursula Schauer and Gerhard Kattner.

Heft-Nr. 482/2004 – „Arctic Coastal Dynamics. Report of the 4th International Workshop. VNIIOkeangeologia, St. Petersburg (Russia), 10-13 November 2003“, edited by Volker Rachold, and Georgy Cherkashov.

Heft-Nr. 483/2003 – „Reproductive trade-offs in benthic decapod crustaceans of high southern latitudes: tolerance of cold and food limitation“, by Sven Thatje.

Heft-Nr. 484/2004 – „Wavelength dependent induction and biosynthesis of UV-absorbing mycosporine-like amino acids in marine macroalgae“, by Gudrun Kräbs.

Heft-Nr. 485/2004 – „A Numerical Model for Short-term Sea Ice Forecasting in the Arctic“, by Jan Leonhard Lieser.

Heft-Nr. 486/2004 – „Zum Einfluß troposphärischer Aerosole auf das Klima der Arktis“, von Martin Fortmann.

Heft-Nr. 487/2004 – „Parallel Filter Algorithms for Data Assimilation in Oceanography“, by Lars Nerger.

Heft-Nr. 488/2004 – „The Expedition ARKTIS XIX/3 of the Research Vessel POLARSTERN in 2003. Reports of Legs 3a, 3b and 3c“, edited by Michael Klages, Jörn Thiede and Jean-Paul Foucher.

Heft-Nr. 489/2003 – „Expeditions in Siberia in 2003“, edited by Lutz Schirrmeister.

Heft-Nr. 490/2004 – „Modern Sedimentation Processes in the Kara Sea (Siberia)“, by Andrea Catalina Gebhardt.

Heft-Nr. 491/2004 – „Bentho-pelagische Kopplungsprozesse im arktischen Mellemfjord (Westgrönland) unter besonderer Berücksichtigung benthischer Peracarida (Malacostraca, Crustacea)“, von Jörg Nickel.

Heft-Nr. 492/2004 – „The coastal ecosystem of Kongsfjorden, Svalbard. Synopsis of biological research performed at the Koldewey Station in the years 1991-2003“, edited by Christian Wiencke.

Heft-Nr. 493/2004 – „Ontogeny of osmoregulatory functions and structures of three decapod crustaceans from the North Sea“, by Ude Cieluch.

Heft-Nr. 494/2005 – „Community dynamics and development of soft bottom macrozoobenthos in the German Bight (North Sea) 1969-2000“, by Alexander Schroeder.

Heft-Nr. 495/2005 – „The Expedition ANTARKTIS-XX of RV ‘Polarstern’ in 2002/2003. Reports of Legs 1 and 2“, edited by Dieter K. Fütterer and Gerhard Kattner.

Heft-Nr. 496/2005 – „Reproduction strategies and distribution of larvae and juveniles of benthic soft-bottom invertebrates in the Kara Sea (Russian Arctic)“, by Ingo Fetzer.

Heft-Nr. 497/2005 – „Großräumige Zirkulationsstrukturen in einem nichtlinearen adaptiven Atmosphärenmodell“, von Matthias Läuter.

Heft-Nr. 498/2005 – „Terrigener Sedimenteintrag und Paläoumwelt im spätquartären Arktischen Ozean: Rekonstruktionen nach Haupt- und Spurenelementverteilungen“, von Frank Schoster.

Heft-Nr. 499/2005 – „Der Einfluss der Großen Meteorbank auf die Ernährungsbiologie und Verteilung dominanter Calanoida (Crustacea, Copepoda)“, von Lutz Fischer.

Heft-Nr. 500/2005 – „The Expeditions ANTARKTIS XXI/3-4-5 of the Research Vessel „Polarstern“ in 2004“, edited by Victor Smetacek, Ulrich Bathmann, Elisabeth Helmke.

Heft-Nr. 501/2005 – „Pechora Sea Environments: Past, Present, and Future“, edited by H. A. Bauch, Yu. A. Pavlidis, Ye. I. Polyakova, G. G. Matishov, N. Koç.

Heft-Nr. 502/2005 – „Distribution and Mobility of Juvenile Polychaeta in a Sedimentary Tidal Environment“, by Norma Angélica Hernández-Guevara.

Heft-Nr. 503/2005 – „The Expedition ANTARKTIS XXI/2 (BENDEX) of RV ‘Polarstern’ in 2003/2004“, edited by Wolf E. Arntz and Thomas Brey.

Heft-Nr. 504/2005 – „Sea ice conditions in the northern North Atlantic in 2003 and 2004. Observations during RV POLARSTERN cruises ARKTIS XIX/1a and b and ARKTIS XX/2“, compiled by Jan L. Lieser.

Heft-Nr. 505/2005 – „Biodiversity, zoogeography and ecology of polychaetes from the Magellan region and adjacent areas“, by Américo Montiel San Martín.

Heft-Nr. 506/2005 – „Arctic Coastal Dynamics. Report of the 5th International Workshop. McGill University, Montreal (Canada), 13-16 October 2004“, edited by Volker Rachold, Hugues Lantuit, Nicole Couture and Wayne Pollard.

Heft-Nr. 507/2005 – „Evolution of Antarctic Fauna. Extended Abstracts of the IBMANT/ANDEEP International Symposium and Workshop in 2003“, edited by Sven Thatje, Javier A. Calcagno and Wolf E. Arntz.

Heft-Nr. 508/2005 – „Calanoid copepod resting eggs – a safeguard against adverse environmental conditions in the German Bight and the Kara Sea?“, by Marcus Engel.

Heft-Nr. 509/2005 – „The Expedition El'gygytgyn Lake 2003 (Siberian Arctic)", edited by Martin Melles, Pavel Minyuk, Julie Brigham-Grette and Olaf Juschus.

Heft-Nr. 510/2005 – „Stability of the Climate System and Extreme Climates in Model Experiments", by Vanya Romanova.

Heft-Nr. 511/2005 – „Untersuchungen zu gezeitenbedingten Höhenänderungen des subglazialen Lake Vostok, Antarktika, von Anja Wendt.

Heft-Nr. 512/2005 – „Demography, Reproductive Biology and Trophic Ecology of Red Coral (Corallium rubrum L.) at the Costa Brava (NW Mediterranean)", by Georgios Tsounis.

Heft-Nr. 513/2005 – „Rekonstruktion tausendjähriger aerosolchemischer Eiskernzeitreihen aus Nordostgrönland: Quantifizierung zeitlicher Veränderungen in Atmosphärenzirkulation, Emission und Deposition", von Birgit Mieding.

Heft-Nr. 514/2005 – „Radiation conditions in an Antarctic environment", by Sigrid Wuttke.

Heft-Nr. 515/2005 – „Südöstlicher Atlantik und südwestlicher Indik. Rekonstruktion der sedimentären und tektonischen Entwicklung seit der Kreide. AISTEK-I: Agulhas Transect. Report of the RV „Sonne" cruise SO-182, Project AISTEK-I. 4 April to 18 May 2005", edited by Gabriele Uenzelmann-Neben.

Heft-Nr. 516/2005 – „***Kontinental-Verschiebungen"***, Originalnotizen und Literaturauszüge von Alfred Wegener, herausgegeben von Reinhard Krause und Jörn Thiede.

Heft-Nr. 517/2005 – „Scientific Cruise Report of the Arctic Expedition ARK-XX/3 of RV „Polarstern" in 2004: Fram Strait, Yermak Plateau and East Greenland Continental Margin", edited by Ruediger Stein.

Heft-Nr. 518/2005 – „Exploring the neogene sedimentation of the eastern South Atlantic with reflection seismic data", by Etienne Wildeboer Schut.

Heft-Nr. 519/2006 – „The Influence of an Improved Soil Scheme on the Arctic Climate in a Regional Climate Model (RCM)", by Subodh Kumar Saha.

Heft-Nr. 520/2006 – „Global Implications of Arctic Climate Processes and Feedbacks. Report of the Arctic Climate Workshop. Alfred Wegener Institute for Polar and Marine Research, Potsdam (Germany), 5-7 September 2005", edited by Annette Rinke and Klaus Dethloff.

Heft-Nr. 521/2006 – „Südöstlicher Atlantik und südwestlicher Indik: Rekonstruktion der sedimentären und tektonischen Entwicklung seit der Kreide. AISTEK-II: Mosambik Rücken und Mosambik Becken. Report of the RV „Sonne" cruise SO-183, Projekt AISTEK-II. 20 May to 7 July 2005", edited by Wilfried Jokat.

Heft-Nr. 522/2006 – „Benthische Foraminiferenvergesellschaftungen als Anzeiger für spätquartäre Positionsänderungen der Fronten des Antarktischen Zirkumpolarstroms im Südatlantik", von Miriam Rudolph.

Heft-Nr. 523/2006 – „Late Weichselian to Holocene Sedimentation in the Inner Kara Sea: Qualification and Quantification of Processes", by Klaus Hauke Dittmers.

Heft-Nr. 524/2006 – „Nichtlineare Dynamik atmosphärischer Zirkulationsregime in einem idealisierten Modell", von Mario Sempf.

Heft-Nr. 525/2006 – „Processing of shipborne magnetometer data und revision of the timing and geometry of the Mesozoic break-up of Gondwana", by Matthias König.

Heft-Nr. 526/2006 – „Effects of ultraviolet radiation on early life stages of cold temperate and Arctic macroalgae: implications for recruitment and vertical depth distribution", by Michael Y. Roleda.

Heft-Nr. 527/2006 – „Kleinskalige Heterogenität in der arktischen Tiefsee: Einfluss kleiner Kaltwasser-Schwämme auf die Diversität benthischer Nematoden-Gemeinschaften", von Christiane Hasemann.

Heft-Nr. 528/2006 – „Makrozoobenthos-Gemeinschaften arktischer Weichböden: Struktur und Bedeutung als Nahrungsgrundlage demersaler Fische", von Marko Herrmann.

Heft-Nr. 529/2006 – „Strategies of cellular ageing in polar and temperate marine Invertebrates", by Eva Philipp.

Heft-Nr. 530/2006 – „Schiffstagebuch der Steam-Bark GROENLAND geführt auf einer Fangreise in die Antarktis im Jahre 1873/1874 unter der Leitung von Capitain Ed. Dallmann", herausgegeben und kommentiert von Reinhard A. Krause und Ursula Rack.

Heft-Nr. 531/2006 – „Aggregations of Arctic deep-sea scavenging amphipods at large food falls", by Katrin Premke.

Heft-Nr. 532/2006 – „Ecological Preferences of Benthic Foraminifera in the Eastern South Atlantic: Distribution Patterns, Stable Carbon Isotopic Composition, and Paleoceanographic Implications", by Laetitia Licari.

Heft-Nr. 533/2006 – „The Expedition ANTARKTIS-XXII/3 of the Research Vessel 'Polarstern' in 2005, edited by Eberhard Fahrbach.

Heft-Nr. 534/2006 – „Sensitivitätsstudien und Analyse von Atmosphäre-Meereis-Wechselwirkungen mit dem regionalen Atmosphärenmodell HIRHAM4 auf Basis eines neu entwickelten beobachtungsgestützten unteren Modellantriebs während ausgewählter Sommer über der Arktis / Laptewsee", von Klaus Görgen.

Heft-Nr. 535/2006 – „Beobachtung und Modellierung der Schneeschmelze und Aufeisbildung auf arktischem und antarktischem Meereis", von Marcel Nicolaus.
[Notice for corrections: The name of the author Nicolaus was regrettably misprinted on the title pages of that volume]

Heft-Nr. 536/2006 – „Tunicaten (Ascidiacea) der Nordsee: Chemische Ökologie und pharmakologisches Potential", von Jana Stefanie Barenbrock.

Heft-Nr. 537/2006 – „The Expeditions ANTARKTIS-XXII/4 and 5 of the Research Vessel 'Polarstern' in 2005", edited by Hans-Werner Schenke and Walter Zenk.

Heft-Nr. 538/2006 – „Radition Measurements and Synoptic Observations at Ny-Ålesund, Svalbard", by Heike Kupfer, Andreas Herber and Gert König-Langlo. – Notice: The report including the large appendix ist published at: http://epic.awi.de/Publications/Kup2006a.pdf

Heft-Nr. 539/2006 – „The Expedition LENA 2004 in Siberia and the Expedition LIVINGSTON 2005 in Antarctica", edited by Dirk Wagner.

Heft-Nr. 540/2006 – „Seafloor analysis based on multibeam bathymetry and backscatter data“, by Andreas Beyer.

Heft-Nr. 541/2006 – „The Exchange of Energy, Water and Carbon Dioxide between Wet Arctic Tundra and the Atmosphere at the Lena River Delta, Northern Siberia“, by Lars Kutzbach.

Heft-Nr. 542/2007 – „Identification of seafloor provinces - specific applications at the deep-sea Håkon Mosby Mud Volcano and the North Sea“, by Kerstin Jerosch.

Heft-Nr. 543/2007 – „Farming in a High Energy Environment: Potentials and Constraints of Sustainable Offshore Aquaculture in the German Bight (North Sea)“, by Bela Hieronymus Buck.

Heft-Nr. 544/2007 – „The Expeditions ARKTIS XX/1 and XX/2 of the Research Vessel ‘Polarstern’ in 2004“, edited by Gereon Budéus and Peter Lemke.

Heft-Nr. 545/2007 – „Lakustrine Sedimente als Archive des spätquartären Umweltwandels in der Amery-Oase, Ostantarktis“, von Nadja Hultzsch.

Heft-Nr. 546/2007 – „Detaillierte Biomarkeruntersuchungen an Sedimentkernen von ODP-Leg 177“, von Petra Weller.

Heft-Nr. 547/2007 – „Development of a novel balloon-borne optical sonde for the measurement of ozone and other stratospheric trace gases“, von Mareile Wolff.

Heft-Nr. 548/2007 – „Holocene and Last Glacial Maximum (paleo-)productivity off Morocco. Evidence from benthic foraminifera and stable carbon isotopes“, by Astrid Eberwein.

Heft-Nr. 549/2007 – „11th International Conference on the Physics and Chemistry of Ice (PCI-2006). Bremerhaven, Germany, 23-28 July 2006. Abstracts“, edited by Frank Wilhelms and Werner F. Kuhs.

Heft-Nr. 550/2007 – „Expeditions in Siberia in 2005“, edited by Lutz Schirrmeister.

Heft-Nr. 551/2007 – „The Expeditions ANTARKTIS-XXII/1 and XXII/2 of the Research Vessel ‘Polarstern’ in 2004/2005“, edited by Saad El Naggar, Gerhard Dieckmann, Christian Haas, Michael Schröder and Michael Spindler.

* vergriffen/out of print.
** nur noch beim Autor/only from the author.